Université de Montréal

Actin cytoskeleton regulates pollen tube growth and tropism

par
Firas Bou Daher

Département de sciences biologiques, Institut de recherche en biologie végétale
Faculté des Arts et des Sciences

Thèse présentée à la Faculté des Arts et des Sciences
en vue de l'obtention du grade de doctorat
en biologie végétale

Avril, 2011

Université de Montréal
Faculté des études supérieures et postdoctorales

Cette thèse intitulée:

Actin cytoskeleton regulates pollen tube growth and tropism

Présentée par :
Firas Bou Daher

a été évaluée par un jury composé des personnes suivantes :

David Morse, président-rapporteur
Anja Geitmann, directeur de recherche
Mohamed Hijri, membre du jury
Alice Cheung, examinateur externe

Résumé

La fertilisation chez les plantes dépend de la livraison des cellules spermatiques contenues dans le pollen à l'ovule. Au contact du stigmate, le grain de pollen s'hydrate et forme une protubérance, le tube pollinique, chargé de livrer les noyaux spermatiques à l'ovule. Le tube pollinique est une cellule à croissance rapide, anisotrope et non autotrophe; ainsi tout au long de sa croissance à travers l'apoplaste du tissu pistillaire, le tube pollinique puise ses sources de carbohydrates et de minéraux du pistil. Ces éléments servent à la synthèse des constituants de la paroi qui seront acheminés par des vésicules de sécrétion jusqu'à l'apex du tube. Ce dernier doit aussi résister à des pressions mécaniques pour maintenir sa forme cylindrique et doit répondre à différents signaux directionnels pour pouvoir atteindre l'ovule. Mon projet de doctorat était de comprendre le rôle du cytosquelette dans la croissance anisotrope du tube pollinique et d'identifier les éléments responsables de sa croissance et de son guidage. Le cytosquelette du tube pollinique est composé des microfilaments d'actine et des microtubules. Pour assurer une bonne croissance des tubes polliniques *in vitro*, les carbohydrates et les éléments de croissance doivent être ajoutés au milieu à des concentrations bien spécifiques. J'ai donc optimisé les conditions de croissance du pollen d'*Arabidopsis thaliana* et de *Camellia japonica* qui ont été utilisés avec le pollen de *Lilium longiflorum* comme modèles pour mes expériences. J'ai développé une méthode rapide et efficace de fixation et de marquage du tube pollinique basée sur la technologie des microondes. J'ai aussi utilisé des outils pharmacologiques, mécaniques et moléculaires couplés à différentes techniques de microscopie pour comprendre le rôle du cytosquelette d'actine lors de la croissance et le tropisme du tube pollinique. J'ai trouvé que le cytosquelette d'actine et plus précisément l'anneau d'actine localisé dans la partie sub-apicale du tube est fortement impliqué dans la croissance et le maintien de l'architecture du tube à travers le contrôle de la livraison des vésicules de sécrétion. J'ai construit une chambre galvanotropique qui peut être montée sur un microscope inversé et qui sert à

envoyer des signaux tropistiques bien précis à des tubes polliniques en croissance. J'ai trouvé que les filaments d'actine sont impliqués dans la capacité du tube pollinique à changer de direction. Ce comportement tropistique dépend de la concentration du calcium dans le milieu de croissance et du flux de calcium à travers des canaux calciques. Le gradient de calcium établi dans le tube pollinique affecte l'activité de certaines protéines qui se lient à l'actine et dont le rôle est la réorganisation des filaments d'actine. Parmi ces protéines, il y a celles de dépolymérisation de l'actine (ADF) dont deux spécifiquement exprimées dans le gamétophyte mâle d'*Arabidopsis* (ADF7 et ADF10). Par marquage avec des proteins fluorescents, j'ai trouvé que l'ADF7 et l'ADF10 ont des expressions différentielles pendant la microsporogenèse et la germination et croissance du tube pollinique et qu'elles partagent entre elles des rôles importants durant ces différents stades.

Mots-clés : Actine, *Arabidopsis thaliana*, ADF, calcium, *Camellia japonica*. cytosquelette, *Lilium longiflorum*, pollen, tropisme, tube pollinique.

Abstract

Fertilization in plants depends on the delivery of the sperm cells in the pollen grain through the pollen tube to the ovule. The pollen tube is a highly anisotropic, fast growing cellular protuberance. Because the pollen tube is non autotrophic, it requires a steady supply of carbohydrates and minerals supplied by the pistil to sustain its growth. These elements serve for the synthesis of cell wall material, delivered to the site of cell wall assembly in secretory vesicles that are transported along the actin cytoskeleton and deposited at the growing apex of the tube. The tube has to resist external deformation forces in order to maintain its cylindrical shape and to respond to various directional signals in order to reach its target. My objectives were to identify the role of the cytoskeleton in the anisotropic growth of the pollen tube and to determine how the tube responds to directional cues. The cytoskeleton in the pollen tube consists of microfilaments and microtubules, both forming long filamentous elements. For *in vitro* growing pollen tubes, carbohydrates and growth minerals have to be added to the growth medium in specific amounts order to sustain pollen tube growth. I optimized the growth conditions of *Arabidopsis thaliana* and *Camellia japonica* pollen tubes which, in addition to pollen from *Lilium longiflorum*, were used as model species for my experiments. I developed a microwave based, fast and efficient fixation and labelling protocol for pollen tubes. I used pharmacological, mechanical, molecular and microscopical tools to study the role of the cytoskeleton in pollen tube growth and tropism. I found that the actin cytoskeleton, and more specifically the subapical actin fringe, plays an important role in the regulation of pollen tube growth and architecture through the controlled delivery of secretory vesicles to the growing apex. I constructed a galvanotropic chamber that can be mounted on an inverted microscope to induce controlled tropic triggers. I found that the actin cytoskeleton is also involved in the ability of the pollen tube to change its direction. This tropic behaviour was shown to be dependent on the concentration of calcium ions in the growth medium and calcium influx through calcium channels.

The cytosolic calcium gradient in the pollen tube regulates the activity of various actin binding proteins that are responsible for remodelling the actin cytoskeleton. Among these proteins are two *Arabidopsis* gametophyte-specific actin depolymerizing factors (ADFs) that I tagged with two intrinsically fluorescent proteins. I found that ADF7 and ADF10 are differentially expressed during microsporogenesis and pollen tube germination and growth and that they likely divide important functions between them.

Keywords: Actin, actin depolymerizing factor, *Arabidopsis thaliana*, calcium, *Camellia japonica*, cytoskeleton, *Lilium longiflorum*, pollen, pollen tube, tropism.

List of abbreviations

ABP: actin binding protein

ADF: actin depolymerizing factor

ADP: adenosine diphosphate

ATP: adenosine triphosphate

BC: before Christ

BDM: 2,3-butanedione monoxine

BSA: bovine serum albumin

Ca^{2+}: calcium

CCD: charged coupled device

CFP: cyan fluorescent protein

DAPI: 4'-6-diamidino-2-phenylindole

DNA: deoxyribonucleic acid

EGFP: enhanced green fluorescent protein

EGTA: ethylene glycol tetraacetic acid

FDA: fluorescein diacetate

FRAP: fluorescence recovery after photobleaching

GFP: green fluorescent protein

MBS: m-maleimidobenzoyl N-hydroxysuccinimide

LatB: latrunculin B

LM: lily medium

MW: microwave

PBS: phosphate buffer saline

PI: phosphatidylinositol

PIP: phosphatidylinositol 4-phosphate

PIP2: phosphatidylinositol 4,5-biphosphate

PM: PIPES and magnesium buffer

PME: pectin methyl esterase

RNA: ribonucleic acid

ROP: Rho of plants

SEM: scanning electron microscope

STICS: spatio-temporal image correlation spectroscopy

sulfo-EGS: ethylene glycol bis[sulfosuccinimidylsuccinate]

TBS: tris buffer saline

TEM: transmission electron microscope

YFP: yellow fluorescent protein

Table of Contents

List of figures

List of tables

...You have been told also that life is darkness, and in your weariness you echo what was said by the weary.

And I say that life is indeed darkness save when there is urge,

And all urge is blind save when there is knowledge,

And all knowledge is vain save when there is work,

And all work is empty save when there is love;

And when you work with love you bind yourself to yourself, and to one another, and to God.

...Work is love made visible.

And if you cannot work with love but only with distaste, it is better that you should leave your work and sit at the gate of the temple and take alms of those who work with joy.

For if you bake bread with indifference, you bake a bitter bread that feeds but half man's hunger.

And if you grudge the crushing of the grapes, your grudge distils a poison in the wine.

And if you sing though as angels, and love not the singing, you muffle man's ears to the voices of the day and the voices of the night.

The Prophet

Gibran Kahlil Gibran

Acknowledgements

I would like to thank Dr Anja Geitmann, for all the support, guidance and tutoring that she provided me with during my PhD journey. I was deeply honoured and privileged for having her as my supervisor. I also want to thank her for whom she was out of the lab; nice, friendly, caring and generous. It all meant a lot to me and I am grateful for that. Thank you Anja!

I would like to thank Leila, Youssef, Olivier and all the members of our lab including Rabah, Gérome, Monisha, Jens, Orlando, Nicolas, Minako and Chloe for all the help provided.

I would like to thank Gabriel Theodorescu, Michel Lemay and Louis-Régens Deschênes for taking care of our plants in the greenhouses.

I would like to thank Louise Pelletier for her help in electron microscopy.

I would like to thank Dr Mario Cappadocia and Jonathan Soulard for kindly providing the pDONR Zeo plasmid.

I would like to thank all the staff of the IRBV for making my life easier.

I would like to thank Mrs Nayla Mouawad for all the care and support.

Nothing of what I achieved would have been done without the support of my father and my mother and my brother. Their blessings and prayers gave me the strength to go all along. Thank you Pa, thank you Ma, thank you Bro!

Finally I would like to thank God Almighty for giving us the talents and the opportunities to use them.

1 Introduction

1.1 Pollen in history

Pollen, the microscopic dust produced by flowers and carried by wind and bees in the spring, is nothing else but the carrier of the plant male gametes. The role of the pollen is to transfer the male gametes to their female counterparts for the fertilization that will produce new plant generations. The importance of pollen has been known for long time. In his travels through Babylonia, Herodotus (ca. 484- ca. 425 BC) describes how the Babylonians treated their date palm trees in order to bear fruits. He writes that the contact between the male and female fruits will allow the "insect" living in the male fruit to enter the female fruit in order for the latter to mature (Lacarrière, 1981). Even though he confused the pollination type of figs that are native to Greece and require an insect for pollination and fruit set with that of date palms that just require pollen transfer by wind from the male to the female flower, Herodotus provides information concerning the early knowledge about pollen and pollination. Clearly the concept has been known for several centuries before Jesus Christ. In fact, several stone reliefs dating from the ninth to the seventh century BC are present in the palace of Ashurnasirpal II (ninth century BC) in Nineveh on the eastern side of the Tigris River that display the manual pollination performed by shaking the male flowers of date palm trees (Porter, 1993).

However, because of their small size, it was not until the seventeenth century and the development of the microscope that pollen grains could be morphologically described. The Englishman Nehemiah Grew and the Italian Marcello Malpighi were the pioneers in this field and they left morphological descriptions of several pollen species. Giovanni Batista Amici, an Italian astronomer, botanist and microscopist, is known to be the first to describe pollen germination on a stigma of *Portulaca* in 1822, although Robert Brown (Brown, 1833) claims that Ferdinand Lucas Bauer describes pollen tube germination and entry into the style before Amici. The

"Brownian motion" was first observed and described by Brown himself in 1828 when he talked about the inherent movement of granules in the pollen of *Clarkia*.

The function of the pollen tube in the reproduction process remained a mystery until the mid of the nineteenth century when Jacob Matthias Schleiden posited that the pollen tube carrying the embryonal globule enters the embryo sac where it forms the embryo. However, Wilhelm Hofmeister demonstrated in 1849 that the ovum present inside the embryo sac forms the embryo thus overturning the theory of Schleiden (Hofmeister, 1962) and opening the new era of recognizing the specific functions of the male and female gametophytes in plants.

1.2 Importance of pollen

The flowers with their wonderful beauty and adorable smell have one reason for being so majestic: ensuring the efficient transfer of the pollen grain between individuals of the same species. Flowers evolved and developed these traits in order to attract pollinators like birds, bats, insects and other arthropods. These pollinators ensure the conservation of the species through the transfer of the male genetic material contained in the pollen grain to the female counterpart allowing fertilization and seed and fruit set. The importance of pollen in agronomy and horticulture as the carrier of the generative nuclei is therefore obvious. However, pollen has also gained an important role in other scientific fields because the biochemical composition and architectural characteristics of the pollen grain exine (the outer cell wall) makes this structure very resistant to chemical, biological and mechanical deterioration (Scott, 1994). This property is exploited in archaeological and geological research due to the presence of fossil pollen. Because of its extraordinary resistance, pollen is often the only remnant of past vegetation. Because of species-specific geometrical variations in its outer structure, a feature that is maintained during petrification, plant species can be identified purely based on the morphology of its pollen (Figure 1.1). Therefore, fossil pollen provides precious information about plant survival and

colonization (Petit *et al.*, 2002; Tollefsrud *et al.*, 2008) and past climatic changes (Webb and Bryson, 1972). It allows retracing species evolution and origin including extant species (Muller, 1981; Gaillard *et al.*, 2008; Schaefer *et al.*, 2009) and it provides plenty of other biologically relevant information including plant-pollinator coevolution (Hu *et al.*, 2008). Freshly shed pollen on the other hand is a very convenient tool for forensic investigations since it readily and unnoticeably attaches to clothes and objects and reveals the location at which these objects must have been, based on the species composition. This scientific field is known as forensic palynology (Bryant and Mildenhall, 1998). Due to its abundance in honey, pollen has been used to verify the quality and authenticity of commercial honey, a science known as melissopalynology. The health issues caused by some pollen species have made pollen also an interesting topic for medical research (Ciprandi *et al.*, 1995; Ciprandi *et al.*, 1997; Jutel *et al.*, 2005).

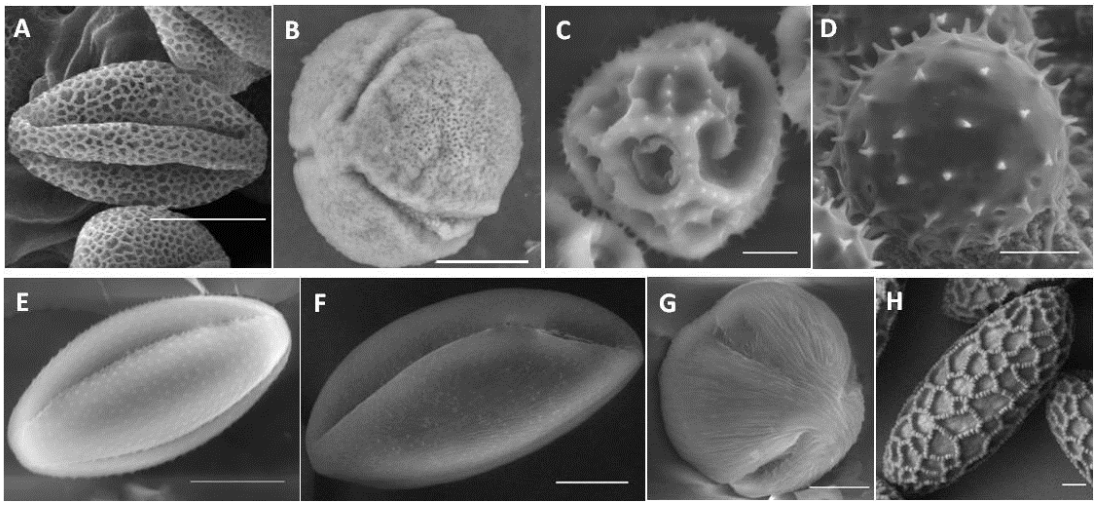

Figure 1.1: Scanning electron micrographs of (A) *Arabidopsis*, (B) *Camellia*, (C) *Taraxacum*, (D) hibiscus, (E) poppy, (F) pear, (G) apple and (H) lily pollen grains. Bars = 10 µm in A, C, E, F, G, H and 50 µm in B, D.

Pollen comes in different shapes and sizes (Figure 1.1). The smallest pollen grains belong to the family of Boraginaceae and are about 2 µm in diameter whereas the biggest are those of *Cymbopetalum odoratissimum* (Annonaceae) which can

measure up to 350 μm (Walker, 1971). In some marine species the pollen is coiled in the anther and once released it can measure up to 5 mm (Ducker *et al.*, 1978).

1.3 Pollination

The male plant gametophytes form in the anther where a sporocyte undergoes meiosis and gives rise to microspores that develop into mature pollen grains (Twell *et al.*, 1998; McCormick, 2004). The last steps in pollen maturity are characterized by water loss and when the pollen is highly dehydrated when shed. This increases the pollen's ability to survive during its travel. Upon pollination, and if favourable conditions are available, the pollen hydrates and produces a tube that grows through the stylar tissue and reaches the ovary (Figure 1.2). Passing the placenta, the pollen tube reaches the ovule through the micropyle and delivers the sperm cells for double fertilization to happen (Lord and Russell, 2002). This delivery process of the sperm cells through the cellular tunnel formed by the pollen tube is known as siphonogamy, contrary to systems in which the motile sperm moves on its own.

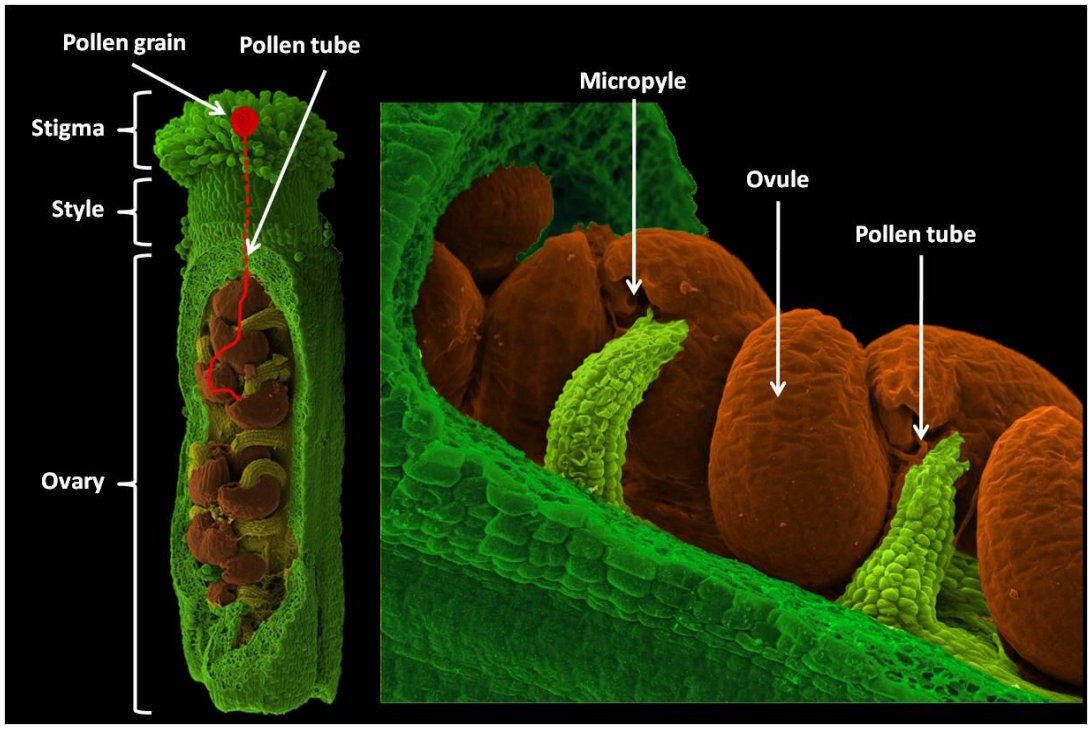

Figure 1.2: *Arabidopsis thaliana* pistil scanning electron micrograph with false colors and a schematic representation of the pollen tube on the left with a close up image of the exposed ovules on the right.

The attachment of the pollen grain to the stigma, its germination and the penetration of the pollen tube through the stigmatic, stylar and ovarian tissues to finally reach the embryo sac require recognition and communication between the pollen tube and the pistil in order for the former to be well guided along its trajectory (Cheung, 1996; Cheung and Wu, 2001; Geitmann and Palanivelu, 2007; Dresselhaus and Márton, 2009). Recognition starts when the pollen lands on the stigma. Stigmas can be either dry, as in the Brassicaceae, or wet as in the Solanaceae (Dafni and Maués, 1998). In the case of dry stigmas, hydration is the critical step. Certain lipid compounds play a role in this process (Preuss *et al.*, 1993) and might generate a water gradient along which the tube is guided into the stigma (Wolters-Arts *et al.*, 1998). In the Brassicaceae, the initial hydration is controlled by *S-locus* specific glycoproteins that are implicated in sporophytic self incompatibility (Trick and Flavell, 1989; Takayama *et al.*, 2000). In species with wet stigmas, hydration is

considered to be a passive process sustained by the readily available stigma exudates (Swanson *et al.*, 2004). Once the pollen germinates, the pollen tube grows by penetrating the papilla cell walls in dry stigmas or through the intercellular spaces of the wet stigmas assisted by cell wall loosening enzymes (Cosgrove *et al.*, 1997; Nieuwland *et al.*, 2005). The passage of the pollen tube through the stigma is important for the tube to be able to accomplish fertilization since its capacity to target a receptive ovule is increased by a process called capacitation (Palanivelu and Preuss, 2006). Depending on the species, following invasion of the stigma, pollen tubes either grow along a hollow style or have to make their way through the intercellular matrix of the transmitting tissue filling a solid style. The intercellular matrix is rich in sugars, glycoproteins, amino acids, and other elements that play a role in pollen tube growth and guidance through interactions at the pollen tube surface or within its cytoplasm after being taken up (Cheung, 1996; Cheung and Wu, 1999; Lord, 2003; Sanchez *et al.*, 2004; Geitmann and Palanivelu, 2007; Hiscock and Allen, 2008). During pollen tube growth through the style, different guidance mechanisms are known to act. In the case of lily which is characterized by a hollow style, a gradient of chemocyanin, a small pistillar protein, guides pollen tube growth (Kim *et al.*, 2003). Recently, a calcium gradient was found to be established in the style after pollination (Ge *et al.*, 2009) which might direct pollen tube growth. In the case of gametophytic self incompatibility, pollen rejection and therefore death is executed in general in the style (poppy being an exception since it does not have a style) in an S-RNase based process (McClure and Franklin-Tong, 2006). When the pollen tube reaches the bottom-end of the style and enters the ovary, it enters the sphere of influence of the female gametophytes located within the ovules. Female gametophyte guidance is based on the production of attractant or repellant substances that help the tube reach an unfertilized embryo sac and deliver the sperm cells (Higashiyama *et al.*, 2003; Tung *et al.*, 2005; Higashiyama and Hamamura, 2008; Dresselhaus and Márton, 2009; Qin *et al.*, 2009; Higashiyama, 2010; Márton and Dresselhaus, 2010). Our understanding of the communication between male and

female gametophytes is poor, but it has been found that the central cell produces transcriptional regulators that affect pollen tube guidance in *Arabidopsis* (Chen *et al.*, 2007). In maize, the egg apparatus (composed of the egg cell and the two synergids) produces an attractant protein (EA1) that passes through the micropyle to attract the pollen tube (Márton *et al.*, 2005). The synergids of *Torenia fournieri* produce a protein called LURE that has an important role in pollen tube attraction (Okuda *et al.*, 2009). In addition to the proteic signals, the synergids are believed to extrude calcium into their extracellular medium thus creating a calcium gradient that will attract the pollen tube to the embryo sac (Chaubal and Reger, 1990; Higashiyama *et al.*, 2003). Once in the embryo sac, the pollen tube contacts one of the synergids and ruptures in a process regulated by calcium (Schiøtt *et al.*, 2004; Higashiyama and Hamamura, 2008; Dresselhaus and Márton, 2009).

During its passage through the pistillar tissue, the pollen tube has to produce an invasive force that will allow it to elongate within the transmitting tissue and to resist external mechanical compression forces against which it needs to maintain its tubular shape. The driving force for this growth process is generated by a combination of the turgor pressure and a continuous supply of new cell wall material deposited at the growing apex. Elongation only takes place at the tip of the cell, contrary to most other plant cells in which growth is characterized as diffuse. Pollen tubes share this growth principle with root hairs, fungal hyphae and to a certain extent with animal nerve axons.

Due to its rapid, one-dimensional type of growth, the ease of *in vitro* culture and the panoply of signaling mechanisms involved, the pollen tube is being used as a model system by numerous researchers around the globe. Its cellular structures are being thoroughly investigated using optical, fluorescence and electron microscopy. Its mechanical parameters are being quantified. Knock out mutants and transgenic lines are being generated for different target genes involved in all aspects of pollen tube growth and finally physical and mathematical models describing pollen tube

growth are being applied to help understand and quantify the biological data generated.

1.4 Pollen tube growth

The pollen tube is a cellular protuberance formed by the pollen grain, and is characterized by a rapid and unidirectional growth. Pollen tubes grow at very rapid rates that can reach up to 2.75 cm/h in the case of *Colchicum autumnale* which represents 9000 times the diameter of the pollen grain each hour (Schleiden, 1849). *Lilium longiflorum*, a species commonly used in pollen studies, has a pollen tube that grows at 2 mm/h *in vivo* (van der Woude and Morré, 1968), while tobacco pollen grows at 1.7 mm/h (Sanchez *et al.*, 2004). It should be mentioned that pollen tube growth *in vitro* is much slower than that of pollen growing in the style of the flower. For instance, *Lilium longiflorum* pollen tube growth *in vitro* is about 0.5 mm/h (data from our lab). Since the pollen tube is not autotrophic due to the lack of chloroplasts, it requires a continuous supply of carbohydrates to sustain the ongoing assembly of cell wall and to maintain the osmotic potential. When pollen tubes are grown *in vitro*, carbohydrates, usually in the form of sucrose, should be added to the medium in addition to several important microelements including boron, calcium, magnesium, nitrogen and sulfur (Brewbaker and Kwack, 1963).

Pollen tube growth is sustained by a continuous and efficient supply of new cell wall material contained in secretory vesicles and deposited at the growing apex through exocytosis (Franklin-Tong, 1999; Bove *et al.*, 2008; Zonia and Munnik, 2008) (Figure 1.3). Organelle transport in pollen tubes occurs on both actin filaments and microtubules (Lovy-Wheeler *et al.*, 2007; Romagnoli *et al.*, 2007). However, inhibition of the microtubules using oryzalin does not affect cytoplasmic streaming (Cai *et al.*, 2005), whereas interference with actin functioning through cytochalasin or latrunculin B rapidly arrests both pollen tube growth and cytoplasmic streaming

(Gibbon *et al.*, 1999; Vidali and Hepler, 2001). Actin-myosin driven motion is, therefore, the principal mechanism that drives and guides the movement of organelles and vesicles. A myosin extracted from lily pollen has been shown to belong to class XI myosins (Yokota and Shimmen, 1994). Treatment with 2,3-butanedione monoxine (BDM) which inhibits myosin ATPases by stabilizing the myosin–ADP–Pi complex (Palmieri *et al.*, 2007) revealed a concentration dependent effect on germination and elongation of *Picea abies* pollen tubes with the threshold concentration being 10 mM (Anderhag *et al.*, 2000). In *Chara corallina* and in lily pollen tubes, BDM reversibly inhibited the cytoplasmic streaming (Tominaga *et al.*, 2000; Funaki *et al.*, 2004) indicating that this process is highly dependent on energy supply through ATP.

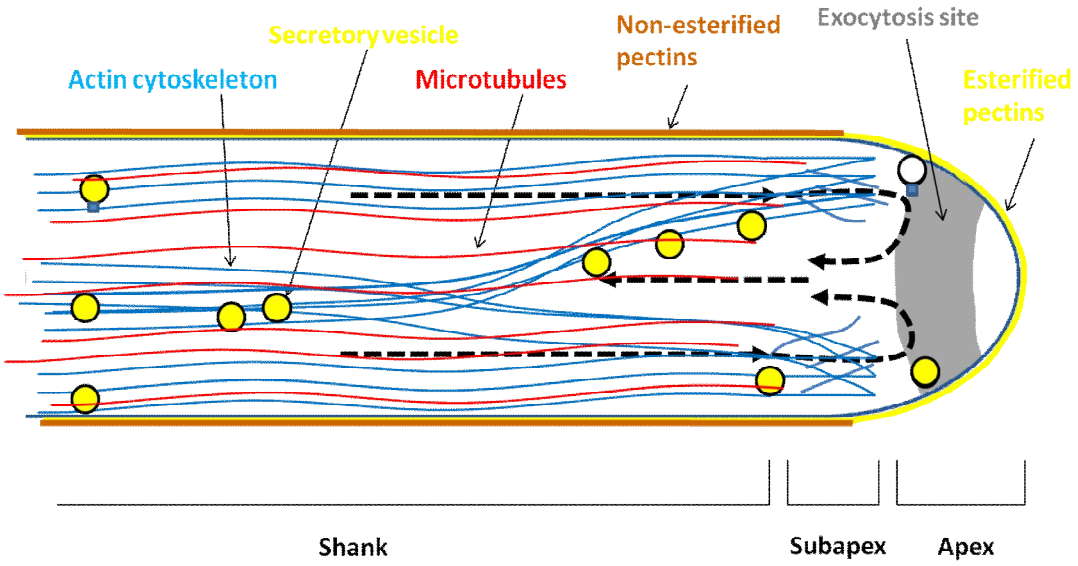

Figure 1.3: Schematic representation of the cytoarchitecture characterising the different zones of the pollen tube. Dashed arrows indicate motion patterns of vesicle flow.

The anisotropic and radially symmetric mode of growth (which is shared with root hairs, fungal hyphae and neurons), has made the pollen tube a model system to study different aspects of cell growth. It has also made pollen tube extremely interesting from a mechanical and modeling point of view. Therefore, research on

pollen tube extends the studies to interdisciplinary field combining biological with physical and mathematical sciences. By modeling pollen tube growth and the panoply of biological phenomena occurring inside the cell and validating the models by biological data, mathematicians and physicists are improving our knowledge about different aspects of cellular growth and development.

1.5 Pollen tube cytoarchitecture

Pollen grains are either bicellular (70% of the species) or tricellular (Brewbaker, 1967). Pollen of the former type consists of a vegetative cell and a generative cell, whereas in the latter the generative cell has already divided into the two sperm cells during pollen maturation. In bicellular pollen this division only takes place during pollen tube growth. The sperm cells move within the cytoplasm of the pollen tube over distances of up to 30 cm from the grain to the ovule. Whereas during animal development, cellular migration is a common phenomenon, plant cells are in general unable to move away from their location of origin. The sperm cell migration through the pollen tube represents, therefore, a quite exceptional situation in the plant kingdom.

The pollen tube cell wall is composed of an inner callose layer and an outer pecto-cellulosic layer (Heslop-Harrison *et al.*, 1987; Steer and Steer, 1989). Callose and cellulose are load bearing materials (Parre and Geitmann, 2005; Aouar *et al.*, 2010). Callose is absent at the tip of the pollen tube and is deposited as a secondary layer in the maturing part of the tube (Heslop-Harrison *et al.*, 1987; Parre and Geitmann, 2005). The abundance of cellulose is very low in the cell wall of the pollen tube which is quite atypical for a plant primary cell wall (Schlüpmann *et al.*, 1994; Aouar *et al.*, 2010). The tip of the pollen tube cell wall is almost exclusively composed of pectin (Ferguson *et al.*, 1998; Holdaway-Clarke and Hepler, 2003). While both callose and cellulose are produced by plasma membrane-located synthases activated in the maturing portion of the tube, the pectic layer is assembled

through exocytosis at the very tip. Secretory vesicles transport pectic polysaccharides, composed of homogalacturonan that has been methyl-esterified in the Golgi, to the growing zone of the pollen tube. This methyl-esterified pectin is a soft material (Parre and Geitmann, 2005). After their insertion into the apical cell wall pectins are gradually de-esterified by pectin methyl-esterases. The action of these enzymes converts the methoxyl groups of the galacturonan into carboxyl groups which can be readily cross linked by calcium ions, thus increasing the stiffness of the pectins present at the subapical region of the pollen tube. The presence of esterified pectins at the tip of the pollen tube creates a spatially confined location of lower mechanical stability that yields under the effect of the growth driving force, the turgor pressure. As a result, the tube elongates in one direction only forming a perfect cylinder (Geitmann and Steer, 2006; Geitmann and Dumais, 2009; Fayant *et al.*, 2010).

The number of vesicles transported to the apical zone exceeds the number that is needed to provide the amount of building material necessary to sustain pollen tube growth (Bove *et al.*, 2008). At the growth rates observed *in vitro*, the supply of vesicles is, therefore, not the factor limiting the speed of growth (Bove *et al.*, 2008). Remarkably, the number of vesicles required to deliver cell wall material is higher than that necessary to form the expanding plasma membrane, so excess membrane in the apical region of the pollen tube must be removed by endocytosis (Picton and Steer, 1983; Derksen *et al.*, 1995; Bove *et al.*, 2008). The vesicles formed by endocytosis and the excess secretory vesicles that are recycled back at the tip of the pollen tube form what is known as the inverted cone of vesicles (Lancelle and Hepler, 1992; Parton *et al.*, 2001; Bove *et al.*, 2008). The apical zone of the pollen tube containing the vesicles is also known as the clear zone because little or no other larger organelles are located here and in brightfield microscopy this zone appears rather smooth compared to the distal region of the cell (Cresti *et al.*, 1977; Heslop-Harrison and Heslop-Harrison, 1990). The apical cytoplasm of the pollen tube is devoid of actin filaments. The vesicular movement in these region is therefore

slower, but still measurable, and probably based on diffusion and/or convective motion (Kroeger *et al.*, 2009).

The cytoplasm in the subapex contains a dense mesh of actin filaments (Kost *et al.*, 1998; Geitmann and Emons, 2000; Lovy-Wheeler *et al.*, 2005) known as the actin fringe. This region is also rich in mitochondria, dictyosomes and endoplasmic reticulum. In the shank region of the pollen tube where long cables of actin filaments and microtubule are oriented parallel to the axis of gowth (Figure 1.3), a high concentration of dictyosomes, endoplasmic reticulum and vacuoles are present in addition to the vegetative nucleus and the generative cell (Mascarenhas, 1993; Åström *et al.*, 1995; de Graaf *et al.*, 2005; Lovy-Wheeler *et al.*, 2007). The non-uniform distribution of cytoplasmic components in the pollen tube clearly reflects the polar activity of the cell which focuses all growth activity to a single site, the tip.

A detailed analysis using STICS (spatio-temporal image correlation spectroscopy) and FRAP (fluorescence recovery after photobleaching) described the spatial patterns by which vesicles reach the apex through the cell cortex, and are recycled backwards through the center of the tube (Bove *et al.*, 2008). The high temporal resolution microscopic study revealed that an annular region of exocytosis spatially coincides exactly with the proximal end of the actin fringe. This suggests an important role for the actin fringe in orienting the direction of pollen tube growth by way of targeting vesicles to spatially confined regions at the cellular surface.

1.6 Pollen tube tropism

For fertilization to happen, the pollen tube has to find its way through the stigma, style, and ovary, to reach the micropyle and deliver the sperm cells (Geitmann and Palanivelu, 2007). To find its target, the embryo sac, it has to respond to external signals, change direction when required, and exhibit tropic behaviour (Cheung and Wu, 2001). Genetic and physiological studies have shown that the pistil (Cheung *et al.*, 1995; Palanivelu *et al.*, 2003) and the female gametophyte

(Higashiyama *et al.*, 2003; Tung *et al.*, 2005; Palanivelu and Preuss, 2006; Higashiyama and Hamamura, 2008; Okuda *et al.*, 2009; Márton and Dresselhaus, 2010) produce directional signals that help the pollen tube reach its target. It is not yet clear how the pollen tube perceives these signals and how the intracellular signalling pathways eventually lead to a change in growth direction. Molecules such as receptor kinases and cell membrane-associated small G proteins, along with variations in ion fluxes, are candidates for pollen effectors of the reorientation reaction (Hepler *et al.*, 2001). Nitric oxide has been also shown to affect pollen tube guidance in lily and *Arabidopsis* probably by affecting calcium influx to the pollen tube (Prado *et al.*, 2004; Prado *et al.*, 2008).

Although we have an increasingly detailed understanding of the molecular players that are involved in determining cellular polarity in the pollen tube, in order to understand how the rapidly growing tube changes growth direction in response to an external signal it is important to also look at the mechanics determining the unidirectional growth behavior. The greatest rate of surface expansion at the tip of the tube is ensured by the precisely targeted delivery of soft cell wall material to this spot. A shift in the growth direction must thus be achieved through vesicle delivery towards a region that is located off the central axis of the tube. The mechanism that spatially controls this delivery process should therefore be at the center of attention when trying to understand the mechanism of the tropic growth response.

Vesicle delivery relies on the myosin mediated propulsion of these cellular organelles along actin filaments. Both the myosin-regulated motion as well as the dynamics of the guiding actin-array are therefore potential regulators of the spatial targeting. Plant myosins are activated by calmodulin binding and inactivated by Ca^{2+}-induced calmodulin dissociation (Vidali and Hepler, 2001). This mechanism might be crucial in the final step of vesicle delivery - the detachment of the vesicle from the actin cytoskeleton in the vicinity of the apical plasma membrane. Given that the cytoplasmic calcium concentration is elevated at the region of exocytosis, an

important regulatory function of this ion might be to allow vesicles to be released from the actin rails into the actin filament free apical region or directly onto the plasma membrane.

To decipher the causal relationships between actin dynamics, vesicle motion and directional growth control, it is useful to be able to trigger changes in growth direction in pollen tubes growing *in vitro*. *In vitro* experiments achieving a redirection of growth have elegantly been done by exposing the tubes to chemical signals (Higashiyama and Hamamura, 2008). However, to successfully achieve redirection using a precisely timed external signal, *in vitro* growing pollen tubes were exposed to electrical fields. The reorientation was postulated to be mediated by ion fluxes in the medium (Malhó *et al.*, 1992). The amplitude of the observed response depends on the calcium concentration in the medium (Nakamura *et al.*, 1991). The importance of ion fluxes in determining growth direction was further emphasized by the finding that the release of injected caged calcium on one side of the pollen tube cytoplasm caused a redirection of the pollen tube growth towards the triggered location (Malhó and Trewavas, 1996). While ion fluxes are undisputedly crucial for pollen tube growth and orientation, it is important to note that by themselves, ions cannot act directly on the direction of cellular growth. Their effect is mediated by structural features such as the cytoskeleton and the synthesis and delivery of new cell wall material.

1.7 The cytoskeleton in the pollen tube

While many studies have been done on the animal cell cytoskeleton and its role in cellular extension, motility, and architecture (Pollard and Borisy, 2003; Pollard and Cooper, 2009), little is known about the mechanical role of the cytoskeletal elements in the control of plant cellular architecture. Focus has hitherto been on the implication of microtubules in anisotropic cell wall expansion (Baskin,

2005; Bisgrove, 2008). The reason for this scarcity of information on cytoskeletal mechanics in plants is that the relationship between turgor pressure and cell wall has been considered to be the dominant player determining plant cell growth in general and pollen tube tip growth in particular (Geitmann and Steer, 2006). Therefore, while the role of the cytoskeleton in vesicle and organelle transport within the pollen tube cytoplasm is well defined (Lovy-Wheeler *et al.*, 2007), its implication in the mechanics of the tip growth process is poorly understood.

The pollen tube cytoskeleton has two main components, the microtubules composed of tubulin dimers and the microfilaments composed of actin monomers (Geitmann and Emons, 2000; Wasteneys and Galway, 2003). Microtubules do not seem to be directly involved in pollen tube tip growth, since inhibition of their polymerization does not prevent pollen tube elongation (Gossot and Geitmann, 2007). However, a pollen specific α-tubulin has been shown to be responsible for pollen tube growth through the oriented deposition of cell wall material at the apex of gymnosperm and *Arabidopsis* pollen tubes (Yu *et al.*, 2009). Actin on the other hand is crucial as revealed by inhibitors that interfere with actin polymerization and consequently pollen tube growth (Vidali and Hepler, 2001). It has been shown that microfilaments play a role in the capacity of pollen tubes to invade a mechanical obstacle and to elongate in stiffened media (Gossot and Geitmann, 2007). Actin filaments in the pollen tube are oriented longitudinally, parallel to the growth axis and they form a fringe of fine filaments in the subapex of the tube (Geitmann and Emons, 2000; Lovy-Wheeler *et al.*, 2005) (Figure 1.2). This fringe coincides with a cytoplasmic alkaline region (Feijó *et al.*, 1999) and was suggested to be formed and maintained by the combination of the severing activity of ADF (actin depolymerizing factor) under high pH conditions and the bundling activity of villin (Cardenas *et al.*, 2008). The actin filaments are polarized in the pollen tube, with the barbed ends pointing towards the apex at the periphery of the cell and away from the apex at the center (Lenartowska and Michalska, 2008). Since myosins move from the pointed (minus) to the barbed (plus) ends on actin, this bidirectional filament polarity

imposes vesicle and organelle movement to be oriented forward in the periphery of the tube and backward in its center (Figure 1.3).

Many proteins are able to bind to the cytoskeletal arrays and either modify their length or stability or form links with other proteins that are responsible for organelle movement or membrane attachment. The majority of these proteins are tissue specific and/or cargo specific. These include the actin binding proteins (ABPs) and the microtubule associated proteins (MAPs). These proteins interact with regulatory kinases, phosphatases, and phosphoinositides. They also bind and release nucleoside phosphates, Ca^{2+}, and other ions (Wasteneys and Galway, 2003). ABPs are responsible for the organization of the cytoskeleton in response to various internal and external signals. These signal-induced cytoskeletal changes may subsequently lead to altered cell functioning, behavior or structure. Among the best characterized ABPs in plants are profilins (Vidali and Hepler, 1997; Gibbon, 2001; Vidali and Hepler, 2001). Profilins are uniformly distributed in the cytoplasm of the pollen tube and they are responsible for sequestering most of the G-actin. They therefore have a buffering function that reduces the formation of spontaneous filaments. The actin-sequestering effect of profilins is optimal at elevated calcium concentrations since the ability of profilin-Ca^{2+}ATP-actin to attach to actin filaments ends is reduced (Kovar *et al.*, 2000). Since the calcium concentration at the pollen tube tip is high, profilin action might be responsible for the absence of prominent actin bundles in this region.

Arp2/3 is a profilin binding complex expressed in pollen tubes. It has an actin polymerization and branching activity. However, this mechanism has not been yet observed in pollen tubes (Cheung and Wu, 2008). Another group of proteins that interact with profilins in a yeast two-hybrid system are the formins (Banno and Chua 2000). This latter group is believed to be the main controller of actin polymerization in plant cells (Wasteneys and Yang, 2004; Michelot *et al.*, 2005). Actin depolymerizing factor (ADF) is a pH sensitive ABP (Carlier *et al.*, 1997). It uses

ATP hydrolysis in actin assembly to enhance filament dynamics (Gungabissoon *et al.*, 1998) by facilitating the loss of subunits from the pointed ends. Therefore, it creates a high rate of treadmilling (Bamburg, 1999) which is important for pollen tube growth (Chen *et al.*, 2002; Chen *et al.*, 2003). When moderately expressed in tobacco pollen tubes, GFP-labelled NtADF1 targets the actin fringe and the long cables in the shank of the tubes, while its overexpression causes a reduction in the number of actin cables and an inhibition of pollen tube growth (Chen *et al.*, 2002). The fact that its activity is enhanced by alkaline conditions may explain the high actin filament dynamics in the actin fringe zone. ADF phosphorylation (and therefore inactivation) is carried out on a conserved serine residue by a Ca^{2+}-dependent protein kinase, whose activity is probably dependent on the (plant Rho GTPase) ROP GTPase signaling system (Chen *et al.*, 2003; Wasteneys and Galway, 2003). Villin is a factor responsible for bundling actin filaments in pollen tubes, and may also play a key role in determining the direction of cytoplasmic streaming (Tominaga *et al.*, 2000). It is a Ca^{2+} dependant ABP and may participate in F-actin fragmentation and nucleation in the apex of the pollen tube (Vidali *et al.*, 1999).

Members of the family of Rho-related GTPases (ROP GTPases) play an important role in polarized tip growth due to their impact on actin dynamics (Smith and Oppenheimer, 2005). ABPs are the downstream targets of the ROP GTPase. Inhibition of ROP function by injecting antibodies in the cytoplasm results in a growth arrest of the pollen tube and a downregulation of the Ca^{2+} gradient (Lin and Yang, 1997) while the overexpression of these GTPases causes excess F-actin polymerization. This demonstrates the importance of these proteins in actin filament organization and F-actin assembly as well as in Ca^{2+} influx. In fact, F-actin assembly and Ca^{2+} influx have been shown to be separate functions of ROP that are mediated by different RIC (ROP-interacting CRIB domain) effector proteins (Gu *et al.*, 2005) and whose overexpression in tobacco pollen tubes causes a swelling and therefore a loss of polarity at the pollen tube apex (Klahre and Kost, 2006). By mediating the external signal to the actin cytoskeleton through ADF, ROP GTPases are believed to

contribute to the fine regulation of actin dynamics allowing growth and reorientation of the pollen tube (Chen *et al.*, 2003).

While the role of the actin cytoskeleton in vesicle and organelle transport within the pollen tube cytoplasm is well defined (Lovy-Wheeler *et al.*, 2007; Bove *et al.*, 2008), its implication in the mechanics of the tip growth process is poorly understood. The inhibition of pollen tube elongation using agents that block actin polymerization such as profilin, DNAse I, cytochalasin D and latrunculin B is achieved at concentrations lower than those needed to block cytoplasmic streaming (Geitmann and Emons, 2000; Vidali and Hepler, 2001). This shows that actin polymerization is intimately connected with the mechanical process of pollen tube elongation. This is further corroborated by the finding that microfilaments play a role in the capacity of pollen tubes to invade a mechanical obstacle and to elongate in stiffened media (Gossot and Geitmann, 2007).

1.8 Calcium plays key roles during different aspects of pollen tube growth

The configuration of the actin cytoskeleton, the dynamics of its remodeling through polymerization, cross-linking, and bundling are controlled by the cytoplasmic Ca^{2+} and H^{+} concentrations through activation and inactivation of actin binding proteins. Ca^{2+} also plays a role in exocytosis and vesicle-membrane fusion at the apex of the pollen tube (Battey *et al.*, 1999; Camacho and Malhó, 2003; Coelho and Malhó, 2006). A supply of Ca^{2+} in the growth medium is, therefore, indispensable for pollen germination and pollen tube growth (Brewbaker and Kwack, 1963; Picton and Steer, 1983; Pierson *et al.*, 1994; Li *et al.*, 1999; Chebli and Geitmann, 2007). For normal pollen tube growth to happen, the *in vitro* growth medium needs to be supplemented with a calcium concentration that is situated within a certain range (Brewbaker and Kwack, 1963; Picton and Steer, 1983; Holdaway-Clarke and Hepler, 2003). This optimal concentration varies between

species (Steer and Steer, 1989). Reflecting the polarized distribution of growth activity and actin configuration in this cell, the cytoplasmic Ca^{2+} concentration displays a steep, tip high gradient (Feijó *et al.*, 1995; Pierson *et al.*, 1996) (Figure 1.4), disruption of which causes the arrest of pollen tube growth (Pierson *et al.*, 1994). The connection between the actin cytoskeleton and calcium is a two-way control mechanism, however, since actin microfilaments were shown to play an important role in the regulation of plasma membrane located Ca^{2+} channels and thus the Ca^{2+} influx into the cell (Wang *et al.*, 2004; Cardenas *et al.*, 2008). The direct link between Ca^{2+} influx and resulting cytosolic gradient on the one hand and pollen tube growth rate on the other is demonstrated by the fact that both are temporally and spatially correlated. Oscillatory changes in the growth rate are accompanied by temporal changes in Ca^{2+} flux and steepness of the gradient (Messerli and Robinson, 1997; Messerli *et al.*, 2000). Artificial displacement of the cytoplasmic calcium gradient to one side of the growing pollen tube apex induces the tube to change direction (Malhó and Trewavas, 1996). Whether this is due to a remodeling of the apical actin cytoskeleton or to a direct effect on the location of exocytosis is unknown. A calcium sensitive vibrating electrode has been used to reveal calcium influx into the pollen tube (Kühtreiber and Jaffe, 1990; Pierson *et al.*, 1994). Calcium channels have been proposed to be present in both pollen tubes (Holdaway-Clarke and Hepler, 2003; Qu *et al.*, 2007) and pollen grains (Dutta and Robinson, 2004; Shang *et al.*, 2005). In the tube they are active at the apex (Pierson *et al.*, 1994; Pierson *et al.*, 1996) thus being responsible for calcium influx into the cell.

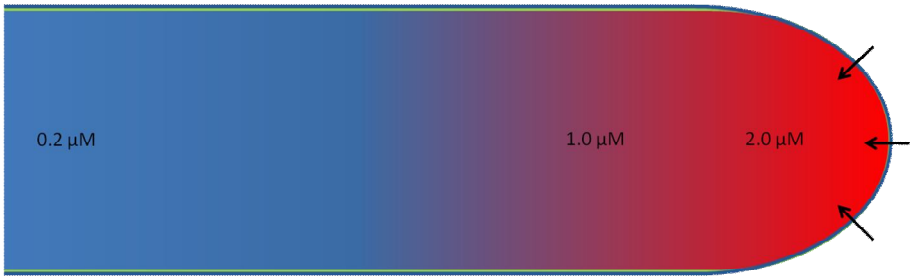

Figure 1.4: Schematic representation of calcium distribution in lily pollen tube adapted from (Pierson *et al.*, 1996). A tip to base calcium gradient is established after calcium influx (arrows) with the highest concentration being at the tip of the pollen tube. These concentrations may vary between species.

The tip-focused gradient of cytosolic calcium and the polymerization of tip-localized F-actin are two processes controlling vesicle delivery. They might also be involved in pollen tube polarity (Fu *et al.*, 2001; Higashiyama *et al.*, 2003). External calcium gradients are believed to affect pollen tube tropism *in vivo* because of their presence along the transmitting tissue of the flower (Ge *et al.*, 2009). A better understanding of the connection between the calcium gradient in the cell and the pollen tube reorientation through the actin cytoskeleton reorganization will allow us to explain how the pollen tube is able to perceive the directional signals and change its direction of growth.

1.9 Objectives

The main focus of my PhD project was to elucidate the function of the cytoskeleton in the highly active anisotropic growth process of pollen tubes. The role of actin filaments in the control of pollen tube shape, growth, and direction were studied. Pollen from three plant species served as model systems for my project: *Arabidopsis thaliana* (*Arabidopsis*), *Camellia japonica* (*Camellia*) and *Lilium longiflorum* (lily). The reason for using *Arabidopsis* is the ease of plant cultivation, the production of flowers in a short period of time (4 weeks under appropriate conditions), and most importantly, the ready access to sequence data and the ease of transformation and production of transgenic lines. Pollen tubes from *Camellia* on the

other hand, are much larger than those of *Arabidopsis*, and their growth behavior under *in vitro* conditions is more reproducible, faster and straighter. Therefore, mechanical experiments were based on cells from this species. Lily has a well studied and characterized actin cytoskeleton and therefore served as my reference for any comparative study at this level. In addition to this, lily pollen can be relatively easily transformed by particle bombardment.

The pollen tube is an ideal experimental system to study the role of the actin cytoskeleton in plant cell growth in general and in the targeting of secretory vesicles to an expanding cellular surface in particular. My project focuses on the following objectives

1- Characterization of the role of the actin cytoskeleton in
    a. the elongation by tip growth,
    b. the maintenance of the tubular shape, and
    c. the tropic behaviour of the growing tube.
2- Determination of the role of calcium ions in the regulation of these processes.
3- Identification of pollen-specific members of the ADF-family, key actin binding proteins during gametogenesis, germination and elongation of the pollen tube.

Necessary prerequisites for these objectives were the following three items that led to a series of preliminary studies:

A- Optimization of *in vitro* growth conditions for *Arabidopsis* and *Camellia* pollen.
B- Optimization of labeling conditions for visualization of the actin cytoskeleton in pollen tubes.
C- Optimization of microwave assisted protocols for faster and more efficient chemical fixation and labeling.

2 Optimization of conditions for germination of cold stored *Arabidopsis thaliana* pollen

One of the rare weak points of the model plant *Arabidopsis* is the technical problem associated with the germination of its male gametophyte and the generation of the pollen tube *in vitro*. It is generally agreed upon that existing protocols are highly unsatisfactory as they do not allow the generation of reproducible percentages of germination, even within a single batch of pollen. Together with my colleague Youssef Chebli we undertook a systematic study to optimize the growth conditions for different experimental approaches. We optimized the germination conditions for *Arabidopsis* pollen that had been freeze stored. The most important differences with previously published *Arabidopsis* pollen growth media (Boavida and McCormick, 2007) are the fact that we used cold-stored pollen (vs. freshly harvested) that was bulk collected (vs. collection from selected, recently opened flowers), and that we determined ideal long-term storage conditions and times. Our optimized protocol differed significantly from that by Boavida and McCormick (Boavida and McCormick, 2007). We also describe how the conditions can be optimized for different experimental setups. In our manuscript we suggest how to optimally use these methods for different practical experiments ranging from morphological observations of pollen tubes in optical and electron microscopy to their bulk use for molecular and biochemical analyses or for experimental setups for which a specific medium stiffness is critical. Contrary to the Boavida and McCormick protocol, our optimized medium allows germination of *Arabidopsis* pollen at a temperature of 4°C, a very important requirement for observation of pollen germination in an environmental scanning electron microscope.

Our manuscript with the title "Optimization of conditions for germination of cold stored *Arabidopsis thaliana* pollen" was published in 2009 in Plant Cell Reports volume 28, number 3, pages 347 - 357.

Optimization of Conditions for Germination of Cold Stored *Arabidopsis thaliana* Pollen

Firas Bou Daher*, Youssef Chebli*, Anja Geitmann

*These authors contributed equally to the work

Abstract

One of the rare weak points of the model plant *Arabidopsis* is the technical problem associated with the germination of its male gametophyte and the generation of the pollen tube *in vitro*. *Arabidopsis* pollen being tricellular has a notoriously low i*n vitro* germination compared to species with bicellular pollen. This drawback strongly affects the reproducibility of experiments based on this cellular system. Together with the fact that pollen collection from this species is tedious, these are obstacles for the standard use of *Arabidopsis* pollen for experiments that require high numbers of pollen tubes and for which the percentage of germination under control conditions need to be highly reproducible. The possibility of freeze storing pollen after bulk collection is a potential way to solve these problems but necessitates methods that ensure continued viability and reproducible capacity to germinate. Our objective was the optimization of germination conditions for *Arabidopsis* pollen that had been freeze stored. We optimized the concentrations of various media components conventionally used for *in vitro* pollen germination. We found that in general 4 mM calcium, 1.62 mM boric acid, 1 mM potassium, 1 mM magnesium, 18% sucrose at pH 7 and a temperature of 22.5°C are required for optimal pollen germination. However, different experimental setups may deviate in their requirements from this general protocol. We suggest how to optimally use these optimized methods for different practical experiments ranging from morphological observations of pollen tubes in optical and electron microscopy to their bulk use for molecular and biochemical analyses or for experimental setups for which a specific medium stiffness is critical.

Key Words

Arabidopsis thaliana - in vitro cell culture - pollen germination - pollen tube

2.1 Introduction

In the last two decades, *Arabidopsis thaliana* has evolved as an extremely useful organism for studying a wide range of issues in plant biology. This species gained even more importance and became the main tool for plant cellular and molecular biology studies after the publication of "The *Arabidopsis* Genome Initiative" (The Arabidopsis Genome Initiative, 2000). It is therefore astonishing that since that date, less than 5% of the PubMed-listed publications on research performed on the male gametophyte of flowering plants have used *Arabidopsis* pollen. Pollen is a widely used cellular system that on one hand is studied to better understand the reproduction process in flowering plants, and on the other hand is used to investigate the principles governing plant cell growth in general. The latter is due to the fact that the pollen tube, a cellular protrusion formed from the pollen grain, elongates extremely rapidly with the purpose of delivering the sperm cells to the ovule. Very conveniently for the researcher, pollen germination and the generation of the pollen tube can be achieved *in vitro,* thus offering an excellent opportunity to observe the processes associated with plant cell growth, cell wall synthesis and intracellular transport in a single cell system.

While microscopic observations are often carried out on few individual cells, other experimental approaches require large amounts of material. Myosin extraction from lily pollen tubes (Yokota and Shimmen, 1994), RNA isolation for transcriptional profiling and gene expression in pollen grains and pollen tubes (Guyon *et al.*, 2000; Becker *et al.*, 2003), and vesicle isolation for biochemical and ultrastructural characterization from germinated lily pollen (van der Woude *et al.*, 1971) and require large amounts of pollen as a starting material. From the need for substantial amounts of *Arabidopsis* pollen material implicated in this type of experiment ensued the necessity to optimize a method for long term storage that would allow pooling pollen from several harvests.

The principal problem associated with large quantity pollen harvest in *Arabidopsis* is the minute size of its flower (1 mm), the resulting low number of pollen grains per flower, as well as the small size of the individual pollen grain. A comparison to other plant species illustrates this point. To obtain the same amount of pollen in weight collected from a single flower of *Camellia*, pollen from approximately 115 000 plants of *Arabidopsis* needs to be harvested, or, in other words, that of more than one million flowers. To automate bulk pollen collection of *Arabidopsis*, Johnson-Brousseau and McCormick (2004) developed a method using a modified vacuum cleaner equipped with three different meshes that has proven to be very useful. Nevertheless, harvesting the mounts of material necessary for biochemical experiments remains time-consuming.

Not only is pollen harvest from *Arabidopsis* comparably tedious, experimentation on germinating pollen is rendered challenging by the fact that *in vitro* germination is notoriously irreproducible in this species. It is generally agreed upon that existing protocols are highly unsatisfactory as they do not allow the generation of reproducible percentages of germination, even within a single batch of pollen. One reason for this may be that *Arabidopsis* pollen is tricellular for which *in vitro* percentages of germination is reduced compared to bicellular species (Brewbaker and Kwack, 1963; Taylor and Hepler, 1997). Moreover, the 6 stamens of the *Arabidopsis* flower form two distinct groups which mature at different times (Smyth *et al.*, 1990), causing a difference in the degree of maturity between the two types of pollen harvested from a single flower (Johnson-Brousseau and McCormick, 2004). It was also reported that mature pollen grains undergo autolysis in *Arabidopsis thaliana* after anthesis favoring autopolination (Yamamoto *et al.*, 2003). This may be an additional factor responsible for the low germination rate *in vitro*.

The need for significant amounts of material associated with certain experimental strategies could be met easier if pollen could be stored without the significant loss of viability or germination capacity. The pollen of many plant species

can be dried on silica gel and stored at -20°C or -80°C to maintain its ability to germinate after several years. Hitherto, this method did not seem to be very successful for *Arabidopsis* pollen. Here we investigated the effect of cold storage on pollen germination and we optimized several parameters of the growth conditions to allow for optimal percentage germination of frozen stored pollen.

Various *Arabidopsis* pollen germination media have been proposed in the literature (Sanders *et al.*, 1999; Fan *et al.*, 2001; Boavida and McCormick, 2007), their principal ingredients comprise calcium, boric acid, magnesium, potassium and sucrose, components that are generally found in pollen germination media at varying concentrations. In addition to these elements, the pH of the medium and the growth temperature are two major factors affecting percentage germination and growth (Boavida and McCormick, 2007; Chebli and Geitmann, 2007).

Here we describe protocols for germination of frozen stored *Arabidopsis thaliana* pollen grains that contain optimized concentrations of these ingredients. In addition, we provide standardized methods for pollen germination and growth in different experimental setups including liquid and solid medium, low and high quantity approaches. These methods are useful for different kinds of studies ranging from morphological observations in electron or optical microscopy (cell wall and cytoskeleton labeling, live observation of vesicle trafficking, monitoring of ion gradients) to the bulk use for molecular and biochemical analyses.

2.2 Materials and methods

2.2.1 *Arabidopsis thaliana* growth and pollen harvest

Arabidopsis thaliana ecotype Columbia 0 plants were grown in trays in a glasshouse at 22°C day temperature and 20°C night temperature, 50% humidity under 16h daylight and 300 µE m^{-2} s^{-1} light intensity. Approximately 150 seeds (prepared by mixing 50 mg of seeds in 40 mL of 0.1% agar in water to avoid seed

clumps) were sown per plate. The mixture was then uniformly dribbled on the soil surface. Plants were irrigated each day and fertilized every second day with Plant-Prod® 20-20-20 fertilizer at 200 ppm. Pollen was collected every day from the time flowers bloomed using a modified vacuum cleaner as described by Johnson-Brousseau and McCormick (Johnson-Brousseau and McCormick, 2004). Briefly, using plumbing fittings, three different sized Lab Pak® nylon meshes (80, 35 and 5µm) were fixed in sequence on a plastic pipe which was then related to a 700 W Shark® vacuum cleaner. Pollen was collected by passing the modified plastic pipe over the *Arabidopsis* flowers with gentle shaking.

2.2.2 Storage of pollen grains

Pollen was removed from the 35 and the 5 µm nylon meshes and used directly or stored in 1.5 ml microfuge tubes. Unless noted otherwise, pollen was dried on silica gel for 2 hours at room temperature prior to cold storage at either -20°C or at -80°C.

2.2.3 Pollen grain rehydration

Pollen was rehydrated before each experiment. For this purpose, after removal from the freezer, pollen was placed in a humid chamber for 30 minutes at room temperature. Care was taken not to let the grains get in direct contact with liquid water.

2.2.4 Germination media

For all experiments, unless specified elsewhere, two different versions of the growth medium were used for pollen germination; a liquid version and a solid version containing 0.5% agar (SIGMA A1296). Unless specified otherwise, the germination medium contained 18% sucrose, 0.01% (1.62 mM) boric acid, 1 mM $CaCl_2$, 1 mM $Ca(NO_3)_2$, 1 mM $MgSO_4$, and 1 mM KCl with a pH adjusted to 7. For solid medium preparation, agar was added to the mix and heated to dissolve.

For comparison, the following media tested were used with a modified concentration of sucrose (18% instead of the concentration originally published): Brewbaker and Kwack (BK) medium (Brewbaker and Kwack, 1963), Lily pollen germination medium (Parre and Geitmann, 2005). The media that were used exactly as published had originally been developed by the following groups: Wu and coworkers (Fan *et al.*, 2001), Yang and coworkers (Sanders *et al.*, 1999), and McCormick and coworkers (Boavida and McCormick, 2007).

2.2.5 Experimental setups

2.2.5.1 Pollen germination on a drop of liquid medium

200 µL liquid growth medium was placed on a microscope slide forming a dome shaped drop. Hydrated pollen grains were sprinkled on top of the drop using a fine brush. The slides were placed in a humid chamber to avoid dehydration of the medium.

2.2.5.2 Pollen germination in liquid medium in Erlenmeyer flasks

3 mL liquid growth medium were put in a 25 mL Erlenmeyer flask. Hydrated pollen grains were mixed with the medium by vigorous shaking to avoid clump formation. Two or three whole *Arabidopsis* flowers were added to the medium unless specified otherwise. The Erlenmeyer flasks were covered with a Parafilm® layer containing small holes and placed on a shaker at 70 rpm.

2.2.5.3 Pollen germination on solid surface

Hot agar containing medium was poured onto a microscope slide to form a layer with a thickness of about 0.5 mm and left to cool. Hydrated pollen was then sprinkled on the surface using a fine brush. The slides were placed in a humid chamber.

2.2.5.4 Pollen germination in solid medium

Solid medium was prepared as described above and left to cool to 42°C. Hydrated pollen grains were rapidly mixed with the medium by vigorous stirring. The medium was then poured onto a microscope slide to form a layer with a thickness of about 0.5 mm and placed in a humid chamber.

Unless specified otherwise, subsequent incubations were carried out at 22.5°C. Temperature control was ensured by placing the samples in a Sanyo® MIR-153 incubator. Images were taken at 2, 4 and 6 hours after the beginning of incubation.

2.2.6 Viability test

Pollen grain viability was assessed using fluorescein diacetate (FDA) which was dissolved in acetone at 10 $mg.mL^{-1}$ and stored at -20°C. Prior to each experiment, FDA was diluted in a 10% sucrose solution to a final concentration of 0.2 $mg.mL^{-1}$. Hydrated pollen was dipped in 250 µL of the FDA solution on a glass slide and kept in the dark for 5 minutes. Observations were made with a Zeiss Imager-Z1® microscope with excitation light at 470 nm and a 515-565 nm band pass emission filter. Only viable pollen grains emit a fluorescence signal under these conditions.

2.2.7 Microscopy

Samples were observed either with a Zeiss Imager-Z1 microscope equipped with a Zeiss AxioCam MRm Rev.2 camera and AxioVision Release 4.5 software or with a Nikon Eclipse TE2000-U inverted microscope equipped with a Roper fx cooled CCD (charged coupled device) camera and ImagePro (Media Cybernetics, Carlsbad, CA) software.

2.2.8 Determination of the germination, growth rate and pollen tube length

For each experiment, at least ten images per sample were taken at random positions and the percentage of germination was quantified. Pollen grains were considered germinated when the pollen tube length was greater than the diameter of the pollen grain (Tuinstra and Wedel, 2000). To determine pollen tube length, at least fifty tubes were measured for each experiment.

2.3 Results and Discussion

2.3.1 Influence of storage conditions on pollen grain viability

Tests using FDA that fluoresces under UV in living cells (Schnurer and Rosswall, 1982) revealed a decrease in pollen viability with duration of cold storage. While 80% viability was observed for fresh pollen or pollen stored at -20°C for 24h only, this percentage decreased to 12% for pollen stored for 10 months with the most significant drop occurring at approximately 6 months (Figure 2.1). Storage temperature (-20°C versus -80°C) did not affect pollen viability differently. At both temperatures viability was around 60% for pollen grains stored for 2 to 5 months (Figure 2.2). To ensure satisfactory germination of cold stored pollen, we therefore suggest using up frozen stored *Arabidopsis* pollen within a 5 month period.

2.3.2 Effect of storage conditions on germination

In order to be able to pool pollen from different harvests for analyses requiring significant amounts of material, the optimization of storage conditions is pivotal. Generally, drying pollen before freeze storing is advantageous and therefore we tested different times for drying of *Arabidopsis* over silica gel. Drying for 24h reduced the percentage of germination of the pollen before freezing by approximately 20%, whereas pollen dried for 2h had the same percentage of

germination as fresh, non-dried pollen. We therefore used the 2h drying period for all subsequent pollen batches.

We then examined the effect of prolonged freeze storage at -20°C on germination. Our data reveal that during the first 5 months of freeze storage the percentage of germination does not decrease significantly compared to fresh pollen. However, after this time the percentage of germination decreased to be below 10% by the time pollen had been in storage for 10 months or longer. These data are consistent with the decrease in pollen viability observed for the same period of time (Figure 2.2).

In contrast to pollen viability, storage temperature strongly affected pollen germination. The percentage of germination of pollen stored at -80°C for four months was 11% while that of pollen of the same age stored at -20°C was 40%. The latter is therefore clearly a preferable temperature for storing *Arabidopsis* pollen - contrary to other species such as lily whose germination activity is conserved very well at the lower temperature. Even though the percentage of germination was lower for pollen stored at -80°C, we observed that this percentage was maintained for periods exceeding one year. This loss of the ability to germinate may in part be due to lysosomal degradation of the cytoplasmic components that is characteristic for *Arabidopsis thaliana* pollen grains (Yamamoto *et al.*, 2003).

2.3.3 Optimization of medium composition for the germination of frozen stored pollen in various experimental setups

In different experimental setups pollen is exposed to different conditions, such as availability of oxygen, that might influence its requirement for the individual elements present in the germination medium. We therefore optimized the concentrations for four different experimental setups:

1. **Liquid drop**: pollen is mixed with liquid medium forming a drop of 180 µl placed on a microscope slide.

2. **Bulk germination in liquid** (Erlenmeyer): pollen is mixed with 3 ml liquid medium in an Erlenmeyer flask.

3. **On solid surface**: pollen is sprinkled onto the surface of an agar-stiffened layer of medium.

4. **Within solid medium**: pollen is mixed into an agar-stiffened medium prior to gelation.

We used a concentration series for each of the components in the liquid germination medium and assessed the percentage of germination at 2, 4, and 6 hours after incubation for each of the experimental setups. While different pollen batches were used for different experiments (thus resulting in different percentages of germination for the control samples), pollen with identical storage durations were used for all the samples of an individual series of experiments. Table 2.1 summarizes the optimized concentrations. In the following we discuss some of the results in more detail.

2.3.3.1 Calcium

The presence of Ca^{2+} in the growth medium is known to be required for *in vitro* pollen germination and tip growth of most plant species (Brewbaker and Kwack, 1963; Picton and Steer, 1983; Sanders *et al.*, 1999; Chebli and Geitmann, 2007). It plays a role in cell wall formation and rigidity, directs vesicle trafficking, controls actin dynamics (Chebli and Geitmann, 2007) and was also found to affect the period and amplitude of growth rate oscillations (Geitmann and Cresti, 1998; Holdaway-Clarke and Hepler, 2003). Normal pollen tube growth can only take place in the presence of a calcium concentration that is situated within a certain range (Brewbaker and Kwack, 1963; Picton and Steer, 1983; Holdaway-Clarke *et al.*, 2003) that varies between species (Steer and Steer, 1989). Within this range, pollen tube tip extension rates are relatively insensitive to small changes in the calcium

concentration (Picton and Steer, 1983), whereas outside of this range, growth is severely hampered.

We used different calcium concentrations, 0 mM, 2 mM, 4 mM and 10 mM. These are the total concentrations of calcium in the medium resulting from the equimolar addition of two different sources of calcium: calcium chloride and calcium nitrate. We found that growth in liquid medium (setups 1 and 2) was optimal at 4 mM Ca^{2+} and could not be enhanced further by higher concentrations, whereas growth in solid medium was augmented by 10 mM calcium compared to 4 mM (Figure 2.3). Pollen tubes growing on the surface of solid medium (setup 3) required only 2 mM of calcium for optimal germination that was not enhanced or inhibited by higher concentrations up to 10 mM (Figure 2.4). In all three cases the optimal percentage of germination was approximately 40%. The difference in calcium requirement between the experimental setups might be due to oxygen availability affecting the metabolism of the pollen tube since oxygen is more readily available for pollen growing on the surface of a solid medium than in liquid or in solid medium.

In all three experimental setups we observed the presence of germinated pollen in the control samples devoid of added calcium. Percentages of germination in these "calcium-free" samples were up to 22% on the surface of solid medium. The addition of EGTA (ethylene glycol tetraacetic acid) at a concentration of 0.1 and 0.2 mM to quench any contamination with calcium did not reduce the percentage of germination (data not shown). Similar observations were made for *Tradescantia virginia* pollen upon Ca^{2+} quenching with EGTA (Picton and Steer, 1983). This may be explained with the presence of a stock of calcium already present in or on the surface of the pollen grains.

Since the two sources of calcium in the medium contained chloride and nitrate ($CaCl_2$ and $Ca(NO_3)_2$), changing the calcium concentration also changed Cl^- and NO_3^- concentrations. To ensure that the observed effects were only related to variations in the calcium concentration and not to the alterations in chloride and/or

nitrate content, we increased the concentrations of these two ions to match those in the 10 mM Ca^{2+} sample using hydrochloric acid and nitric acid. Results showed that there were no significant differences between the controls (pollen tubes germinating without addition of Cl^- and NO_3^-) and the respective media containing the increased amounts of chloride and nitrate ions (Figure 2.4). From this we conclude that the effect observed under different calcium concentrations was only due to the variations in the concentration of calcium ions.

2.3.3.2 Boron

In the pollen tube, boron is involved in cell wall formation and protein assembly into membranes and cell wall (Blevins and Lukaszewski, 1998). Through its effect on H^+-ATPase activity, boron affects pollen germination, tube growth (Feijó *et al.*, 1995; Wang *et al.*, 2003) and oscillation behavior (Holdaway-Clarke *et al.*, 2003). 100 ppm boric acid was found to be essential for pollen germination (Brewbaker and Kwack, 1963). In *Picea meyeri*, boron deficiency decreases pollen germination and affects callose and non-esterified pectin accumulation on the cell wall (Wang *et al.*, 2003).

Five different concentrations of boric acid (0 mM, 0.49 mM, 1.17 mM, 1.62 mM and 3.24 mM) were used. Germination of pollen growing on the surface of solid medium (setup 3) was the highest for 1.62 mM of boron whereas higher concentrations were inhibitory (Figure 2.5A). In liquid media (setups 1 and 2) the highest percentage of germination was obtained for concentrations as low as 0.49 mM (Figure 2.5B). Similar results were observed in *Picea meyeri* where 0.01% boric acid (1.62 mM) yielded optimal germination and higher concentrations were detrimental for pollen tube germination (Wang *et al.*, 2003). One possible reason for why higher boron concentrations are required for optimal germination when using a solidified medium is that the boron may be sequestered by the agar molecules (residues of algal cell walls).

2.3.3.3 Potassium

Many pollen species such as lily and *Solanum* require potassium for optimal *in vitro* germination, perhaps due to its possible involvement in the initiation of the osmotic water influx required for pollen germination (Fan *et al.*, 2001). The effect of potassium on growth was proposed to be in the maximization of the association of the calcium ions to the cell wall (Brewbaker and Kwack, 1963). In *Arabidopsis*, a potassium channel has been shown to be present in pollen protoplast membrane (Fan *et al.*, 2001) and its mutation reduces the growth of pollen tubes (Mouline *et al.*, 2002). Therefore, we investigated whether or not varying the concentration of potassium in the medium influences pollen germination in *Arabidopsis*.

Different concentrations ranging between 0 mM and 10 mM of potassium chloride were tested. Results showed that in liquid growth medium (setups 1 and 2), potassium concentrations of 1 mM or higher increased the percentage of germination by more than 30% whereas this increase was more than 60% in solid medium (setups 3 and 4). No inhibitory effect was observed for higher concentrations of potassium (Figure 2.6).

2.3.3.4 Sucrose

Since the pollen tube does not perform photosynthesis, a carbon source is required for energy supply and carbohydrate skeleton formation. Therefore, sucrose is generally added to pollen germination media, but the optimal concentration varies greatly between species. For instance, optimal *Papaver* pollen growth *in vitro* occurs at 5% sucrose, *Camellia* at 8%, *Lilium* and *Solanum* at 10% (unpublished data). While it was previously observed that sucrose concentrations higher than 15% reduced or prevented *Arabidopsis* pollen germination (Boavida and McCormick, 2007), we tested concentrations of sucrose ranging from 0 to 25%. For our optimized medium, 18% sucrose yielded the highest percentage germination (50%) regardless of the stiffness of the medium (Figure 2.7). This percentage was significantly

reduced when sucrose concentration was outside the optimal range of 15 to 20%. In addition to lowering the percentage germination, higher sucrose concentrations reduced pollen tube elongation (Figure 2.8). The requirement for relatively high sucrose concentration for *Arabidopsis* pollen when compared to other species might be related to the fact that this species has a dry stigma (Elleman *et al.*, 1992; Zinkl and Preuss, 2000) thus providing an environment with high osmolarity. *Arabidopsis* culture medium with 18% sucrose might provide the environment that is closest to the situation *in planta*.

2.3.3.5 pH

Medium pH is a critical condition for *in vitro* pollen tube growth. For *Lilium*, *Solanum* and *Camellia* pollen tubes, the optimum pH is situated between 5 and 6. Lower or higher pH values drastically reduce the percentage of germination and are unable to sustain pollen tube growth (Chebli and Geitmann, 2007). To optimize the pH for *Arabidopsis*, we tested different values: 5, 6, 6.8, 7 and 8. Adjustment of the pH was made immediately prior to each experiment. For solid media, pH was adjusted prior to the addition of agar. In solid medium the optimum pH for pollen germination was 7. When pollen was grown at a slightly different pH (6.8), the percentage of germination was reduced by 40% when quantified after 6 hours of growth (Figure 2.9A).

However, interestingly, we observed that in a solid medium (setup 4) with a slightly acidic pH, pollen grains were able to germinate faster than in a medium with pH 7. After four hours of germination the percentage of germination reached a high value that at this point of time was higher than in medium with pH 7 (Figure 2.9A).

In liquid medium (setup 1) we noticed that the pH variation did not have a dramatic effect on the percentage of germination achieved after 6h. However, the pollen germinated fastest at pH 6.8 as seen by the greater percentages of germination at 2h in these samples (Figure 2.9B). Therefore, in experiments focusing on shorter

time periods after germination, a slight acidification of the liquid medium would be advantageous to obtain optimal percentage of germination. On the other hand, total germination as quantified after 6h is not significantly higher at pH 6.8 then pH 7.

In our experiments, we noticed a decrease by 0.4 pH units after 6 hours of growth in liquid medium. This acidification of the medium may affect pollen germination with time. This is consistent with earlier reports that with time, growing pollen tubes tend to acidify the medium with time eventually resulting in growth arrest (Tupý and Říhová, 1984). An acidification of 0.1 units was also observed in a control liquid sample without any pollen. This decrease in the pH might be due to the metabolism of microorganisms, present in the medium, on the glassware and in higher amounts on the pollen itself. It may also be due to the metabolism of the pollen and pollen tubes where a high degree of ions exchange happens between intra- and extracellular compartments. The use of Tris buffer (5 and 10 mM) reduced the percentage of germination (not shown), which is why we did not pursue further experimentation with buffers.

2.3.3.6 Temperature

Pollen germination shows a temperature dependent behavior. A controlled temperature was proven to be important for optimal germination and pollen growth in *Arabidopsis thaliana* (Boavida and McCormick, 2007). Since various experimental strategies may require incubation temperatures other than room temperature, we tested a temperature range from 4 to 42°C. Best germination for pollen tubes growing on solid medium was obtained for temperatures ranging from 22 to 25°C (Figure 2.10). The same was observed for pollen grown in liquid medium in Erlenmeyer flasks, whereas the optimal temperature for pollen in a liquid drops was 30°C (Table 1). A similarly surprising optimal germination temperature was observed by Boavida *et al.* (2007) who describe that 28°C increases germination in the Colombia ecotype.

Approximately 5% of the pollen grains were able to germinate at 4°C in liquid medium and these tubes displayed normal morphology (Figure 2.11) with a mean length of 110 µm after 24 h of growth. We tested this condition since it would allow image acquisition of living pollen tubes in the environmental scanning electron microscope as image quality decreases with increasing temperature.

2.3.3.7 Comparison with other media

To demonstrate the difference between our optimized medium and other media that had been developed for pollen germination of various species, we compared them side by side. Using pollen that had been cold-stored for 3 months, our optimized medium yielded significantly higher percentages of germination than the Lily pollen medium (Parre and Geitmann, 2005), the BK medium (Brewbaker and Kwack, 1963) and several *Arabidopsis* media (Sanders *et al.*, 1999; Fan *et al.*, 2001; Boavida and McCormick, 2007) (Figure 2.12A). The tube length of those grains that had succeeded in germinating was significantly longer in our medium than that in the other media (Figure 2.12B). Furthermore, our medium resulted in pollen tubes without apparent morphological disorders, whereas in our hands pollen tubes grown on the Boavida and McCormick medium (2007) were frequently aberrant with apical swellings. One of the reasons why our medium appeared superior to the others might be that it had been optimized for bulk collected, cold stored pollen while the others were optimized for freshly collected pollen and/or for pollen from the most recently opened flowers of the *Arabidopsis* plant.

2.3.4 Conclusions

Given the importance of *Arabidopsis thaliana* as a model system, the optimization of the conditions for bulk storage and germination of frozen stored pollen should contribute to the increased use of this species in pollen research. Furthermore, we provided optimized conditions for different experimental setups that either use large amounts of pollen or require specific conditions such as low

temperatures or medium stiffness. Our optimized *Arabidopsis* pollen growth medium is composed of 18% sucrose, 1 mM potassium chloride, 1.62 mM boric acid, 1 mM magnesium sulphate, 2 mM calcium chloride and 2 mM calcium nitrate, at a pH of 7 with an incubation temperature of 22.5°C. For pollen grown in solid medium, twice the amount of calcium is ideal. For pollen grown in a liquid drop, the optimum growth temperature is 30°C (Table 1).

The two main advantages of these methods of *Arabidopsis* pollen germination are the high reproducibility compared to other media described in the literature and the possibility of using large amounts of pollen that has been collected and stored frozen. Therefore, the availability of flowering *Arabidopsis* plants at the time of the experiment is not a limiting factor. Whenever a batch of flowers is mature, all its pollen can be collected and stored for experiments to be carried out at a later time.

The bulk pollen germination makes our methods useful for a variety of experiments requiring large amount of nucleic acid, proteins, or organelles to be extracted from *Arabidopsis* pollen tubes. The wide range of germination conditions make them appropriate for other experiments where low germination temperatures are required (environmental scanning electron microscopy) or different medium stiffness is a limiting factor to the success of the experiments.

2.4 Acknowledgements

Research in the Geitmann lab is supported by grants from the Natural Sciences and Engineering Research Council of Canada (NSERC), the *Fonds Québécois de la Recherche sur la Nature et les Technologies* (FQRNT), and the Human Frontier Science Program (HFSP).

2.5 Table

	Setup 1	Setup 2	Setup 3	Setup 4
Temperature (^{o}C)	30.0	22.5	22.5	22.5
pH	7.0	7.0	7.0	7.0
Calcium (mM)	4.0	4.0	2.0	4.0
Boron (mM)	0.49	0.49	1.62	1.62
Magnesium (mM)	1.0	1.0	1.0	1.0
Potassium (mM)	1.0	1.0	1.0	1.0
Sucrose (%)	18	18	18	18

Table 2.1: Optimized conditions for *in vitro Arabidopsis* pollen germination in four different experimental setups. Setup 1: Pollen in liquid drop. Setup 2: Pollen in Erlenmeyer. Setup 3: Pollen on solid surface. Setup 4: Pollen within solid medium.

2.6 Figures

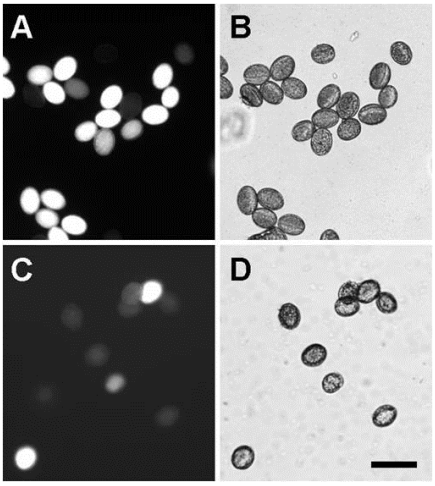

Figure 2.1: *Arabidopsis thaliana* pollen viability test using fluorescein diacetate (FDA). Viable pollen fluoresces bright white under UV light. Fresh pollen (A,B) and pollen stored for 12 months at -20°C (C,D). Bar = 20 µm.

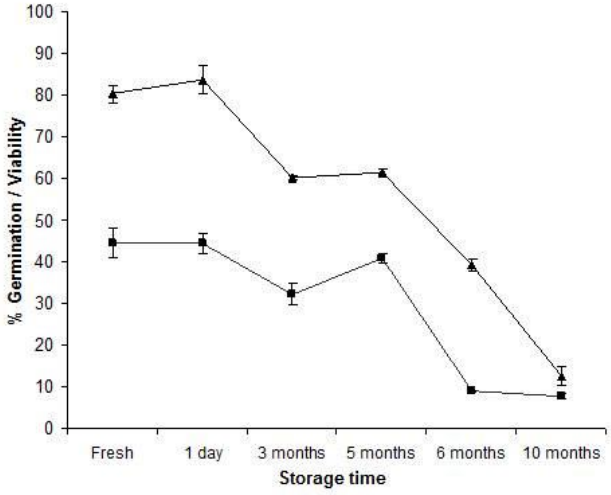

Figure 2.2: Change of *Arabidopsis* pollen viability (▲) and percentage germination (■) with duration of cold storage. Stored pollen was kept at -20°C after 2 hours of dehydration following harvest. Vertical bars represent the standard deviation (n=5).

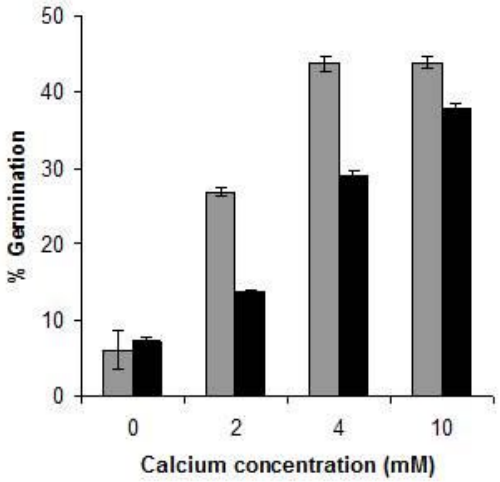

Figure 2.3: Effect of calcium concentration on the percentage of germination of *Arabidopsis thaliana* pollen grown in liquid drop (grey) and in solid medium (black) after 6 hours of growth. Vertical bars represent the standard deviation (n=5).

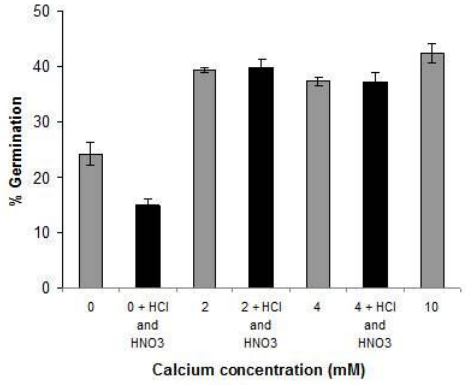

Figure 2.4: Effect of calcium concentration on percentage germination of *Arabidopsis thaliana* pollen grown on solid medium after 6 hours of growth. In a parallel series (black bars), chloride and nitrate concentrations were adjusted to equal those in the 10 mM Ca^{2+} sample. Vertical bars represent the standard deviation (n=5).

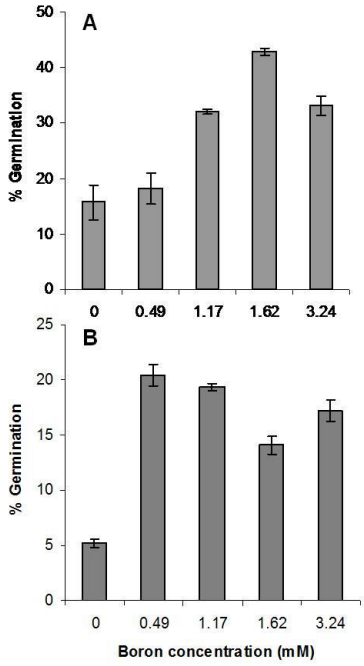

Figure 2.5: Effect of boron concentration on the percentage germination of *Arabidopsis thaliana* pollen grown on solid medium (A) and in liquid medium (B) after 6 hours of growth. Vertical bars represent the standard deviation (n=5).

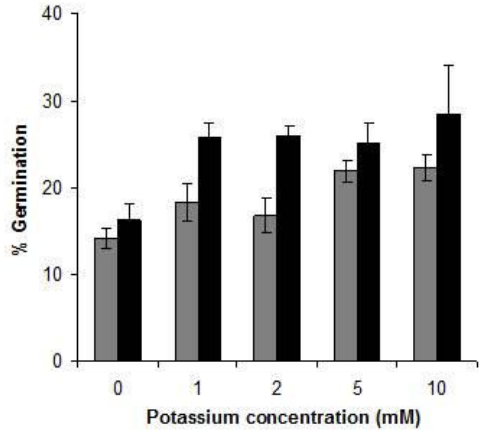

Figure 2.6: Effect of potassium concentration on the percentage germination of *Arabidopsis thaliana* pollen grown in liquid drop (grey) and in solid medium (black) after 6 hours of growth. Vertical bars represent the standard deviation (n=5).

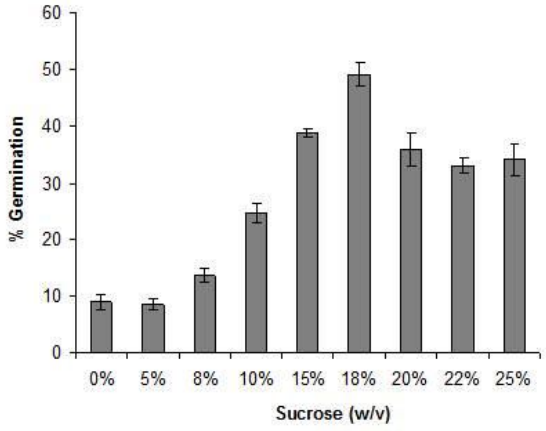

Figure 2.7: Effect of the sucrose concentration on the percentage germination of *Arabidopsis thaliana* pollen after 6 hours of growth on solid medium. Vertical bars represent the standard deviation (n=5).

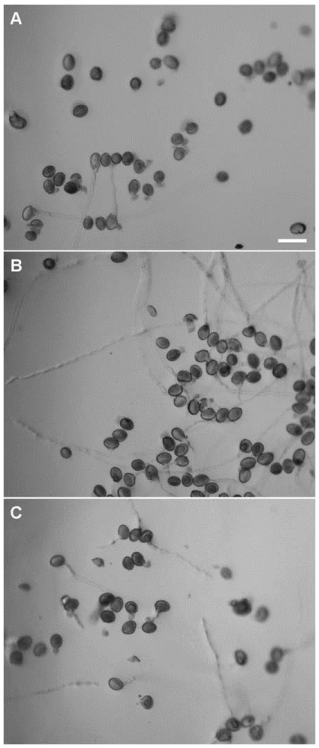

Figure 2.8: *Arabidopsis* pollen germination on agarose medium containing 5% (A), 18% (B), and 25% sucrose (C). Bar = 50 µm.

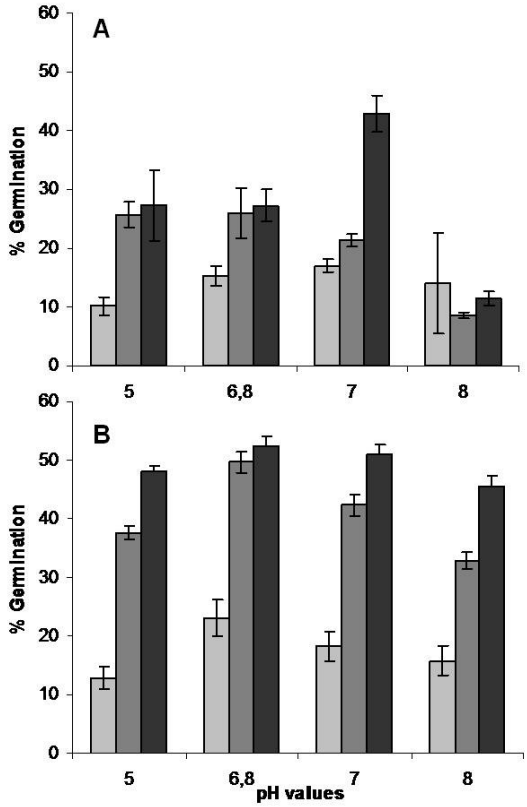

Figure 2.9: Effect of the pH on the percentage germination of *Arabidopsis thaliana* pollen grown on solid surface (A) or in liquid medium (B) after 2 hours (light grey), 4 hours (dark grey) and 6 hours (black) of growth. Vertical bars represent the standard deviation (n=5).

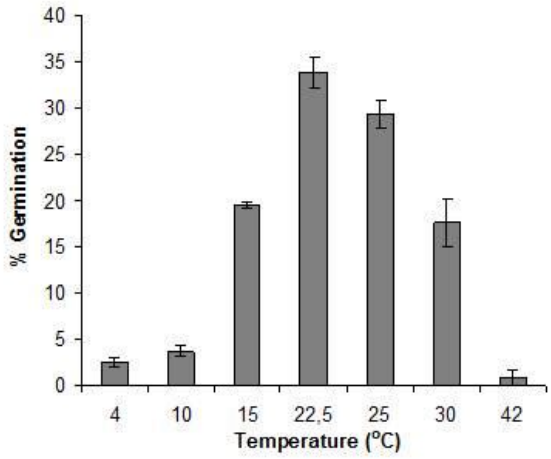

Figure 2.10: Effect of the temperature on the percentage germination of *Arabidopsis thaliana* pollen grown on solid medium. Vertical bars represent the standard deviation (n=5).

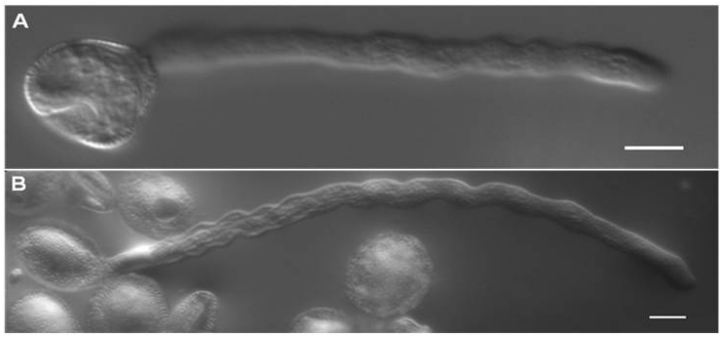

Figure 2.11: Micrographs of *Arabidopsis* pollen tubes grown at 4°C for 24 hours (A) in liquid medium and (B) on solid medium. Bars = 10 µm

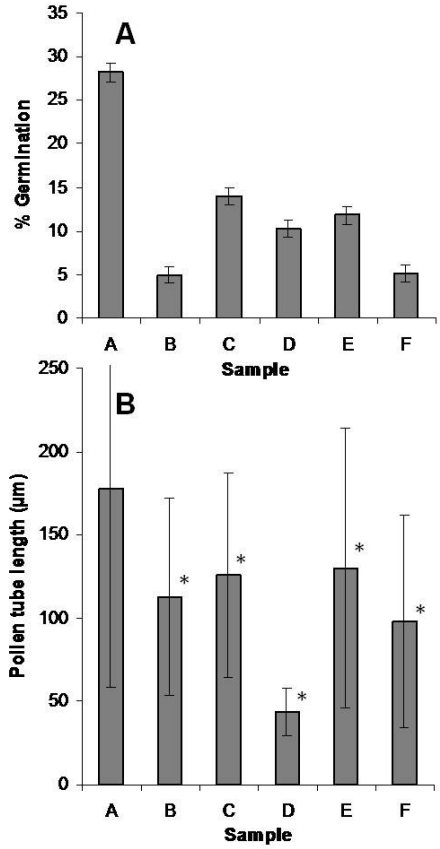

Figure 2.12: *Arabidopsis* pollen percentage of germination (A) and pollen tube length (B) after five hours of growth on agarose stiffened media based on our optimized protocol (sample A), Boavida and McCormick (2007) (sample B), Li *et al.* (1999) (sample C), Fan *et al.* (2001) (sample D), Brewbaker and Kwack (1963) modified with 18% sucrose (sample E), and lily medium (Parre and Geitmann 2005) modified with 18% sucrose (sample F). Bars represent the standard deviation (n=5). * Despite large standard deviations for pollen tube length (B), mean values of samples B through F are significantly different from that of sample A with $p<0.05$ (samples B and E) and $p<0.01$ (samples C, D, F) (two tailed student t-test).

3 Microwave-assisted processing of plant cells for optical and electron microscopy

Together with the members of my lab Youssef Chebli, Monisha Sanyal and Leila Aouar, we optimized microwave (MW)-assisted sample processing for single plant cells for both optical and electron microscopy. Two important variables that are critical for MW-assisted sample preparation were optimized: wattage, correct adjustment of which is responsible for tissue stabilization, and exposure time, which is sample and treatment dependent. Furthermore, the application of a vacuum simultaneously to microwave processing, allows further reduction of experimentation time.

This technique was applied to label actin cytoskeleton and cell wall components of the pollen tube. It resulted in a dramatic reduction of experimentation time. More importantly, structural integrity and antigenicity were not compromised when comparing to conventional bench-top processing methods for chemically fixed samples. A technical report with the title "Microwave-assisted processing of plant cells for optical and electron microscopy" was published in the November issue of 2008 of the Bulletin of the Microscopical Society of Canada, pages 15 - 19. I performed all the fluorescence and immunolabelling experiments. The manuscript was written in equal parts by Youssef Chebli and myself.

Microwave Assisted Processing of Plant Cells for Optical and Electron Microscopy

Youssef Chebli, Firas Bou Daher, Monisha Sanyal, Leila Aouar and Anja Geitmann

The technological development of microscope hardware has led to a significant breakthrough by pushing the resolution from the micro to the nano-scale range. During the past century high end electron, optical and atomic force microscopes have been developed for better ultra-structural viewing and 3D visualization of the specimen. Compared to these impressive hardware developments, progress in specimen processing techniques has been far less dramatic. Despite the increased use of living material in microscopy, numerous applications still require specimens to be fixed and bench time is a major constraint in any kind of sample preparation. The first and one of the most important steps in biological tissue processing for microscopy is fixation. Depending on the specimen, times for chemical fixation may range from half an hour to as much as 24 hours. The entire procedure required for processing biological samples for transmission electron microscopy (TEM) can therefore take between a few days and a week. While this time is necessary to completely fix, dehydrate and embed the specimen, it also allows unintended processes to occur such as the dissolving of membranes leading to the release of organelle content. This can result in the dilution of the applied solutions and to alterations in their pH value (Russin and Trivett, 2001) which in turn may generate structural artifacts. The fixation time is even more critical in case of immunohistochemistry where antigen preservation is crucial for successful labeling. Therefore, efforts to minimize fixation and processing times not only aim to reduce bench time but also to prevent structural impact on the tissue.

In the 1970s, the use of microwave (MW) ovens was first introduced to accelerate sample processing (Mayers, 1970; Demaree and Giberson, 2001). The first report on MW-assisted aldehyde tissue fixation for the purpose of light microscopy and TEM was made in the 1980s (reviewed by (Giberson, 2001). The early MW ovens had no control of power or temperature and the only variable was the exposure

time. Currently, MW ovens are available with variable power (wattage), temperature control and MW transparent vacuum system.

Because of the presence of cell walls, vacuoles, plastids and intracellular air space (Russin and Trivett, 2001), plant cells generally require rather prolonged incubation times with fixation and dehydration solutions and thus would profit greatly from an accelerated protocol. In the present study, we aimed at optimizing MW-assisted sample processing for single plant cells for both optical and electron microscopy. We used leaf trichomes and pollen tubes as test specimens. The former are cells differentiated from the leaf epidermis. They stick out from the leaf surface into the air space and are thus not mechanically stabilized by any surrounding tissue. The latter are cellular protuberances formed by germinating pollen grains upon contact with a receptive stigma. They function in delivery of the two sperm cells to the ovary to ensure double fertilization. Pollen tubes are commonly used as a model for the study of anisotropic cell growth and also to understand the structural dynamics and material properties associated with polarized cellular expansion (Geitmann, 2006; Geitmann and Steer, 2006). Due to their extremely rapid growth and active intracellular transport processes, high quality fixation of pollen tubes is critical for the preservation of cellular ultrastructure and polarity. We optimized two important variables critical for MW-assisted sample preparation: wattage, correct adjustment of which is responsible for tissue stabilization, and exposure time, which is sample and treatment dependent (Russin and Trivett, 2001). During experiments, sample temperature was monitored to control the effect of heating (Demaree and Giberson, 2001), and vacuum was used for better infiltration of the cells with the fixation solution (Russin and Trivett, 2001). All experiments were carried out in a PELCO cold spot®.

3.1 Optical microscopy

Due to the highly polarized mode of growth, the pollen tube cell wall has a characteristic spatial profile of non-uniformly distributed cell wall polysaccharides. The tip is composed of methyl-esterified pectins that permit, due to their plastic characteristics, pollen tube elongation at this location (Geitmann and Parre, 2004; Parre and Geitmann, 2005). On the other hand, the basal part of the tube is composed of non-esterified, stiffer pectins and it is further characterized by the deposition of cellulose and callose (Chebli and Geitmann, 2007). The latter component plays a role in the mechanical resistance of the cell wall against tension and compression stress in the cylindrical part of the cell (Parre and Geitmann, 2005). In longer pollen tubes, callosic plugs compartmentalize the cell allowing the older parts of the cell to degenerate. To sustain the active growth of the pollen tube, cell wall material is constantly added to the growing tip through the fusion of secretory vesicles which are transported to the growing zone via the highly dynamic actin cytoskeleton.

Visualization of both cell wall components and cytoplasmic structures such as the cytoskeleton can be performed by combining specific labels with fluorescence and confocal microscopy. Due to the extremely fast growth behavior and the polar distribution of cytoplasmic components by selective and directed cytoplasmic streaming, fixation of pollen tubes needs to be rapid to capture the ultrastructure reality. We tested several staining and immunohistochemical procedures to assess the efficiency and quality of MW-assisted fixation protocols on pollen tubes. Given that we have extensive experience with this cell type and its characteristic labeling profiles we were able to judge the quality of the samples obtained with the MW-assisted protocols comparing them to conventional chemical fixation and rapid freeze fixation.

3.2 Methodology

In the optimized protocol all steps were carried out in a microwave operating at 150 W under 21inches of Hg vacuum and a controlled temperature of 26^{o}C ± 2^{o}C.

3.2.1 Pectin labeling

Pollen tubes were fixed for 40 seconds in 3% formaldehyde in phosphate buffer saline (PBS) solution. After 3 washes in PBS with 2% bovine serum albumine (BSA), they were incubated for 10 minutes in JIM5 (monoclonal antibody specific for pectins with low degree of methyl-esterification; Figure 3.1A) or JIM7 (monoclonal antibody specific for pectins with high degree of methyl-esterification; Figure 3.1B) followed by 3 washes of 40 seconds each in a 2% BSA solution. Tubes were then incubated for 10 minutes in Alexa 594 anti-rat secondary antibody (Molecular Probes), washed 3 times and mounted on glass slides for observations.

3.2.2 Callose labeling

Pollen tubes were fixed in 3% formaldehyde in PIPES buffer for 40 seconds and washed 3 times in the same buffer. A 10 minute incubation with 0.2% aniline blue solution was used to label callose. Samples were then washed 4 times in PIPES buffer before observation (Figure 3.2).

3.2.3 Actin labeling

Pollen tubes were fixed for 40 seconds in a pH 9 PIPES buffer containing 3% formaldehyde, 0.5% glutaraldehyde and 0.05% Triton. After 3 washes with the same buffer, pollen tubes were incubated with rhodamine phalloidin for 10 minutes in a pH 7 PIPES buffer, washed 5 times and then observed immediately, since actin tends to be unstable even when fixed (Figure 3.3).

3.2.4 Electron Microscopy

3.2.4.1 Transmission electron microscopy

Sample preparation for TEM is very critical due to the necessity to preserve the cellular ultrastructure. Any inappropriate handling during fixation, dehydration or embedding will be flagrantly expressed in the observed samples as artifacts. MW technology has the potential to strongly reduce sample preparation time while preserving tissue subcellular integrity and antigenicity.

We optimized different conditions for microwave sample processing for pollen tubes. Application of a fixative consisting of 2% formaldehyde and 2.5% glutaraldehyde in phosphate buffer (PB) to pollen tubes growing in a 0.5% agar medium for 40 seconds was sufficient for a very good fixation. Post-fixation was performed using 2% osmium tetroxide solution following 3 washes in PB and 3 additional washes in deionized water. Samples were then washed twice with PB followed by two other washes in water. Dehydration was done using an increasing acetone gradient ranging from 25 to 100% with the last step repeated thrice. All fixation, washing and dehydration steps were conducted under 150 W and 21 in of Hg vacuum for 40 seconds each.

For resin infiltration we used SPURR resin in 4 steps with increasing resin concentration up to 100%. These steps were conducted at 300 W for 3 minutes each and under 21in Hg vacuum. Resin polymerization was done in a regular oven at 64^{o}C overnight. This polymerization can also be carried out in a water bath at 60^{o}, 70^{o} and 80^{o}C for 10 minutes each then at 100^{o}C for 45 minutes (Demaree and Giberson, 2001). Ultrathin sections were cut with a Leica Ultracut and samples were observed with a JEOL JEM 1005 transmission electron microscope operating at 80 kV (Figure 3.4).

3.2.4.2 Scanning electron microscopy

Pollen tubes and trichomes were fixed and dehydrated using the same protocol as that for TEM sample preparation. Samples were then dehydrated, critical point dried, gold-palladium coated and observed with a JEOL JSM 35 (Figure 3.5).

3.3 Results and Discussion

Plant cell fixation and processing for microscopical observations are a challenge due to the presence of cell wall, vacuoles as well as high internal turgor pressure. Osmotic changes upon the addition of a chemical fixation solution easily causes cellular collapse or bursting, or, less dramatically but nevertheless critical, spatial rearrangement of cytoplasmic contents (e.g. loss of polar distribution of organelles). The cell wall surrounding the plasma membrane hampers effective penetration of the fixative. Using MW-assisted protocols we succeeded in improving and accelerating sample processing while preserving the cellular integrity. Cytochemical labeling of callose in the pollen tube cell wall reproduced the same characteristic profiles as those described previously using conventional chemical fixation. While antigenicity was enhanced in some cases (Giberson, 2001), in our case, we noticed that it was preserved as revealed by immunolabelling for two different types of pectin. The actin cytoskeleton, a very dynamic and unstable structure, was preserved using MW-assisted fixation and resulted in a spatial configuration similar to that observed after freeze fixation, the gold standard for the quality of fixed plant cell cytoskeleton (Lovy-Wheeler *et al.*, 2005). In electron microscopy, cell structure and subcellular compartments were well preserved when comparing with bench top processed plant cells. This was observed when comparing structural integrity of the subcellular components on pictures taken using both methods.

In addition to this, experimentation time was dramatically reduced using the MW-assisted methods (Figures 3.6 and 3.7). For optical microscopy, sample

preparation time reduction varied from 5 fold for cytochemical labeling to 8 fold for actin labeling while time reduction for TEM sample preparation was 26 fold.

3.4 Conclusion

The use of MW-assisted protocols resulted in a dramatic reduction of experimentation time. More importantly, structural integrity and antigenicity were not compromised when comparing to conventional bench-top processing methods for chemically fixed samples. Vacuum MW processing for electron microscopy of pollen tubes gave the same results as compared to the traditional method despite much shorter fixation and incubation times.

On a more practical level, MW technology is affordable, user friendly, does not require specific installations and older models can be upgraded with a temperature control device. Furthermore, it is very flexible allowing an easy switch mid-protocol to the conventional bench-top method if necessitated by time constraints or logistics.

3.5 Figures

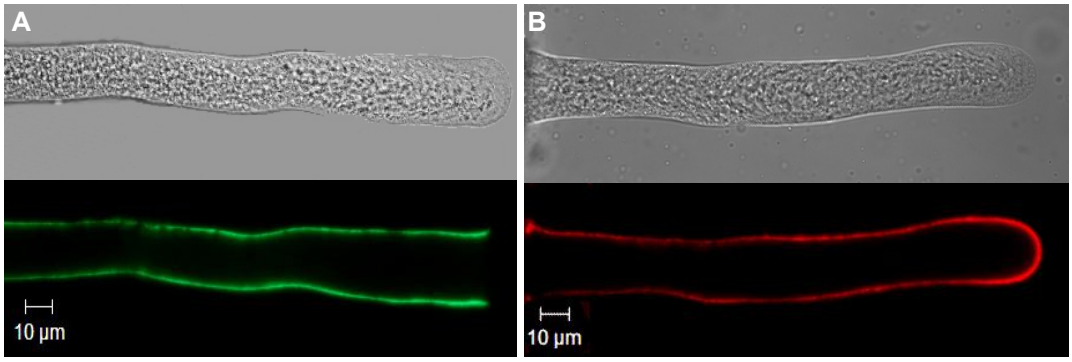

Figure 3.1: Immunofluorescence label of lily pollen tubes. (A) JIM5 label of non-esterified pectins reveals the presence of the polymer in the distal region. (B) JIM7 label of esterified pectins is predominantly present at the apex. Pictures represent median pollen tube sections taken with a Zeiss LSM-510 META confocal microsocope.

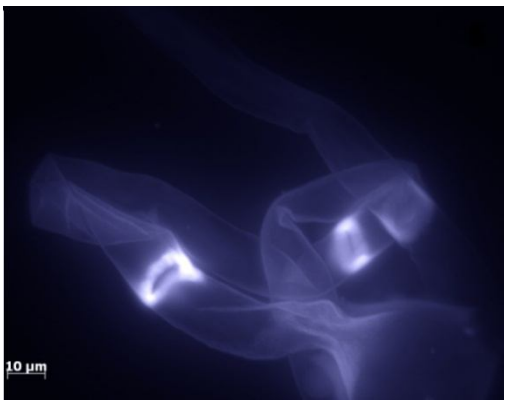

Figure 3.2: Callose rings observed with aniline blue staining in *Camellia* pollen tubes. These callose rings will develop into callose plugs. Picture represents a Z-stack projection taken with a Zeiss Imager-Z1 microscope equipped with a Zeiss AxioCam MRm Rev 2 camera.

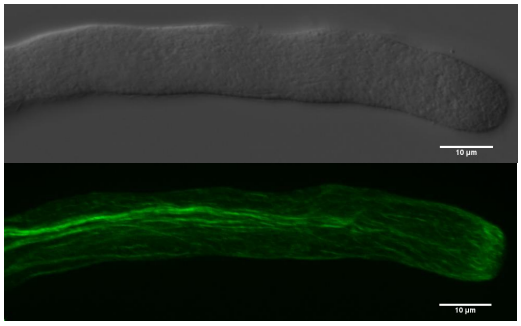

Figure 3.3: *Camellia* pollen tube actin cytoskeleton as visualized by rhodamin-phalloidin label. Picture represents a Z-stack projection taken with a Zeiss Imager-Z1 microscope equipped with a Zeiss AxioCam MRm Rev 2 camera.

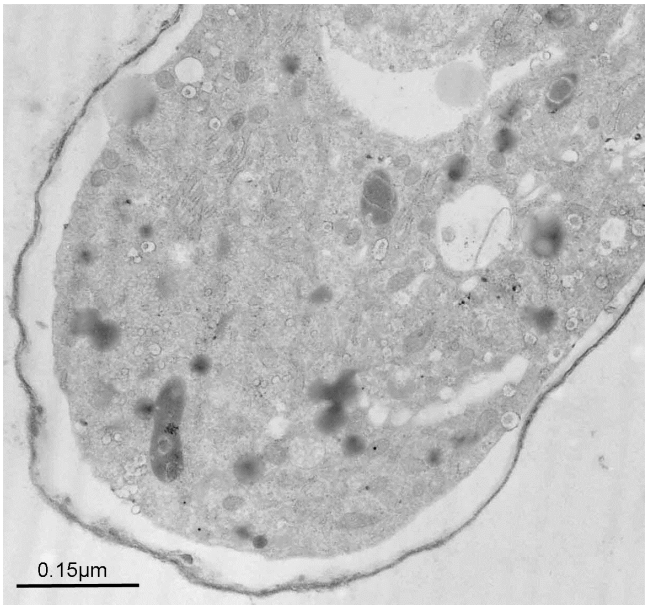

Figure 3.4: Transmission electron micrograph of a cross-section of a *Camellia* pollen tube. Picture was taken with a JEOL JEM 1005 transmission electron microscope operating at 80 kV.

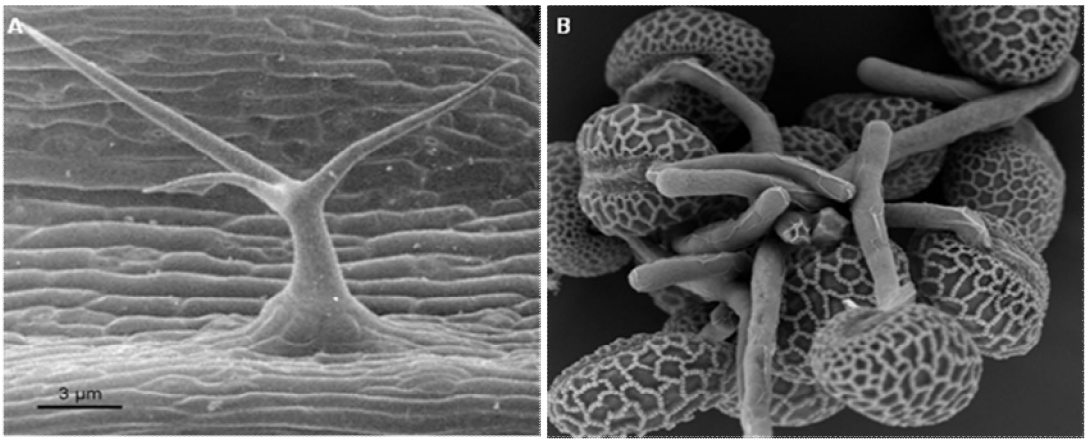

Figure 3.5: Scanning electron micrograph of an *Arabidopsis* leaf trichome (A) and germinated lily pollen grains (B). Pictures were taken with a JEOL JSM 35 (A) and a Hitachi TM 1000 (B)

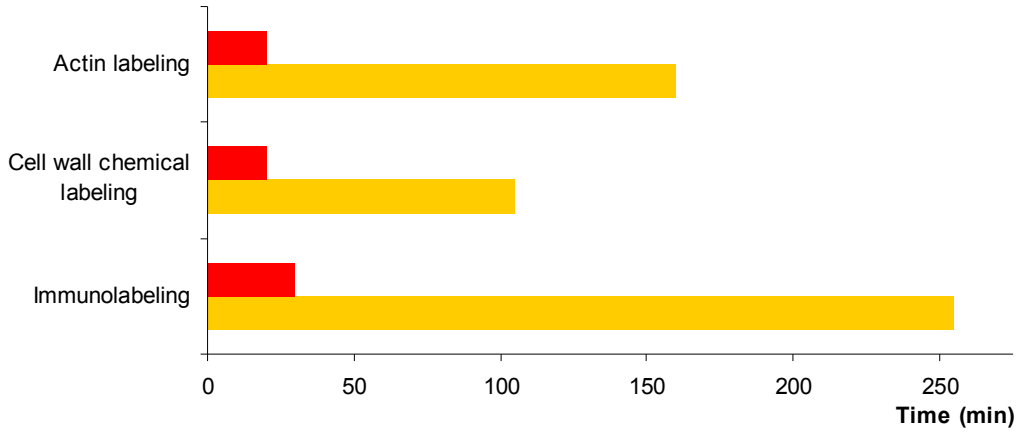

Figure 3.6: Comparison of experimentation time between bench-top (orange) and microwave assisted (red) methods of sample preparation for optical microscopy.

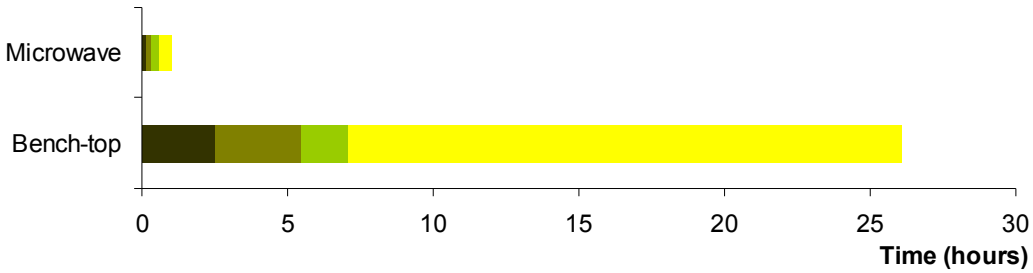

Figure 3.7: Comparison of experimentation time between conventional bench-top and microwave assisted methods of sample preparation for transmission electron microscopy. Fixation (black), post-fixation (brown), dehydration (green) and resin infiltration (yellow).

4 Actin regulates pollen tube shape and growth

4.1 Introduction

Pollen tubes are highly anisotropic cylindrical structures produced by the male gametophyte of higher plants. These tubes will grow along the transmitting tissue of the pistil with the aim of transporting the sperm cells to the embryo sac where double fertilization will happen. To be able to accomplish this function, the pollen tube has to interact with the various types of signals that are produced by the pistil to guide the pollen tube to its target (Geitmann and Palanivelu, 2007; Cheung and Wu, 2008).

Given the very high growth rate of the pollen tube, a considerable amount of cell wall material must be added in order to sustain this growth. The pollen tube has an apical mode of growth and addition of new material happens in a zone at the shoulders of the pollen tube tip (Geitmann and Dumais, 2009). Cell wall material is composed mainly of methyl-esterifed pectins (Parre and Geitmann, 2005) that are transported by secretory vesicles to an exocytosis zone located in the subapex of the tube (Franklin-Tong, 1999; Bove *et al.*, 2008; Zonia and Munnik, 2008). Secretory vesicle transport is a highly dynamic process as can be observed when labeling vesicles with styril dyes. In plant cells in general and in pollen tubes in particular, vesicular transport occurs along arrays of the actin cytoskeleton and requires myosin motor proteins (DePina and Langford, 1999; Geitmann and Steer, 2006; Yokota and Shimmen, 2006) and is therefore energy-consuming. Class XI myosins have been shown to be expressed in lily pollen tubes (Yokota and Shimmen, 1994).

The animal cytoskeleton has been extensively studied and its roles in cell motility and architecture are well understood. On the other hand, very little is known

about the role of the cytoskeleton in determining plant cell architecture in general and pollen tube growth in particular. The reason for this lack of knowledge is that turgor pressure due to water uptake and cell wall yielding are dominant mechanical features whose interaction governs plant cell expansion (Cosgrove, 1986; Geitmann and Steer, 2006; Geitmann and Ortega, 2009). The pollen tube cytoskeleton is composed of microtubules and actin microfilaments (Geitmann and Emons, 2000). Microtubules have been shown to be implicated in anisotropic plant cell expansion (Baskin, 2005) but they are unlikely to play an important role in pollen tube elongation since their depolymerization does not prevent *in vitro* pollen tube growth (Gossot and Geitmann, 2007). The actin cytoskeleton on the other hand is very important for organelle transport (Lovy-Wheeler *et al.*, 2007) and pollen tube growth as has been shown by experiments using actin depolymerizing drugs (Gibbon *et al.*, 1999; Miller *et al.*, 1999; Vidali and Hepler, 2001). Actin filaments were also found to be involved in the ability of the pollen tube to invade solid obstacles and to grow in stiff media (Gossot and Geitmann, 2007). Nevertheless, the role of this cytoskeletal array in the mechanics of pollen tube apical growth is poorly understood. The pollen tube actin cytoskeleton is composed of long actin cables in the shank of the pollen tube (Geitmann and Emons, 2000; Lovy-Wheeler *et al.*, 2005). These long filaments are polarized and point with their barbed (plus) ends towards the pollen tube apex at the periphery of the tube and in the opposite direction at the center (Lenartowska and Michalska, 2008). At the subapex of the tube, densely arranged actin filaments are organized in a ring shaped actin fringe (Lovy-Wheeler *et al.*, 2005). This array is believed to be the site of high actin dynamics (Chen *et al.*, 2002). At the very apex of the pollen tube, no or very few actin filaments are present (Lovy-Wheeler *et al.*, 2005; Lenartowska and Michalska, 2008). Actin dynamics in the growing pollen tube is regulated by several actin binding proteins whose activity is controlled by calcium ions and protons (Hepler *et al.*, 2006; Yokota and Shimmen, 2006; Ren and Xiang, 2007).

Despite the description of the actin fringe in several pollen tube species (Kost *et al.*, 1998; Lovy-Wheeler *et al.*, 2005), its exact function is still unknown. In the present chapter I visualized this structure at high spatial resolution in order to provide a detailed description of its three-dimensional configuration in the pollen tubes of the most commonly used species. Furthermore, I investigated whether the subapical actin fringe was involved in determining the precisely controlled cylindrical shape of the elongating tube. For this purpose I pharmacologically altered actin dynamics by enhancing bundling of actin filaments and I interfered with the myosin-mediated transport of secretory vesicles along actin cables.

4.2 Materials and methods

4.2.1 Plant material

Pollen was collected from plants grown in the Montreal Botanical Garden. *Camellia japonica* pollen was dehydrated in gelatin capsules on anhydrous silica gel overnight and stored at -20°C. *Camellia* pollen growth medium contained 1.62 mM H_3BO_3, 2.54 mM $Ca(NO_3)_2 \cdot 4H_2O$, 1 mM KNO_3, 0.81 mM $MgSO_4 \cdot 7H_2O$, 8% sucrose (w/v). After collection, *Lilium longiflorum* pollen was packed in gelatin capsules, dried overnight on silica gel and stored at -80°C. Lily pollen germination medium contained 1 mM KNO_3, 130 nM $Ca(NO_3)_2$, 160 nM H_3BO_3, 10 % sucrose (w/v), and 5 mM MES buffer adjusted to pH 5.5. *Arabidopsis thaliana* pollen was treated as described in chapter 1. Pollen was rehydrated in humid atmosphere for 30 min prior to *in vitro* culture.

4.2.2 Actin labeling

After one hour of growth for *Camellia*, one hour and a half for lily and four hours for *Arabidopsis*, pollen tubes were fixed for 40 seconds in the microwave (PELCO cold spot® biowave 34700) set at 150 Watts in 3% formaldehyde, 0.5% glutaraldehyde and 0.05% Triton X-100 solution in a buffer composed of 100 mM

PIPES, 5 mM $MgSO_4$ and 0.5 mM $CaCl_2$ at pH 9. Pollen tubes were then washed 3 times for one minute each in the same buffer then incubated overnight at 4°C in a rhodamine-phalloidin (Molecular Probes) in a buffer composed of 100 mM PIPES, 5 mM $MgSO_4$, 0.5 mM $CaCl_2$ and 10 mM EGTA at pH 7. Next day, pollen was washed 5 times for one minute each in the same buffer. All washing steps were conducted in the microwave at 150 Watts. Pollen was then mounted on glass slides in a drop of citifluor (Electron Microscopy Sciences), covered with a cover slip, sealed and immediately observed in the fluorescence microscope.

4.2.3 Microtubule labeling

Pollen was fixed in PIPES and magnesium (PM) buffer (50 mM PIPES, 1 mM EGTA, 1 mM $MgCl_2$ at pH 6.9) with 4% formaldehyde for 45 minutes then washed twice (5 minutes each) in PM buffer. Pollen was then treated with 2% cellulysine for 6 minutes, washed twice then treated with cold ethanol for 5 minutes at -20°C. After 2 washes with tris buffer saline (TBS) (50 mM Tris, 150 mM NaCl at pH 7.5) with 2% bovine serum albumin (BSA), an anti-α-tubulin (Molecular Probes) mouse monoclonal antibody (diluted 1:200) was added and incubation was conducted overnight at 4°C. Second day and after 2 washes with TBS plus 2% BSA, Alexa Fluor 594 (Molecular Probes) goat anti-mouse secondary antibody (diluted 1:100) was added and left to incubate for 2 hours at room temperature. Before mounting, pollen was washed 4 times in TBS plus 2% BSA.

4.2.4 Callose and cellulose labeling

After pollen fixation for 40 seconds in a buffer composed of 100 mM PIPES, 5 mM $MgSO_4$ and 0.5 mM $CaCl_2$ at pH 9 with 3% formaldehyde and 0.5% glutaraldehyde in the microwave, 3 washes were done before adding few drops of 0.2% aniline blue (for callose labeling) or 1 mg/ml calcofluor white (for cellulose labeling). Pollen was then incubated in the microwave under 1.5 in Hg vacuum at

26°C and 150 Watts. After 5 washing steps, pollen was mounted on glass slides for microscopic observations.

4.2.5 Immunofluorescent labeling of pectins

Pollen tubes were fixed in 3% formaldehyde and 0.5% glutaraldehyde in PIPES buffer (100 mM PIPES, 5 mM $MgSO_4$ and 0.5 mM $CaCl_2$ at pH 9) and subsequently treated with monoclonal antibodies JIM5 or JIM7 diluted 1:50 in PBS for (10 minutes under vacuum). After washes in buffer, the secondary antibody, goat-anti-rat conjugated with alexa fluor 594 diluted 1:100, was applied overnight at 4°C in the dark. After several washes, pollen tubes were mounted and observed in a fluorescence microscope.

4.2.6 Vesicle labelling

Vesicles in living pollen tubes were labelled using the lipophilic styryl dye FM1-43 (Molecular probes, Invitrogen). FM1-43 was added to the pollen growth medium at 160 nM five minutes prior to observation.

4.2.7 Microscopic Observations

Fluorescence microscope observations were done using a Zeiss Axio Imager.Z1 equipped with a Zeiss AxioCam MRm Rev.2 camera. Z-Stacks acquired at 1 μM intervals were taken and image reconstruction and surface rendering were conducted using AxioVision Release 4.5 software. Confocal images were taken on a Zeiss LSM 510 META Live Duo confocal microscope equipped with a LSM 5 LIVE CCD detector and pictures were acquired with the LSM Image Examiner software. Images for the galvanotropic experiment were taken with a Nikon TE2000 microscope equipped with a Roper fx cooled CCD camera and ImagePro software (Media Cybernetics, Carlsbad, CA). To improve the representation of the 3D data, I used surface rendering after the *in silico* reconstruction of z-stack images. This image processing technique replaces voxels by polygonal surfaces. Since this technique

takes into consideration the intensity of each voxel, it makes it easier to schematize a 2D image in 3D with the possibility of rotation and tilting of the resulting images.

4.3 Results and Discussion

4.3.1 Optimization of actin labeling after chemical fixation

Actin in the pollen tube can be visualized in fixed or in living pollen tubes. The first method uses fluorescent-labeled phalloidin, a fungal toxin that binds actin (Wieland *et al.*, 1978). The second is based on the use of actin binding proteins or selected domains from these proteins that have been tagged with a fluorescent protein (Kost *et al.*, 1998; Vidali *et al.*, 2009). The disadvantage of using live actin visualization is that due to the introduction of additional actin binding proteins into the cytoplasm, the technique may affect pollen tube growth, alter actin conformation and is likely to label only a portion of the actin population in the pollen tube (Wilsen *et al.*, 2006). Also, not all pollen tube species are easily transformed. To obtain a reproducible, high spatial resolution, 3D reconstruction image of the actin arrays in different pollen tube species, we therefore chose to use fixed samples.

It is rather difficult to preserve the configuration of the actin cytoskeleton during fixation since actin filaments are very unstable; any changes in the subunit state will cause filament fragmentation. Therefore, fixation should be as quick as possible (Galkin *et al.*, 2003). In recent years, the preservation of actin arrays in chemically fixed pollen tubes has been enhanced by using a pre-fixation step with m-maleimidobenzoyl N-hydroxysuccinimide (MBS) ester or ethylene glycol bis[sulfosuccinimidylsuccinate] (sulfo-EGS). However, not surprisingly, the administration of these cross-linking agents prior to aldehyde fixation had the tendency to slightly alter the native actin arrays to appear more cross-linked (Geitmann and Emons, 2000). Rapid freeze fixation has so far yielded the best results for the conservation of the actin cytoskeleton in pollen tubes (Lovy-Wheeler *et al.*, 2005). In the absence of a freeze fixation facility in our hands, we optimized our

protocols for aldehyde-based chemical fixation using microwave-enhanced and thus extremely rapid incubation protocols.

Using microwave exposure, a fixation treatment with 3% formaldehyde, 0.5% glutaraldehyde and 0.05% Triton X-100 in a buffer composed of 100 mM PIPES, 5 mM $MgSO_4$ and 0.5 mM $CaCl_2$ at pH 9, could be shortened from 30 min on the bench to 40 seconds in the microwave at 150 Watts and 26°C. Each of the washing steps was also conducted in the microwave for 1 minute at the same conditions. Subsequent label with rhodamine-phalloidin revealed excellent preservation of the actin cytoskeleton (Figure 4.1) whose configuration was virtually identical to that of rapid freeze fixation preparations from other labs (Lovy-Wheeler *et al.*, 2005).

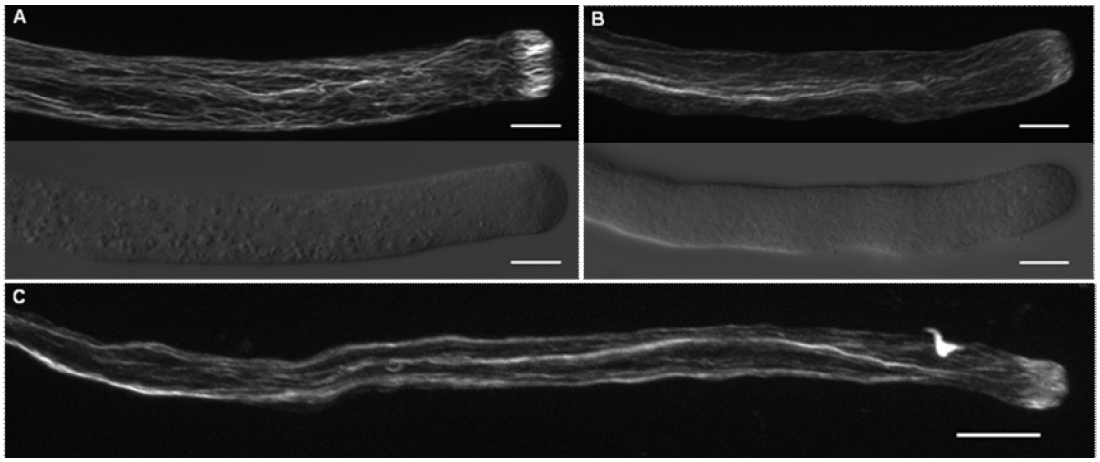

Figure 4.1: Confocal laser scanning micrographs showing phalloidin-based actin labelling of lily (A), *Camellia* (B) and *Arabidopsis* (C) pollen tubes after microwave-enhanced chemical fixation. The fluorescence micrographs are maximum projections of the images of a z-stack and the accompanying brightfield micrographs were taken with DIC optics. Bars = 10 μm.

The protocol worked equally well on pollen tubes from three species: lily, *Camellia* and *Arabidopsis*. In all of the pollen tubes, the very apex was devoid of prominent actin filaments, the collar region between apex and shank displayed an actin fringe and long filaments parallel to the axis of growth characterized the basal part of the tube (Figure 4.1).

Our optimized actin labeling protocol represents a significant improvement in the visualization of pollen tube microfilaments upon conventional chemical fixation protocols. It allowed us to obtain, in very short experimental time and with less labor, actin label in terms of image detail and definition equal to or better than what was observed in the literature using rapid freeze fixation (Lovy-Wheeler *et al.*, 2005). In addition to this, no additional cross linkers (other than the aldehydes) were added to the fixative. Cross-linkers such as MBS or sulfo-EGS have the potential to alter the native conformation of the actin arrays by connecting two or more filaments that are in close proximity making them look like one filament or cable. The fact that our optimzed procedure avoids this cross-linking was demonstrated by the preservation of fine actin filaments in very close vicinity to each other that were clearly distinct.

4.3.2 Spatial configuration of actin

Although the general geometry of the actin arrays in the three species investigated here was very similar, there were small differences. Compared to lily, *Camellia* and *Arabidopsis* had more bundled and thicker actin cables in the shank region (Figure 4.1 B,C). The differences in bundling patterns that were observed in the three species could for example be explained by a specific activity or expression of actin bundling proteins such as villin (Vidali *et al.*, 1999). In *Camellia* and *Arabidopsis,* villins might have a higher expression level or activity in the shank of the pollen tube compared to that of lily which could explain the differences in actin bundling patterns in these three species. Differences in villin activity could be due to differences in cytoplasmic calcium levels between these species since villin is a calcium dependent ABP (Vidali *et al.*, 1999).

Image processing using surface rendering revealed the 3D conformation of the actin cytoskeleton in lily pollen tubes (Figure 4.2). The actin fringe was represented as a dense group of fine actin filaments arranged principally in a direction parallel to the long-axis of the cell, in a ring-shaped arrangement at the subapex of the pollen tube (Figure 4.2B). In the surface rendering, depending on the

choice of threshold, the fine filaments did not necessarily appear as distinct objects but were often grouped. By contrast, the actin arrays located in the shank appeared as longer, thicker bundles that were almost evenly distributed throughout the tube diameter (Figure 4.2C). In order to be able to visualize the relative distribution in 3D of the actin cytoskeleton and the secretory vesicles, I applied surface rendering to the 3D reconstruction of a z-stack of confocal images of the vesicles labeled with the styryl dye FM1-43 (Figure 4.2D). I subsequently merged the resulting image with that of the actin fringe, which demonstrates that in 3D the inverted cone of vesicles fits exactly inside the ring formed by the actin fringe (Figure 4.2F).

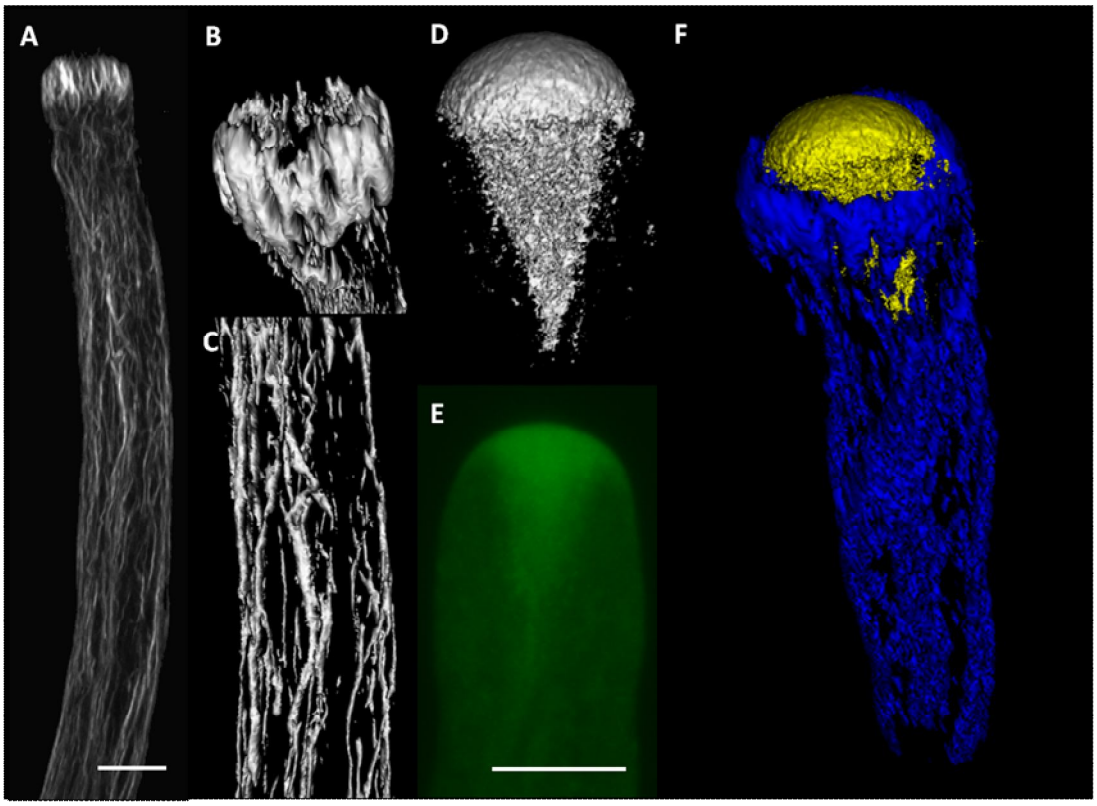

Figure 4.2: Spatial configuration of actin arrays and vesicles in pollen tubes of lily. (A) Confocal laser scanning micrographs of the actin cytoskeleton labeled with rhodamine phalloidin. The image represents a maximum projection of the images of a z-stack taken at 1 µm interval. (B,C) 3D reconstruction and surface rendering of details from pollen tube shown in (A). (B) The structure is tilted slightly to reveal the absence of actin in the center of the subapical fringe. (C) Shank region of the tube. (D) 3D reconstruction and surface rendering image of the vesicles at the tip of the pollen tube that were labeled with FM1-43 shown in (E). (F) Merged image of the cone of vesicles and the actin cytoskeleton showing the 3D distribution of the two elements of the same tube. A-C and D-E are images of two different tubes. Bars = 10µm.

In wavy pollen tubes, these bundles located in the shank of the tube had the tendency to follow the shortest way through the cell lumen (Figure 4.3). The fact that thick actin bundles follow the shortest track (Figure 4.3) may be a strategy by the cell to minimize energy spent on the actions of bundling and cytoplasmic streaming or a

mechanical resistance of the bundled actin filaments to bending. The acto-myosin system consumes energy and reducing the distance on which vesicle have to travel to reach the tip or to be transported backwards. Since villins are involved in cytoplasmic streaming (Tominaga *et al.*, 2000) this can connect actin bundling to vesicle trafficking and energy spent in these two processes.

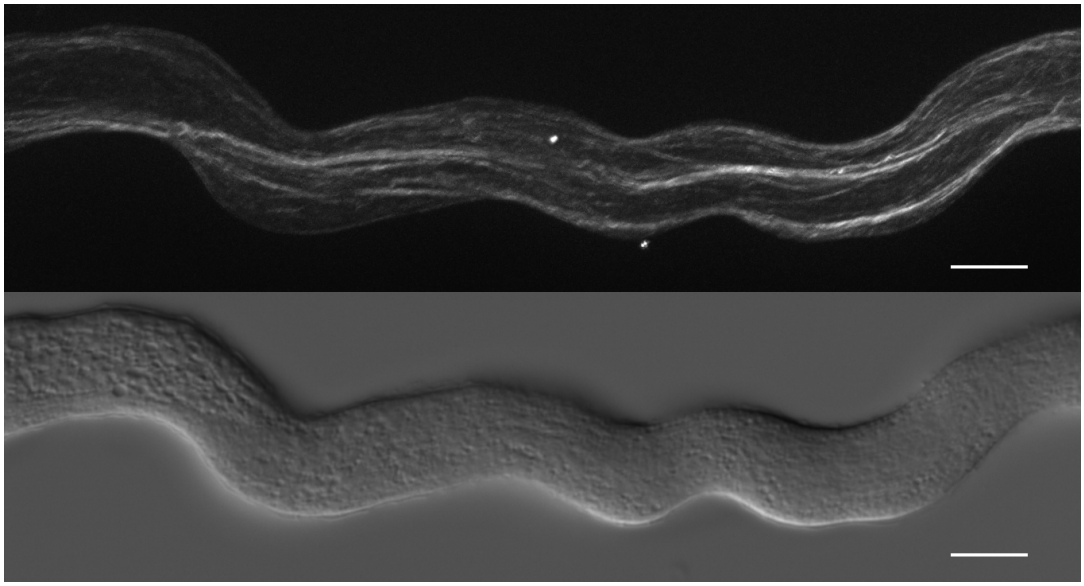

Figure 4.3: Conformation of actin bundles in the shank of an undulating *Camellia* pollen tube labelled with rhodamine phalloidin. Bar = 10 μm.

4.3.3 The dynamic behavior of the actin fringe varies with growth rate

Comparison between the subapical actin fringes of the three pollen tube species investigated here revealed that the structure had the tendency to be shorter relative to the tube diameter and less dense in *Camellia*, and longer in *Arabidopsis*. Incidentally, *Camellia* has the fastest growing pollen tube under *in vitro* conditions and *Arabidopsis thaliana* the slowest among the three species I tested. To assess whether there is any correlation between the velocity of the pollen tube and the shape of the actin fringe, I cultured lily pollen tubes at a temperature of 15°C and compared

their actin fringe to that of lily pollen grown at 24°C (Figure 4.4). The colder temperature reduced the growth velocity in this species since the average pollen tube length of 317±106 μm obtained after 2h at 24°C was reduced to 221±105 μm at 15°C. To quantify the size of the actin fringe, its length along the longitudinal axis of the cell and the surface area of the region occupied by the fringe on images obtained by maximal projection of z-stacks were measured. At 15°C, the fringe length was 9±0.8 μm and the fringe area was 107.0±13.7 μm^2 while for pollen tubes growing at 24°C the fringe length was significantly shorter with 6.6±1.2 μm and its area reduced to 82.8±15.3 μm^2. The differences in fringe length and area were significant ($p<0.02$). Temperature has been shown not to affect actin protein levels in the pollen tube (Åström *et al.*, 1991). Therefore, the change in filament length at the level of the actin fringe is either due to a change in actin polymerization and treadmilling rates or due to differential activity level of actin bundling proteins. Several actin binding proteins (ABP) expressed in the pollen tube regulate actin severing, polymerization and bundling. Among these proteins is the actin depolymerizing factor (ADF) which binds to the pointed ends of the actin filaments and accelerates actin depolymerization at this slow growing end. In conditions where the amount of monomeric actin is limiting, this depolymerization enhances actin polymerization at the barbed or fast growing end (Carlier *et al.*, 1997; Cooper and Schafer, 2000; Bamburg and Bernstein, 2008). ADF is present at the fringe zone of the pollen tube (Chen *et al.*, 2002). At low concentrations, ADF is known to promote actin severing at the pointed end (Yeoh *et al.*, 2002; Andrianantoandro and Pollard, 2006). This may be the reason why expression levels of ADF in different pollen species might affect severing levels and therefore induce actin polymerization by increasing the actin monomer pool. Actin monomers are bound to profilin (Vidali and Hepler, 1997; Gibbon, 2001; Vidali and Hepler, 2001; Wasteneys and Galway, 2003) which binds G-actin and makes it readily available for polymerization. Stability of newly formed filaments is increased by the bundling activity of villin (Friederich *et al.*, 1990). The different growth rates observed in pollen tubes from different species might be

related to differences in metabolic levels and protein expression levels including ABP which could explain the differences in the pollen tube actin fringe length.

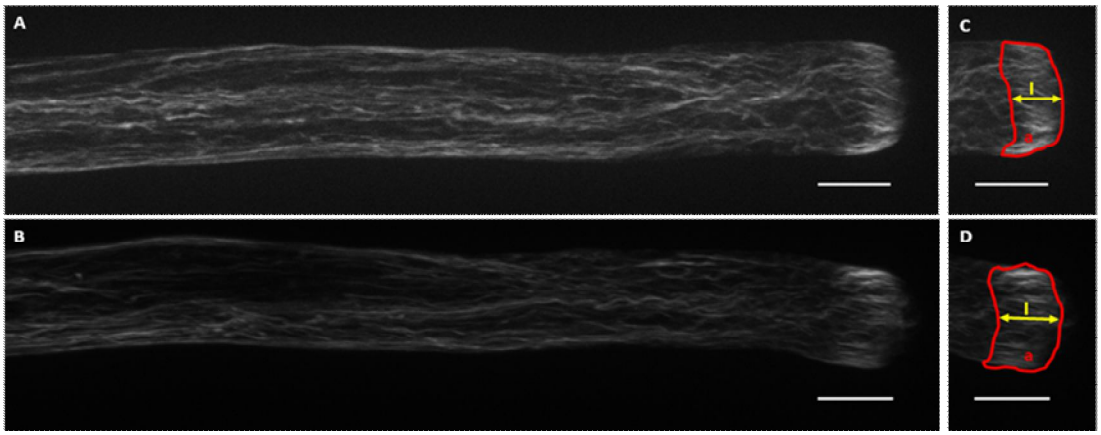

Figure 4.4: Effect of growth temperature on the actin fringe of lily pollen tubes. (A) Pollen tube grown at 24°C and (B) 15°C. (C) and (D) show the measurements made on tubes A and B respectively; the yellow double headed arrow represents the length of the fringe (l) and the red line is the border of the area (a) occupied by the fringe. Bar = 10µm.

Actin filament elongation is the result of interplay between actin polymerization and depolymerization. Actin polymerization is promoted by formins while ADF/cofilins are responsible for actin depolymerization. This interplay affects filament length and pollen velocity. The difference in actin fringe pattern could be explained by different expression levels of these two protein families where filaments are longer in *Arabidopsis* due to a lower turnover, and they are the shortest in *Camellia* where the turnover maybe very high. One piece of evidence supporting this hypothesis is the difference in growth rate between the three species where *Camellia* has the fastest growing pollen tubes while *Arabidopsis* pollen tubes have the lowest velocity *in vitro*.

4.3.4 The actin fringe regulates pollen tube growth and shape

It is intriguing how the pollen tube is able to strictly control its diameter and form a perfectly tubular shape. The actin cytoskeleton and in particular the subapical actin fringe are likely to be crucial in the control of the growth process as they deliver the secretory vesicles to precisely identified sites on the cellular surface as is shown by their complementary 3D locations (Figure 4.2F). In order to identify the role of the actin fringe in maintaining the tubular shape of the pollen tube, we used pharmacological agents that affect the degree of crosslinking between actin filaments. Ethylene glycol bis[sulfosuccinimidylsuccinate] (sulfo-EGS) is known to be a strong actin cross-linker (Lovy-Wheeler *et al.*, 2005; Gossot and Geitmann, 2007). It has been used to block the advancement of the actin fringe in poppy and lily pollen tubes (Gossot, unpublished data). I tested different concentrations of sulfo-EGS on *Camellia* pollen tubes and monitored pollen tube velocity and tip shape. At 500 mM sulfo-EGS, and after just few seconds of application of the drug, pollen tube velocity was decreased by half (from 0.2 to 0.1 μm/sec) followed by a swelling at the tip (Figure 4.5B). After few minutes, pollen tube recovered its original shape (Figure 4.5D) but failed to recover its original velocity during the remaining observation time.

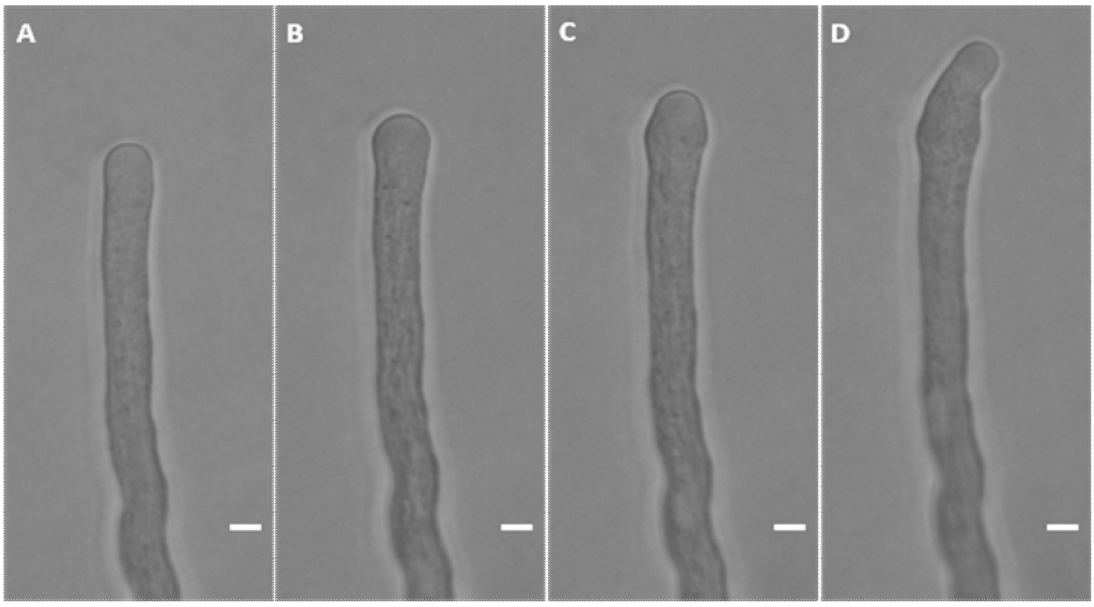

Figure 4.5: Time lapse series of *Camellia japonica* pollen tubes treated with sulfo-EGS. (A) Before the application of the drug, (B) 1 minute after the application, (C) 6 minutes after and (D) 15 minutes after. Bars = 10µm.

To determine how this drug affects the actin cytoskeleton, I labeled sulfo-EGS treated tubes with rhodamine-phalloidin. At 10 minutes of treatment with sulfo-EGS, the pollen tube lost its specific actin conformation at the tip; the actin fringe was lost and the actin arrays in the swelling tip were disorganized (Figure 4.6B). After 20 minutes, the actin arrays seemed to assemble at the very tip of the apical swelling (Figure 4.6C) and subsequently these form a fringe-like structure, that seemed to preceed the recovery of the pollen tube growth in its original diameter in less than 30 minutes (Figure 4.6D).

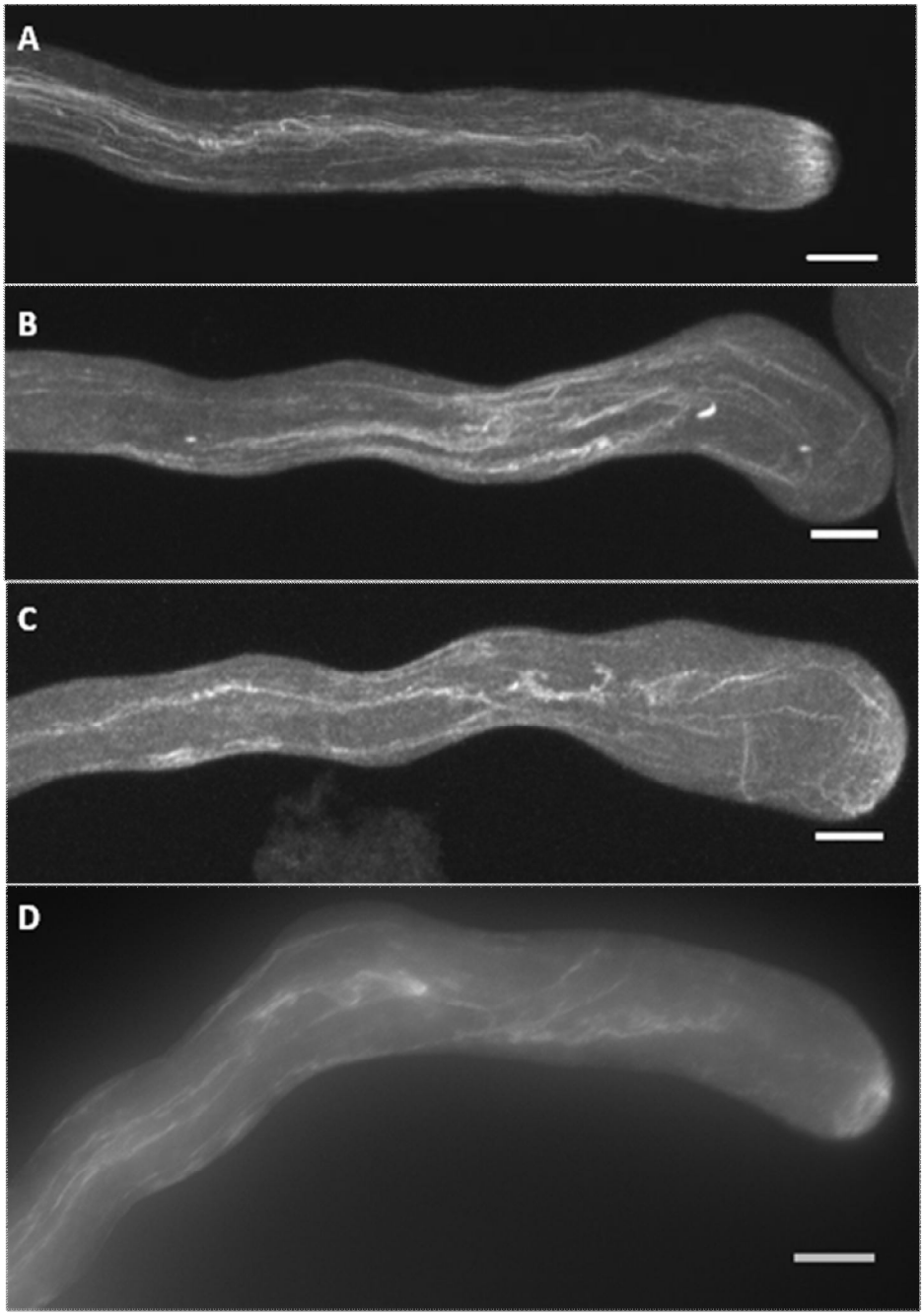

Figure 4.6: Actin cytoskeleton in *Camellia* pollen tubes labeled with rhodamine-phalloidin. (A) control tube. Growing pollen tubes were treated with 500 mM sulfo-EGS (B-D) for 10 (B), 20 (C) and 30 minutes (D). Bar = 10μm.

The reduction in pollen tube growth rate and the loss of its cylindrical shape associated with the loss of the actin fringe and the reassembly of the actin fringe

prior to resumption of pollen tube shape, indicate the importance of the role of this cytoskeletal structure in maintaining the integrity of the pollen tube tubular shape and the normal growth rate.

4.3.5 Role of the actin-myosin mediated vesicle delivery to the tip

From studies in our lab (Bove *et al.*, 2008), we know that secretory vesicles are delivered to precisely identified locations in an annular region around the very tip of the pollen tube. While subsequent vesicle movement through the apical inverted vesicle cone is likely to be based on diffusion and/or convective flow (Kroeger *et al.*, 2009), the delivery to the exocytosis site is probably mediated by the interaction of actin and myosin. Inhibition of myosin activity by 2,3-butanedione monoxine (BDM), an inhibitor of myosin ATPases that acts by stabilizing the myosin–ADP–Pi complex (Palmieri *et al.*, 2007; Radford and White, 2010) slows cytoplasmic streaming as demonstrated on *Chara corallina* and in lily pollen tubes (Tominaga *et al.*, 2000; Funaki *et al.*, 2004). Pollen of *Picea abies* treated with this agent show a concentration dependent reduction in germination and pollen tube elongation rates (Anderhag *et al.*, 2000). In order to interfere with the vesicle delivery to growing zone of the pollen tube, I treated *Camellia* pollen tubes with different concentrations of BDM and assessed its effect on tube elongation, the actin cytoskeleton and cell wall components. 12 mM BDM was the threshold concentration between normal and morphologically affected growth. At this or higher concentrations of the drug, pollen tube growth rate was reduced and accompanied by a swelling at the tip shortly after application of the treatment. At concentrations above 25 mM, pollen tubes stopped growing and a severe swelling followed by pollen tube tip explosion was observed. A balance between turgor pressure and cell wall mechanical properties governs the apical growth of the pollen tube (Chebli and Geitmann, 2007). The reason for bursting may therefore be the BDM induced reduction in the delivery of cell wall material to the expanding cell wall. While the apical cell wall continuously expands

under the effect of the turgor generated hydrostatic pressure, it thins and thus bursts, likely because exocytosis does not take place.

To assess the configuration of the actin cytoskeleton following BDM treatment, I labeled drug treated pollen tubes with rhodamine phalloidin. After 50 minutes of growth in control conditions, *Camellia* pollen tubes were treated with 12 mM BDM and incubated for 10 more minutes after which they were immediately fixed and stained. The highly organized actin fringe was displaced more distally and appeared less organized (Figure 4.7). Remarkably, the clear zone was longer and extended to more than 20 μm from the tip. Facing the clear zone there were thin actin filaments organized in a circular shape. In the shank region of the pollen tube bundling of actin seemed reduced as actin was more homogeneously dispersed through lumen of the cell. We do not know whether this is a direct effect of the drug or whether this is linked to the reduced amount of trafficking on the actin bundles.

The extension of the clear zone together with the distal position of the actin fringe seems to indicate the during BDM treatment, vesicles still get delivered to the tip, but they do not seem to get transported away from the tip, thus accumulating there. This might indicate that rather than affecting forward transport, interfering with myosin functioning reduced in particular rearward transport of vesicles.

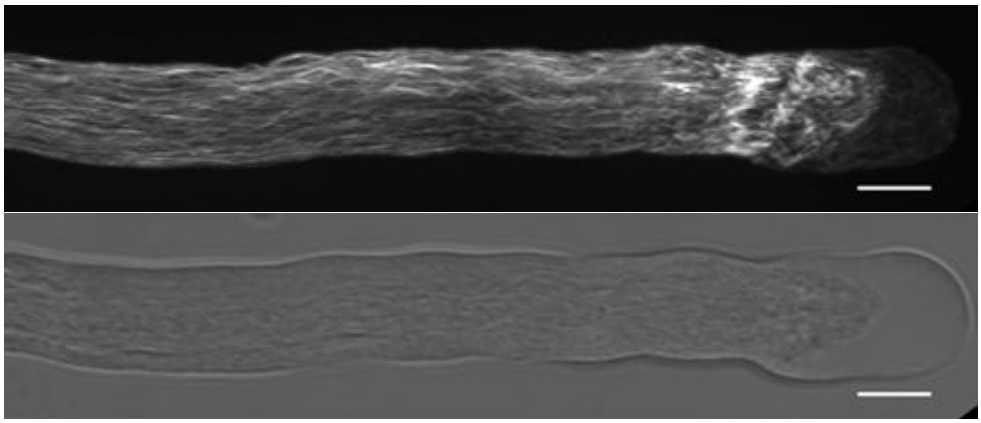

Figure 4.7: Actin cytoskeleton in a *Camellia japonica* pollen tube treated with 12 mM BDM. The upper image is the fluorescent image and the lower one is a DIC image. Bar = 10 μm.

Pollen tube morphology has been shown to be controlled by the mechanical properties of its cell wall (Fayant *et al.*, 2010). Since BDM caused morphological changes, I assessed whether incubation with the drug caused any variations in the cell wall composition of the pollen tube. Using histochemical and immunolabel methods I investigated the distribution of callose, cellulose and pectic components of the cell wall.

Aniline blue treatment of *Camellia* pollen tubes after one hour of growth in the presence of 12mM BDM showed no clear difference in callose distribution between control and treated pollen tubes. Callose was mostly present at the base of the tube and decreased closer to the tip (Figure 4.8), which is typical for growing pollen tubes of most species (Ferguson *et al.*, 1998).

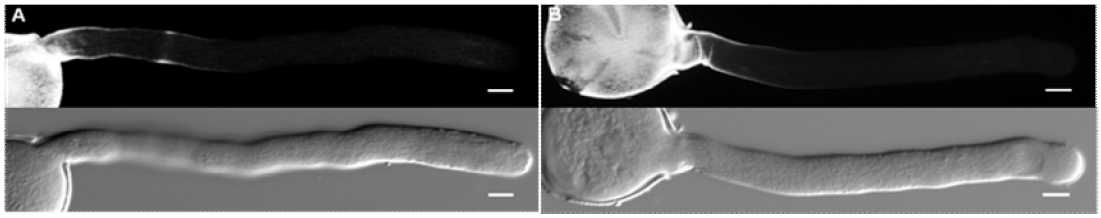

Figure 4.8: Callose staining of *Camellia japonica* pollen tubes with aniline blue. (A) control tube and (B) 12 mM BDM treated pollen tube. Images are median optical sections. Bar = 10 μm.

Calcofluor white label for cellulose revealed an increased cellulose deposition in the normally cellulose free apical region in BDM treated tubes (Figure 4.9). In addition, there seemed to be a cytoplasmic region containing cellulose in the center of the border region separating the clear zone from the rest of the pollen tube. Cellulose was mostly present in the distal part of the pollen tube but less visible in regions closer to the tip than callose (Derksen *et al.*, 2002). Callose and cellulose deposition result from the activity of membrane-localized synthases and cellulose synthesis is activated earlier during the longitudinal maturation of the cell wall than that of callose synthesis (Ferguson *et al.*, 1998; Geitmann and Steer, 2006). Therefore, a reduction in growth rate may allow cellulose synthase activity to "catch

up" with the continuously elongating tip leading to ectopic deposition of visible amounts of cellulose in the apical region.

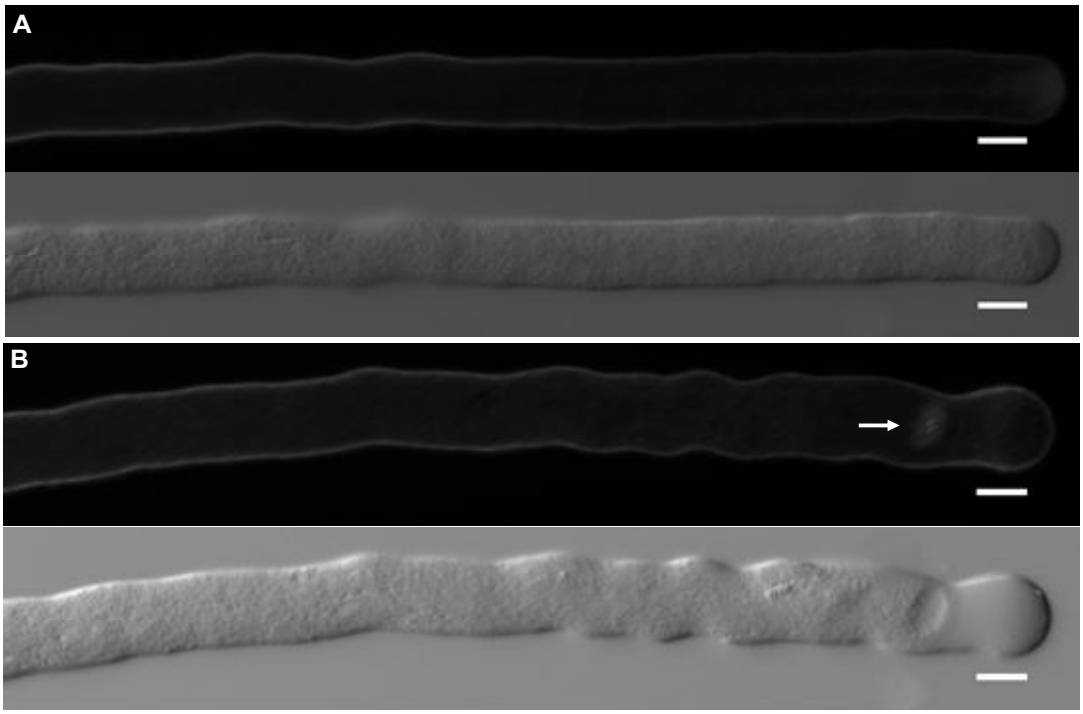

Figure 4.9: Cellulose staining of *Camellia japonica* pollen tubes. (A) control tube and (B) 12 mM BDM treated pollen tubes. The arrow shows a dense subapical cellulose deposition. The upper images are projections of images taken at 1 µm interval. Bar = 10 µm.

Immunolabeling of pectins revealed that methylesterified pectins (labeled with JIM7 monoclonal antibody) in BDM treated tubes showed the same labeling pattern as the control (Figure 4.10A,B). Label for non-esterified pectins (JIM5 monoclonal antibody) was clearly different, however. While non-esterified pectins were absent at the tip of control *Camellia* pollen tubes, they were present at the tip of the BDM treated tubes (Figure 4.10C,D).

This phenomenon can possibly be explained the behavior of the enzyme pectin methyl esterase (PME). During maturation of the apically deposited pectic cell wall, this enzyme de-esterifies pectin molecules allowing them to be cross-linked by Ca^{2+} resulting in the formation of a relatively stiff three dimensional pectate gel.

PME is deposited at the apex together with its target molecule and catalyses the de-esterification in time-dependent manner. A slower growth rate might result in PME activity to "catch up" with the elongating apex leading to visible amounts of acidic pectin in this region. Alternative, and not mutually exclusive is an explanation that is based on the fact that the activity of different isoforms of PME is affected by the pH of the apoplast (Bosch and Hepler, 2005) which could be different as a result of the drug treatment.

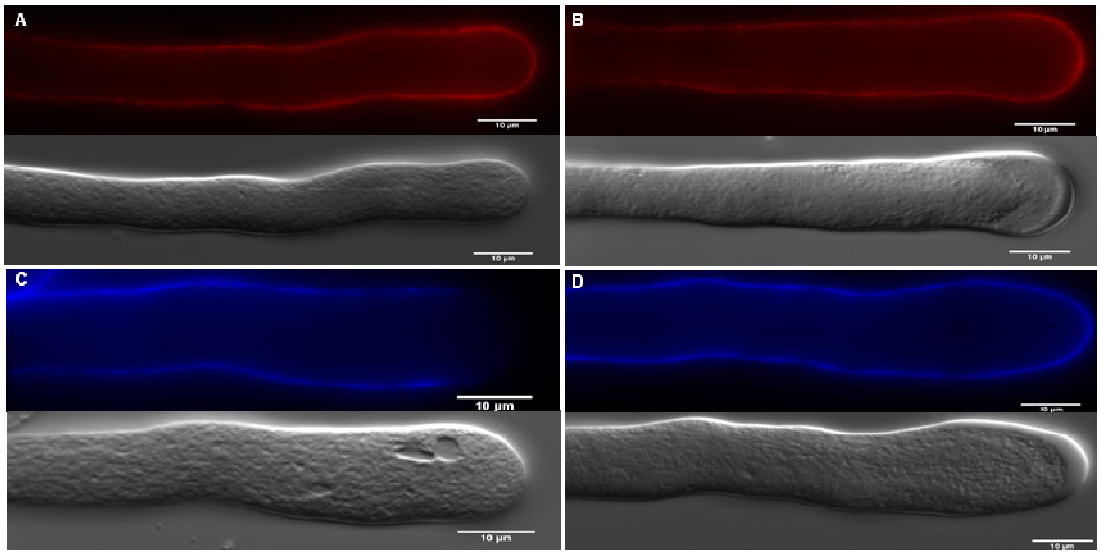

Figure 4.10: Effect of disruption of vesicle transport by BDM on the distribution of esterified (A,B) and non-esterified (C,D) pectins in the cell wall of *Camellia japonica* pollen tubes. A and C represent the controls and B and D represent the 12 mM BDM treated pollen tubes. Upper images are median optical sections. Bars = 10 µm.

4.4 Conclusion

The pollen tube actin cytoskeleton is strongly involved in the regulation of pollen tube growth and architectural integrity. The actin fringe located at the subapex of the pollen tube is the site of high actin dynamics. The use of cross linkers that block the actin fringe strongly reduced pollen tube growth and induce a swelling at

the tip of the tube. The tube recovered its shape preceded by a progressive reconstruction of the actin mesh at the subapex. Normal rates of vesicle delivery are crucial for a growing pollen tube. Any modification in the rate of delivery of secretory vesicles is likely to affect the entire machinery controlling pollen tube growth. After the treatment with the BDM, the actin conformation changed, the actin fringe shifted location and the clear zone increased in volume due to changes in the vesicle transport pattern.

5 Actin regulates pollen tube tropism through redirection of secretory vesicles

I wanted to investigate the role of the actin cytoskeleton and calcium ions in controlling the capacity of the pollen tube to change its growth direction and hence to respond to an external signal. I devised an assay that allowed me to apply a directional signal in precisely timed and calibrated manner and to assess the detailed time course of events associated with the cellular response. *In vitro* grown pollen tubes were exposed to an electrical field and their response was monitored using brightfield and fluorescence microscopy. Different treatments that interfere with cytoskeleton integrity or calcium channels were also used and the responses monitored.

The article was submitted to the journal Traffic

Actin regulates pollen tube tropism through redirection of secretory vesicles

Firas Bou Daher and Anja Geitmann*

Abstract

In order to accurately target the embryo sac and deliver the sperm cells, the pollen tube has to find an efficient path through the pistil and respond to precise directional cues produced by the female tissues. Although many chemical and proteic signals have been identified to guide pollen tube growth, the mechanism by which the tube changes direction in response to these signals is poorly understood. We designed an experimental setup using a microscope mounted galvanotropic chamber that allowed us to induce the redirection of in vitro pollen tube growth through a precisely timed and calibrated external signal. Actin depolymerization, reduced calcium concentration in the growth medium and inhibition of calcium channel activity decreased the responsiveness of the pollen tube to a tropic trigger. An increased calcium concentration in the medium enhanced this response and was able to rescue the effect of actin depolymerization. Time lapse imaging revealed that the motion pattern of vesicles and the dynamics of the subapical actin array undergo spatial reorientation prior to the onset of a tropic response. Together these results suggest that the precise targeting of the delivery of new wall material represents a key component in the growth machinery that determines directional elongation in pollen tubes.

Key words

Pollen tube, galvanotropism, actin, calcium, vesicle, tip growth.

5.1 Introduction

Cellular differentiation often entails changes to cell shape. These shape changes can affect the overall aspect ratio of the cell dimensions or give rise to complex geometric features. The formation of cellular protrusions is an important example of a morphogenetic process that in numerous cell types is crucial for attaining full functionality. Cellular protrusions typically allow the cell to reach out into other areas of the organism or the surrounding environment. This activity can have different purposes such as making contact with other cells or tissues, exchanging signals, transporting material over long distances or finding sources of water and nutrients. In mammals, the growth of neuronal growth cones is an extreme example of a cellular protrusion formed with the aim of reaching distant regions of the organism. In plant and fungal cells, in which cellular migration is prevented by a relatively stiff cell wall, reaching out is the only way for cells to move. Cellular protuberances formed by walled cells are generally cylindrical extensions with approximately hemisphere-shaped ends. In fungi, hyphal extensions elongate rapidly and they are able to colonize the soil, plant roots or any other substance providing nutrients (Gow, 1994; Riquelme et al., 1998). In plants, typical cellular protuberances include root hairs, unicellular trichomes, and pollen tubes. Although neuronal axons, fungal hyphae and pollen tubes are evolutionary distant, they share a common feature that enables them to direct their elongation growth towards particular targets: the capacity to respond to directional cues and display tropic behaviour. Rapid redirection of cellular growth relies on a specialized growth mechanism: tip growth. Contrary to the diffuse expansion characterizing determinate protuberances such trichomes, in tip growing cells all growth activity is confined to the extreme end of the cell (Harold, 1997; Bachewich and Heath, 1998; Alessa and Kropf, 1999; Gomez and Spitzer, 1999; Baluška *et al.*, 2000; Geitmann and Ortega, 2009). This spatially confined expansion allows for instant changes in growth direction upon the perception of vectorial signals (Geitmann, 2010). In order to execute this redirection,

the machinery generating the polar growth activity must be reoriented in space. Although we have an increasingly detailed understanding of the molecular players involved in the perception of directional signals in plants (Geitmann and Palanivelu, 2007; Mortimer *et al.*, 2008; Mortimer *et al.*, 2009; Stewman *et al.*, 2010), many questions remain on how exactly the growth machinery is redirected in walled cells.

Cellular expansion in plant cells is driven by the internal hydrostatic pressure, the turgor. Turgor is generally recognized to be the motor, but not the controller of plant cell growth (Schopfer, 2006), even though local increases in turgor were purported to be able to direct cellular growth in plants (Zonia *et al.*, 2006). However, since pressure is a scalar quantity and not a vector quantity it is safe to state that morphogenesis in walled cells is regulated by the spatial distribution and anisotropy of mechanical properties in the cell wall (Geitmann and Ortega, 2009; Fayant *et al.*, 2010; Winship *et al.*, 2010). Spatial biomechanical gradients in the primary wall of individual plant cell are generated by two processes: the spatially targeted delivery of new, relatively softer cell wall material and the maturation and hence stiffening of cell material through enzymatic action causing cross-linking between cell wall polymers. Insertion of soft material promotes expansion; cross-linking reduces it. In tip growing plant cells, both processes occur in close spatial proximity with the delivery of soft material being focused to the pole of the cell and the annular region around it (Bove *et al.*, 2008; Zonia and Munnik, 2008; Geitmann and Dumais, 2009) and the rigidification occurring in the transition region linking the hemisphere shaped apex and the cylindrical shank (Fayant *et al.*, 2010). The targeting of both cell wall material and cell wall modifying enzymes to the apex of the cell is, therefore, crucial for tip growth. It is ensured by the long-distance transport of secretory vesicles towards the apical cytoplasm and the subsequent exocytosis that deposits the material into the existing wall. The intracellular delivery of vesicles towards the apex is mediated by the actin cytoskeleton thus pointing at this cytoskeletal array as a potential regulator of material targeting and thus controller of the growth machinery. However, this concept is awaiting experimental proof.

To investigate the mechanism of growth redirection in walled cells, we examined this process in pollen tubes, the cylindrical extensions formed from pollen grains. Efficient directional growth of the tube towards the ovule, located deep within the pistillar tissues, necessitates several drastic changes in growth orientation in response to a variety of cues that are of mechanical, chemical, proteic and physical nature (Geitmann and Palanivelu, 2007). Genetic and physiological studies have shown that both the pistil and the female gametophyte produce directional signals (Higashiyama *et al.*, 2003; Tung *et al.*, 2005; Higashiyama and Hamamura, 2008; Dresselhaus and Márton, 2009; Qin *et al.*, 2009; Márton and Dresselhaus, 2010), but it is not clear how the pollen tube perceives these signals and how they are translated into changes in growth direction. Signaling pathways involving receptor kinases and cell membrane-associated small G proteins along with variations in ion fluxes are likely to be involved in the reorientation response (Muschietti *et al.*, 1998; Hepler *et al.*, 2001; Kaothien *et al.*, 2005), but all signaling pathways must eventually effect a change in a mechanical structure of the cell to accomplish a change in growth behavior.

In angiosperm pollen tubes, material carrying vesicles are delivered to the growing tip in an inverse fountain shaped, cytplasmic streaming pattern that results in the aggregation of vesicles in a cone-shaped region within the apical cytoplasm (Parton *et al.*, 2001; Bove *et al.*, 2008; Zonia and Munnik, 2008; Geitmann and Dumais, 2009). The vesicles in the center of this cone-shaped aggregation display movement in rearward direction and correspond either to vesicles that had failed to undergo exocytosis and or to those taken up by endocytosis at the pole of the cell (Bove *et al.*, 2008). The delivery of vesicles towards the apex on the other hand occurs in the periphery of the tube, towards a region forming an annulus around the pole of the pollen tube tip. This annulus is thought to correspond to the region of highest exocytosis (Bove *et al.*, 2008; Zonia and Munnik, 2008). It coincides with the front end or leading edge of the cortical actin fringe, a dense array of actin filaments dominating the periphery of the subapical cytoplasm in growing pollen tubes (Lovy-

Wheeler *et al.*, 2005). Actin filaments in the periphery of the fringe point forward with their barbed ends, whereas actin arrays in the central region of the cell point rearward (Lenartowska and Michalska, 2008) thus enabling the myosin-driven bidirectional motion of vesicles (Cai and Cresti, 2008; Kroeger *et al.*, 2009). The cone-shaped aggregation of vesicles is known to tilt during a reorientation of pollen tube growth (Camacho and Malhó, 2003; Bove *et al.*, 2008), but whether this occurs before or after the change in the pollen tube geometry has not been determined in detail. It is equally unclear whether this deviation from the radial symmetry is accompanied by or possibly even a result of a change in the spatial configuration of the actin fringe. Here we investigated at high spatial and temporal resolution how changes in vesicle flow pattern and spatial configuration of the subapical actin array are connected to effect a redirection of pollen tube growth. To analyze the time-course and causality of events, we also assessed the role of calcium, an ion that has the potential to influence the turning response at several levels. It functions as a cross-linker of pectin molecules (Jarvis, 1984; Carpita and Gibeaut, 1993) and may thus be involved in determining the spatial profile of the cell wall mechanical properties. The ion also enters the pollen tube cytoplasm by way of tip-localized calcium channels (Pierson *et al.*, 1994; Pierson *et al.*, 1996) resulting in a tip-focused cytosolic calcium gradient the presence of which is required for pollen tube growth (Pierson *et al.*, 1994). To reproducibly trigger a turning response in growing pollen tubes, we used a galvanotropic setup designed to operate in a confocal laser scanning microscope allowing for time lapse imaging of vesicle motion patterns and actin filament dynamics.

5.2 Results

5.2.1 Application of an electrical field induces a reproducible, tropic response in *Camellia japonica* pollen tubes

In planta, growing pollen tubes orient their growth direction in response to chemical and mechanical cues. However, chemical signals have the disadvantage of having to diffuse which is a difficult to control, time-dependent process. To allow us to switch on and off a directional trigger at precisely determined points in time and at exactly defined parameter settings, we used an electrical trigger, which has been shown to induce tropic behavior in pollen tubes (Nakamura *et al.*, 1991; Malhó *et al.*, 1992). We devised a miniature electrophoresis chamber which can be mounted on an inverted microscope (Figure. 5.1A) to allow live observation.

For most experiments, we used pollen from *Camellia japonica*, a species forming large pollen tubes that grow extremely straight under in vitro conditions. With the current switched off, *Camellia japonica* pollen was placed in a line parallel to the future electrical field (Figure. 5.1A) resulting in pollen tubes growing mostly perpendicular to the field (Figure. 5.1B). After 105 minutes of undisturbed growth, the electrical field was switched on and left on for 10 minutes. To confirm that the resulting reorientation of the growth direction was not arbitrary but a result of the electrical field, in several experiments the orientation of the field was reversed after 10 min. In all cases, this reversed the direction of the response (Figure. 5.1C). To assess pollen tube response, we quantified the percentage of pollen tubes displaying a change in growth direction, the angle between new and old growth direction, and the time delay between application of the field and appearance of the first change of outer morphology (Figure. 5.1C). In preliminary trials, different voltages had been tested. 1.5 V/cm was the optimal setting at which 35% of the tubes responded by changing their growth direction towards the cathode. No tubes were observed to turn towards the anode. At higher current potentials, pollen tubes exploded and at lower

voltages no visual effect was observed. At 1.5 V/cm, two populations of pollen tubes could clearly be distinguished. One population of tubes turned with an average angle of 19.95±4.15° (Figure. 5.2), the other did not turn visibly within the observation time. Within the population displaying a turning response, the average response time between application of the electrical field and onset of the redirection was 209 seconds (Figure. 5.3; $n > 100$). Importantly, the growth rate was not affected by the electric field. Neither the growth rate between trigger and onset of response nor that after onset of the growth redirection was statistically different from the growth rate before application of the field (Figure. 5.4).

5.2.2 Modification of the calcium concentration in the growth medium affects the tropic response

Calcium is taken up by pollen tubes at the growing apex (Feijó *et al.*, 1995) resulting in a strong tip-focused gradient of the ion in the cytoplasm (Pierson *et al.*, 1994). Changing the spatial distribution of this gradient causes the pollen tube to change its growth direction (Malhó *et al.*, 1992). Dissipation of the calcium gradient causes growth arrest (Pierson *et al.*, 1994) confirming that calcium is a crucial element in the signaling pathway controlling both growth rate and growth direction. Therefore, we wanted to assess whether altering the calcium concentration in the growth medium would affect the behavior of *Camellia* pollen tubes upon a galvanotropic trigger.

To culture *Camellia japonica* pollen tubes in vitro, we used a standard growth medium (Gossot and Geitmann, 2007) that had been optimized for this species by modifying the calcium concentration to be 2.54 mM (in form of calcium nitrate). This modified medium consistently yielded a germination percentage of approximately 87% and, after one hour of incubation, the *Camellia* pollen tubes had an average length of 380 µm (Figure. 5.5). To determine the range of calcium concentrations within which growth rate would not be affected dramatically, we

determined the dose-dependence of the behavior of *Camellia* pollen in the absence of an electrical field. Growth media containing half of the optimized calcium concentration (1.27 mM) or twice the optimal concentration (5.08 mM) caused mild reductions in germination percentage by about 10%, while the tube elongation was reduced by 14 and 19%, respectively (Figure. 5.5). This behavior is consistent with the postulated optimal calcium range within which the response of pollen tubes to concentration changes is known to be minor (Brewbaker and Kwack, 1963; Picton and Steer, 1983; Steer and Steer, 1989; Holdaway-Clarke and Hepler, 2003; Bou Daher *et al.*, 2009). Outside of this range, *Camellia* pollen tube growth was affected dramatically, as was demonstrated by the presence of very short tubes with morphological aberrations in growth medium without added calcium.

To test the effect of altered calcium concentration on the galvanotropic response, we compared pollen tube redirection in the optimal medium (2.54 mM calcium) to that in media with higher (5.08 mM) and lower (0.63 mM) calcium concentrations. Lowered calcium decreased the percentage of responsive pollen tubes to 25% and increased the response time to 268 seconds. Increased calcium on the other hand, did not statistically alter the percentage of responsive tubes (35%), but the response time was strongly reduced to 159 seconds (Figure. 5.3). In both cases, the average deviation angle of the responsive tubes did not differ significantly from that in the control treatment (Figure. 5.2).

The cytosolic calcium gradient in the pollen tube has been shown to be dissipated by the application of calcium channel blockers (Malhó *et al.*, 1995). This treatment also affects pollen tube growth (Malhó *et al.*, 1994; Malhó and Trewavas, 1996; Geitmann and Cresti, 1998). To test whether the effect of calcium on the galvanotropic behavior of *Camellia* pollen tubes was due to the activation of putative surface receptors or whether it necessitated the channel mediated passage of calcium into the cytosol we partially blocked calcium channels using lanthanum chloride (La) (Malhó *et al.*, 1995; Malhó and Trewavas, 1996; Geitmann and Cresti, 1998; Qu *et*

al., 2007). Preliminary tests had shown that at a concentration of 1 µM, La only slightly decreased pollen tube length when assessed after one hour of incubation. In the presence of 1 µM La, the average deviation angle of pollen tubes upon application of the galvanotrigger was not different from any other treatment (Figure. 5.2), but the percentage of responsive tubes was reduced to 21.5% ($p<0.05$) and the response time significantly increased to 273 seconds (Figure. 5.3). Doubling the calcium concentration in the growth medium in the presence of La was able to rescue the La induced reduction in response time to a value similar to that obtained with the control medium (219 seconds), while the percentage of responsive tubes increased only slightly to 24% (Figure. 5.3).

5.2.3 Reducing the polymerization rate of actin filaments affects the tropic response

The pollen tube cytoskeleton has two main components: microtubules and actin microfilaments (Geitmann and Emons, 2000). Microtubules do not seem to be directly involved in pollen tube tip growth, since inhibition of their polymerization does not prevent pollen tube elongation (Åström *et al.*, 1995; Gossot and Geitmann, 2007). However, depolymerization of the microtubule cytoskeleton results in straighter tubes in poppy indicating a potential role for this cytoskeletal element in the execution of turning events (Gossot and Geitmann, 2007). Actin on the other hand is crucial for pollen tube growth in general, as revealed by inhibitors that interfere with actin polymerization (Vidali and Hepler, 2001; Gossot and Geitmann, 2007). This role is most likely linked to the involvement of actin in vesicle and organelle transport. However, elongation of pollen tubes is inhibited at much lower concentrations of actin drugs than those required to impede long distance organelle movement. Therefore, actin also seems to be more directly involved in the growth process, but this role remains to be defined.

To assess whether the pollen tube cytoskeleton is involved in the execution of a change of growth direction in the pollen tube, we pharmacologically disrupted microtubule and microfilament functioning. Latrunculin B (LatB) is a toxin isolated from the red sea sponge *Latrunculia magnifica* that sequesters G-actin leading to F-actin depolymerization due to treadmilling (Gibbon *et al.*, 1999). Since pollen tube growth is very sensitive to actin depolymerization, we needed to identify a concentration of LatB that would only mildly interfere with *Camellia* pollen tube elongation. For this purpose, germination percentage, tube growth (Figure. 5.6), and configuration of actin arrays (Figure. 5.7) were assessed after one hour incubation with various concentrations of the drug. Germination percentage of *Camellia* pollen was reduced by half at 5 nM LatB and higher concentrations were almost completely lethal (Figure. 5.6). At concentrations as low as 1 nM LatB, pollen tube length was moderately reduced although germination percentage was not affected (Figure. 5.6). Phalloidin labelling of the actin cytoskeleton revealed that 1 nM LatB treated tubes seemed indistinguishable from the control as the apical actin fringe and the subapical actin bundles were not visually affected (Figure. 5.7A,B). At higher LatB concentrations, the density of actin filaments in the region close to the apex was reduced (Figure. 5.7C,D). In the galvanotropic setup, the presence of 1nM LatB resulted in a significant reduction in the percentage of responsive pollen tubes (16.8%), and a significant increase in the response time to 272 seconds ($p=<0.05$) (Figure. 5.3). This suggests that the actin cytoskeleton is involved in the execution of a tropic response.

Oryzalin, a dinitroaniline herbicide, has high affinity to tubulin monomers resulting in the degradation of the microtubules (Morejohn *et al.*, 1987). Since inhibition of microtubules is known to fail to interfere with pollen tube growth, we exposed growing pollen tubes to 1 µM oryzalin, a concentration that caused complete disruption of microtubule arrays in *Camellia* pollen tubes as evidenced with immuno-fluorescence label (Figure. 5.8). To ascertain the specificity of the drug effect, we labelled the actin cytoskeleton in oryzalin-treated pollen tubes using

rhodamine-phalloidin. The configuration of the actin cytoskeleton was indistinguishable from that of control tubes (Figure. 5.9). As expected, 1 μM oryzalin did not alter the pollen tube growth rate in *Camellia* (Figure. 5.4). Using the drug in the galvanotropic setup revealed that neither the percentage of responsive pollen tubes (32%) nor the time delay between trigger and response (209 seconds) were different from the control treatment (Figure. 5.3). This suggests that microtubules have no visible effect on the galvanotropic response of the pollen tube *in vitro*. In both LatB and oryzalin treated samples, the average change in growth direction of responsive tubes (20°) was not significantly different from that of the control treatment (Figure. 5.2).

5.2.4 The effect of drug mediated scavenging of actin monomers can be rescued by calcium

The polymerization of actin filaments is calcium dependent since the ion controls the activity of various actin binding proteins (Vidali and Hepler, 2001; Ren and Xiang, 2007; Chen *et al.*, 2009). Since increasing the calcium concentration accelerated the tropic response and mild inhibition of actin polymerization delayed it, we wanted to test whether one treatment could compensate for the effect of the other. We assessed the galvano-response of pollen tubes grown in a medium supplemented with 1 nM LatB and 5.08 mM calcium. The number of tubes displaying a response was significantly higher than that of tubes exposed to LatB alone (Figure. 5.3) and the response time decreased to the same value (209 seconds) as that of the control without drug and normal calcium concentration (Figure. 5.3).

5.2.5 Vesicle transport patterns change preceding pollen tube redirection

Growth events in plant cells are preceded by a relaxation of the cell wall (Lockhart, 1965; Cosgrove, 1993; Cosgrove, 2000). This principle was shown to be

true in pollen tubes by temporal and spatial correlation studies which revealed that a reduction in cellular stiffness precedes the apical expansion of the cell wall (Zerzour *et al.*, 2009). This concept is not uncontested, however, since local increases in turgor pressure have been proposed to be responsible for the spatially confined expansion of the pollen tube cell wall at the apex (Zonia *et al.*, 2006). If turgor was able to locally deform the cell wall, then delivery of new cell wall material to the apex would simply be a compensatory mechanism to prevent cell wall failure wherever the cell wall expands. If spatial control of growth activity was associated with active manipulation of cell wall mechanics on the other hand, the delivery of new cell wall material would likely have the important function of controlling the local mechanical properties of the wall through the targeted addition of soft or fluid wall material. If the "local turgor" hypothesis was applicable, one would expect the secretory machinery to follow a reorientation in growth direction, whereas according to the "cell wall" hypothesis the secretory machinery should reorient prior to such a new direction of cell expansion.

To distinguish between these two hypotheses, we monitored the spatial orientation of the cone-shaped aggregation of vesicles in the pollen tube apex preceding galvano-induced reorientation of the growth response. To obtain a precise time course of events, we labeled vesicles with FM1-43 at 15 minutes prior to the administration of the galvanotropic trigger. Time lapse imaging with the confocal laser scanning microscope revealed that switching on the electrical field did not visibly alter intracellular vesicle dynamics (not shown). However, during the delay period between application of the electric trigger and redirection of growth, the location and orientation of the apical inverted cone of vesicles changed. The inverted vesicle cone started reorienting towards the cathode prior to a visible change in outer cell geometry suggests that secretory vesicles were now targeted to an annular location that was tilted towards the cathode (Figure. 5.10A). To quantify this shift in the vesicle targeting we monitored the spatial profile of the fluorescence intensity in the periphery of the vesicle cone (Figure 5.10C,B). In a straight growing tube, the

cathodal and anodal sides of the pollen tube periphery had similar fluorescence intensity profiles that were characterized by a maximum at 2 µm meridional distance from the pole and a local minimum at the pole (0 µm meridional distance). At 17.2±4.4 sec (n=5) seconds prior to the morphological deviation from radial symmetry, this local minimum and the two maxima began to shift resulting in the local minimum to being located at approximately 2 µm off the symmetry axis towards the cathodal side (Figure. 5.10B image 126s). Given an average tube diameter of 18 µm, this corresponds to a lateral shift of approximately 13° on the hemisphere shaped apex by the time a morphological asymmetry became visible. The fact that this value was lower than the final turning angle of 20° suggests that the tilting of the growth machinery is a gradual process that continues after the initiation of asymmetric cell wall expansion.

5.2.6 Actin fringe remodeling precedes the change in pollen tube direction

Since the actin cytoskeleton is responsible for vesicular transport and delivery to the growing apex, we wanted to assess whether the reorientation of the apical vesicle cone, and thus vesicle targeting, was caused by a change in the configuration of the actin arrays. *Camellia japonica* pollen tubes do not have a known gene expression promoter and do not express genes under the control of Lat52 (Twell *et al.*, 1990) or zmC13 (Hamilton *et al.*, 1998), two widely used, pollen tube specific promoters. We therefore used lily pollen tubes transiently transformed with lifeact (under the zmC13 promoter control) to visualize actin (Figure. 5.11). The targeting of vesicles towards the annular site of exocytosis (Geitmann and Dumais, 2009) is likely accomplished by the forward pointing ends of the actin filaments forming the leading edge of the subapical actin fringe (Cardenas *et al.*, 2008). We therefore measured the density of actin filaments at the front end of the fringe across the diameter of the tube. Before application of a galvanotrigger, the fluorescence intensity profile across the tube was approximately symmetrical. After application of

the galvanotrigger, but prior to pollen tube redirection, the density of actin filaments became higher on the anodal side suggesting that the leading edge of polymerizing actin filaments had advanced further into the tip in this half of the tube (Figure 5.11B,C). This change in actin array symmetry likely resulted in delivery of vesicles further towards the pole in the anodal side leading to an off-center displacement of the delivery of new cell wall material.

5.3 Discussion

Shape changes during cellular morphogenesis in plants generally occur in order to endow the cell with a particular functionality. In many cases, these shape changes alter the aspect ratio, for example by generating long fibers (high flexibility despite tensile resistance) or large vessel elements (efficient water transport). Although these shape changes are influenced by environmental conditions and interaction with neighboring cells, they typically do not represent spatially oriented responses to directional signals at the single cell level. Even during organ curvature following a gravitropic or light signal, the individual cells of a shoot or a root expand differentially but are not directed in relation to the vector of the external trigger. Only a few plant cell types have been identified to display growth activities that occur as directional responses to vectorial cues and that can thus be classified as tropic at the cellular level. These cell types represent excellent model systems for the investigation of the spatial control of plant cell growth.

5.3.1 An electrical field induces directional growth in pollen tubes

Electrical fields are clearly able to modulate the behavior of many cell types. For example cell division in human epithelial cells (Zhao *et al.*, 1999) and growth in chicken neurites are affected by electrical fields (Jaffe and Poo, 1979). In addition, hyphae of *Candida albicans* (Crombie *et al.*, 1990; Brand *et al.*, 2007) and several filamentous fungi (McGillivray 1986, Gow 1994, Lever 1994) display galvanotropic behaviour which was shown to be dependent on the activity of calcium channels

(Brand 2007, Lever 1994). Earlier studies on pollen tubes successfully used electrical fields in the range of 0.5-2 V/cm to reorient growth (Wang *et al.*, 1989; Nakamura *et al.*, 1991; Nozue and Wada, 1993). With an optimal response at 1.5 V/cm, the *Camellia* pollen tubes tested here responded in a similar range of electrical potential as the pollen tubes of other plant species confirming that our conditions were appropriate. Despite the multitude of earlier studies, it remains poorly understood how the cell perceives the electrical signal. It has been proposed that as a result of exposure to an electrical field, ions in the growth matrix are driven by electrophoresis and move to form gradients to which the cell responds (Malhó *et al.*, 1992). For a chemical gradient to be responsible for reorientation in our experimental setup, it would have to be established within the observed delay time between trigger and growth response, i.e. less than 2 min. Whether electrophoresis would be able to generate a significant chemical gradient within such a short time remains to be elucidated since available data on calcium gradients were obtained after much longer times of exposure to an electrical field (Malhó *et al.*, 1992).

Another hypothesis proposes that the electrical field induces electrophoretic displacement of ions or molecules within the cell. However, *Camellia japonica* pollen tubes in our experiments moved solely to the cathode, a behavior that would be inconsistent with the fact that the cell surface and most of the cellular constituents are negatively charged (Weisenseel *et al.*, 1975; Bosch and Hepler, 2005) and would therefore rather be expected to move towards the anode. Alternatively, the application of the electrical field may depolarize the side of the pollen tube facing the cathode (Robinson, 1985), thus opening voltage gated calcium channels at this location, a phenomenon that has been described in yeast and filamentous fungi (Lever *et al.*, 1994; Brand *et al.*, 2007). This would increase the conductance of the plasma membrane for calcium ions at the cathodal side. This phenomenon has been observed in mouse neuroblastoma cells subjected to electrical fields between 1 and 10 V/cm (Bedlack *et al.*, 1992). Whatever the precise molecular mechanism, the electrical trigger has proven to be an excellent tool to study tropic behavior of pollen

tubes because it is immediate, specific, reproducible and does not affect pollen tube growth rate.

5.3.2 Calcium affects pollen tube growth and tropism

Calcium ions are required for in vitro pollen germination and elongation in most plant species (Brewbaker and Kwack, 1963; Picton and Steer, 1983; Li *et al.*, 1999; Bou Daher *et al.*, 2009). Pollen tubes are known to follow gradients in calcium concentration in vitro (Mascarenhas and Machlis, 1964; Reger *et al.*, 1992) and likely also in vivo (Ge *et al.*, 2009). A tip focused, tip high Ca^{2+} gradient is established in the cytosol of the growing pollen tube (Pierson *et al.*, 1994; Feijó *et al.*, 1995) and any disruption of this gradient causes inhibition of growth. Calcium affects various processes involved in pollen tube growth and signalling (Trewavas and Malhó, 1998; Cheung and Wu, 2008; Zhou *et al.*, 2009). Although growth in *Camellia* pollen tubes was only mildly affected by changes in the external calcium concentration within the tolerance range, their ability to respond to a tropic trigger was strongly calcium dependent. Importantly, the shortened response time observed at increased calcium concentration was not due to a faster growth rate because at this higher calcium concentration, pollen tubes actually grow slightly slower than under control conditions (Figure. 5.5). This means that directionality is more sensitive to calcium than growth rate per se. The question is how does calcium act to accomplish a change in growth direction? Does it act on the outside of the cell or does it enter the cell? Calcium has the ability to cross-link cell wall polymers. A rigidification of the wall on one side of the cell could putatively lead to the redirection of tip growth in the opposite direction. However, since calcium stiffens the wall, the bend would occur in the direction of the lower calcium concentration in the case of a concentration gradient (Steer and Steer, 1989). Since tubes bend towards the cathode, and a putative, electrophoresis-induced calcium gradient in the medium would be high at the cathode, this explanation does not seem to hold. On the other hand, the electrical field could cause calcium ions to leach out of the cell wall on the cathodal

side of the tube thus potentially causing a weakening of the cell wall at this side. Proof for this hypothesis would require quantification of the local calcium concentration in the cell wall and biomechanical tests of the effect of calcium concentration on cell wall mechanical properties.

A more likely scenario is the asymmetric uptake of calcium in tubes exposed to an electrical field. The characteristic tip-high cytosolic calcium gradient is fed by calcium ions taken up through membrane located channels at the tip of the tube (Dutta and Robinson, 2004; Wang *et al.*, 2004) at least some which are voltage activated (Shang *et al.*, 2005; Qu *et al.*, 2007). Certain stretch activated calcium channels are also known to be voltage sensitive (Guharay and Sachs, 1985; Cosgrove and Hedrich, 1991). Since the application of an electrical field induces membrane depolarization (Gross *et al.*, 1986; Tsien *et al.*, 1988; Tester and MacRobbie, 1990), the activity of these voltage-dependent calcium channels may be affected and create a biased calcium entry at the cathodal side as suggested for fungal hyphae (Lever et al., 1994) (Figure. 5.12). The negative effect of the channel blocker lanthanum on the rapidity and frequency of the turning response and the fact that this effect could be rescued by increased availability of calcium in the medium confirm that in reorienting *Camellia* pollen tubes, calcium ions exert their role within the cytoplasm. This is consistent with the observation that artificial displacement of the point of highest cytosolic calcium concentration towards the side of the growing pollen tube apex induces the tube to change direction (Malhó *et al.*, 1994; Malhó *et al.*, 1995; Malhó and Trewavas, 1996). which has been posited to be mediated by a control of vesicle fusion (Camacho and Malhó, 2003; Coelho and Malhó, 2006).

5.3.3 The actin cytoskeleton mediates the turning response

Our time-lapse studies suggest that the effect of the putative localized calcium influx is likely mediated by the actin cytoskeleton. Elevated cytosolic calcium is known to trigger actin fragmentation (Kohno and Shimmen, 1987; Eun and Lee, 1997) or block polymerization (Vantard and Blanchoin, 2002). The effect of calcium

on actin can be direct or indirect, via the activation or deactivation of actin binding proteins (ABP) that in turn control the dynamics of the actin cytoskeleton (Vidali and Hepler, 2001; Chen *et al.*, 2009). Actin dynamics are the product of a fine equilibrium between actin polymerization and depolymerization. Many of the ABP regulating these processes are calcium- or calcium- calmodulin-dependent. Among these proteins are actin depolymerizing factors (ADF) (Ressad *et al.*, 1998; Smertenko *et al.*, 1998; Vidali and Hepler, 2001), profilin, a protein able to sequester actin monomers (Staiger, 2000) and prevent actin polymerization (Gibbon *et al.*, 1998; Kovar *et al.*, 2000; Snowman *et al.*, 2000; Snowman *et al.*, 2002), villin, a protein that bundles actin filaments (Yokota *et al.*, 2000; Yokota *et al.*, 2005), and gelsolin, an actin severing protein (Yin *et al.*, 1990; T'Jampens *et al.*, 1997; Huang *et al.*, 2004). LatB competes with profilin for actin monomers (Gibbon *et al.*, 1999) thus reducing the total amount of available G-actin resulting in a reduction of total F-actin density in the pollen tube. Upon application of LatB at a moderate concentration (1 nM), pollen tube length was somewhat reduced but no structural changes in the appearance of the F-actin arrays were visible. However, despite the absence of a dramatic effect of this drug concentration on growth rate or actin configuration, the number of tubes responding to the galvano-stimulus was drastically reduced and the response delayed. This suggests that the dynamic nature of the actin arrays, their continuous polymerization and depolymerization, are crucial for the ability of the pollen tube to rapidly change direction. Confirmation for this concept was provided by the tilt of the leading edge of the subapical actin fringe prior to growth redirection. This indicates that polymerization activities of the actin filaments facing cathode and anode were different resulting in a faster advancement of the leading edge on the anodal side and a deviation from radial symmetry. The fact that increased calcium in the medium was able to rescue the effect of LatB corroborates the notion that actin dynamics controlled by actin binding proteins is crucial for the galvanotropic response.

The apparent role of actin in pollen tube tropism contrasts with findings in the hyphae of *Neurospora crassa* (Riquelme et al., 1998). In these fungal hyphae, the turning response depends on a functional microtubule cytoskeleton, whereas in the pollen tubes studied here, no effect on the tropic response was observed after complete depolymerization of microtubules. This confirms that there are crucial differences between hyphal and pollen tube growth. Despite the similarity of the outer morphology of these two tip growing cell types, the intracellular growth machineries are organized differently. Secretory vesicles in the tips of fungal hyphae are aggregated into a centrally located, structural feature that also comprises cytoskeletal elements, the Spitzenkörper, from which the vesicles are thought to depart towards the apical plasma-membrane (Bartnicki-Garcia, 1990). Vesicles in pollen tubes, on the other hand, are delivered along the periphery of the cell by the cortically positioned subapical actin fringe (Bove *et al.*, 2008; Cai and Cresti, 2008; Cardenas *et al.*, 2008). Microtubules in pollen tubes are known to be involved in the mobility of the vegetative nucleus and the sperm cells (Åström *et al.*, 1995) as well as that of bigger organelles (Cai and Cresti, 2008), but their depolymerization does not prevent pollen tube elongation (Åström *et al.*, 1995). Therefore, the absence of an effect of oryzalin on the turning response in *Camellia* pollen tubes was not surprising, since within the short experimental time used in the present setup (10 minutes) a failure in nuclear transport was not expected to have any significant effect.

In order to understand how the actin arrays function in redirecting tip growth in pollen tubes, it is important to recognize the fundamental differences between animal and plant cells. In mammalian cells, the polymerization of actin filaments is able to push forward the adjacent plasma membrane and thus to redirect the crawling movement of cells as is seen with fibroblasts (Onuma and Hui, 1988). In walled cells, the polymerization of cytoskeletal arrays cannot produce a force sufficiently high to compete with that generated by the turgor pressure (Money, 1997; Money and Hill, 1997). Any morphogenetic effect of a change in cytoskeletal dynamics in

turgid cells with walls must therefore be achieved indirectly by manipulation of cell wall assembly. While microtubules are able to orient plant cell expansion by influencing the deposition of cellulose microfibrils, actin filaments deliver new, pectic material to the cellular surface creating local soft spots in the wall. It is this delivery of soft cell wall material that enables the pollen tube to expand at the apex (Geitmann and Dumais, 2009; Zerzour et al., 2009). The tilting of the apical vesicle aggregation prior to pollen tube reorientation observed here clearly confirms that it is a change in the spatial targeting pattern of vesicles that leads to the change in tube shape and that the dynamic behavior of the actin array is responsible for this targeted delivery.

5.4 Conclusion

The timing of the tilting in the leading edge of the actin fringe and in the pattern of vesicle dynamics prior to a change in outer morphology clearly suggest that it is the cytoplasmic growth machinery that reorients to accomplish a change in growth direction in pollen tubes. The tilt is achieved by a differential modulation of actin dynamics in the two sides of the tube and this seems to be brought about by an increased local influx of calcium which we propose to be the result of an asymmetric opening of calcium channels.

5.5 Materials and methods

5.5.1 Plant material

Camellia japonica pollen was collected from a plant growing in the Montreal Botanical Garden, dehydrated in gelatin capsules on anhydrous silica gel overnight and stored at -20°C. *Camellia* pollen growth medium contained 1.62 mM H_3BO_3, 2.54 mM $Ca(NO_3)2{\cdot}4H_2O$ (unless mentioned otherwise), 1 mM KNO_3, 0.81 mM $MgSO_4{\cdot}7H_2O$, 8% sucrose (w/v). Lily (*Lilium longiflorum*) pollen was grown in lily

medium (LM) composed of 1mM KNO_3, 1.6 mM H_3BO_3, 0.13 mM $Ca(NO_3)_2$, 5 mM MES and 8% w/v final sucrose concentration with a pH adjusted to 5.5.

5.5.2 Actin labeling

After one hour of growth, *Camellia* pollen tubes were fixed for 40 seconds in a freshly prepared fixative containing 3% formaldehyde, 0.5% glutaraldehyde and 0.05% Triton X-100 solution in a buffer composed of 100 mM PIPES, 5 mM $MgSO_4$, 0.5 mM $CaCl_2$ at pH 9. Subsequently, samples were washed in the same buffer, 3 times for one minute each. Fixation and washing steps were accelerated by exposure to microwaves at 150 Watts in a PELCO cold spot® biowave 34700. Actin was labeled by incubating overnight at 4°C in rhodamine-phalloidin (Molecular Probes) diluted 30 times in a buffer composed of 100 mM PIPES, 5 mM $MgSO_4$, 0.5 mM $CaCl_2$, 10 mM EGTA at pH 7. Next day, samples were washed with buffer 5 times for one minute in the microwave at 150 Watts. Pollen was then mounted on glass slides in a drop of citifluor (Electron Microscopy Sciences), covered with a cover slip, sealed and immediately observed.

Particle bombardment was used to visualize live actin dynamics in lily pollen tubes using *zmC13::Lifeact-mEGFP*, an actin probe that does not affect pollen tube growth (Vidali *et al.*, 2009). DNA was extracted using alkaline lysis followed by RNAse treatment, phenol-chloroform extraction and PEG precipitation. 3 µg of DNA were used to coat 1.1 µm microcarrier, tungsten M-17 beads (BIORAD). Bombardment of pollen grains, placed on a filter paper, was carried out in an in-house made biolistic device at an accelerating pressure of 62 psi for 50 ms under 600 mm.Hg vacuum. Pollen was left to grow in 1 ml of 16% sucrose LM to which 200 mL LM without sucrose were added every 10 minutes until the final sucrose concentration in the medium reached 8%. After 4 hours of growth, pollen was deposited in the galvanotropic chamber and observation was done in the confocal laser scanning microscope.

5.5.3 Microtubule labeling

Pollen was fixed in PIPES magnesium (PM) buffer (50 mM PIPES, 1 mM EGTA, 1 mM $MgCl_2$ at pH 6.9) with freshly prepared 4% formaldehyde for 45 minutes, then washed twice (5 minutes each) in PM buffer. Fixed pollen was treated with 2% cellulysin (Calbiochem) for 6 minutes, washed twice and treated with cold methanol for 5 minutes at -20°C. After two washes with tris buffer saline (TBS) (50 mM Tris, 150 mM NaCl at pH 7.5) with 2% bovine serum albumin (BSA), the samples were incubated overnight in anti-α-tubulin (Molecular Probes) mouse monoclonal antibody (diluted 1:200) at 4°C. After two washes with TBS buffer containing 2% BSA, samples were incubated with Alexa Fluor 594 (Molecular Probes) goat anti-mouse secondary antibody (diluted 1:100) for 2 hours at room temperature. Before mounting, pollen was washed four times in TBS buffer with 2% BSA.

5.5.4 In vivo vesicle labeling

Vesicles in growing pollen tubes were labelled by adding 160 nM of the lipophilic styryl dye FM1-43 (Molecular probes, Invitrogen) to the growth medium fifteen minutes prior to observation.

5.5.5 Microscopy and statistical analysis

Widefield fluorescence microscopy was done in a Zeiss Axio Imager.Z1 equipped for structured illumination microscopy (Apotome) and with a Zeiss AxioCam MRm Rev.2 camera. Z-Stacks acquired at 1 μM intervals were used for image reconstruction using AxioVision Release 4.5 software.

Confocal laser scanning micrographs were taken on a Zeiss LSM 510 META confocal laser scanning microscope equipped with a LSM 5 LIVE setup. Images were acquired with the LSM Image Examiner software. Images for the galvanotropic experiment used for experimental optimizations and statistical analysis were taken

with a Nikon TE2000 microscope equipped with a Roper fx cooled CCD camera and ImagePro software (Media Cybernetics, Carlsbad, CA). Images were processed and fluorescent profiles quantitatively analysed using ImageJ 1.41o (National Institutes of Health, USA, http://rsb.info.nih.gov/ij). Changes in the geometry of pollen tubes were detected by drawing a line following the outline of the growing pollen tube apex before exposure to a tropic trigger. This outline was copied onto subsequent images in a time series to identify the moment at which the shape of the apex changed asymmetrically compared to the original outline. The student t-test was used to determine statistic significance.

5.5.6 Galvanotropic setup

A miniature electrophoresis chamber was designed to be compatible with observation in an inverted microscope. It consists of a 3.5 cm Petri dish with a 2x1 cm rectangular opening to which a coverslip (thickness #1) was glued using silicone. Each of the 1 cm sides of the chamber was connected to an electrode using a platinum wire (Figure. 5.1A). The electrodes were connected to a direct-current (DC) power supply (TEKPOWER HY1803D). Heated *Camellia* growth medium complemented with 1% agarose type VII (Sigma-Aldrich) was precooled to 40°C before addition of latrunculin B, oryzalin or lanthanum chloride. The medium was spread into a thin layer on the coverslip of the chamber and left for 5 minutes to solidify. Pollen was then applied in a line parallel to the electrical field inside the agarose layer.

5.6 Acknowledgements

Research in the Geitmann lab is funded by grants from the Natural Sciences and Engineering Research Council of Canada (NSERC) and the Fonds Québécois de

la Recherche sur la Nature et les Technologies (FQRNT). The authors wish you thank Luis Vidali for the Lifeact construct.

5.7 Figures and Legends

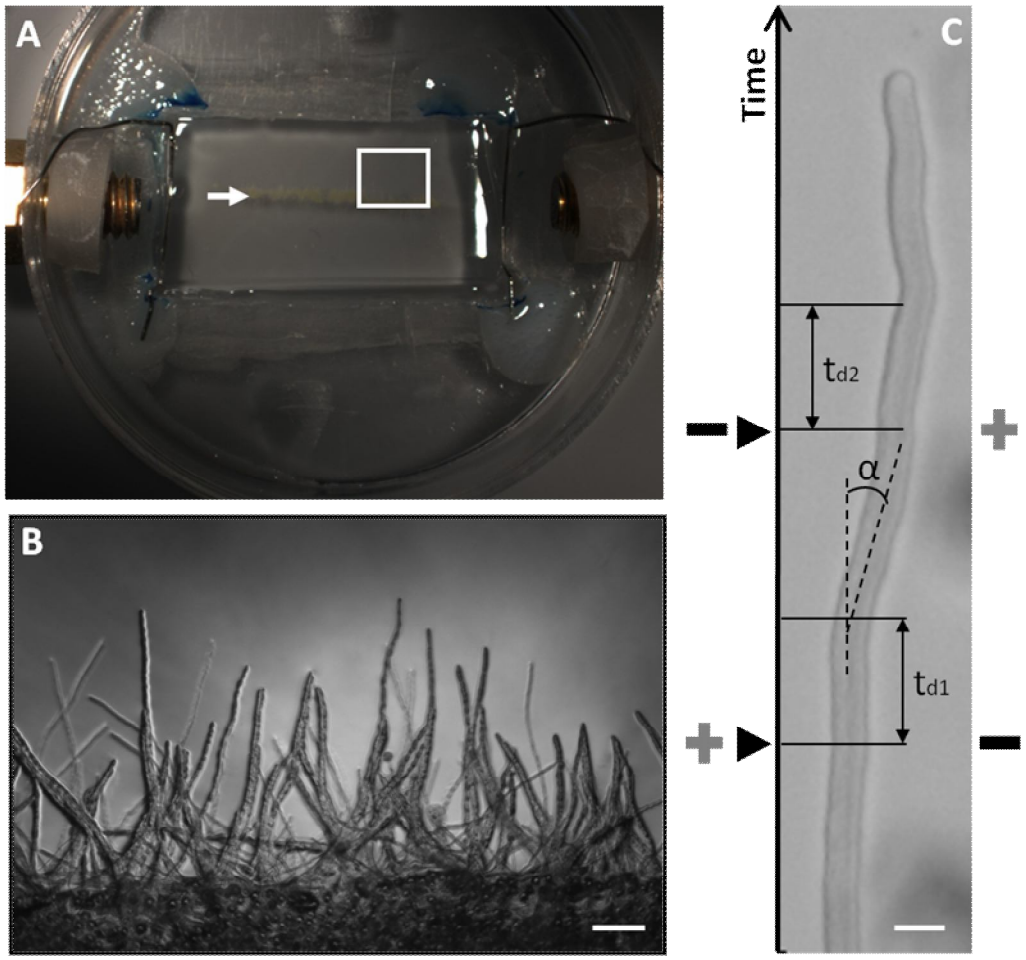

Figure 5.1**:** Galvanotropic setup devised to expose *Camellia* pollen tubes to an electrical field. (A) Galvanotropic chamber with pollen applied on a line (arrow) oriented parallel to the field. The square indicates the position of the close-up in (B). (B) Pollen tubes emerging from the aligned pollen grains grow mainly perpendicular to the line and thus to the future electrical field. (C) Pollen tube changing growth direction by an angle α after the application of an electrical field of 1.5 V/cm perpendicular to the growth direction. Arrowheads indicate the time of field application and minus and plus signs indicate the cathodal and anodal sides of the field, respectively. t_{d1} and t_{d2} represent the delay times between the application of the electrical field and the appearance of a visible change in growth direction. In this example, the electrical field was continuously applied and reversed upon completion of growth redirection to demonstrate that the tropic response is due to the presence of the electrical field in a particular orientation. Bars = 100 µm (B), 20 µm (C).

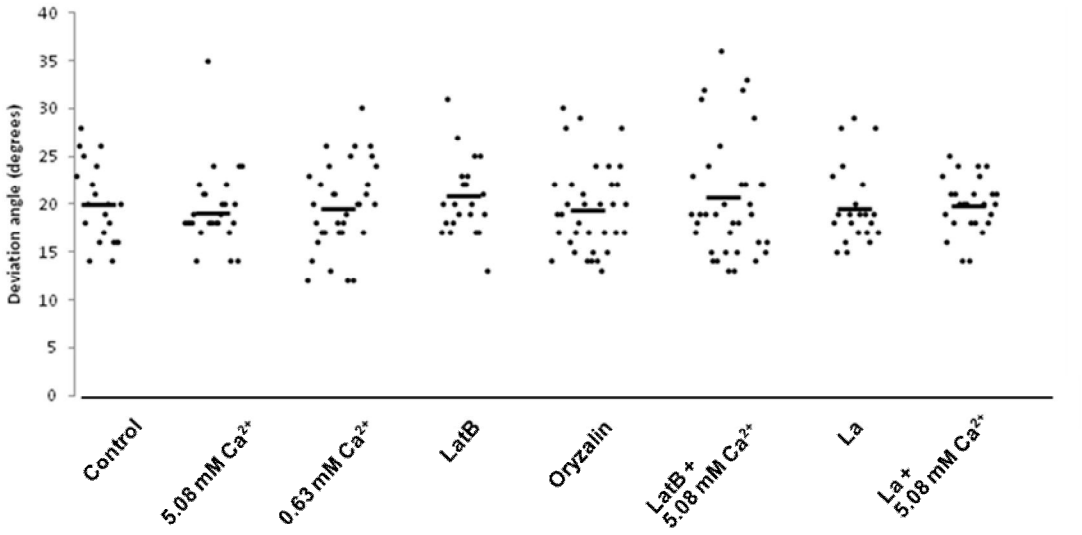

Figure 5.2: Deviation angle of *Camellia* pollen tubes subjected to a 1.5 V/cm DC electrical field under different experimental conditions. Deviation angles of tubes displaying a turning response varied between 12 and 35 degrees. No difference was observed in the mean values (horizontal lines) of the deviation angle (approximately 20 degrees) between the eight treatments. Points represent individual pollen tubes.

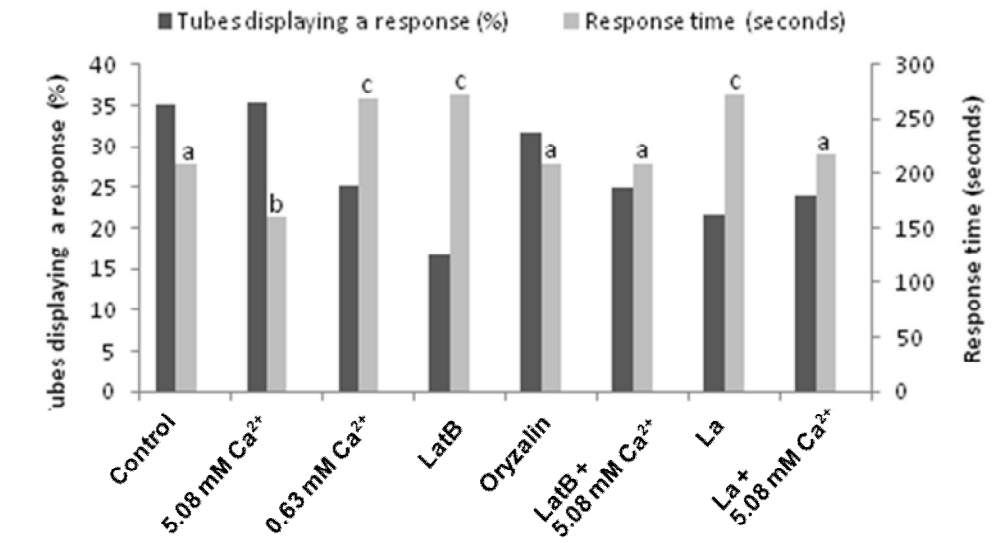

Figure 5.3: Percentage of tubes displaying a turning response and response times of *Camellia* pollen tubes subjected to a 1.5 V/cm electric trigger under different experimental conditions. Letters represent the statistical difference in the response time ($p<0.05$).

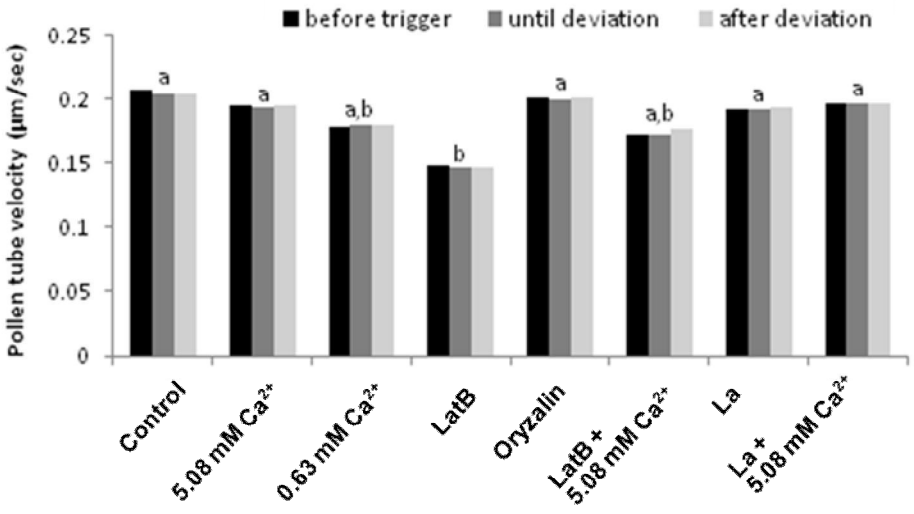

Figure 5.4: Velocity of *Camellia* pollen tubes before application of the electrical trigger (black), during delay time between application and deviation (grey) and after pollen tube deviation (white). Letters represent the statistical differences between treatments. No effect of the electrical field was found on pollen tube elongation during the three time periods within individual treatment conditions.

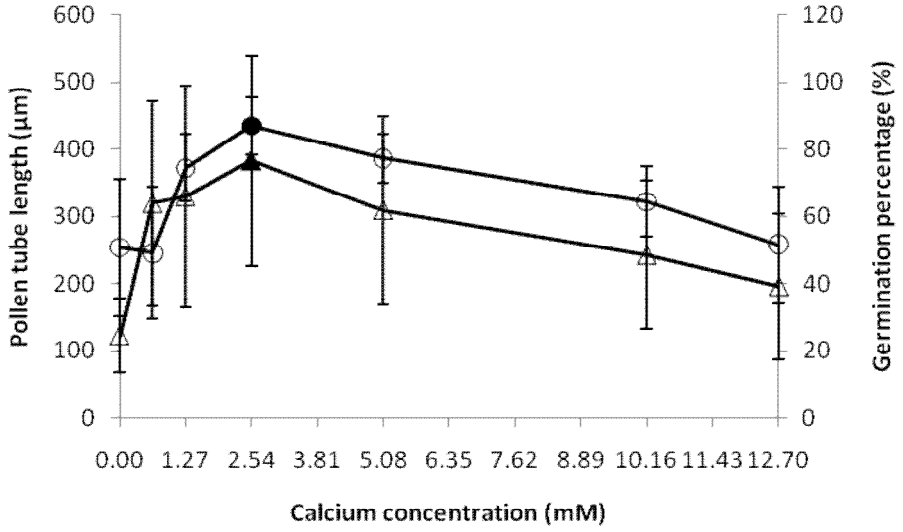

Figure 5.5**:** Effect of calcium concentration in the medium on tube length (triangles) and germination percentage (circles) of *Camellia* pollen after one hour of growth. Optimal germination percentage is marked (full symbol). Data points represent the mean values of n>100 tubes and vertical bars represent standard deviations.

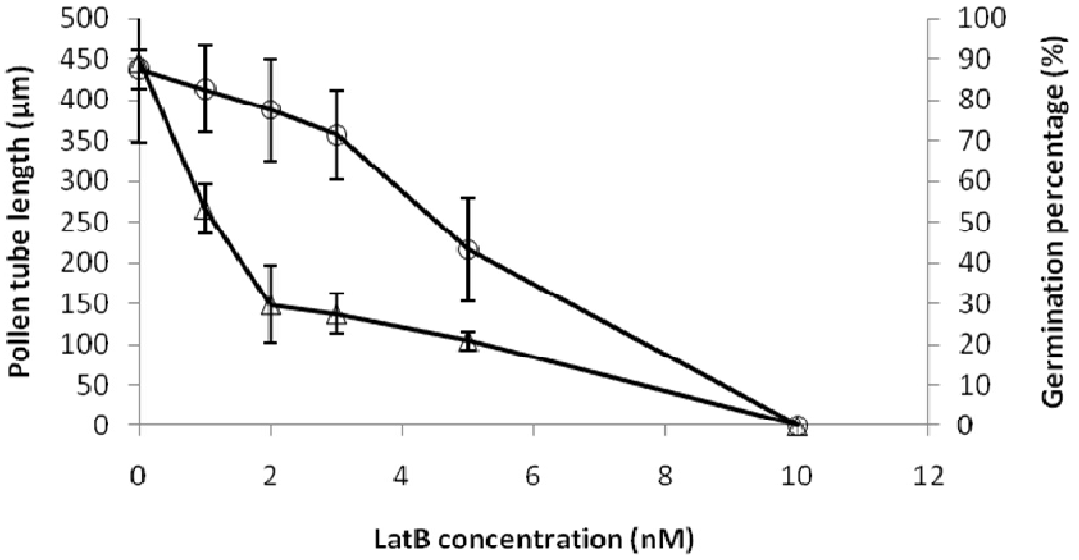

Figure 5.6: Effect of LatB on *Camellia* germination percentage (circles) and pollen tube length (triangles) at one hour of growth. Points represent mean values (n>100) and vertical bars represent the standard deviations.

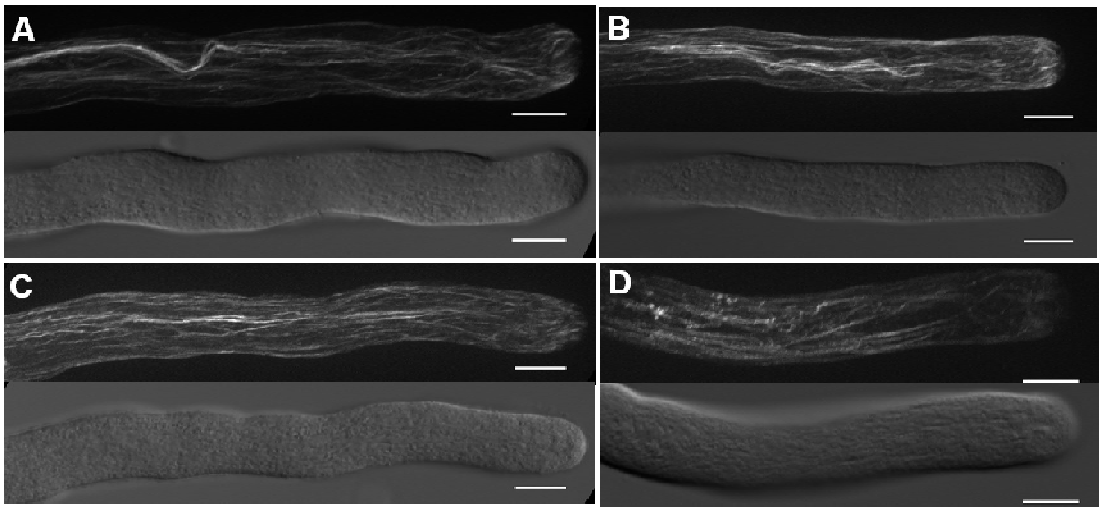

Figure 5.7: Effect of LatB on the spatial configuration of the actin arrays in *Camellia japonica* pollen tubes. Fluorescent micrographs of actin labeled with rhodamine phalloidin after treatment with 1 nM LatB (B), 3 nM LatB (C) and 10 nM LatB (D). Images represent maximum projections of Z-stacks acquired with the Apotome shown with their corresponding DIC micrographs. (A) Control tube. Bar = 10 µm.

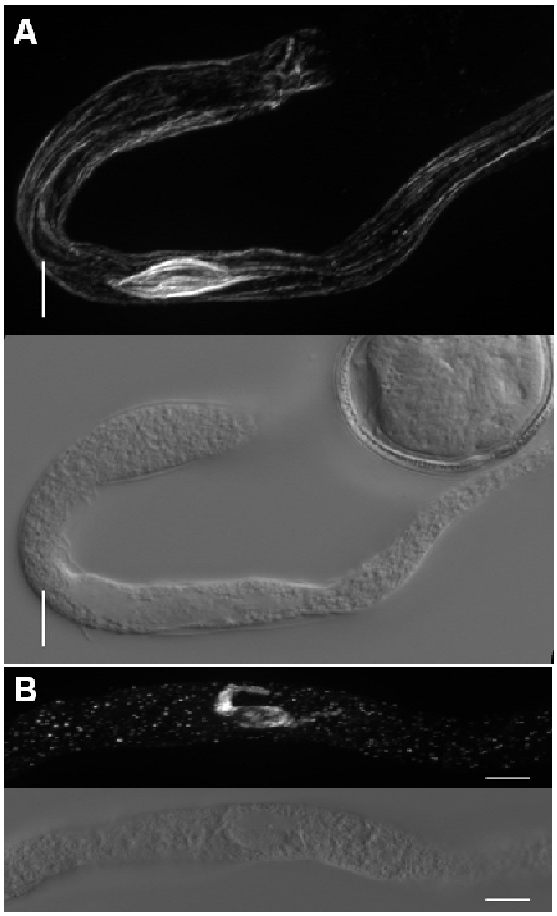

Figure 5.8: Effect of oryzalin on the microtubule arrays in *Camellia* pollen tubes. Fluorescent micrographs represent Z-projections of images taken with the Apotome of pollen tubes labeled for α-tubulin, shown with their corresponding DIC images. (A) Control tube, (B) 1 μM oryzalin. Bars = 10 μm.

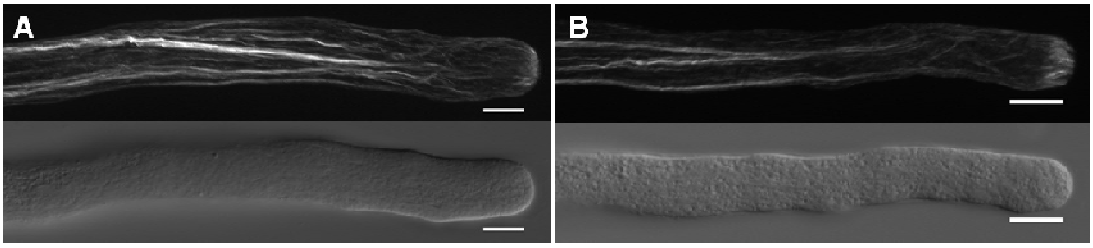

Figure 5.9**:** Effect of oryzalin on the actin cytoskeleton in *Camellia* pollen tubes. Pollen tube labeled with rhodamine phalloidin after treatment with 1 μM oryzalin (B). (A) Control tube. Fluorescent micrographs represent projections of Z-images taken on the Apotome, shown with their corresponding DIC images. Bars = 10 μm.

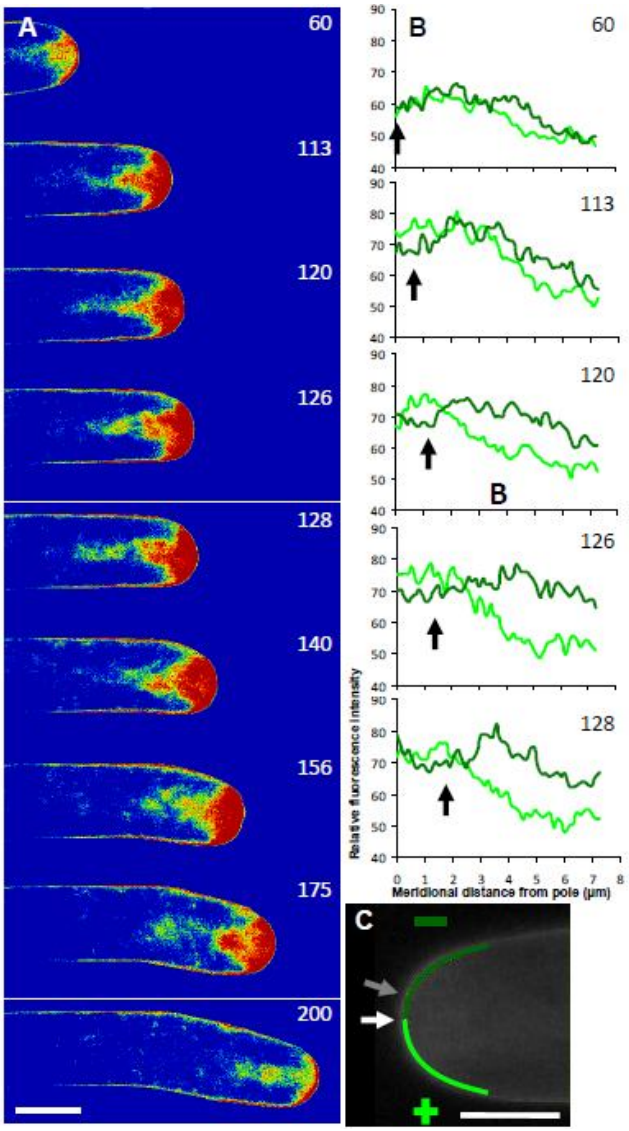

Figure 5.10: Vesicle targeting during the tropic growth response in a *Camellia* pollen tube. (A) Vesicles labelled with FM1-43 styryl dye. False colors are used to indicate relative fluorescence intensity. Red stands for high, blue for lower intensity. Numbers indicate the time in sec after the application of the directional trigger. (B) Spatial profiles of the relative fluorescence intensity along the periphery of the tube on the anodal (light green) and cathodal (dark green) sides. x-axis shows meridional distance from the pole of the tube. The arrow indicates the position of the local minimum in fluorescence intensity. (C) Position of the line plot on the anodal (light green) and cathodal (dark green) side. The white arrow indicates the position of the local minimum in fluorescence intensity before galvano-trigger. The grey arrow indicates the position of the fluorescence minimum at 126 sec when outer tube geometry started changing. Bars = 10 µm.

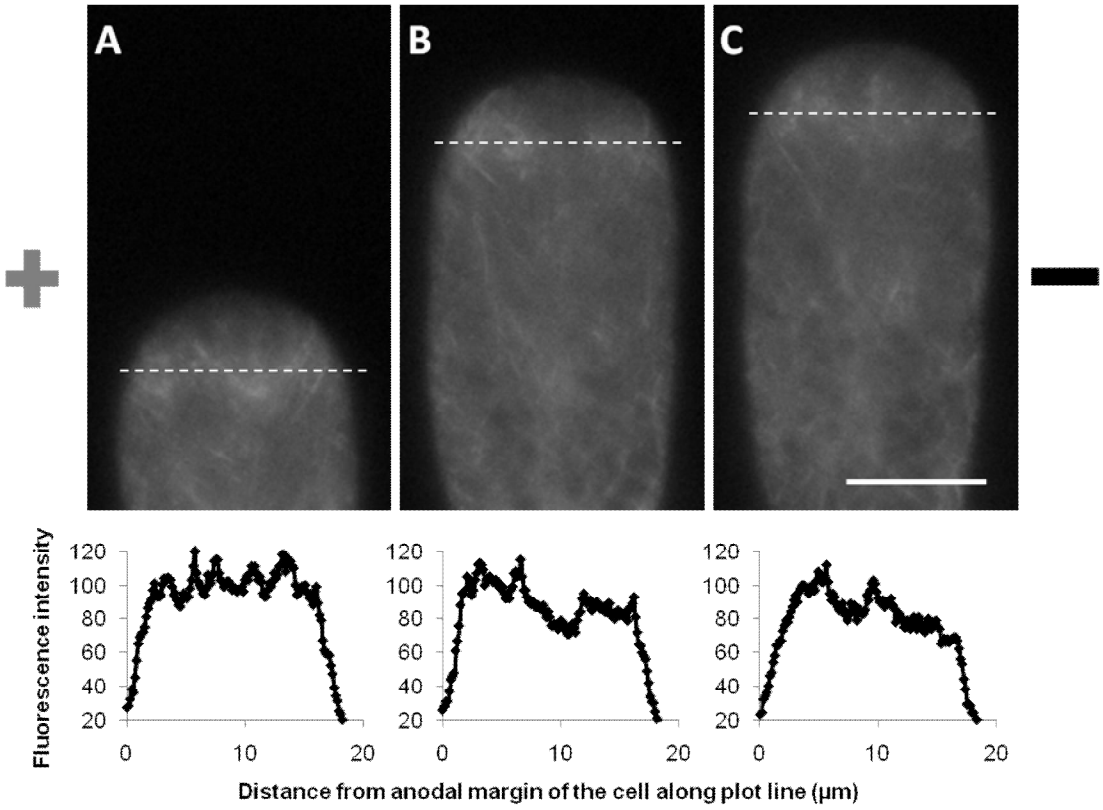

Figure 5.11: Confocal micrographs of median optical sections of *Lilium* pollen tube expressing *zmC13::Lifeact-mEGFP* (top) and the corresponding fluorescence intensity profiles on a line plot (dashed) perpendicular to the growth axis and situated 5µm from the tip of the tube (bottom). (A) Normally growing pollen tube, (B) the same tube subjected to the electric trigger and observed prior to the change in its geometry and (C) the same tube after the change in geometry appeared. + Anodal side, - cathodal side. Bar = 10µm.

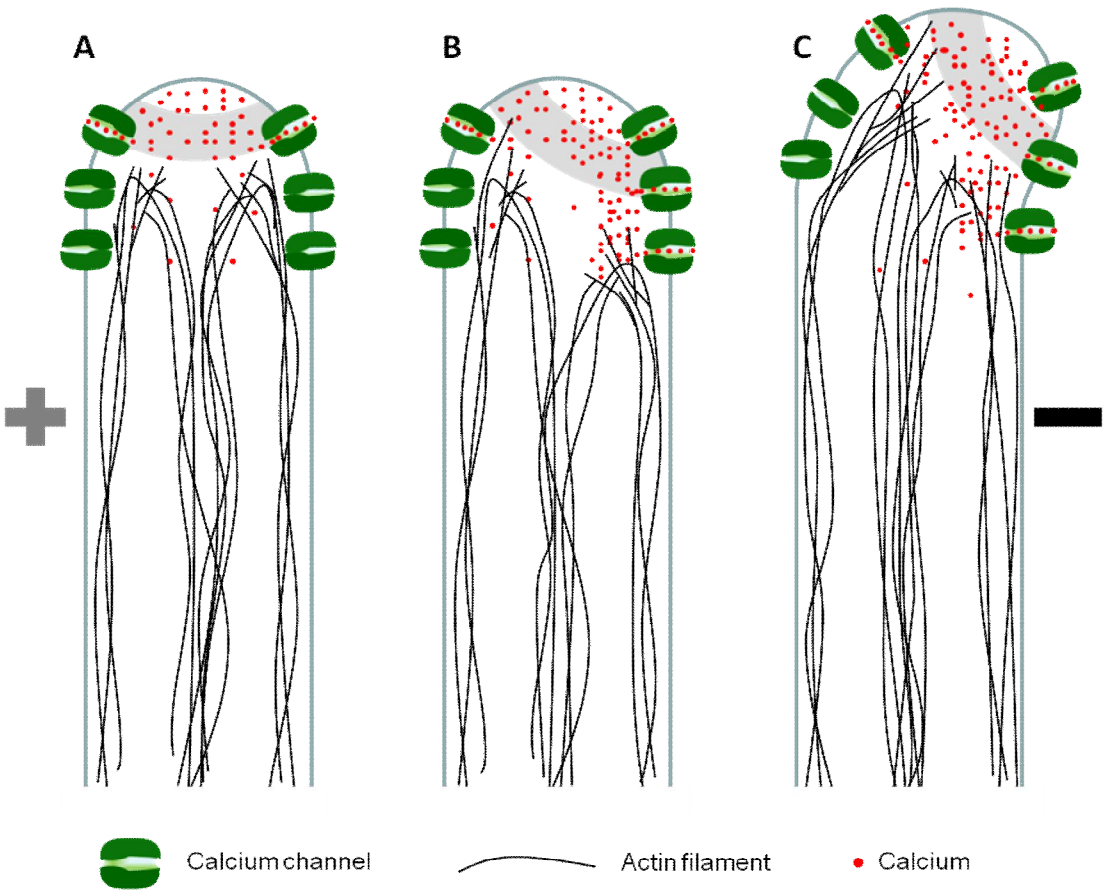

Figure 5.12: Proposed model for cellular events during the reorientation of a pollen tube following a galvanotropic trigger. (A) Calcium channel activity, actin dynamics and cytosolic calcium concentration are symmetric in a normally growing pollen tube. (B) Upon application of the electrical trigger, calcium channels on the depolarized (cathode facing) side of the pollen tube are opened leading to the elevation of the cytosolic calcium concentration at this side of the tube. This in turn reduces actin polymerization at this side. (C) Actin filaments in the anodal side deliver vesicles closer towards the pole causing the exocytosis annulus (grey) to tilt towards the cathode. Elements are not drawn to scale.

6 Spatial and Temporal Expression of Actin Depolymerizing Factors ADF7 and ADF10 during Male Gametophyte Development in *Arabidopsis thaliana*

To have a clear idea on how actin polymerization and dynamics in the pollen tube are regulated, the activities of the proteins controlling actin dynamics need to be investigated in more detail. One of the actin binding proteins involved in actin remodeling in the pollen tube that I considered to be a primary candidate is ADF. I used the fluorescent tagging of full length protein technique to monitor the expression and subcellular localization of ADF7 and ADF10, two pollen specific ADFs, during *Arabidopsis thaliana* male gametophye development, pollen germination and pollen tube growth.

This manuscript was submitted to Plant and Cell Physiology.

Title

Spatial and Temporal Expression of Actin Depolymerizing Factors ADF7 and ADF10 during Male Gametophyte Development in *Arabidopsis thaliana*

Authors:

Firas Bou Daher and Anja Geitmann

Université de Montréal, Département de sciences biologiques, Institut de recherche en biologie végétale. 4101 Sherbrooke East, Montreal, Quebec, Canada.

Abbreviations:

ADF, actin depolymerizing factor; CFP, cyan fluorescent protein; DAPI, 4'-6-diamidino-2-phenylindole; LatB, latrunculin B; YFP, yellow fluorescent protein

Abstract

The actin cytoskeleton plays a crucial role in many aspects of plant cell development. During male gametophyte development, the actin arrays are conspicuously remodeled both during pollen maturation in the anther as well as after pollen hydration on the receptive stigma and pollen tube elongation. Remodeling of actin arrays results from the highly orchestrated activities of numerous actin binding proteins. A key player in actin remodeling is the actin depolymerizing factor (ADF) which increases actin filament treadmilling rates. We prepared fluorescent protein fusions of two *Arabidopsis* pollen specific ADFs, ADF7 and ADF10. We monitored the expression and subcellular localization of these proteins during male gametophyte development, pollen germination and pollen tube growth. *ADF7* and *ADF10* were differentially expressed with the ADF7 signal appearing in the microspore stage and that of ADF10 only during the polarized microspore stage. ADF7 was associated with the vegetative nucleus during less metabolically active stages, but in germinating pollen grains and elongating pollen tubes, it was associated with the subapical actin fringe. On the other hand, ADF10 was associated with filamentous actin in the developing gametophyte, in particular with the arrays surrounding the apertures of the mature pollen grain. In the shank of elongating pollen tubes, ADF10 was associated with thick actin cables. We propose possible specific functions of these two ADFs based on their differences in expression and localization.

Keywords

Actin depolymerizing factor, *Arabidopsis thaliana*, cyan fluorescent protein, male gametophyte, pollen tube, yellow fluorescent protein.

6.1 Introduction

The actin cytoskeleton fulfills various functions in plant cells, some of which differ significantly from their animal counterparts. Actin arrays are the structural basis for cyclosis, the rapid motion of organelles within the plant cytoplasm (Woods *et al.*, 1984), they are associated with the phragmoplast, a cytoskeletal configuration regulating plant cytokinesis (Higaki *et al.*, 2008), and they seem to be involved in the perception of mechanical stimuli such as those leading to gravitropism (Kordyum *et al.*, 2009; Stanga *et al.*, 2009). Actin filaments also play a crucial role in the regulation of cell shape generation and the initiation of local growth events that lead to the morphogenesis of the complex shapes characterizing certain plant cell types (Smith and Oppenheimer, 2005). Whereas in mammalian cells actin mediated morphogenesis is accomplished by a direct effect of the forces exerted by actin polymerization and contraction on the surrounding plasma membrane, the morphogenetic role of actin in plant cells is thought to be exerted through the targeting of cell wall material to defined surface domains designated for cell expansion (Mathur, 2006; Geitmann and Dumais, 2009). How exactly this plant specific mechanism operates is poorly understood, however. Therefore, although actin dynamics is known to be a crucial feature during plant development, its precise regulatory role in many of these developmental processes remains elusive.

The spatial configuration of actin arrays and their dynamic behavior are largely controlled by the activity of proteins that influence actin filament polymerization, depolymerization, branching and bundling. Many of the proteins identified in mammalian cells are also known to be expressed in plant tissues with a varying degree of similarity in amino acid sequence and 3D structures (McCurdy *et al.*, 2001; Hussey *et al.*, 2006; Yokota and Shimmen, 2006). One of the protein families involved in the control of plant actin dynamics is the actin depolymerizing factor (ADF)/cofilin. ADF is phylogenetically conserved in plants, animals and fungi

(Hussey *et al.*, 2002) and it is known to specifically bind the ADP-bound form of both monomeric and filamentous actin. ADF binding to filamentous actin occurs preferentially at the pointed ends where this interaction causes a change in the helical twist of the actin filament and accelerates the dissociation of actin subunits (Lopez *et al.*, 1996; Carlier *et al.*, 1997; Jiang *et al.*, 1997; McGough *et al.*, 1997; Hussey *et al.*, 1998; Bamburg, 1999; Bowman *et al.*, 2000; Cooper and Schafer, 2000; Bamburg and Bernstein, 2008). Under conditions of limited actin monomer supply, the resulting increased availability of the monomer promotes actin filament polymerization at the barbed end thus accelerating treadmilling (Carlier *et al.*, 1997; Michelot *et al.*, 2007). ADF/cofilin is also capable of severing actin filaments which reduces filament length but simultaneously increases the number of available barbed ends that serve as nucleators for more polymerization activity (Hayden *et al.*, 1993; Blanchoin and Pollard, 1999; Staiger and Blanchoin, 2006; Staiger *et al.*, 2009). ADF/cofilin activity is concentration dependent - it promotes actin severing at low concentrations and induces actin nucleation and actin assembly at higher concentrations (Yeoh *et al.*, 2002; Andrianantoandro and Pollard, 2006). The ability of ADF to depolymerize actin is also pH dependent with alkaline conditions favoring this process (Carlier *et al.*, 1997; Allwood *et al.*, 2001; Chen *et al.*, 2002).

ADF activity is controlled by the phosphorylation state of a serine residue present at the N-terminal region of the protein (Smertenko *et al.*, 1998; Allwood *et al.*, 2001; Chen *et al.*, 2003). The phosphorylation of ADF, and therefore ADF activity, was found to be controlled by a calcium stimulated protein kinase present in plant cells (Smertenko *et al.*, 1998). ADF can also be inactivated by phosphatidylinositol (PI), phosphatidylinositol 4-phosphate (PIP) and phosphatidylinositol 4,5-biphosphate (PIP2) through their binding to the actin binding domain of ADF (Yonezawa *et al.*, 1990; Yonezawa *et al.*, 1991; Gungabissoon *et al.*, 1998; Kusano *et al.*, 1999). ADF activity was also found to be controlled by Rop GTPases (Chen *et al.*, 2003) a plant member of the Rho family of

GTP binding proteins, thus providing a downstream element through which many regulatory pathways are likely to act on cellular morphogenesis.

The functional analysis of plant ADF through downregulation has been challenging because of the presence of numerous isoforms in the plant genome. While unicellular eukaryotes typically possess only one ADF gene and one ADF and two cofilin genes are found in most vertebrate genomes, several ADF genes exist in most higher plant species analyzed so far (Maciver and Hussey, 2002; Bamburg and Bernstein, 2008). The ADF family in *Arabidopsis thaliana* comprises 11 genes (Arabidopsis.org) that are divided into four subclasses (Mun *et al.*, 2000; Ruzicka *et al.*, 2007). A member of subclass 1, *ADF2*, was shown to be involved in the regulation of plant cell growth and differentiation, since RNAi knockdown interfered with plant development (Clement *et al.*, 2009). The members of subclass 2, *ADF7*, *ADF8*, *ADF10* and *ADF11*, are suspected to have roles in tip growth, a type of highly polarized growth activity that is regulated by the actin cytoskeleton. Transcriptomics and proteomics, promoter-GUS assays and immunolocalization data have shown that *ADF8* and *ADF11* are expressed in trichoblasts and root hairs (Ruzicka *et al.*, 2007), whereas *ADF7* and *ADF10* are specifically expressed in pollen and pollen tubes (Becker *et al.*, 2003; Honys and Twell, 2003; Honys and Twell, 2004; Noir *et al.*, 2005; Pina *et al.*, 2005; Hruz *et al.*, 2008; Zou *et al.*, 2009). Because of the expression of multiple *ADF* isoforms even within individual cell types, the precise functions of the proteins specific to tip-growing cells remain elusive. However, downregulation of ADF in the tip-growing moss *Physcomitrella*, that only has a single gene coding for ADF, severely interferes with tip growth (Augustine *et al.*, 2008), whereas partial antisense silencing increased the actin dynamics and root hair elongation in *Arabidopsis* (Dong *et al.*, 2001). This suggests that the regulation of actin dynamics through ADF activity is likely to be a crucial component of the tip growth process in higher plants.

Several functional investigations of ADF in plant cells have exploited the pollen tube, a tip-growing plant cell type that grows fastest and that can therefore be expected to have an extremely dynamic actin cytoskeleton. This cylindrical, cellular protuberance is formed by the pollen after contact with a receptive stigma and can grow at rates of up to 3 mm/h. Its purpose is to deliver of the immotile sperm cells from the pollen grain to the female gametophyte which is nestled deep within the pistillar tissues. The importance of the actin cytoskeleton for the growth process is readily demonstrated by drugs resulting in actin depolymerization such as latrunculin B or cytochalasin which halt the process immediately (Gibbon *et al.*, 1999; Miller *et al.*, 1999; Vidali *et al.*, 2001; Gossot and Geitmann, 2007). A principal function of actin in pollen tubes is logistic in nature. Pollen tube growth requires significant amounts of membrane and cell wall material to be delivered to the growing surface domain in order to sustain continuous elongation over distances as long as many centimeters (Franklin-Tong, 1999). This material is transported by secretory vesicles from Golgi bodies located anywhere in the cytoplasm to the small region on the cellular surface where it is needed, the growing tip (Bove *et al.*, 2008; Zonia and Munnik, 2008). Vesicles and other organelles are therefore shuttled rapidly along the tube in a bidirectional movement that is largely myosin-mediated (Vidali and Hepler, 2001) and occurs on actin filaments oriented in opposite directions in the periphery and central regions of the cytoplasm (Lenartowska and Michalska, 2008). Close to the apex, a fine mesh of actin filaments forms a cortical fringe (Lovy-Wheeler *et al.*, 2005) that colocalizes with an alkaline cytoplasmic region (Feijó *et al.*, 1999). There are almost no actin filaments at the very tip of the pollen tube where vesicles accumulate during a transition phase between forward and backward movement (Kroeger *et al.*, 2009). The guidance of vesicles to a precisely determined annular region around the pole of the cell is thought to be crucial for the generation of a perfectly cylindrical tube, since exocytosis must be under tight spatial control for geometrically correct morphogenesis (Cardenas *et al.*, 2008; Geitmann and Dumais, 2009; Fayant *et al.*, 2010) as well as for the control of growth direction

(Bou Daher and Geitmann) and invasive activity (Gossot and Geitmann, 2007). The crucial role of the subapical actin fringe for morphogenesis can be demonstrated experimentally since drug- or mutation induced alterations in the cytoskeletal functioning are known to cause apical swelling and hence a loss of the perfectly polar growth activity (Hepler *et al.*, 2001; Cheung and Wu, 2008; Yang, 2008; Zerzour *et al.*, 2009). Importantly, the subapical fringe and pollen tube elongation are more sensitive to actin-depolymerizing drugs than the long-distance organelle transport occurring in the cylindrical shank of the cell (Vidali *et al.*, 2001).

For the actin arrays in the rapidly growing pollen tube to maintain their well defined spatial configuration and to respond to external signals, their dynamics need to be tightly regulated. Actin filament polymerization, depolymerization, branching, capping and bundling must be finely tuned in order for the cell to accomplish specific functions. ADF is among the actin binding proteins known to operate in the subapical actin fringe as demonstrated on tobacco and lily pollen tubes (Chen *et al.*, 2002; Lovy-Wheeler *et al.*, 2006; Wilsen *et al.*, 2006). This role is clearly critical since overexpression of *NtADF1* inhibits tobacco pollen tube growth in a concentration dependent manner (Chen *et al.*, 2002; Chen *et al.*, 2003). Similarly, the overexpression of a pollen specific ADF from cotton (*GhADF7*) decreases pollen viability and reduces pollen tube growth (Li *et al.*, 2010).

Not only pollen tube growth but also the earlier phases of male gametophyte development are characterized by a precisely coordinated remodeling of the actin cytoskeleton (Heslop-Harrison *et al.*, 1986; Tiwari and Polito, 1988; Heslop-Harrison and Heslop-Harrison, 1992; Tanaka and Wakabayashi, 1992; Derksen *et al.*, 1995; Taylor and Hepler, 1997; Cai *et al.*, 2005). Without this reorganization of the cytoskeleton, pollen germination inevitably fails and fertilization becomes impossible (Gibbon *et al.*, 1999). In order to characterize the potential roles of ADF in this cytoskeletal reorganization, we examined the subcellular localization of ADF7 and ADF10 coupled to the cyan fluorescent protein (CFP) and the yellow fluorescent

protein (YFP), respectively, during the different stages of pollen development in *Arabidopsis thaliana*.

6.2 Results

6.2.1 Expression pattern of *ADF7* and *ADF10* in *Arabidopsis*

Transcriptomic and proteomic data have shown that in *Arabidopsis*, *ADF7* and *ADF10* seem to be expressed specifically in pollen (Becker *et al.*, 2003; Honys and Twell, 2003; Honys and Twell, 2004; Noir *et al.*, 2005; Pina *et al.*, 2005; Ruzicka *et al.*, 2007; Hruz *et al.*, 2008; Zou *et al.*, 2009). ADF7 and ADF10 share 94% similarity in their amino acid sequences using NCBI blast (Altschul *et al.*, 1997). ADF7 shares between 77 and 92% similarity with the other members of the *Arabidopsis* ADF family members while for ADF10 this similarity is somewhat lower with between 74 and 90%. ADF7 and ADF10 share more that 90% similarity in their amino acid sequence with the other two members of the subclass 2 ADFs, i.e. ADF8 and ADF11. A prediction search for possible nuclear export signals using NetNES 1.1 server of the Technical University of Denmark (la Cour *et al.*, 2004) yielded a positive peak at amino acid 21 for both ADFs with a 0.592 score for ADF10 and a 0.743 score for ADF7.

In order to visualize ADF7 and ADF10, we transformed *Arabidopsis thaliana* with chimeric *ADF7* and *ADF10* genes tagged with the genes for cyan fluorescent protein (*CFP*) and yellow fluorescent protein (*YFP*), respectively, under the control of their respective native promoter and terminator sequences. To test the expression pattern of the fusion proteins in the transformed plants, we examined CFP and YFP expression in roots, root hairs, stems, leaves, trichomes and all flower organs. With the exception of the male gametophyte, we did not observe any fluorescence above the background level in any of these organs. This confirms that *Arabidopsis ADF7* and *ADF10*, when expressed as fluorescent protein chimeras under the control of their own promoters, are indeed pollen specific.

6.2.2 ADF7 and ADF10 localization during male gametophyte development

To determine the subcellular localization of ADF7 and ADF10 during the development of the male gametophyte, we harvested different stages of pollen from transformed *Arabidopsis* plants and observed them by confocal microscopy. The developmental stages were annotated based on the description of gametophyte morphology by Twell and coworkers (Borg *et al.*, 2009). In order to visualize the nuclei, pollen grains were also stained with DAPI prior to observation.

ADF7-CFP expression appeared for the first time during the early microspore stage just after tetrad separation. Prior to this stage no significant label was visible in the developing gametophyte (not shown). After tetrad separation, ADF7-CFP labeled microspores displayed diffuse fluorescence in the cytoplasm and slightly more intense label in the nucleus (Figure 6.1A). At this stage, ADF10-YFP expression was not yet visible (not shown). At the polarized microspore stage, ADF7-CFP was still present in the nucleus (Figure 6.1B) and ADF10-YFP started to appear in short, rod shaped aggregates in the cytoplasm (Figure 6.2A). Just before the bicellular stage, ADF7-CFP disappeared from the nucleus and diffusely labeled the cytoplasm (Figure 6.1C), while ADF10-YFP was associated with longer filamentous structures in the cytoplasm (Figure 6.2B). At the bicellular stage, some ADF7-CFP accumulated around the vegetative nucleus and slightly denser aggregates started appearing in the periphery of the cytoplasm (Figure 6.1D). At this developmental stage, ADF10-YFP appeared to be associated with longer filamentous structures a portion of which was aggregated around the vegetative nucleus but most were concentrated at the periphery of the cell (Figure 6.2C). At the mature pollen stage, short filamentous elements labeled for ADF7-CFP were present around the vegetative nucleus while longer and more densely packed filaments dominated the periphery of the cytoplasm that also contained diffuse CFP fluorescence (Figure 6.1E). ADF10-YFP at this stage displayed a very similar localization as that in the bicellular stage with filamentous

structures around the vegetative nucleus and a dense mesh of filaments mostly at the periphery of the cytoplasm (Figure 6.2D). Just before anthesis, ADF7-CFP formed a dense mesh of long filaments in the periphery of the cytoplasm and diffuse fluorescence was present throughout the cytoplasm and in the vegetative nucleus (Figure 6.1F). Label intensity was higher at the apertures. Before anthesis, ADF10-YFP on the other hand more specifically targeted filamentous structures in the periphery of the cytoplasm with very little diffuse label and no fluorescence in the nucleus (Figure 6.2E). In pollen from open flowers, ADF7-CFP labeled the vegetative nucleus and was present as a dense filamentous mesh in the periphery with high concentration at the apertures (Figure 6.1F). ADF10-YFP label assumed the shape of longer and thicker filaments located at the apertures and oriented parallel to their long axes (Figure 6.2F). Optical sections and surface rendering demonstrate that the label was located in the periphery of the cytoplasm (Figure 6.3) and it was not detectable in the central regions of the cytoplasm.

6.2.3 ADF7 and ADF10 target the actin cytoskeleton

To identify the filamentous structures associated to which ADF7 and ADF10 label was observed, we labeled mature pollen expressing ADF7-CFP and ADF10-YFP from open flowers with rhodamine phalloidin following chemical fixation (Figure 6.4 A,B,G,H). The spatial configuration of the filamentous structures labeled for the ADF and for actin were near identical. Surprisingly, the filamentous structures labeled for ADF7 were frequently longer than the corresponding structures labeled with phalloidin (Figs. 6.3G, H). A possible explanation may be that ADF7-CFP sterically blocks potential phalloidin binding sites on the actin filaments. Moreover, it has been shown that ADF saturated actin filaments lose their phalloidin binding sites due to changes in the actin filament twist (Ressad *et al.*, 1998; Bamburg, 1999).

In order to further confirm the nature of the filamentous structures labeled with ADF7 and ADF10, we administered latrunculin B (LatB) to pollen grains. LatB

is a toxin isolated from the red sea sponge *Latrunculia magnifica* that sequesters G-actin leading to F-actin depolymerization due to the ongoing disassembly at the minus ends of the filaments (Gibbon *et al.*, 1999). Following LatB treatment, the filamentous structures labeled with phalloidin disappeared partly or entirely (Figure 6.4E,K). Similarly, label for ADF7 and ADF10 lost its filamentous configuration (Figure 6.4D,J). Any remaining filamentous structures coincided with structures labeled by phalloidin (Figure 6.4D,E,J,K). Diffuse fluorescence of ADF7 in the cytoplasm was strongly enhanced as a result of the LatB treatment (Figure 6.4D). Interestingly, after treatment of pollen from dehiscent flowers with LatB, ADF10-CFP was associated with the vegetative nucleus (Figure 6.4D).

Actin arrays are typically highly dynamic. In order to assess whether the ADF labeled structures behaved similarly, we acquired time-lapse series of hydrated pollen grains from open flowers of *ADF7-CFP* and *ADF10-YFP* mutants. The structures labeled with CFP and YFP were highly dynamic (Supplementary videos 1, 2), as would be consistent with the behavior of actin filaments.

6.2.4 ADF7 and ADF10 localization in the germinating pollen and the pollen tube

Pollen germination requires the delivery of secretory vesicles to the aperture (Cresti *et al.*, 1977; Cresti *et al.*, 1985) and the actin cytoskeleton is known to form characteristic arrays prior to and during germination (Heslop-Harrison *et al.*, 1986; Tiwari and Polito, 1988; Heslop-Harrison and Heslop-Harrison, 1992; Tanaka and Wakabayashi, 1992; Derksen *et al.*, 1995; Taylor and Hepler, 1997; Cai *et al.*, 2005). In order to assess whether ADF7 or ADF10 are involved in the remodeling of the actin cytoskeleton prior to and during pollen germination, we placed mature pollen in germination medium for one hour before observation. When the pollen grain started germinating, the filamentous elements labeled by ADF7-CFP disappeared from the grain and appeared associated with long filamentous cables seemingly winding

around the tip of the newly emerging tube (Figure 6.5A). In newly developed pollen tubes (shorter than 60 µm), filaments labeled with ADF7-CFP were associated with the tip of the tube and a significant amount of diffuse label was visible in the shank of the cell (Figure 6.5B) and in the pollen grain. In older pollen tubes (longer than 60 µm), ADF7-CFP targeted long filamentous cables in the subapical region of the tube and throughout the shank region (Figure 6.5C).

In germinating pollen grains expressing *ADF10-YFP*, fluorescence was confined to the periphery of the emerging pollen tube (Figure 6.6A). Once the tube had almost attained a length that corresponded to the diameter of the grain, most of the label was found inside the tube and almost no label was left in the grain. The label was associated with longer filamentous structures that were densely packed (Figure 6.6B) and could be observed to form loops (Figure 6.6C). Compared to ADF7-CFP, the number of individual filaments labeled by ADF10-YFP seemed much higher and their arrangement denser (compare Figure 6.4A with 5B). As the tube continued to grow, the fluorescence label for ADF10-YFP became more concentrated in the subapex where it formed shorter filaments (Figure 6.6D). Pollen grains with longer tubes displayed few, thick cables that continued from the grain into the tube (Figure 6.6E, F). Less pronounced but clearly visible label was associated with the subapical fringe in longer tubes pollen tube (Figure 6.6G,H). To confirm the nature of the filamentous structure in the pollen tubes, ADF10-YFP expressing pollen tubes were fixed and labeled for actin with rhodamine phalloidin. The label patterns for YFP and rhodamine fluorescence were identical (Figure 6.7) confirming that ADF is associated with the actin cytoskeleton.

6.3 Discussion

Actin remodeling is of great importance in the process of plant fertilization since the movement of secretory vesicles, and hence cell wall assembly, in the growing pollen tube is based on acto-myosin transportation (DePina and Langford,

1999; Geitmann and Steer, 2006; Yokota and Shimmen, 2006). Actin remodeling occurs during male gametophyte development, pollen grain hydration and continues during pollen germination (Heslop-Harrison *et al.*, 1986; Tiwari and Polito, 1988; Heslop-Harrison and Heslop-Harrison, 1992; Tanaka and Wakabayashi, 1992; Derksen *et al.*, 1995; Taylor and Hepler, 1997; Cai *et al.*, 2005). Actin dynamics relies on the activities of several ABPs including members of the ADF family, several of which are expressed in or specific to pollen.

Given that that male gametophyte expresses several *ADF* isoforms, we suspected that they might have distinct functions and differ in their temporal expression profile or subcellular localization. We focused on *ADF7* and *ADF10*, which are both specifically expressed in pollen but whose functions have not been characterized. We opted for a technique for the construction of chimeric genes with intrinsically fluorescent proteins that respects three conditions. First, our strategy conserved the native expression levels of the proteins by using their native promoter and terminator sequences. This was important since changing the expression level, for example by using a highly expressing promoter such as Lat52, can alter protein function and affect cell growth especially in highly dynamic and sensitive tip growth of the pollen tube. Overexpression of several genes in the pollen tube has been demonstrated to cause swelling, reduced growth rates, abnormal morphology and altered subcellular organization (Kost *et al.*, 1999; Li *et al.*, 1999; Fu *et al.*, 2001; Chen *et al.*, 2002; Chen *et al.*, 2003; Gu *et al.*, 2003; Cheung and Wu, 2004; Bosch and Hepler, 2005; Yoon *et al.*, 2006; Chang *et al.*, 2007; Frietsch *et al.*, 2007; Ischebeck *et al.*, 2008; Röckel *et al.*, 2008; Sousa *et al.*, 2008; Wang *et al.*, 2008; Ye *et al.*, 2009). Second, we used the entire sequence of the gene including the introns. Introns were shown to have an enhancement effect on gene expression (Rose, 2008), specifically in actin genes (McElroy *et al.*, 1990; Jeong *et al.*, 2009) and actin binding proteins (Jeong *et al.*, 2006). Expression of *Petunia ADF* in *Arabidopsis* was particularly enhanced by the presence of the first intron (Mun *et al.*, 2002; Jeong *et al.*, 2007). Third, in order to conserve binding sites, functional domains and proper

targeting of the proteins, insertion of the fluorescent protein in these particular sites was avoided. The technique used here, high throughput fluorescent tagging of full length protein (FTFLP) (Tian *et al.*, 2004) respected these three conditions and was clearly successful since pollen grains germinated and formed perfectly shaped tubes whose morphology was indistinguishable from that of wild type plants. Furthermore, the gene expression pattern was consistent with that predicted by transcriptomic, proteomic and protein immunolabeling data (Honys and Twell, 2003; Honys and Twell, 2004; Pina *et al.*, 2005; Ruzicka *et al.*, 2007) with exclusive expression in the male gametophyte and absence in all other organs. This confirms that our transformation strategy preserved native expression levels and developmental temporal and spatial expression profiles.

Confocal laser scanning microscopy of different stages during gametophyte development revealed that ADF7 and ADF10 displayed different patterns of expression and subcellular localization. ADF7 was expressed earlier, starting from the microspore stage immediately after tetrad separation, whereas ADF10 was only visible at the polarized microspore stage. ADF7 showed nuclear localization at these early stages and at the late pollen grain stage. It is unclear what role ADF plays in the nucleus. ADF/cofilin have been shown to enter the nucleus in animal cells subjected to stress (Sanger *et al.*, 1980; Nishida *et al.*, 1987; Lida *et al.*, 1992; Yahara *et al.*, 1996) and in maize root cells treated with cytochalasin D (Jiang *et al.*, 1997). However, while vertebrate ADF and cofilin have a nuclear localization sequence which allows them to chaperone actin into the nucleus (Bamburg and Bernstein, 2008), these sequences have not been found in plant ADFs. Nevertheless, ADF localization to the plant nucleus has been reported using immunolabeling (Jiang *et al.*, 1997; Ruzicka *et al.*, 2007; Augustine *et al.*, 2008). Two explanations for the nuclear localization have been proposed. ADF in the nucleus may serve to protect actin and reduce ATP loss due to the actin dynamics. Alternatively, actin and ADF enter the nucleus to accomplish chromatin remodeling, to ensure structural stability of the nucleus, and to contribute to proper gene expression through the possible

effect of ADF on actin and therefore on RNA polymerase activity (Jockusch *et al.*, 2006).

Our data showed that the association of ADF7 with the vegetative nucleus was limited to the microspore and to the polarized microspore stages. During the subsequent developmental stages, ADF7 was not again associated with the nucleus anymore, until it returned to the nucleus during late mature stages. This time course suggests that ADF7 is absent from the nucleus during high metabolic activity associated with cell division and it is present in the nucleus during stages of low metabolic activity such as the microspore and the late mature or dormant pollen. This is consistent with the notion that the nuclear localization may serve as a storage form of either ADF or ADF bound actin that can be recruited when cell division or pollen germination requires it. Unlike ADF7, ADF10 was not localized in the nucleus at any of the developmental stages observed here, but it entered the nucleus upon LatB treatment. Since our sequence search showed that both ADF7 and ADF10 possess a positive peak for nuclear export signals with a score of 0.743 and 0.592 respectively, it is possible that the ADF10 score is below the threshold for normal nuclear export and allows ADF10 nuclear targeting only during high stress conditions. The stress-induced behavior of ADF10 is consistent with the notion that ADF inhibits actin denaturation, supporting the hypothesis that actin is packed into the nucleus to protect it during stress and make it available after the stress is removed (Hayden *et al.*, 1993).

ADF10 was not expressed in the *Arabidopsis* male gametophyte until the polarized microspore stage. Label for ADF10 was associated much more frequently with longer actin filaments than ADF7. It also displayed a denser distribution around the apertures (compare Figure 6.1G with Figure 6.2F). These differences suggest that ADF10 has a different function from ADF7 and that it might rather be involved in regulating actin dynamics required for the physical process of pollen tube germination, possibly by ensuring that the actin array correctly directs vesicles

towards the site of pollen tube emergence. This is consistent with the fact that different *ADF* genes expressed in the same cell type show variable expression levels that might be related to functional diversity (Zhang *et al.*, 2007).

In short pollen tubes, ADF7 seemed to be more abundant in the subapical region of the pollen tube tip than ADF10 indicating an important role for ADF7 in the initial phase of cell expansion process occurring at the apex of the emerging pollen tube. In pollen tubes of the same developmental stage, ADF10 was more concentrated on thick bundles of actin filaments in the shank of the pollen tube and in the grain, suggesting that ADF10 has the function to mark older filaments for turnover. It remains unknown where the actin monomers liberated from these distal filaments are used again. They would certainly be expected to be consumed at the pollen tube tip since the elongating tube requires a continuous advancement of the subapical fringe and hence substantial actin polymerization activity. However, even in the shank region of the tube polymerization of actin may be ongoing. An increased number of filaments could serve to produce thicker actin bundles which could ensure efficient long-distance organelle transport and continuous vesicle supply towards the apical zone. This is supported by the notion that acto-myosin mediated vesicular transport is known to happen faster on highly bundled actin filaments (Holweg, 2007). The expression level of ADFs within a given cell might influence the subcellular localization and therefore modulate specific subcellular functions. Transient expression of *NtADF1* in tobacco pollen under the control of the Lat52 promoter was observed to cause this protein to target thicker actin cables in highly expressing pollen grains, whereas in grains with lower expression level label was associated with thinner cables (Chen *et al.*, 2002). The preferential association of ADF10 with thick actin bundles in the shank of the pollen tubes might therefore be a consequence of its relatively high expression level compared to ADF7.

It must be pointed out that the interpretation of ADF expression profiles and subcellular localization needs to be done cautiously, since the presence of ADF does

not necessarily mean that the protein is active. Phosphorylation is able to deactivate ADF (Smertenko *et al.*, 1998; Allwood *et al.*, 2001; Chen *et al.*, 2003) even if it remains bound to actin. On the other hand, phosphoinositides are also able to inactivate ADF (Yonezawa *et al.*, 1990; Yonezawa *et al.*, 1991; Gungabissoon *et al.*, 1998; Kusano *et al.*, 1999) by binding to the actin specific site of free ADF. The fact that diffuse cytoplasmic label was more abundant for ADF7 than ADF10 could be either a result of a lower affinity of ADF7 to actin, of a different steady-state-equilibrium between bound and free ADF, or of a different control mechanism based on phosphoinositide binding. Other proteins could also regulate the activities of ADF7 and ADF10 differently. Lily ADF has for example been shown to be activated by actin interacting protein 1 (AIP1) (Allwood *et al.*, 2002). Finally, although we qualitatively compared fluorescence intensities of ADF7-YFP and ADF10-CFP, direct quantitative comparison is proscribed, of course, since different lasers and light channels were used for image acquisition.

Our data clearly show that ADF7 and ADF10 display different spatial profiles, with ADF7 showing nuclear localization during stages of lower cell activity whereas ADF10 appears in the nucleus only after exposure to stress. This suggests that ADF7 is responsible for ensuring the presence of an actin-ADF stock in the nucleus that can be activated when required for cell division or pollen tube formation, whereas ADF10 protects actin from denaturation during stress conditions. Although ADF7 labels actin filaments in the periphery of the pollen grain, ADF10 showed stronger localization in the peripheral cytoplasm of the developing gametophyte, at the apertures, in the grain after germination and at the tip of the young elongating pollen tube. In elongating pollen tubes, ADF10 seemed to be more highly expressed than ADF7 and it was associated with older actin filaments, likely marking them for recycling. ADF7 on the other hand seemed to be involved in the rapid turnover that characterizes the subapical actin fringe and that is crucial for vesicle targeting to the growing surface (Kroeger *et al.*, 2009). The dynamics of actin filaments in the fringe is known to be crucial for pollen tube growth since its loss

results in a loss of polarity and eventual growth arrest (Cardenas *et al.*, 2005) and the ability of the pollen tube to redirect its growth upon application of external triggers is compromised (Bou Daher and Geitmann). The difference in expression profiles and subcellular localization between ADF7 and ADF10 are summarized in Figure 8. The different profiles suggest that there is a division of labor between different ADF isoforms in the *Arabidopsis* male gametophyte. Proof for this concept awaits experimental evidence on whether the suppression of either protein causes differential effects on pollen development, pollen tube elongation, and the control of polarized and directional growth. Similarly, it will be important to determine whether the individual ADF isoforms are the targets of different signaling pathways.

6.4 Materials and methods

6.4.1 Fluorescent tagging and native expression of ADF

To reproduce the expression level and pattern of the target gene, the construct included the 5' UTR and promoter sequences (about 1000 base pairs), the coding region with introns, and the 3' UTR and the terminator region. To minimize further effects of the fluorescent tag on native subcellular localization and function of the chimeric protein, the location of the tag relative to the target gene was determined based on computer-assisted predictions of protein folding and functional domains. *Arabidopsis* plants expressing *ADF7* (At4g25590) and *ADF10* (At5g52360) were generated using the fluorescent tagging of full length protein (FTFLP) technique (Tian *et al.*, 2004). Two sets of primers P1-P2 and P3-P4 were designed to amplify each of the target genes in two fragments. P1 and P4 contained attB1 and attB2 recombination sites respectively in addition to gene specific sequences. P2 and P3 contained gene specific sequences and fluorescent tag specific sequences. ADF7 was labeled with the cyan variant of the yellow fluorescent protein (CFP) while ADF10 was labeled with yellow fluorescent protein (YFP). Both tags contained a glycine rich linker peptide at the N-terminal side and an alanine rich linker peptide at the C-

terminal region to reduce the interference with the protein folding (Tian *et al.*, 2004).
ADF7 primer sequences:

P1: 5’ gctcgatccacctaggctatcgctgaaacgaggaacagaaag 3’,
P2: 5’ cacagctccacctccacctccaggccggcccactgccatccccgacgc 3’,
P3: 5’ tgctggtgctgctgcggccgctggggccgaggacgagtgcaagctgaag 3’ and
P4: 5’ cgtagcgagaccacaggatcctttctaatgtgcgttgtggtt 3’.
ADF10 primer sequences:
P1: 5’ gctcgatccacctaggctcaatctgtttgcgctttcttttatt 3’,
P2: 5’ cacagctccacctccacctccaggccggcccaccgccatccccgacgc 3’,
P3: 5’ tgctggtgctgctgcggccgctggggccgaggacgagtgtaagctgaag 3’ and
P4: 5’ cgtagcgagaccacaggacgaaagtgagctattacacgagaa 3’.

The fluorescent tag was combined to the two PCR fragments using a triple template PCR with a forward primer containing the attB1 site 5’ ggggacaagtttgtacaaaaaagcaggctgctcgatccacctaggct 3’ and a reverse primer containing the attB2 site 5’ ggggaccactttgtacaagaaagctgggtcgtagcgagaccacagga 3’. Individual PCR fragments were amplified using Phusion (Finnzymes) DNA polymerase and the triple template PCR was performed using ExTaq (TaKaRa) DNA polymerase. DNA was extracted from gel using QIAquick (Qiagen) gel extraction kit. Final PCR fragments were introduced into pDONR Zeo (Invitrogen) entry vector using a BP (Invitrogen) recombination reaction according to the industrial manual. Sequencing was used to verify the positive clones. The chimeric gene was introduced in pBIN-GW (Tian *et al.*, 2004) destination vector using LR (Invitrogen) recombination reaction according to the manufacturer's manual. Plasmid extraction from bacteria was done with QIAprep spin (Qiagen) miniprep kit.

6.4.2 Plant material and pollen tube growth

Arabidopsis thaliana Col-0 plants were grown in soil at 22°C-20°C day-night temperatures, at 60% relative humidity in growth chambers with 16h light/8h dark

light cycle. For pollen tube growth *in vitro*, pollen was collected from flowers at anthesis. Germination was conducted in *Arabidopsis* pollen tube growth medium for 5 hours as described in (Bou Daher *et al.*, 2009). For microspore collection at different stages of development, flowers were dissected under a stereomicroscope and only gametophytes from long anthers were mounted for observation.

6.4.3 Actin and DNA labeling

After five hours of growth, *Arabidopsis* pollen tubes were chemically fixed for 40 seconds in the microwave oven (PELCO Cold Spot® Biowave 34700) under 150 Watts in 3% formaldehyde, 0.5% glutaraldehyde and 0.05% Triton X-100 solution in a buffer composed of 100 mM PIPES, 5 mM $MgSO_4$ and 0.5 mM $CaCl_2$ at pH 9. Pollen tubes were then washed 3 times for one minute each in the same buffer then incubated overnight at 4°C in rhodamine phalloidin (Molecular Probes) in a buffer composed of 100 mM PIPES, 5 mM $MgSO_4$, 0.5 mM $CaCl_2$ and 10 mM EGTA at pH 7. Next day, pollen was washed 5 times for one minute each in the same buffer. All washing steps were conducted in the microwave at 150 Watts. Pollen was then mounted on glass slides in a drop of Citifluor (Electron Microscopy Sciences), covered with a cover slip, sealed and immediately observed in the microscope. DNA was labelled by placing the gametophytes in 1 µg/ml 4'-6-diamidino-2-phenylindole (DAPI) solution in *Arabidopsis* pollen medium. For latrunculin B (LatB) treatment, pollen was incubated in *Arabidopsis* medium containing 100 nM LatB before fixation and actin labeling.

6.4.4 Microscopic observations

Arabidopsis gametophytes from lines expressing the fluorescent proteins were observed in a Zeiss Imager-Z1® microscope equipped for structured illumination microscopy (Apotome) and with a Zeiss AxioCam MRm camera. A filter set of BP 450-490 excitation, FT 510 beamsplitter and BP 515-565 emission was used. For confocal imaging, a Zeiss LSM 510 META / LSM 5 LIVE / Axiovert

200M system confocal microscope was used. A 488 nm argon laser was used for YFP and 458 nm for CFP excitation. For surface rendering and to show a view from inside the pollen grain, the upper half of the z-stack was used to produce a 3D reconstruction of half a grain using the inside 4D function of AxioVision 4.8 (Zeiss) software.

6.5 Funding

This work was supported by grants from the Natural Sciences and Engineering Research Council of Canada (NSERC) and the *Fonds Québécois de la Recherche sur la Nature et les Technologies* (FQRNT) to A.G.

6.6 Acknowledgements

The authors would like to thank professor Natasha Raikhel for kindly providing the p-Citrine3, p-CFP and pMN-GW plasmids.

6.7 Figures

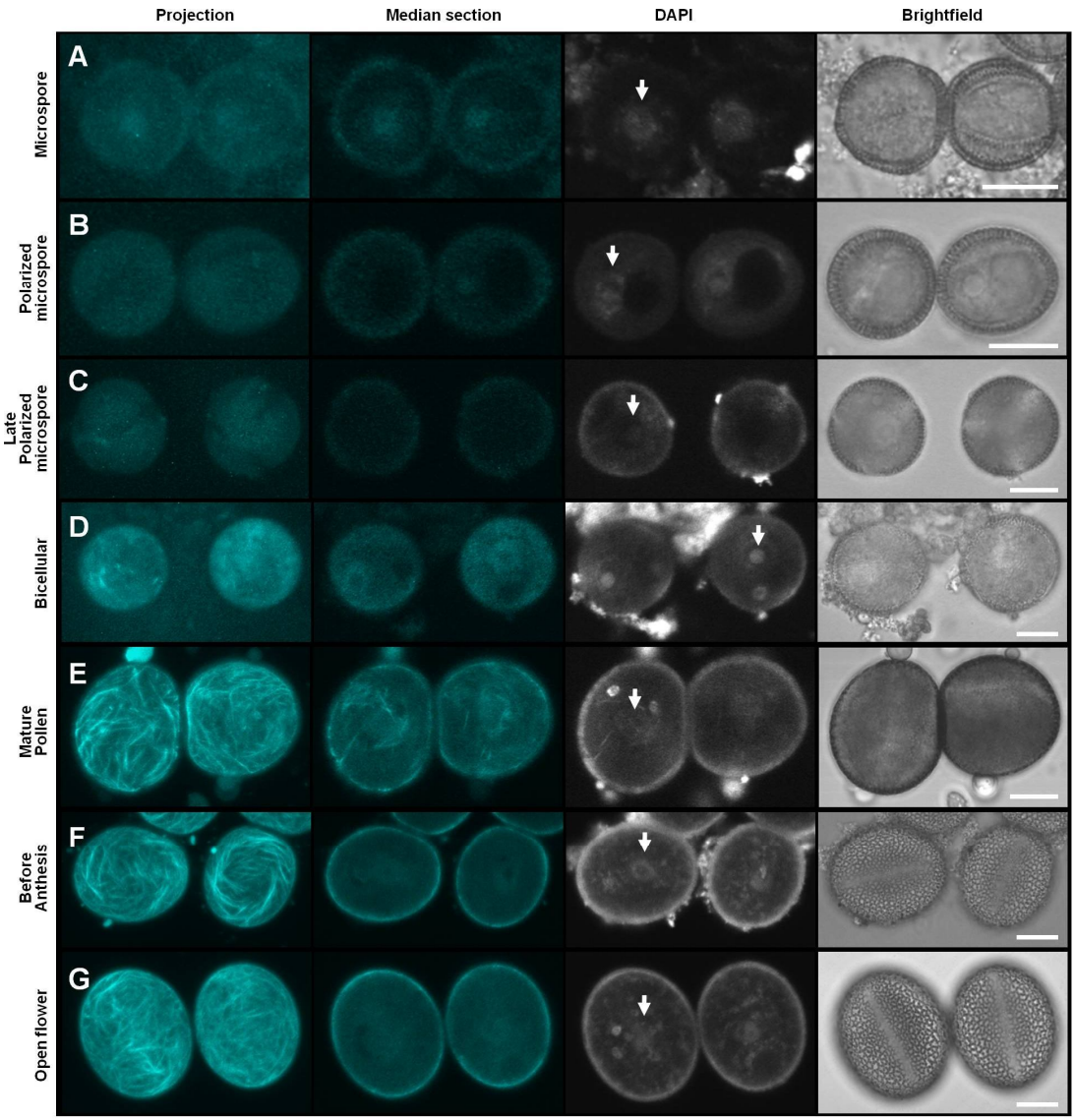

Figure 6.1 : ADF7-CFP expression during different stages of the male gametophyte development. The first column shows maximum projections of Z-stack images acquired with the confocal microscope and the second column shows the corresponding median optical sections. The third column represents single optical sections of the same cells labeled with DAPI and the fourth column represents the corresponding brightfield images. Vegetative nuclei are indicated with an arrow. Scale bars = 10 µm.

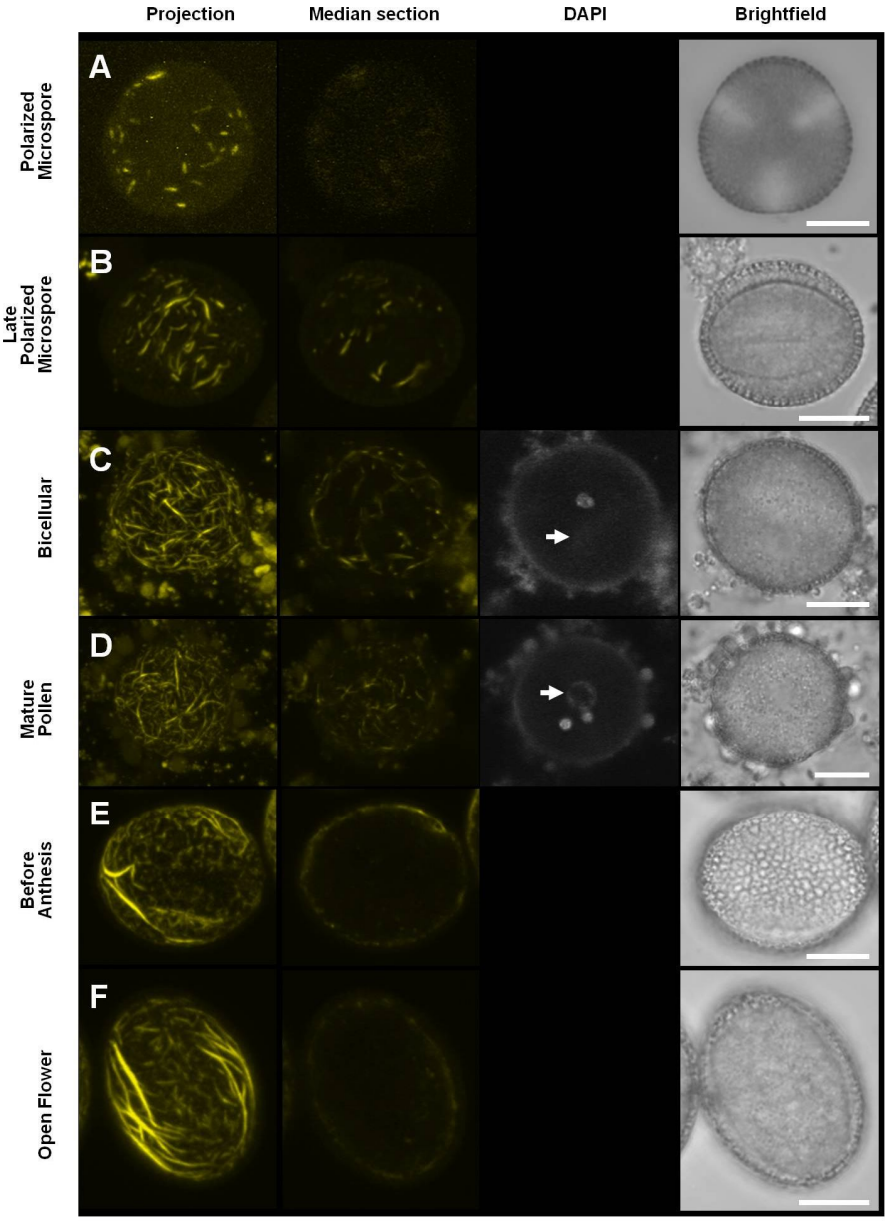

Figure 6.2: ADF10-YFP expression during different stages of the male gametophyte development. The first column represents projections of Z-images taken on the confocal microscope. The first column shows maximum projections of Z-stack images acquired with the confocal microscope and the second column shows the corresponding median optical sections. The third column represents single optical sections of the same cells labeled with DAPI and the fourth column represents the corresponding brightfield images. Vegetative nuclei are shown with an arrow. Scale bars = 10 µm.

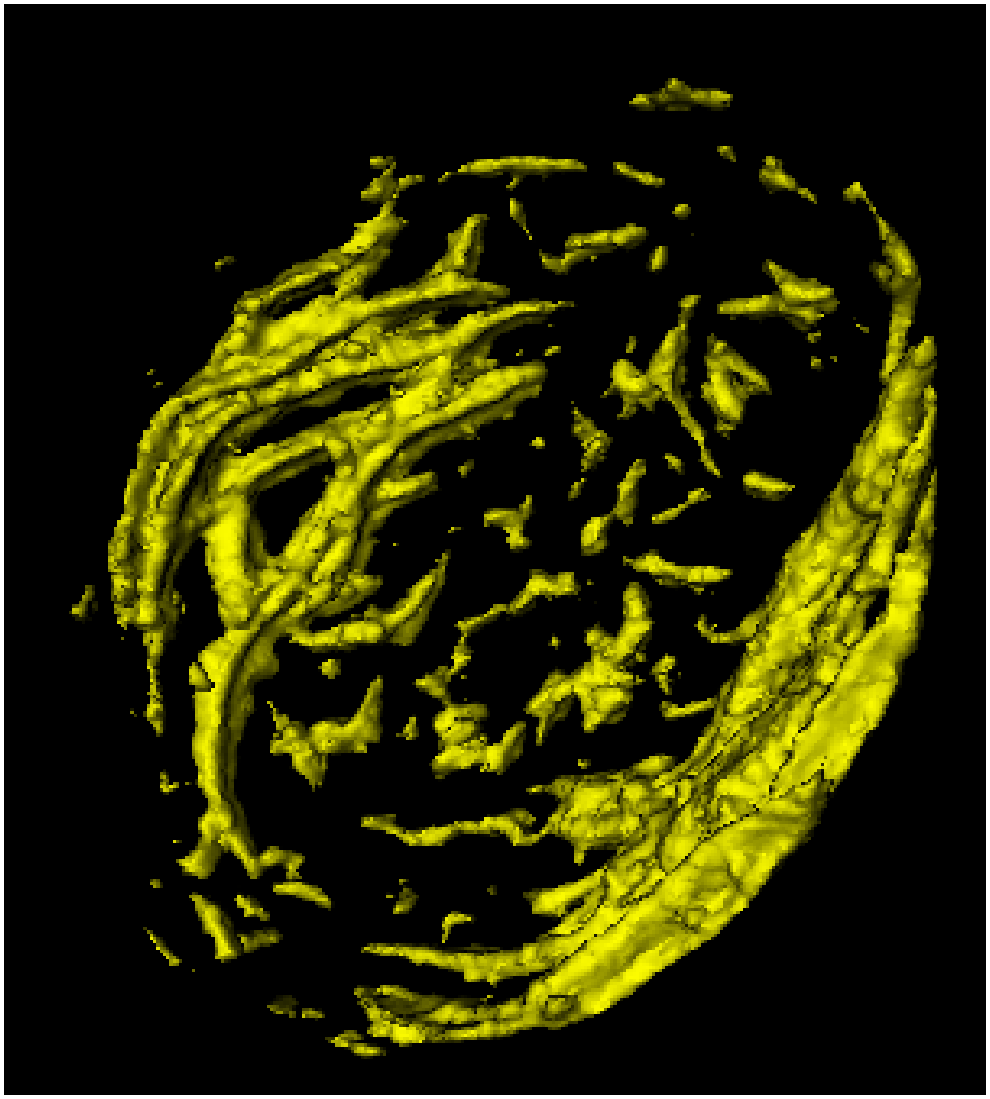

Figure 6.3: Surface rendering image of the pollen grain at the open flower stage expressing ADF10-YFP shown in Figure 2F. Only the upper half of the Z-stack has been used to reveal ADF localization to the peripheral region of the grain. The two groups of long filaments are located at the two apertures present in the half of the grain shown here.

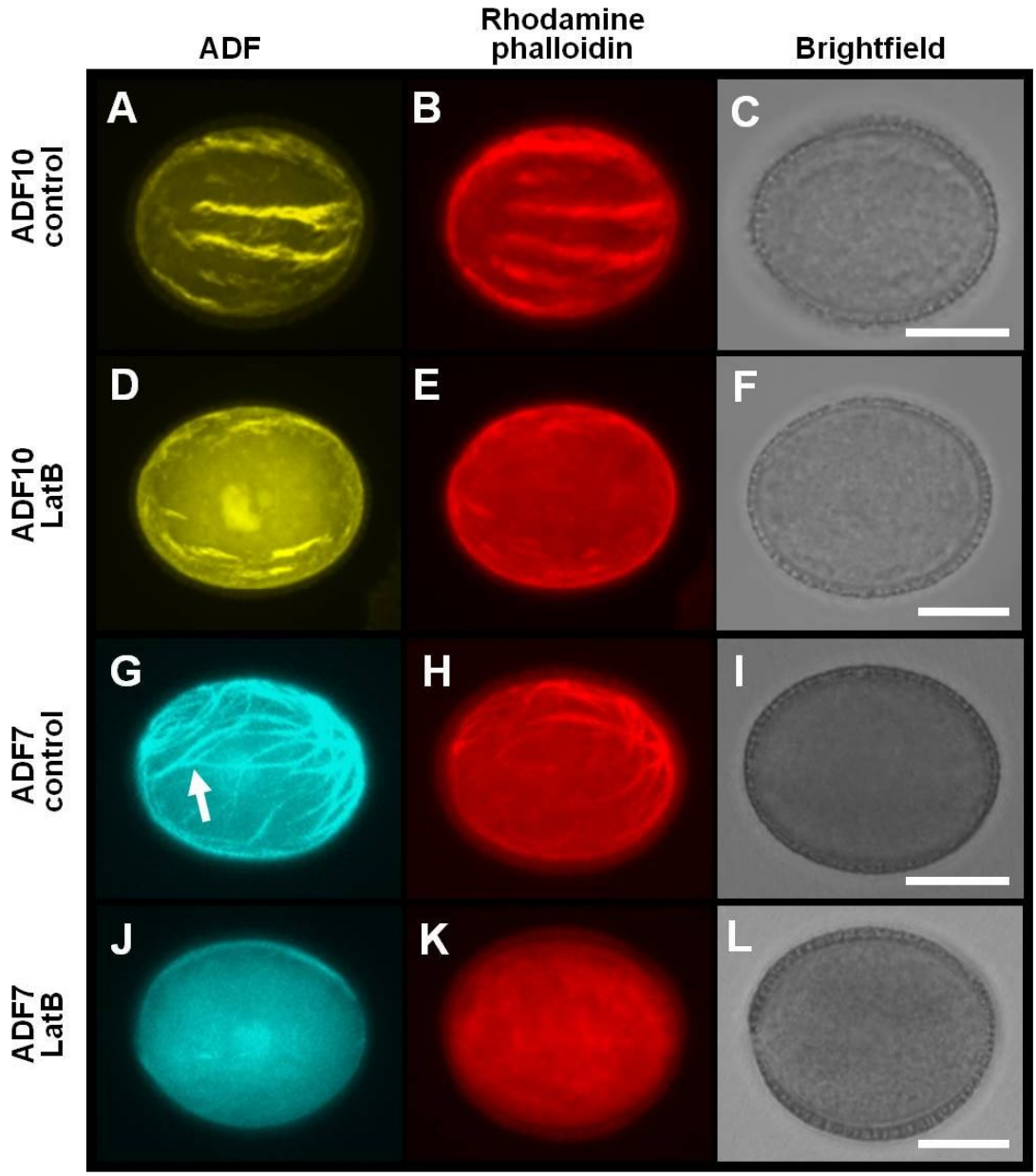

Figure 6.4: Subcellular localization of fluorescent ADF and actin labeled with rhodamine-phalloidin in mature pollen from open flowers. The first column represents ADF label, the second column shows actin labeled with rhodamine phalloidin and last column is the corresponding brightfield image. (D-F, J-L) Pollen grains were treated with LatB prior to fixation and phalloidin label. Certain longer filaments labeled by ADF7 were not labeled with phalloidin (arrow). All fluorescence micrographs are maximum projections of Z-stacks acquired with the confocal microscope. Scale bars = 10 μm.

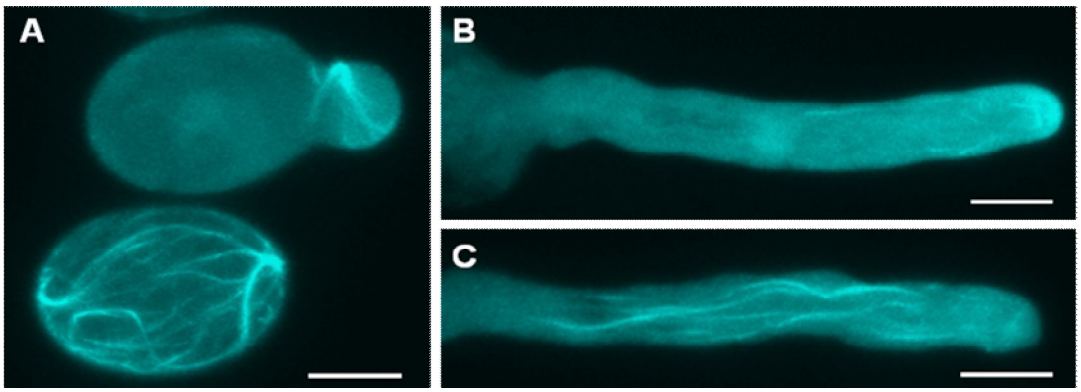

Figure 6.5: Localization of ADF7-CFP in germinating *Arabidopsis* pollen grain (A), in short pollen tube (B) and in long pollen tube (C). All micrographs are maximum projections of Z-stacks acquired with the confocal microscope. Scale bars = 10 µm.

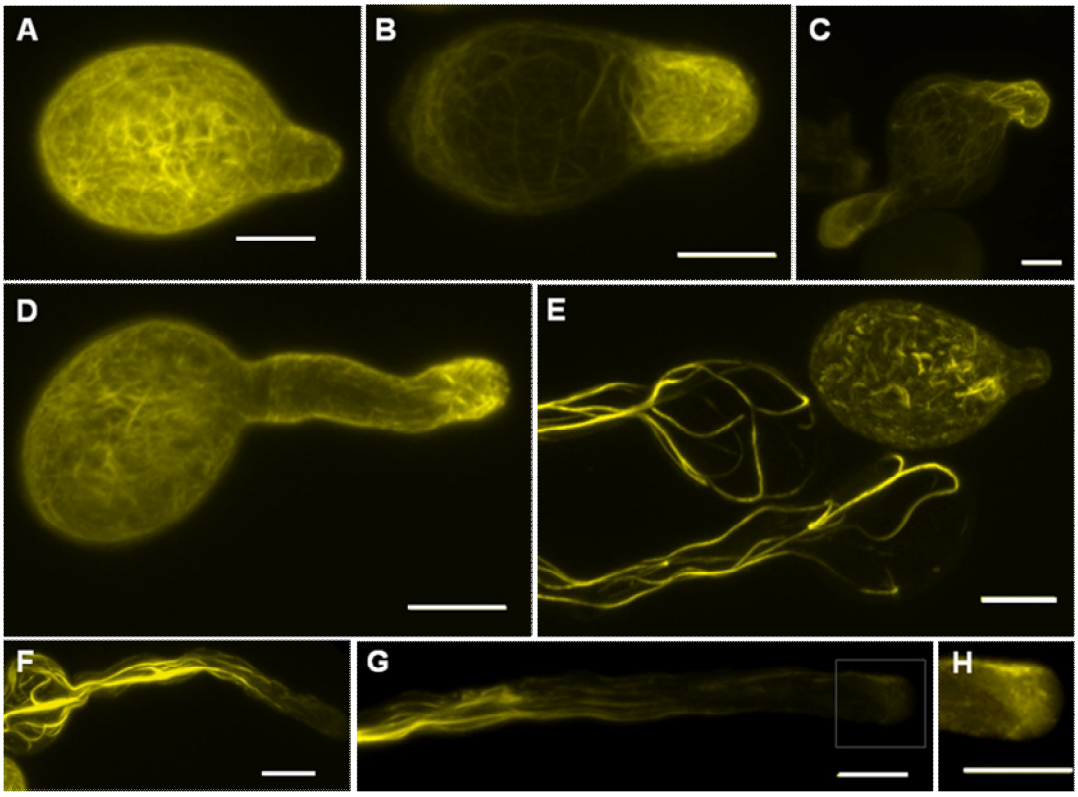

Figure 6.6: Localization of ADF10-YFP in germinating *Arabidopsis* pollen grain (A,B,C), in short pollen tube (D,F) and in long pollen tubes (E,G). (C) is a pollen grain with two emerging pollen tubes. (H) is a magnified and contrast-enhanced image of the tip of the pollen tube in (G) to show the actin fringe. All micrographs are maximum projections of Z-stacks acquired with the confocal microscope. Scale bars = 10 µm.

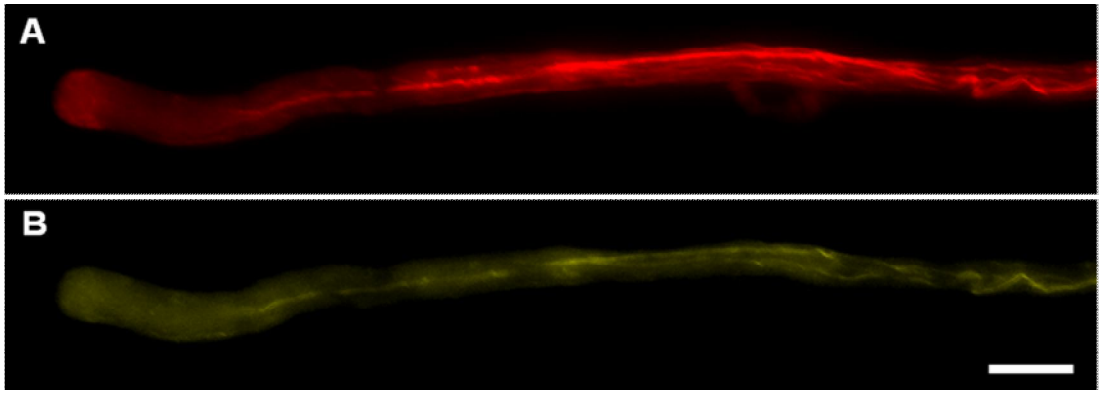

Figure 6.7: *Arabidopsis* pollen tube expressing ADF10-YFP (B) labeled with rhodamine phalloidin (A). Images are maximum projections of Z-stacks of images taken with the Zeiss Apotome. Scale bar = 10 μm.

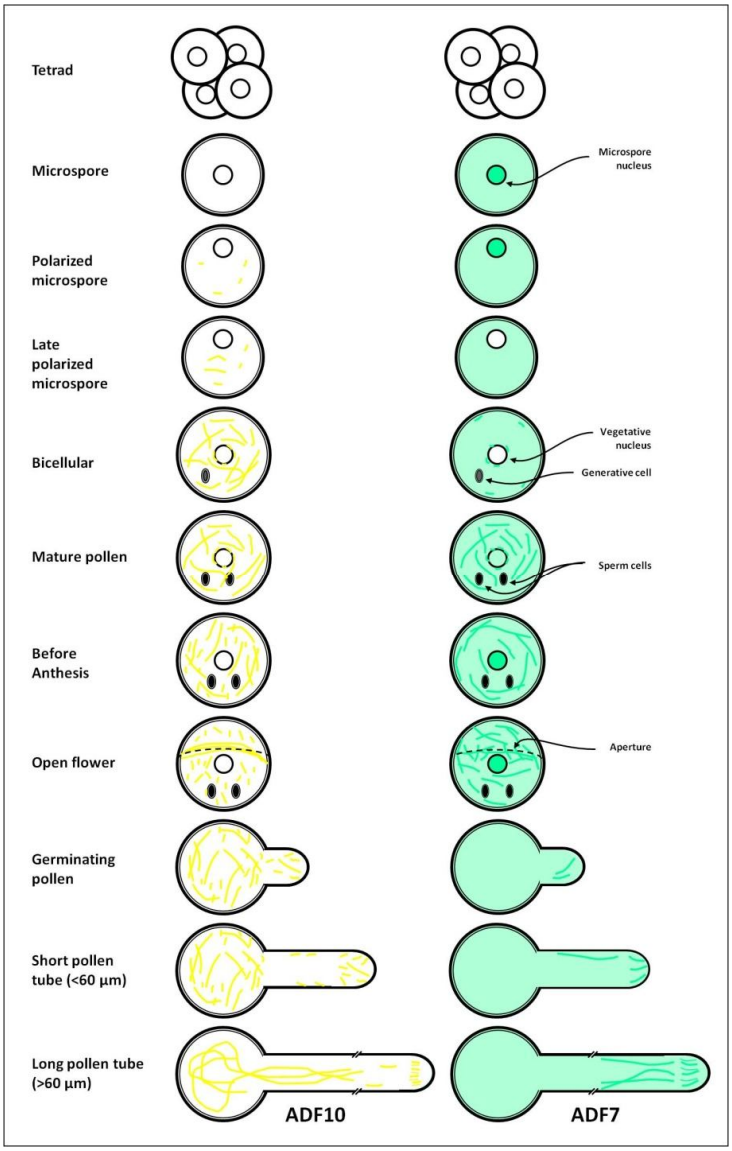

Figure 6.8: ADF7-CFP (cyan) and ADF10-YFP (yellow) distribution in the developing male gametophyte, germinating pollen and elongating pollen tube of *Arabidopsis thaliana*. Elements are not drawn to scale. The dashed line indicates the position of one of the three apertures. For simplicity, nuclei are not shown in the germinated pollen.

6.8 Supplementary material

Supplementary video 1 Time lapse imaging of ADF7-CFP dynamics in *Arabidopsis thaliana* hydrated pollen grain from an open flower. Images were acquired at 1 frame/sec and are played at 7 frames/sec.

Supplementary video 2 Time lapse imaging of ADF10-YFP dynamics in *Arabidopsis thaliana* hydrated pollen grain from an open flower. Images were acquired at 1 frame/sec and are played at 7 frames/sec.

7 Conclusion and perspectives

Reproduction in higher plants requires the transfer of sperm nuclei from the pollen grain to the ovule. Since the ovule is protected in the ovary at the base of the pistil, the pollen grain has to produce a protuberance, the pollen tube, that grows through the pistillar tissues and transports the sperm cells to the embryo sac. Compared to the diameter of the pollen itself, the distance traveled by the pollen tube is extremely long. Therefore, a huge supplement of nutrients is necessary for the non autotrophic pollen tube to grow. Not only is the path to the ovule long, it is also winding and complex, bringing the tube into contact with different cell types and tissues of the pistil. A finely calibrated guidance mechanism based on communication between the pistil and the pollen tube is, therefore, necessary for the latter to follow the right path and reach its target (Cheung *et al.*, 1995; Higashiyama *et al.*, 2003; Palanivelu *et al.*, 2003; Palanivelu and Preuss, 2006; Geitmann and Palanivelu, 2007; Higashiyama and Hamamura, 2008; Okuda *et al.*, 2009; Márton and Dresselhaus, 2010).

The pollen tube has an anisotropic mode of growth shared with root hairs, fungal hyphae and to a certain extent with animal neurons. The cylindrical pollen tube elongates only at the apical region resulting in a unidirectional growth pattern (Geitmann and Dumais, 2009; Geitmann and Ortega, 2009). Because of its simple geometry and rapid growth, the pollen tube has emerged as a model system to study different aspects of polar growth. It presents several advantages over other cell types including the availability of pollen and simplicity of collection and storage on one hand and the relative ease of germination *in vitro* on the other hand. In an attempt to understand how the cytoskeleton regulates pollen tube growth, architecture and tropism, I used molecular, pharmacological, mechanical and microscopical techniques applied to three different pollen species *Lilium longiflorum*, *Camellia japonica* and *Arabidopsis thaliana*.

Lily pollen has been extensively used in pollen tube research. The structure of its cytoskeleton is very well described (Lovy-Wheeler *et al.*, 2005). Lily pollen tube specific gene promoters and constructs with chimeric genes targeting the actin cytoskeleton and tagged with fluorescent proteins are available (Vidali *et al.*, 2009), making lily pollen a useful model for comparative studies focusing on actin configuration and dynamics. *Camellia* pollen is not largely used, most probably due to the growth conditions of this shrub that requires a certain number of chilling hours per year in order to flower. Pollen of *Camellia* turned out to be very easy to germinate, and with few modifications of the standard medium used in our lab (Gossot and Geitmann, 2007), I was able to obtain very high germination percentages and pollen tube growth rates. Importantly, *Camellia* pollen germinates very quickly (20 to 30 minutes after imbibition), it grows very fast (0.2 µm/sec) thus allowing for short experiment time. Furthermore, compared to other species, it has a large diameter (approximately 18 µm), making *Camellia* pollen tube an excellent model to study the mechanical properties of the pollen tube. *Arabidopsis thaliana* is of particular interest for investigation of pollen tube biology because its genome sequence is known, a great number of genes have been identified and characterized and *Arabidopsis* plants are easy to handle because of their small size and short life cycle. The only and major disadvantage this species presents in my context is that its pollen is difficult to germinate and available protocols are often not reproducible. I optimized an *Arabidopsis thaliana* pollen germination and pollen tube growth protocol based on the use of bulk-collected, cold-stored pollen. This protocol produced high and reproducible rates of pollen tube germination and growth *in vitro* and opened the way for use of this promising species in my experiments. Other labs (e.g. Palanivelu, Tucson) have adopted our optimized protocol demonstrating its general usefulness.

A crucial prerequisite for my ultrastructural studies was the availability of a highly reliable, reproducible protocol for the visualization of the actin cytoskeleton of the pollen tube. The actin cytoskeleton is highly dynamic and very sensitive to any

external disturbance. Its structure is easily lost with inappropriate fixation methods. Rapid freeze fixation is the method that has yielded the best results so far based on the conservation of actin arrays when labelled. Given the absence of rapid freeze fixation equipment in our lab, and the long experimental time required for this method, I developed a pollen tube fixation and actin labelling method based on microwave-accelerated chemical fixation. This method proved to be very efficient and very fast with results matching those obtained with freeze fixation. I also used the microwave facility to optimize labelling protocols for cell wall components of the pollen tube.

The actin cytoskeleton in the pollen tube is characterized by an actin fringe located at the subapex of the tube (Kost *et al.*, 1998; Geitmann and Emons, 2000; Lovy-Wheeler *et al.*, 2005). This fringe is the site of high actin dynamics and remodelling (Chen *et al.*, 2002) and is believed to represent a transition between actin filaments located at the periphery of the pollen tube and oriented with their barbed ends pointing to the apex, and filaments oriented in opposite direction and located in the center of the pollen tube (Lenartowska and Michalska, 2008). To further characterize the role of the actin cytoskeleton in pollen tube growth, I treated *Camellia* pollen tubes with s-EGS, a cross linker known to block polymerization of the actin fringe. This treatment caused a loss of the structure of the actin fringe, a strong reduction in pollen tube growth and a swelling at the tip. Normal cylindrical shape and growth could not be resumed before reestablishment of the actin fringe at the subapex of the pollen tube. This highlights the importance of the actin fringe in the pollen tube growth and architecture. This is consistent with the finding that overexpression of ROP, RIC3 or the application of actin stabilizing drugs in pollen tubes lead to the loss of the actin fringe and a swelling of the pollen tube tip (Li *et al.*, 1999; Fu *et al.*, 2001; Cardenas *et al.*, 2005; Gu *et al.*, 2005).

The high sensitivity of the growth process towards the manipulation of the functionality of the actin fringe can be explained by the fact that the fringe is

responsible for the delivery of vesicles to their site of secretion, an annulus located at the shoulder of the pollen tube tip (Geitmann and Dumais, 2009). Whereas the peripheral portion of the fringe moves vesicles forward, the central portion of the subapical actin array is involved in carrying endocytotic vesicles rearward, away from the tip towards the shank. The precise spatial arrangement of the actin fringe at the subapex of the tube with correct actin filament polarity maintains the highly choreographed vesicle flow pattern (Kroeger *et al.*, 2009). Plant cells in general and pollen tubes in particular grow by the deformation of the existing cell wall and the addition of new cell wall material. In pollen tubes, newly added cell wall material is mainly composed of methyl-esterified pectins which is a soft material (Parre and Geitmann, 2005). It is the delivery of these pectins from the Golgi bodies to the growing apical zone that makes the bulk of the vesicle movement (Bove *et al.*, 2008). Treating pollen tubes with BDM, a myosin ATPase inhibitor that inhibits vesicle transport, caused a reduced growth rate in the pollen tube and a change in the composition of its cell wall. This confirms that a balance between expansive growth and cell wall deposition is crucial for correct morphogenesis during pollen tube growth.

Although I provided a detailed time course of the changes in the actin cytoskeleton during BDM treatment and recovery, it will now be important to compare this with the effect of the drug on vesicle motion. This could be done by labeling vesicles in BDM treated tubes and monitoring their movement using high temporal resolution confocal laser scanning microscopy. Movement patterns could be analyzed using spatio-temporal image correlation spectroscopy (STICS), similar to studies done in regularly growing tubes (Bove *et al.*, 2008). This will help us understand the exact effect of BDM on vesicle movement and to determine whether or not the drug preferentially affects the rearward streaming as was suggested by the brightfield micrographs.

It is important for the pollen tube to be able to change its growth direction in order to reach the embryo sac located deep in the ovarian tissues. While various directional signals are produced by the pistil and the female gametophyte to guide the pollen tube (Cheung, 1996; Cheung and Wu, 2001; Geitmann and Palanivelu, 2007), the mechanisms by which they act on the pollen tube are not well understood. Calcium ions are believed to be a crucial element in the signal pathway controlling pollen tube tropism since the release of caged calcium in one side of the pollen tube cytoplasm causes a growth redirection to the same side (Malhó and Trewavas, 1996). To understand how the pollen tube is able to redirect its growth and to determine the elements in the tube regulating its tropic behavior, it was necessary to have a means to induce pollen tube tropic growth *in vitro*. Electric fields were shown to induce tropic growth in several pollen species (Nakamura *et al.*, 1991; Malhó *et al.*, 1992). I designed a miniature galvanotropic chamber that can be mounted on an inverted microscope and in which pollen tubes can grow. I used this chamber to induce precisely timed and calibrated tropic triggers to pollen tubes and to monitor their effects microscopically under different experimental conditions. I found that the actin cytoskeleton is strongly implicated in the ability of the pollen tube to perform directional change. This tropic reaction is also dependent on Ca^{2+} in the growth medium and the calcium influx to the pollen, since blocking calcium channels reduced the capacity of the pollen tube to perform tropic growth. Calcium influx at the pollen tube apex creates a gradient of calcium concentration in the tube (Pierson *et al.*, 1994; Feijó *et al.*, 1995). Calcium ions affect the activity of different actin binding proteins located in the vicinity of the actin fringe. These proteins are responsible for remodeling the actin cytoskeleton. The entry of calcium to one side of the pollen tube after application of the electrical trigger may activate certain actin binding proteins located on one side of the tube and change the symmetry of the actin fringe as was shown when I visualized the actin fringe in a pollen tube upon electrically induced tropic growth. This asymmetric actin distribution is likely to cause vesicle delivery to be shifted to a region further into the apex on one side of the

pollen tube thus causing a tilt in the orientation of the zone of exocytosis. With the addition of soft material being repositioned asymmetrically at the apex, cell wall deformation is biased to one side and tropic growth results.

The question is, how does the electrical field cause a differential influx of calcium? The apical region of the pollen tube plasma membrane is equipped with calcium channels whose activity is crucial for pollen tube growth (Reiss and Herth, 1985; Geitmann and Cresti, 1998; Shang *et al.*, 2005; Qu *et al.*, 2007). Partial blockage of these calcium channels in *Camellia* pollen tubes using lanthanum chloride strongly affected the tropic response, but this effect could be rescued by additional calcium in the growth medium. At least some of the calcium channels in pollen tubes are voltage activated (Shang *et al.*, 2005; Qu *et al.*, 2007). Since the application of an electrical field induces membrane depolarization (Gross *et al.*, 1986; Tsien *et al.*, 1988; Tester and MacRobbie, 1990), we propose that the activity of these voltage-gated calcium channels is affected in our system. We suggest that the calcium channels located on the cathode facing side of the pollen tube are activated by the electric field, creating a biased calcium entry at this side (Figure 5.12B). Since elevated cytosolic calcium is known to trigger actin fragmentation (Eun and Lee, 1997; Eun *et al.*, 2001) or block polymerization (Vantard and Blanchoin, 2002), this results in a tilting of the leading edge and, consequentially of the exocytosis annulus. It is noteworthy that in different pollen tube species, the galvanotropic growth response differed with a cathodotropic response observed in *Vinca*, *Camellia, Erithrina, Tulipa* and *Agapanthus* (Marsh and Beams, 1945; Nakamura *et al.*, 1991; Malhó *et al.*, 1994; Malhó *et al.*, 1995) and an anodotropic response demonstrated in tomato, tobacco, *Lycoris, Hedychinum, Eriobotyia, Impatiens* (Wulff, 1935; Wang *et al.*, 1989; Nakamura *et al.*, 1991). This apparent contradiction could be due to the presence of different types of voltage activated calcium channels or voltage dependent stretch-activated calcium channels or a combination of all these types at the tip of pollen tubes of the different species. A similar explanation had been brought forward for the behavior of fungal hyphae

which are known to turn in different directions (Gow, 1994). Remarkably, the majority of *Agapanthus* pollen tubes were observed to grow towards the cathodal side when they were growing near the cathode and to the anodal side when they were positioned near the anode (Malhó *et al.*, 1992). Even more puzzling, fission yeast *Schizosaccharomyces pombe* subjected to an electrical field grow perpendicular to the direction of the field (Minc and Chang, 2010). Further work on the nature and type of calcium channels present in growing pollen tubes of different species is warranted to clarify the mechanism of calcium entrance and specific difference in pollen tube responses to applied electric trigger.

To eventually understand how actin polymerization and dynamics in the turning pollen tube are regulated, the activities of the proteins controlling actin dynamics must be investigated in more detail. One of the actin binding proteins involved in actin remodeling in the pollen tube that I considered to be a primary candidate is ADF (Chen *et al.*, 2002; Chen *et al.*, 2003). As a crucial step into the direction of a functional analysis, I prepared fluorescent protein fusions of two *Arabidopsis* pollen specific full length ADFs (ADF7 and ADF10) and monitored their expression during male gametophyte development. ADF7 and ADF10 were differentially expressed during microsporogenesis, pollen germination and pollen tube growth. ADF7 showed protein expression directly after the tetrad stage and ADF10 appeared in the polarized microspore stage. ADF7 targeted the vegetative nucleus in the less active developmental stages of the microspore while ADF10 appeared only in the late polarized microspore stage. Just before germination both proteins are highly abundent at the pollen grain apertures suggesting that they might be involved in pollen tube germination through remodeling of the actin cytoskeleton. It would be interesting to test pollen tubes transformed with both ADF7-CFP and ADF10-YFP and to compare their spatial and temporal expression in the same cell.

Understanding the activity state of ADFs in the different stages of male gametophyte development will shed light on the importance of these actin

remodeling proteins during each of the male gametophyte stages of development. ADF activity is regulated by Rop (plant Rho GTPases) proteins (Chen *et al.*, 2003) and by the phosphorylation state of a serine residue contained at the N-terminal side of the protein (Smertenko *et al.*, 1998; Allwood *et al.*, 2001; Chen *et al.*, 2003). This phosphorylation is accomplished by a calcium dependant protein kinase (Smertenko *et al.*, 1998). Since Rop is known to control cell polarity in the pollen tube (Xu and Scheres, 2005; Yalovsky *et al.*, 2008; Hwang *et al.*, 2010), ADF might mediate the effect of Rop on pollen tube growth polarity through site specific actin remodeling in the actin fringe of a growing pollen tube. The fact that ADF7 was found to target the nucleus in less active stages of gametophyte development, on the other hand, might be of great physiological importance. Actin has been found in the nuclei of various animal cells (Bettinger *et al.*, 2004; Jockusch *et al.*, 2006) and was suggested to play a role in RNA polymerase based transcription. It would be of great interest to test the effect of knockdown of ADF7 on transcription and cell division during male gametophyte development since these stages are very well characterized (Borg *et al.*, 2009).

Although the pollen tube has an extremely polarized type of growth, general principles for the mechanism of plant cell growth can be extrapolated from research on the male gametophyte. For example, the interactions between actin arrays and microtubules are believed to contribute to the spatial regulation of growth in both isotropic and diffuse growing cells (Smith and Oppenheimer, 2005; Mathur, 2006). In root hairs, the actin cytoskeleton configuration resembles that of the pollen tube, since filamentous actin is absent at the very apex, fine actin filaments characterize the subapex and long bundled actin filaments are present in the shank. Similar to pollen tubes, treatment with actin depolymerizing drugs inhibits root hair elongation (Miller *et al.*, 1999; Ketelaar *et al.*, 2003; Ketelaar and Emons, 2009). The actin cytoskeleton in trichomes is also organized in long filaments parallel to the growth axis and treatment with cytochalasin D affects trichome morphogenesis (Mathur *et al.*, 1999; Szymanski *et al.*, 1999), but after an initial phase of polar outgrowth,

trichome elongation proceeds by diffuse growth. Consistent with this difference, there is no subapical actin fringe near the tips of elongating trichomes (Mathur *et al.*, 1999). In the zygotes of the marine brown alga *Fucus*, establishment of polarity of the cell is associated with F-actin deposition at the protruding site (Kropf *et al.*, 1989; Goodner and Quatrano, 1993; Kropf, 1997) and this process is affected by actin depolymerization possibly through the disruption of the cell secretory machinery (Fowler and Quatrano, 1997). In *Arabidopsis* pavement cells that are characterized by anisotropically protruding surface areas creating interlocking lobes similar to short polarized outgrowths, the site of cell expansion is associated with fine F-actin deposition (Fu *et al.*, 2002). In all these cell types and in plant cells in general, localized expansion is due to deposition of cell wall material transported by the actin cytoskeleton to the growing surface region. This is very different from the growth or migrating mechanism in animal cells. Although the actin array of the leading edge in migrating fibroblasts looks superficially similar to the subapical actin fringe in pollen tubes, the protrusion of the forward moving cell edge is directly pushed by actin polymerization. The crucial difference between these animal and plant cells is the presence of the relatively stiff outer matrix in the latter. The extracellular matrix in migrating animal cells is highly pliable, whereas the deformation of the cell wall requires forces that are an order of magnitude larger than those that could be produced even by a dense actin array (Money and Hill, 1997). Local growth events in plant cells are therefore spatially controlled by the differences in mechanical properties within the surrounding cell wall which in turn are only indirectly influenced by the actin cytoskeleton through the targeting of new cell wall material (Geitmann and Ortega, 2009).

The dynamic behavior of actin is controlled *in vivo* by ABPs responsible for actin polymerization, depolymerization, nucleation, severing, branching, bundling and capping. The activities of several ABPs in plants is controlled by calcium (Yokota and Shimmen, 2006). In the pollen tube, , Rop was shown to regulate the formation of the calcium gradient at the tip of the pollen tube (Li *et al.*, 1999) and

was found to be strongly implicated in cell polarity (Fu *et al.*, 2001; Molendijk *et al.*, 2001; Fu *et al.*, 2002; Chen *et al.*, 2003; Xu and Scheres, 2005; Nibau *et al.*, 2006; Yalovsky *et al.*, 2008). Monitoring cytosolic calcium and identifying Rop activity during tropic pollen tube growth would yield important information related to the flow of ions and their effect on actin dynamics and precise vesicle deposition. Vesicle deposition determines the soft site in the cell wall, i.e. the site whose mechanical properties allow yielding under turgor pressure (Mathur, 2006). This applies to all plant cells with heterotropic mode of growth (Geitmann and Ortega, 2009) even though the specific molecular players or the concentrations of these players may vary in different cellular systems. The use of probes to localize calcium channels in addition to experiments applying calcium channel inhibitors showed the presence and the effect of these channels on plant cell growth. The nature and activity control of calcium channels at these anisotropically growing zones is a domain that warrants exploration because of the presence of a multitude of cellular mechanisms controlled by calcium. The exact molecular nature of these proteins remains to be identified through the analysis of mutants and the use of fluorescent fusion proteins and complementation of knockouts. Their interaction with other players such as the cytoskeleton will help understand the regulation of their activities and therefore the fascinating mechanisms affected by the calcium influx and actin remodeling including cell growth and cell polarity.

The actin cytoskeleton is also involved in several signalling processes in plants including self incompatibility in pollination (Geitmann *et al.*, 2000; Thomas *et al.*, 2006) and gravitropism in root cells (Baluška and Hasenstein, 1997; Perbal and Driss-Ecole, 2003; Morita, 2010). These signalling processes are also associated with calcium and calcium influx (Kordyum *et al.*, 2007; Toyota *et al.*, 2008; Sobol and Kordyum, 2009). The adaptation of approaches similar to those I used in my research could be used to mimic specific responses of plant cells such as the self incompatibility response of pollen tubes or the gravitropic response of roots which are thought to be mediated by calcium mobilization and actin remodelling or

depolymerization. The galvanotropic setup could be used to force calcium influx into the apex of growing pollen tubes or the root tips in symmetric manner by orienting elongating cells to point towards the cathode. Instead of causing an asymmetric turning response, this would likely simply increase the amount of calcium influx enabling us to monitor the effect of an altered cytosolic calcium concentration on actin, microtubules and amyloplasts sedimentation, a phenomenon believed to be implicated in gravity response (Palmieri and Kiss, 2005). This setup would allow the assessment cellular responses under different conditions such as varying calcium concentrations in the medium or the presence of pharmacological agents affecting signalling. Transgenic lines, whether knockouts or expressing fluorescently tagged proteins, could also be tested and monitored live under the microscope.

References

Alessa, L. and D. L. Kropf (1999). F-actin marks the rhizoid pole in living *Pelvetia compressa* zygotes. Development **126**: 201-209.

Allwood, E. G., R. G. Anthony, A. P. Smertenko, S. Reichelt, B. K. Drobak, J. H. Doonan, A. G. Weeds and P. J. Hussey (2002). Regulation of the pollen-specific actin-depolymerizing factor LlADF1. Plant Cell **14**: 2915-2927.

Allwood, E. G., A. P. Smertenko and P. J. Hussey (2001). Phosphorylation of plant actin-depolymerising factor by calmodulin-like domain protein kinase. FEBS Letters **499**: 97-100.

Altschul, S. F., T. L. Madden, A. A. Schäffer, J. Zhang, Z. Zhang, W. Miller and D. J. Lipman (1997). Gapped BLAST and PSI-BLAST: a new generation of protein database search programs. Nucleic Acids Research **25**: 3389-3402.

Anderhag, P., P. K. Hepler and M. D. Lazzaro (2000). Microtubules and microfilaments are both responsible for pollen tube elongation in the conifer *Picea abies* (Norway spruce). Protoplasma **214**: 141-157.

Andrianantoandro, E. and T. D. Pollard (2006). Mechanism of actin filament turnover by severing and nucleation at different concentrations of ADF/Cofilin. Molecular Cell **24**: 13-23.

Aouar, L., Y. Chebli and A. Geitmann (2010). Morphogenesis of complex plant cell shapes: the mechanical role of crystalline cellulose in growing pollen tubes. Sexual Plant Reproduction **23**: 15-27.

Åström, H., O. Sorri and M. Raudaskoski (1995). Role of microtubules in the movement of the vegetative nucleus and generative cell in tobacco pollen tubes. Sexual Plant Reproduction **8**: 61-69.

Åström, H., I. Virtanen and M. Raudaskoski (1991). Cold-stability in the pollen tube cytoskeleton. Protoplasma **160**: 99-107.

Augustine, R. C., L. Vidali, K. P. Kleinman and M. Bezanilla (2008). Actin depolymerizing factor is essential for viability in plants, and its phosphoregulation is important for tip growth. The Plant Journal **54**: 863-875.

Bachewich, C. and I. Heath (1998). Radial F-actin arrays precede new hypha formation in *Saprolegnia*: implications for establishing polar growth and regulating tip morphogenesis. Journal of Cell Science **111**: 2005-2016.

Baluška, F. and K. H. Hasenstein (1997). Root cytoskeleton: its role in perception of and response to gravity. Planta **203**: S69-S78.

Baluška, F., J. Salaj, J. Mathur, M. Braun, F. Jasper, J. Samaj, N.-H. Chua, P. W. Barlow and D. Volkmann (2000). Root hair formation: F-actin-dependent tip growth is initiated by local assembly of profilin-supported F-actin meshworks accumulated within expansin-enriched bulges. Developmental Biology **227**: 618-632.

Bamburg, J. R. (1999). Proteins of the ADF/cofilin family: Essential regulators of actin dynamics. Annual Review of Cell and Developmental Biology **15**: 185-230.

Bamburg, J. R. and B. W. Bernstein (2008). ADF/Cofilin. Current Biology **18**: R273-R275.

Bartnicki-Garcia, S. (1990). Role of vesicles in apical growth and a new mathematical model of hyphal morphogenesis. In Tip Growth in Plant and Fungal Cells. I. B. Heath. San Diego, Academic Press**:** 211-232.

Baskin, T. I. (2005). Anisotropic expansion of the plant cell wall. Annual Review of Cell and Developmental Biology **21**: 203-222.

Battey, N. H., N. C. James, A. J. Greenland and C. Brownlee (1999). Exocytosis and endocytosis. Plant Cell **11**: 643-659.

Becker, J. D., L. C. Boavida, J. Carneiro, M. Haury and J. A. Feijó (2003). Transcriptional profiling of *Arabidopsis* tissues reveals the unique characteristics of the pollen transcriptome. Plant Physiology **133**: 713-725.

Bedlack, R. S., M. d. Wei and L. M. Loew (1992). Localized membrane depolarizations and localized calcium influx during electric field-guided neurite growth. Neuron **9**: 393-403.

Bettinger, B. T., D. M. Gilbert and D. C. Amberg (2004). Actin up in the nucleus. Nature Reviews Molecular Cell Biology **5**: 410-415.

Bisgrove, S. R. (2008). The roles of microtubules in tropisms. Plant Science **175**: 747-755.

Blanchoin, L. and T. D. Pollard (1999). Mechanism of interaction of *Acanthamoeba* actophorin (ADF/cofilin) with actin filaments. Journal of Biological Chemistry **274**: 15538-15546.

Blevins, D. G. and K. M. Lukaszewski (1998). Boron in plant structure and function. Annual Review of Plant Physiology and Plant Molecular Biology **49**: 481-500.

Boavida, L. C. and S. McCormick (2007). Temperature as a determinant factor for increased and reproducible in vitro pollen germination in *Arabidopsis thaliana*. The Plant Journal **52**: 570-582.

Borg, M., L. Brownfield and D. Twell (2009). Male gametophyte development: a molecular perspective. Journal of Experimental Botany **60**: 1465-1478.

Bosch, M. and P. K. Hepler (2005). Pectin methylesterases and pectin dynamics in pollen tubes. Plant Cell **17**: 3219-3226.

Bou Daher, F., Y. Chebli and A. Geitmann (2009). Optimization of conditions for germination of cold-stored *Arabidopsis thaliana* pollen. Plant Cell Reports **28**: 347-357.

Bou Daher, F. and A. Geitmann (submitted). Actin regulates pollen tube tropism through redefining the spatial targeting of secretory vesicles. Traffic.

Bove, J., B. Vaillancourt, J. Kroeger, P. K. Hepler, P. W. Wiseman and A. Geitmann (2008). Magnitude and direction of vesicle dynamics in growing pollen tubes using spatiotemporal image correlation spectroscopy and fluorescence recovery after photobleaching. Plant Physiology **147**: 1646-1658.

Bowman, G. D., I. M. Nodelman, Y. Hong, N.-H. Chua, U. Lindberg and C. E. Schutt (2000). A comparative structural analysis of the ADF/Cofilin family. Proteins: Structure, Function, and Bioinformatics **41**: 374-384.

Brand, A., S. Shanks, V. M. S. Duncan, M. Yang, K. Mackenzie and N. A. R. Gow (2007). Hyphal orientation of *Candida albicans* is regulated by a calcium-dependent mechanism. Current Biology **17**: 347-352.

Brewbaker, J. and B. Kwack (1963). The essential role of calcium ion in pollen germination and pollen tube growth. American Journal of Botany **50**: 859–865.

Brewbaker, J. L. (1967). The distribution and phylogenetic significance of binucleate and trinucleate pollen grains in the angiosperms. American Journal of Botany **54**: 1069-1083.

Brown, R. (1833). On the organs and mode of fecundation in Orchidec and Asclepiadec. Transactions of the Linnean Society of London **16**: 685-738.

Bryant, V. and D. Mildenhall (1998). Forensic palynology: a new way to catch crooks. New development in palynomorph sampling, extraction ad analysis: 145-155.

Cai, G. and M. Cresti (2008). Organelle motility in the pollen tube: a tale of 20 years. Journal of Experimental Botany: ern321.

Cai, G., C. Del Casino, S. Romagnoli and M. Cresti (2005). Pollen cytoskeleton during germination and tube growth. Current Science **89**: 1853–1860.

Camacho, L. and R. Malhó (2003). Endo/exocytosis in the pollen tube apex is differentially regulated by Ca^{2+} and GTPases. Journal of Experimental Botany **54**: 83-92.

Cardenas, L., A. Lovy-Wheeler, J. G. Kunkel and P. K. Hepler (2008). Pollen tube growth oscillations and intracellular calcium levels are reversibly modulated by actin polymerization. Plant Physiology **146**: 1611-1621.

Cardenas, L., A. Lovy-Wheeler, K. L. Wilsen and P. K. Hepler (2005). Actin polymerization promotes the reversal of streaming in the apex of pollen tubes. Cell Motility and the Cytoskeleton **61**: 112-127.

Carlier, M.-F., V. Laurent, J. Santolini, R. Melki, D. Didry, G.-X. Xia, Y. Hong, N.-H. Chua and D. Pantaloni (1997). Actin depolymerizing factor (ADF/Cofilin) enhances the rate of filament turnover: implication in actin-based motility. Journal of Cell Biology **136**: 1307-1322.

Carpita, N. C. and D. M. Gibeaut (1993). Structural models of primary cell walls in flowering plants: consistency of molecular structure with the physical properties of the walls during growth. The Plant Journal **3**: 1-30.

Chang, F., A. Yan, L.-N. Zhao, W.-H. Wu and Z. Yang (2007). A putative calcium-permeable cyclic nucleotide-gated channel, CNGC18, regulates polarized pollen tube growth. Journal of Integrative Plant Biology **49**: 1261-1270.

Chaubal, R. and B. J. Reger (1990). Relatively high calcium is localized in synergid cells of wheat ovaries. Sexual Plant Reproduction **3**: 98-102.

Chebli, Y. and A. Geitmann (2007). Mechanical principles governing pollen tube growth. Functional Plant Science and Biotechnology **1**: 232-245.

Chen, C. Y.-h., A. Y. Cheung and H.-m. Wu (2003). Actin-depolymerizing factor mediates Rac/Rop GTPase-regulated pollen tube growth. Plant Cell **15**: 237-249.

Chen, C. Y., E. I. Wong, L. Vidali, A. Estavillo, P. K. Hepler, H.-m. Wu and A. Y. Cheung (2002). The Regulation of actin organization by actin-depolymerizing factor in elongating pollen tubes. Plant Cell **14**: 2175-2190.

Chen, N., X. Qu, Y. Wu and S. Huang (2009). Regulation of actin dynamics in pollen tubes: control of actin polymer level. Journal of Integrative Plant Biology **51**: 740-750.

Chen, Y., H. Li, D. Shi, L. Yuan, J. Liu, R. Sreenivasan, R. Baskar, U. Grossniklaus and W. Yang (2007). The central cell plays a critical role in pollen tube guidance in *Arabidopsis*. Plant Cell **19**: 3563 - 3577.

Cheung, A. Y. (1996). Pollen-pistil interactions during pollen-tube growth. Trends in Plant Science **1**: 45-51.

Cheung, A. Y., H. Wang and H.-m. Wu (1995). A floral transmitting tissue-specific glycoprotein attracts pollen tubes and stimulates their growth. Cell **82**: 383-393.

Cheung, A. Y. and H.-m. Wu (2001). Plant biology: pollen tube guidance--right on target. Science **293**: 1441-1442.

Cheung, A. Y. and H.-m. Wu (2004). Overexpression of an *Arabidopsis* formin stimulates supernumerary actin cable formation from pollen tube cell membrane. Plant Cell **16**: 257-269.

Cheung, A. Y. and H.-m. Wu (2008). Structural and signaling networks for the polar cell growth machinery in pollen tubes. Annual Review of Plant Biology **59**: 547-572.

Cheung, A. Y. and H. M. Wu (1999). Arabinogalactan proteins in plant sexual reproduction. Protoplasma **208**: 87-98.

Ciprandi, G., C. Pronzato, V. Ricca, P. Varese, G. S. D. Giacco and G. W. Canonica (1995). Terfenadine exerts antiallergic activity reducing ICAM-1 expression on nasal epithelial cells in patients with pollen allergy. Clinical and Experimental Allergy **25**: 871-878.

Ciprandi, G., M. Tosca, V. Ricca, G. Passalacqua, A. M. Riccto, M. Bagnasco and G. W. Canonica (1997). Cetirizine treatment of rhinitis in children with pollen allergy: evidence of its antiallergic activity. Clinical and Experimental Allergy **27**: 1160-1166.

Clement, M., T. Ketelaar, N. Rodiuc, M. Y. Banora, A. Smertenko, G. Engler, P. Abad, P. J. Hussey and J. de Almeida Engler (2009). Actin-depolymerizing factor2-mediated actin dynamics are essential for root-knot nematode infection of *Arabidopsis*. Plant Cell **21**: 2963-2979.

Coelho, P. and R. Malhó (2006). Correlative analysis of $[Ca^{2+}]_C$ and apical secretion during pollen tube growth and reorientation. Plant Signaling and Behavior **1**: 152-157.

Cooper, J. A. and D. A. Schafer (2000). Control of actin assembly and disassembly at filament ends. Current Opinion in Cell Biology **12**: 97-103.

Cosgrove, D. (1986). Biophysical control of plant cell growth. Annual Review of Plant Physiology **37**: 377-405.

Cosgrove, D. J. (1993). How do plant cell walls extend? Plant Physiology **102**: 1-6.

Cosgrove, D. J. (2000). Expansive growth of plant cell walls. Plant Physiology and Biochemistry **38**: 109-124.

Cosgrove, D. J., P. Bedinger and D. M. Durachko (1997). Group I allergens of grass pollen as cell wall-loosening agents. Proceedings of the National Academy of Sciences of the United States of America **94**: 6559-6564.

Cosgrove, D. J. and R. Hedrich (1991). Stretch-activated chloride, potassium, and calcium channels coexisting in plasma membranes of guard cells of *Vicia faba* L. Planta **186**: 143-153.

Cresti, M., F. Ciampolini, D. L. M. Mulcahy and G. Mulcahy (1985). Ultrastructure of *Nicotiana alata* pollen, its germination and early tube formation. American Journal of Botany **72**: 719-727.

Cresti, M., E. Pacini, F. Ciampolini and G. Sarfatti (1977). Germination and early tube development *in vitro* of *Lycopersicum peruvianum* pollen: Ultrastructural features. Planta **136**: 239-247.

Crombie, C., N. A. R. Gow and G. W. Gooday (1990). Influence of applied electrical fields on yeast and hyphal growth of *Candida albicans*. Journal of General Microbiology **136**: 311-317.

Dafni, A. and M. M. Maués (1998). A rapid and simple procedure to determine stigma receptivity. Sexual Plant Reproduction **11**: 177-180.

de Graaf, B. H. J., A. Y. Cheung, T. Andreyeva, K. Levasseur, M. Kieliszewski and H.-m. Wu (2005). Rab11 GTPase-regulated membrane trafficking is crucial for tip-focused pollen tube growth in tobacco. Plant Cell **17**: 2564-2579.

Demaree, R. S. and R. T. Giberson (2001). Overview of microwave-assisted tissue processing for transmission electron microscopy. In Microwave Techniques and Protocols**:** 1-11.

DePina, A. S. and G. M. Langford (1999). Vesicle transport: The role of actin filaments and myosin motors. Microscopy Research and Technique **47**: 93-106.

Derksen, J., B. Knuiman, K. Hoedemaekers, A. Guyon, S. Bonhomme and E. S. Pierson (2002). Growth and cellular organization of *Arabidopsis* pollen tubes *in vitro*. Sexual Plant Reproduction **15**: 133-139.

Derksen, J., T. Rutten, I. K. Lichtscheidl, A. H. N. de Win, E. S. Pierson and G. Rongen (1995). Quantitative analysis of the distribution of organelles in tobacco pollen tubes: implications for exocytosis and endocytosis. Protoplasma **188**: 267-276.

Dong, C.-H., G.-X. Xia, Y. Hong, S. Ramachandran, B. Kost and N.-H. Chua (2001). ADFproteins are involved in the control of flowering and regulate F-actin organization, cell expansion, and organ growth in *Arabidopsis*. Plant Cell **13**: 1333-1346.

Dresselhaus, T. and M. L. Márton (2009). Micropylar pollen tube guidance and burst: adapted from defense mechanisms? Current Opinion in Plant Biology **12**: 773-780.

Ducker, S., J. Pettitt and R. Knox (1978). Biology of Australian seagrasses: Pollen development and submarine pollination in *Amphibolis antarctica* and

Thalassodendron ciliatum (Cymodoceaceae). Australian Journal of Botany **26**: 265-285.

Dutta, R. and K. R. Robinson (2004). Identification and characterization of stretch-activated ion channels in pollen protoplasts. Plant Physiology **135**: 1398-1406.

Elleman, C., V. Franklin-Tong and H. Dickinson (1992). Pollination in species with dry stigmas: the nature of the early stigmatic response and the pathway taken by pollen tubes. New Phytologist **121**: 413-424.

Eun, S.-O., S.-H. Bae and Y. Lee (2001). Cortical actin filaments in guard cells respond differently to abscisic acid in wild-type and *abi1*-1 mutant *Arabidopsis*. Planta **212**: 466-469.

Eun, S. O. and Y. Lee (1997). Actin filaments of guard cells are reorganized in response to light and abscisic acid. Plant Physiology **115**: 1491-1498.

Fan, L. M., Y. F. Wang, H. Wang and W. H. Wu (2001). *In vitro Arabidopsis* pollen germination and characterization of the inward potassium currents in *Arabidopsis* pollen grain protoplasts. Journal of Experimental Botany **52**: 1603-1614.

Fayant, P., O. Girlanda, Y. Chebli, C.-E. Aubin, I. Villemure and A. Geitmann (2010). Finite element model of polar growth in pollen tubes. Plant Cell **22**: 2579-2593.

Feijó, J. A., R. Malhó and G. Obermeyer (1995). Ion dynamics and its possible role during *in-vitro* pollen germination and tube growth. Protoplasma **187**: 155-167.

Feijó, J. A., J. Sainhas, G. R. Hackett, J. G. Kunkel and P. K. Hepler (1999). Growing pollen tubes possess a constitutive alkaline band in the clear zone and a growth-dependent acidic tip. Journal of Cell Biology **144**: 483-496.

Ferguson, C., T. T. Teeri, M. Siika-aho, S. M. Read and A. Bacic (1998). Location of cellulose and callose in pollen tubes and grains of *Nicotiana tabacum*. Planta **206**: 452-460.

Fowler, J. E. and R. S. Quatrano (1997). Plant cell morphogenesis: Plasma membrane interactions with the cytoskeleton and cell wall. Annual Review of Cell and Developmental Biology **13**: 697-743.

Franklin-Tong, V. E. (1999). Signaling and the modulation of pollen tube growth. Plant Cell **11**: 727-738.

Friederich, E., E. Pringault, M. Arpin and D. Louvard (1990). From the structure to the function of villin, an actin-binding protein of the brush border. Bioessays **12**: 403-408.

Frietsch, S., Y.-F. Wang, C. Sladek, L. R. Poulsen, S. M. Romanowsky, J. I. Schroeder and J. F. Harper (2007). A cyclic nucleotide-gated channel is essential for polarized tip growth of pollen. Proceedings of the National Academy of Sciences **104**: 14531-14536.

Fu, Y., H. Li and Z. Yang (2002). The ROP2 GTPase controls the formation of cortical fine F-actin and the early phase of directional cell expansion during *Arabidopsis* organogenesis. Plant Cell **14**: 777-794.

Fu, Y., G. Wu and Z. Yang (2001). ROP Gtpase–dependent dynamics of tip-localized F-actin controls tip growth in pollen tubes. Journal of Cell Biology **152**: 1019-1032.

Funaki, K., A. Nagata, Y. Akimoto, K. Shimada, K. Ito and K. Yamamoto (2004). The motility of *Chara corallina* myosin was inhibited reversibly by 2,3-butanedione monoxime (BDM). Plant and Cell Physiology **45**: 1342-1345.

Gaillard, M.-J., S. Sugita, M. Bunting, R. Middleton, A. Broström, C. Caseldine, T. Giesecke, S. Hellman, S. Hicks, K. Hjelle, C. Langdon, A.-B. Nielsen, A. Poska, H. von Stedingk and S. Veski (2008). The use of modelling and simulation approach in reconstructing past landscapes from fossil pollen data: a review and results from the POLLANDCAL network. Vegetation History and Archaeobotany **17**: 419-443.

Galkin, V. E., A. Orlova, M. S. VanLoock, A. Shvetsov, E. Reisler and E. H. Egelman (2003). ADF/cofilin use an intrinsic mode of F-actin instability to disrupt actin filaments. The Journal of Cell Biology **163**: 1057-1066.

Ge, L., C. Xie, H. Tian and S. Russell (2009). Distribution of calcium in the stigma and style of tobacco during pollen germination and tube elongation. Sexual Plant Reproduction **22**: 87-96.

Geitmann, A. (2006). Plant and fungal cytomechanics: quantifying and modeling cellular architecture. Canadian Journal of Botany **84**: 581-593.

Geitmann, A. (2010). How to shape a cylinder: pollen tube as a model system for the generation of complex cellular geometry. Sexual Plant Reproduction **23**: 63-71.

Geitmann, A. and M. Cresti (1998). Ca^{2+} channels control the rapid expansions in pulsating growth of *Petunia hybrida* pollen tubes. Journal of Plant Physiology **152**: 439-447.

Geitmann, A. and J. Dumais (2009). Not-so-tip-growth. Plant Signaling and Behavior **4**: 136-138.

Geitmann, A. and A. M. C. Emons (2000). The cytoskeleton in plant and fungal cell tip growth. Journal of Microscopy **198**: 218-245.

Geitmann, A. and J. K. E. Ortega (2009). Mechanics and modeling of plant cell growth. Trends in Plant Science **14**: 467-478.

Geitmann, A. and R. Palanivelu (2007). Fertilization requires communication: signal generation and perception during pollen tube guidance. Floriculture and Ornamental Biotechnology **1**: 77-89.

Geitmann, A. and E. Parre (2004). The local cytomechanical properties of growing pollen tubes correspond to the axial distribution of structural cellular elements. Sexual Plant Reproduction **17**: 9-16.

Geitmann, A., B. N. Snowman, A. M. C. Emons and V. E. Franklin-Tong (2000). Alterations in the actin cytoskeleton of pollen tubes are induced by the self-incompatibility reaction in *Papaver rhoeas*. Plant Cell **12**: 1239-1251.

Geitmann, A. and M. Steer (2006). The architecture and properties of the pollen tube cell wall. In The Pollen Tube. R. Malhó, Springer Verlag**:** 177-200.

Gibbon, B. C. (2001). Actin monomer-binding proteins and the regulation of actin dynamics in plants. Journal of Plant Growth Regulation **20**: 103-112.

Gibbon, B. C., D. R. Kovar and C. J. Staiger (1999). Latrunculin B has different effects on pollen germination and tube growth. Plant Cell **11**: 2349-2364.

Gibbon, B. C., L. E. Zonia, D. R. Kovar, P. J. Hussey and C. J. Staiger (1998). Pollen profilin function depends on interaction with proline-rich motifs. Plant Cell **10**: 981-994.

Giberson, R. T. (2001). Vacuum-assisted microwave processing of animal tissues for electron microscopy. In Microwave Techniques and Protocols**:** 13-23.

Gomez, T. M. and N. C. Spitzer (1999). *In vivo* regulation of axon extension and pathfinding by growth-cone calcium transients. Nature **397**: 350-355.

Goodner, B. and R. S. Quatrano (1993). *Fucus* embryogenesis: A model to study the establishment of polarity. Plant Cell **5**: 1471-1481.

Gossot, O. and A. Geitmann (2007). Pollen tube growth: coping with mechanical obstacles involves the cytoskeleton. Planta **226**: 405-416.

Gow, N. A. R. (1994). Growth and guidance of the fungal hypha. Microbiology **140**: 3193-3205.

Gross, D., L. M. Loew and W. W. Webb (1986). Optical imaging of cell membrane potential changes induced by applied electric fields. Biophysical Journal **50**: 339-348.

Gu, Y., Y. Fu, P. Dowd, S. Li, V. Vernoud, S. Gilroy and Z. Yang (2005). A Rho family GTPase controls actin dynamics and tip growth via two counteracting downstream pathways in pollen tubes. Journal of Cell Biology **169**: 127-138.

Gu, Y., V. Vernoud, Y. Fu and Z. Yang (2003). ROP GTPase regulation of pollen tube growth through the dynamics of tip-localized F-actin. Journal of Experimental Botany **54**: 93-101.

Guharay, F. and F. Sachs (1985). Mechanotransducer ion channels in chick skeletal muscle: the effects of extracellular pH. The Journal of Physiology **363**: 119-134.

Gungabissoon, R. A., C.-J. Jiang, B. K. Drøbak, S. K. Maciver and P. J. Hussey (1998). Interaction of maize actin-depolymerising factor with actin and phosphoinositides and its inhibition of plant phospholipase C. The Plant Journal **16**: 689-696.

Guyon, V. N., J. D. Astwood, E. C. Garner, A. K. Dunker and L. P. Taylor (2000). Isolation and characterization of cDNAs expressed in the early stages of flavonol-induced pollen germination in *Petunia*. Plant Physiology **123**: 699-710.

Hamilton, D. A., Y. H. Schwarz and J. P. Mascarenhas (1998). A monocot pollen-specific promoter contains separable pollen-specific and quantitative elements. Plant Molecular Biology **38**: 663-669.

Harold, F. M. (1997). How hyphae grow: morphogenesis explained? Protoplasma **197**: 137-147.

Hayden, S. M., P. S. Miller, A. Brauweiler and J. R. Bamburg (1993). Analysis of the interactions of actin depolymerizing factor with G- and F-actin. Biochemistry **32**: 9994-10004.

Hepler, P., A. Lovy-Wheeler, S. McKenna and J. Kunkel (2006). Ions and pollen tube growth. In The Pollen Tube. R. Malhó, Springer Berlin / Heidelberg. **3:** 47-69.

Hepler, P. K., L. Vidali and A. Y. Cheung (2001). Polarized cell growth in higher plants. Annual Review of Cell and Developmental Biology **17**: 159-187.

Heslop-Harrison, J., K. W. J. G.H. Bourne and F. Martin (1987). Pollen germination and pollen-tube growth. In International Review of Cytology, Academic Press. **107:** 1-78.

Heslop-Harrison, J. and Y. Heslop-Harrison (1990). Dynamic aspects of apical zonation in the angiosperm pollen tube. Sexual Plant Reproduction **3**: 187-194.

Heslop-Harrison, J., Y. Heslop-Harrison, M. Cresti, A. Tiezzi and F. Ciampolini (1986). Actin during pollen germination. Journal of Cell Science **86**: 1-8.

Heslop-Harrison, Y. and J. Heslop-Harrison (1992). Germination of monocolpate angiosperm pollen: evolution of the actin cytoskeleton and wall during hydration, activation and tube emergence. Annals of Botany **69**: 385-394.

Higaki, T., N. Kutsuna, T. Sano and S. Hasezawa (2008). Quantitative analysis of changes in actin microfilament contribution to cell plate development in plant cytokinesis. BMC Plant Biology **8**: 80.

Higashiyama, T. (2010). Peptide signaling in pollen-pistil interactions. Plant and Cell Physiology **51**: 177-189.

Higashiyama, T. and Y. Hamamura (2008). Gametophytic pollen tube guidance. Sexual Plant Reproduction **21**: 17-26.

Higashiyama, T., H. Kuroiwa and T. Kuroiwa (2003). Pollen-tube guidance: beacons from the female gametophyte. Current Opinion in Plant Biology **6**: 36-41.

Hiscock, S. J. and A. M. Allen (2008). Diverse cell signalling pathways regulate pollen-stigma interactions: the search for consensus. New Phytologist **179**: 286-317.

Hofmeister, W. (1962). On the germination, development, and fructification of the higher cryptogamia and on the fructification of the Coniferae. London, Ray Society. 491.

Holdaway-Clarke, T. L. and P. K. Hepler (2003). Control of pollen tube growth: role of Ion gradients and fluxes. New Phytologist **159**: 539-563.

Holdaway-Clarke, T. L., N. M. Weddle, S. Kim, A. Robi, C. Parris, J. G. Kunkel and P. K. Hepler (2003). Effect of extracellular calcium, pH and borate on growth oscillations in *Lilium formosanum* pollen tubes. Journal of Experimental Botany **54**: 65-72.

Holweg, C. L. (2007). Living markers for actin block myosin-dependent motility of plant organelles and auxin. Cell Motility and the Cytoskeleton **64**: 69-81.

Honys, D. and D. Twell (2003). Comparative analysis of the *Arabidopsis* pollen transcriptome. Plant Physiology **132**: 640-652.

Honys, D. and D. Twell (2004). Transcriptome analysis of haploid male gametophyte development in *Arabidopsis*. Genome Biology **5**: R85.

Hruz, T., O. Laule, G. Szabo, F. Wessendorp, S. Bleuler, L. Oertle, P. Widmayer, W. Gruissem and P. Zimmermann (2008). Genevestigator V3: A a reference expression database for the meta-analysis of transcriptomes, Hindawi Publishing Corporation.

Hu, S., D. L. Dilcher, D. M. Jarzen and D. Winship Taylor (2008). Early steps of angiosperm–pollinator coevolution. Proceedings of the National Academy of Sciences **105**: 240-245.

Huang, S., L. Blanchoin, F. Chaudhry, V. E. Franklin-Tong and C. J. Staiger (2004). A gelsolin-like protein from *Papaver rhoeas* pollen (PrABP80) stimulates calcium-regulated severing and depolymerization of actin filaments. Journal of Biological Chemistry **279**: 23364-23375.

Hussey, P. J., E. G. Allwood and A. P. Smertenko (2002). Actin–binding proteins in the *Arabidopsis* genome database: properties of functionally distinct plant actin–depolymerizing factors/cofilins. Philosophical Transactions of the Royal Society of London. Series B: Biological Sciences **357**: 791-798.

Hussey, P. J., T. Ketelaar and M. J. Deeks (2006). Control of the actin cytoskeleton in plant cell growth. Annual Review of Plant Biology **57**: 109-125.

Hussey, P. J., M. Yuan, G. Calder, S. Khan and C. W. Lloyd (1998). Microinjection of pollen-specific actin-depolymerizing factor, ZmADF1, reorientates F-actin strands in *Tradescantia* stamen hair cells. The Plant Journal **14**: 353-357.

Hwang, J.-U., G. Wu, A. Yan, Y.-J. Lee, C. S. Grierson and Z. Yang (2010). Pollen-tube tip growth requires a balance of lateral propagation and global inhibition of Rho-family GTPase activity. Journal of Cell Science **123**: 340-350.

Ischebeck, T., I. Stenzel and I. Heilmann (2008). Type B phosphatidylinositol-4-phosphate 5-kinases mediate *Arabidopsis* and *Nicotiana tabacum* pollen tube growth by regulating apical pectin secretion. Plant Cell **20**: 3312-3330.

Jaffe, L. F. and M.-M. Poo (1979). Neurites grow faster towards the cathode than the anode in a steady field. Journal of Experimental Zoology **209**: 115-127.

Jarvis, M. C. (1984). Structure and properties of pectin gels in plant cell walls. Plant, Cell & Environment **7**: 153-164.

Jeong, Y.-M., E.-J. Jung, H.-J. Hwang, H. Kim, S.-Y. Lee and S.-G. Kim (2009). Roles of the first intron on the expression of Arabidopsis (*Arabidopsis thaliana*) genes for actin and actin-binding proteins. Plant Science **176**: 58-65.

Jeong, Y.-M., J.-H. Mun, H. Kim, S.-Y. Lee and S.-G. Kim (2007). An upstream region in the first intron of petunia actin-depolymerizing factor 1 affects tissue-specific expression in transgenic Arabidopsis (*Arabidopsis thaliana*). The Plant Journal **50**: 230-239.

Jeong, Y.-M., J.-H. Mun, I. Lee, J. C. Woo, C. B. Hong and S.-G. Kim (2006). Distinct roles of the first introns on the expression of *Arabidopsis* profilin gene family members. Plant Physiology **140**: 196-209.

Jiang, C.-J., A. G. Weeds and P. J. Hussey (1997). The maize actin-depolymerizing factor, ZmADF3, redistributes to the growing tip of elongating root hairs and can be induced to translocate into the nucleus with actin. The Plant Journal **12**: 1035-1043.

Jiang, C.-J., A. G. Weeds, S. Khan and P. J. Hussey (1997). F-actin and G-actin binding are uncoupled by mutation of conserved tyrosine residues in maize actin depolymerizing factor (ZmADF). Proceedings of the National Academy of Sciences of the United States of America **94**: 9973-9978.

Jockusch, B. M., C.-A. Schoenenberger, J. Stetefeld and U. Aebi (2006). Tracking down the different forms of nuclear actin. Trends in Cell Biology **16**: 391-396.

Johnson-Brousseau, S. A. and S. McCormick (2004). A compendium of methods useful for characterizing *Arabidopsis* pollen mutants and gametophytically-expressed genes. Plant Journal **39**: 761-775.

Jutel, M., L. Jaeger, R. Suck, H. Meyer, H. Fiebig and O. Cromwell (2005). Allergen-specific immunotherapy with recombinant grass pollen allergens. Journal of Allergy and Clinical Immunology **116**: 608-613.

Kaothien, P., S. H. Ok, B. Shuai, D. Wengier, R. Cotter, D. Kelley, S. Kiriakopolos, J. Muschietti and S. McCormick (2005). Kinase partner protein interacts with the LePRK1 and LePRK2 receptor kinases and plays a role in polarized pollen tube growth. The Plant Journal **42**: 492-503.

Ketelaar, T., N. C. A. de Ruijter and A. M. C. Emons (2003). Unstable F-actin specifies the area and microtubule direction of cell expansion in *Arabidopsis* root hairs. Plant Cell **15**: 285-292.

Ketelaar, T. and A. Emons (2009). The actin cytoskeleton in root hairs: A cell elongation device. In Root Hairs. A. Emons and T. Ketelaar, Springer Berlin / Heidelberg. **12:** 211-232.

Kim, S., J.-C. Mollet, J. Dong, K. Zhang, S.-Y. Park and E. M. Lord (2003). Chemocyanin, a small basic protein from the lily stigma, induces pollen tube chemotropism. Proceedings of the National Academy of Sciences of the United States of America **100**: 16125-16130.

Klahre, U. and B. Kost (2006). Tobacco RhoGTPase ACTIVATING PROTEIN1 spatially restricts signaling of RAC/Rop to the apex of pollen tubes. Plant Cell **18**: 3033-3046.

Kohno, T. and T. Shimmen (1987). Ca^{2+}-induced fragmentation of actin filaments in pollen tubes. Protoplasma **141**: 177-179.

Kordyum, E., M. Sobol, I. Kalinina, N. Bogatina and A. Kondrachuk (2007). Cyclotron-based effects on plant gravitropism. Advances in Space Research **39**: 1210-1217.

Kordyum, E. L., G. V. Shevchenko, I. M. Kalinina, O. T. Demkiv and Y. D. Khorkavtsiv (2009). The role of the cytoskeleton in plant cell gravisensitivity. In The Plant Cytoskeleton: a Key Tool for Agro-Biotechnology. Y. B. Blume, W. V. Baird, A. I. Yemets and D. Breviario, Springer Netherlands**:** 173-196.

Kost, B., E. Lemichez, P. Spielhofer, Y. Hong, K. Tolias, C. Carpenter and N.-H. Chua (1999). Rac homologues and compartmentalized phosphatidylinositol 4, 5-bisphosphate act in a common pathway to regulate polar pollen tube growth. The Journal of Cell Biology **145**: 317-330.

Kost, B., P. Spielhofer and N.-H. Chua (1998). A GFP-mouse talin fusion protein labels plant actin filamentsin vivoand visualizes the actin cytoskeleton in growing pollen tubes. The Plant Journal **16**: 393-401.

Kovar, D. R., B. K. Drobak and C. J. Staiger (2000). Maize profilin isoforms are functionally distinct. Plant Cell **12**: 583-598.

Kroeger, J. H., F. B. Daher, M. Grant and A. Geitmann (2009). Microfilament orientation constrains vesicle flow and spatial distribution in growing pollen tubes. Biophysical Journal **97**: 1822-1831.

Kropf, D. L. (1997). Induction of polarity in fucoid zygotes. Plant Cell **9**: 1011-1020.

Kropf, D. L., S. K. Berge and R. S. Quatrano (1989). Actin localization during fucus embryogenesis. Plant Cell **1**: 191-200.

Kühtreiber, W. M. and L. F. Jaffe (1990). Detection of extracellular calcium gradients with a calcium-specific vibrating electrode. The Journal of Cell Biology **110**: 1565-1573.

Kusano, K.-i., H. Abe and T. Obinata (1999). Detection of a sequence involved in actin-binding and phosphoinositide-binding in the N-terminal side of cofilin. Molecular and Cellular Biochemistry **190**: 133-141.

la Cour, T., L. Kiemer, A. Mølgaard, R. Gupta, K. Skriver and S. Brunak (2004). Analysis and prediction of leucine-rich nuclear export signals. Protein Engineering Design and Selection **17**: 527-536.

Lacarrière, J. (1981). En cheminant avec Hérodote. Paris, Seghers. 309.

Lancelle, S. A. and P. K. Hepler (1992). Ultrastructure of freeze-substituted pollen tubes of *Lilium longiflorum*. Protoplasma **167**: 215-230.

Lenartowska, M. and A. Michalska (2008). Actin filament organization and polarity in pollen tubes revealed by myosin II subfragment 1 decoration. Planta **228**: 891-896.

Lever, M. C., B. E. M. Robertson, A. D. B. Buchan, P. F. P. Miller, G. W. Gooday and N. A. R. Gow (1994). pH and Ca^{2+} dependent galvanotropism of filamentous fungi: implications and mechanisms. Mycological Research **98**: 301-306.

Li, H., Y. K. Lin, R. M. Heath, M. X. Zhu and Z. B. Yang (1999). Control of pollen tube tip growth by a pop GTPase-dependent pathway that leads to tip-localized calcium influx. Plant Cell **11**: 1731-1742.

Li, X.-B., D. Xu, X.-L. Wang, G.-Q. Huang, J. Luo, D.-D. Li, Z.-T. Zhang and W.-L. Xu (2010). Three cotton genes preferentially expressed in flower tissues encode actin-depolymerizing factors which are involved in F-actin dynamics in cells. Journal of Experimental Botany **61**: 41-53.

Lida, K., S. Matsumoto and I. Yahara (1992). The KKRKK sequence is involved in heat shock-induced nuclear translocation of the 18-kDa acting-binding protein, cofilin. Cell structure and function **17**: 39-46.

Lin, Y. and Z. Yang (1997). Inhibition of pollen tube elongation by microinjected anti-Rop1Ps antibodies suggests a crucial role for Rho-type GTPases in the control of tip growth. Plant Cell **9**: 1647-1659.

Lockhart, J. A. (1965). An analysis of irreversible plant cell elongation. Journal of Theoretical Biology **8**: 264-275.

Lopez, I., R. G. Anthony, S. K. Maciver, C. J. Jiang, S. Khan, A. G. Weeds and P. J. Hussey (1996). Pollen specific expression of maize genes encoding actin depolymerizing factor-like proteins. Proceedings of the National Academy of Sciences of the United States of America **93**: 7415-7420.

Lord, E. M. (2003). Adhesion and guidance in compatible pollination. Journal of Experimental Botany **54**: 47-54.

Lord, E. M. and S. D. Russell (2002). The mechanisms of pollination and fertilization in plants. Annual Review of Cell and Developmental Biology **18**: 81-105.

Lovy-Wheeler, A., L. Cardenas, J. G. Kunkel and P. K. Hepler (2007). Differential organelle movement on the actin cytoskeleton in lily pollen tubes. Cell Motility and the Cytoskeleton **64**: 217-232.

Lovy-Wheeler, A., J. G. Kunkel, E. G. Allwood, P. J. Hussey and P. K. Hepler (2006). Oscillatory increases in alkalinity anticipate growth and may regulate actin dynamics in pollen tubes of lily. Plant Cell **18**: 2182-2193.

Lovy-Wheeler, A., K. L. Wilsen, T. I. Baskin and P. K. Hepler (2005). Enhanced fixation reveals the apical cortical fringe of actin filaments as a consistent feature of the pollen tube. Planta **221**: 95-104.

Maciver, S. and P. Hussey (2002). The ADF/cofilin family: actin-remodeling proteins. Genome Biology **3**: reviews3007.1 - reviews3007.12.

Malhó, R., J. A. Feijó and M. S. S. Pais (1992). Effect of electrical fields and external ionic currents on pollen-tube orientation. Sexual Plant Reproduction **5**: 57-63.

Malhó, R., N. D. Read, M. S. Pais and A. J. Trewavas (1994). Role of cytosolic free calcium in the reorientation of pollen tube growth. The Plant Journal **5**: 331-341.

Malhó, R., N. D. Read, A. J. Trewavas and M. S. Pais (1995). Calcium channel activity during pollen tube growth and reorientation. Plant Cell **7**: 1173-1184.

Malhó, R. and A. J. Trewavas (1996). Localized apical increases of cytosolic free calcium control pollen tube orientation. Plant Cell **8**: 1935-1949.

Marsh, G. and H. W. Beams (1945). The orientation of pollen tubes of *Vinca* in the electric current. Journal of Cellular and Comparative Physiology **25**: 195-204.

Márton, M.-L. and T. Dresselhaus (2010). Female gametophyte-controlled pollen tube guidance. Biochemical Society Transactions **038**: 627-630.

Márton, M. L., S. Cordts, J. Broadhvest and T. Dresselhaus (2005). Micropylar pollen tube guidance by egg apparatus 1 of maize. Science **307**: 573-576.

Mascarenhas, J. P. (1993). Molecular mechanisms of pollen tube growth and differentiation. Plant Cell **5**: 1303-1314.

Mascarenhas, J. P. and L. Machlis (1964). Chemotropic response of the pollen of *Antirrhinum majus* to calcium. Plant Physiology **39**: 70-77.

Mathur, J. (2006). Local interactions shape plant cells. Current Opinion in Cell Biology **18**: 40-46.

Mathur, J., P. Spielhofer, B. Kost and N. Chua (1999). The actin cytoskeleton is required to elaborate and maintain spatial patterning during trichome cell morphogenesis in *Arabidopsis thaliana*. Development **126**: 5559-5568.

Mayers, C. P. (1970). Histological fixation by microwave heating. Journal of Clinical Pathology **23**: 273-275.

McClure, B. and V. Franklin-Tong (2006). Gametophytic self-incompatibility: understanding the cellular mechanisms involved in "self" pollen tube inhibition. Planta **224**: 233-245.

McCormick, S. (2004). Control of male gametophyte development. Plant Cell **16**: S142-153.

McCurdy, D. W., D. R. Kovar and C. J. Staiger (2001). Actin and actin-binding proteins in higher plants. Protoplasma **215**: 89-104.

McElroy, D., W. Zhang, J. Cao and R. Wu (1990). Isolation of an efficient actin promoter for use in rice transformation. Plant Cell **2**: 163-171.

McGough, A., B. Pope, W. Chiu and A. Weeds (1997). Cofilin changes the twist of F-actin: implications for actin filament dynamics and cellular function. The Journal of Cell Biology **138**: 771-781.

Messerli, M. and K. Robinson (1997). Tip localized Ca^{2+} pulses are coincident with peak pulsatile growth rates in pollen tubes of *Lilium longiflorum*. Journal of Cell Science **110**: 1269-1278.

Messerli, M. A., R. Créton, L. F. Jaffe and K. R. Robinson (2000). Periodic increases in elongation rate precede increases in cytosolic Ca^{2+} during pollen tube growth. Developmental Biology **222**: 84-98.

Michelot, A., J. Berro, C. Guerin, R. Boujemaa-Paterski, C. J. Staiger, J.-L. Martiel and L. Blanchoin (2007). Actin-filament stochastic dynamics mediated by ADF/Cofilin. Current Biology **17**: 825-833.

Michelot, A., C. Guerin, S. J. Huang, M. Ingouff, S. Richard, N. Rodiuc, C. J. Staiger and L. Blanchoin (2005). The formin homology 1 domain modulates the actin nucleation and bundling activity of *Arabidopsis* FORMIN1. Plant Cell **17**: 2296-2313.

Miller, Deborah D., Norbert C. A. De Ruijter, T. Bisseling and Anne M C. Emons (1999). The role of actin in root hair morphogenesis: studies with lipochito-oligosaccharide as a growth stimulator and cytochalasin as an actin perturbing drug. The Plant Journal **17**: 141-154.

Minc, N. and F. Chang (2010). Electrical control of cell polarization in the fission yeast *Schizosaccharomyces pombe*. Current Biology **20**: 710-716.

Molendijk, A. J., F. Bischoff, C. S. V. Rajendrakumar, J. Friml, M. Braun, S. Gilroy and K. Palme (2001). *Arabidopsis thaliana* Rop GTPases are localized to tips of root hairs and control polar growth. EMBO Journal **20**: 2779-2788.

Money, N. P. (1997). Wishful thinking of turgor revisited: The mechanics of fungal growth. Fungal Genetics and Biology **21**: 173-187.

Money, N. P. and T. W. Hill (1997). Correlation between endoglucanase secretion and cell wall strength in oomycete hyphae: Implications for growth and morphogenesis. Mycologia **89**: 777-785.

Morejohn, L. C., T. E. Bureau, J. Molè-Bajer, A. S. Bajer and D. E. Fosket (1987). Oryzalin, a dinitroaniline herbicide, binds to plant tubulin and inhibits microtubule polymerization *in vitro*. Planta **172**: 252-264.

Morita, M. T. (2010). Directional gravity sensing in gravitropism. Annual Review of Plant Biology **61**: 705-720.

Mortimer, D., J. Feldner, T. Vaughan, I. Vetter, Z. Pujic, W. J. Rosoff, K. Burrage, P. Dayan, L. J. Richards and G. J. Goodhill (2009). A Bayesian model predicts the response of axons to molecular gradients. Proceedings of the National Academy of Sciences **106**: 10296-10301.

Mortimer, D., T. Fothergill, Z. Pujic, L. J. Richards and G. J. Goodhill (2008). Growth cone chemotaxis. Trends in Neurosciences **31**: 90-98.

Mouline, K., A. A. Very, F. Gaymard, J. Boucherez, G. Pilot, M. Devic, D. Bouchez, J. B. Thibaud and H. Sentenac (2002). Pollen tube development and competitive ability are impaired by disruption of a Shaker K^+ channel in *Arabidopsis*. Genes and Development **16**: 339-350.

Muller, J. (1981). Fossil pollen records of extant angiosperms. Botanical Review **47**: 1-142.

Mun, J.-H., S.-Y. Lee, H.-J. Yu, Y.-M. Jeong, M.-Y. Shin, H. Kim, I. Lee and S.-G. Kim (2002). Petunia actin-depolymerizing factor is mainly accumulated in vascular tissue and its gene expression is enhanced by the first intron. Gene **292**: 233-243.

Mun, J.-H., H.-J. Yu, H.-S. Lee, Y. M. Kwon, J. S. Lee, I. Lee and S.-G. Kim (2000). Two closely related cDNAs encoding actin-depolymerizing factors of petunia are mainly expressed in vegetative tissues. Gene **257**: 167-176.

Muschietti, J., Y. Eyal and S. McCormick (1998). Pollen tube localization implies a role in pollen–pistil interactions for the tomato receptor-like protein kinases LePRK1 and LePRK2. Plant Cell **10**: 319-330.

Nakamura, N., A. Fukushima, H. Iwayama and H. Suzuki (1991). Electrotropism of pollen tubes of *Camellia* and other plants. Sexual Plant Reproduction **4**: 138-143.

Nibau, C., H.-m. Wu and A. Y. Cheung (2006). RAC/ROP GTPases: 'hubs' for signal integration and diversification in plants. Trends in Plant Science **11**: 309-315.

Nieuwland, J., R. Feron, B. A. H. Huisman, A. Fasolino, C. W. Hilbers, J. Derksen and C. Mariani (2005). Lipid transfer proteins enhance cell wall extension in tobacco. Plant Cell **17**: 2009-2019.

Nishida, E., K. Iida, N. Yonezawa, S. Koyasu, I. Yahara and H. Sakai (1987). Cofilin is a component of intranuclear and cytoplasmic actin rods induced in cultured cells. Proceedings of the National Academy of Sciences of the United States of America **84**: 5262-5266.

Noir, S., A. Bräutigam, T. Colby, J. Schmidt and R. Panstruga (2005). A reference map of the *Arabidopsis thaliana* mature pollen proteome. Biochemical and Biophysical Research Communications **337**: 1257-1266.

Nozue, K. and M. Wada (1993). Electrotropism of *Nicotiana* pollen tubes. Plant and Cell Physiology **34**: 1291-1296.

Okuda, S., H. Tsutsui, K. Shiina, S. Sprunck, H. Takeuchi, R. Yui, R. Kasahara, Y. Hamamura, A. Mizukami, D. Susaki, N. Kawano, T. Sakakibara, S. Namiki, K. Itoh, K. Otsuka, M. Matsuzaki, H. Nozaki, T. Kuroiwa, A. Nakano, M. Kanaoka, T. Dresselhaus, N. Sasaki and T. Higashiyama (2009). Defensin-like polypeptide LUREs are pollen tube attractants secreted from synergid cells. Nature **458**: 357 - 361.

Onuma, E. K. and S.-W. Hui (1988). Electrical-field directed cell shape changes, displacement, and cytoskeletal reorganization are calcium dependent. Journal of Cell Biology **106**: 2067-2075.

Palanivelu, R., L. Brass, A. F. Edlund and D. Preuss (2003). Pollen tube growth and guidance Is regulated by POP2, an *Arabidopsis* gene that controls GABA levels. Cell **114**: 47-59.

Palanivelu, R. and D. Preuss (2006). Distinct short-range ovule signals attract or repel *Arabidopsis thaliana* pollen tubes *in vitro*. BMC Plant Biology **6**: 7.

Palmieri, M. and J. Z. Kiss (2005). Disruption of the F-actin cytoskeleton limits statolith movement in *Arabidopsis* hypocotyls. Journal of Experimental Botany **56**: 2539-2550.

Palmieri, M., M. A. Schwind, M. H. H. Stevens, R. E. Edelmann and J. Z. Kiss (2007). Effects of the myosin ATPase inhibitor 2,3-butanedione monoxime on amyloplast kinetics and gravitropism of *Arabidopsis* hypocotyls. Physiologia Plantarum **130**: 613-626.

Parre, E. and A. Geitmann (2005). More than a leak sealant. The mechanical properties of callose in pollen tubes. Plant Physiology **137**: 274-286.

Parre, E. and A. Geitmann (2005). Pectin and the role of the physical properties of the cell wall in pollen tube growth of *Solanum chacoense*. Planta **220**: 582-592.

Parton, R. M., S. Fischer-Parton, M. K. Watahiki and A. J. Trewavas (2001). Dynamics of the apical vesicle accumulation and the rate of growth are related in individual pollen tubes. Journal of Cell Science **114**: 2685-2695.

Perbal, G. and D. Driss-Ecole (2003). Mechanotransduction in gravisensing cells. Trends in Plant Science **8**: 498-504.

Petit, R. J., S. Brewer, S. Bordács, K. Burg, R. Cheddadi, E. Coart, J. Cottrell, U. M. Csaikl, B. van Dam, J. D. Deans, S. Espinel, S. Fineschi, R. Finkeldey, I. Glaz, P. G. Goicoechea, J. S. Jensen, A. O. König, A. J. Lowe, S. F. Madsen, G. Mátyás, R. C. Munro, F. Popescu, D. Slade, H. Tabbener, S. G. M. de Vries, B. Ziegenhagen, J.-L. de Beaulieu and A. Kremer (2002). Identification of refugia and post-glacial colonisation routes of European white oaks based on chloroplast DNA and fossil pollen evidence. Forest Ecology and Management **156**: 49-74.

Picton, J. M. and M. W. Steer (1983). Evidence for the role of Ca^{2+} ions in tip extension in pollen tubes. Protoplasma **115**: 11-17.

Pierson, E. S., D. D. Miller, D. A. Callaham, A. M. Shipley, B. A. Rivers, M. Cresti and P. K. Hepler (1994). Pollen tube growth is coupled to the extracellular calcium ion flux and the intracellular calcium gradient: effect of BAPTA-type buffers and hypertonic media. Plant Cell **6**: 1815-1828.

Pierson, E. S., D. D. Miller, D. A. Callaham, J. van Aken, G. Hackett and P. K. Hepler (1996). Tip-localized calcium entry fluctuates during pollen tube growth. Developmental Biology **174**: 160-173.

Pina, C., F. Pinto, J. A. Feijó and J. D. Becker (2005). Gene family analysis of the *Arabidopsis* pollen transcriptome reveals biological implications for cell growth, division control, and gene expression regulation. Plant Physiology **138**: 744-756.

Pollard, T. D. and G. G. Borisy (2003). Cellular motility driven by assembly and disassembly of actin filaments. Cell **112**: 453-465.

Pollard, T. D. and J. A. Cooper (2009). Actin, a central player in cell shape and movement. Science **326**: 1208-1212.

Porter, B. N. (1993). Sacred trees, date palms, and the royal persona of Ashurnasirpal II. Journal of Near Eastern Studies **52**: 129-139.

Prado, A. M., R. Colaço, N. Moreno, A. C. Silva and J. A. Feijó (2008). Targeting of pollen tubes to ovules is dependent on nitric oxide (NO) signaling. Molecular Plant **1**: 703-714.

Prado, A. M., D. M. Porterfield and J. A. Feijó (2004). Nitric oxide is involved in growth regulation and re-orientation of pollen tubes. Development **131**: 2707-2714.

Preuss, D., B. Lemieux, G. Yen and R. W. Davis (1993). A conditional sterile mutation eliminates surface components from *Arabidopsis* pollen and disrupts cell signaling during fertilization. Genes & Development **7**: 974-985.

Qin, Y., A. R. Leydon, A. Manziello, R. Pandey, D. Mount, S. Denic, B. Vasic, M. A. Johnson and R. Palanivelu (2009). Penetration of the stigma and style elicits a novel transcriptome in pollen tubes, pointing to genes critical for growth in a pistil. PLoS Genetics **5**: e1000621.

Qu, H.-Y., Z.-L. Shang, S.-L. Zhang, L.-M. Liu and J.-Y. Wu (2007). Identification of hyperpolarization-activated calcium channels in apical pollen tubes of *Pyrus pyrifolia*. New Phytologist **174**: 524-536.

Radford, J. and R. White (2010). Inhibitors of myosin, but not actin, alter transport through *Tradescantia* plasmodesmata. Protoplasma: 1-12.

Reger, B. J., R. Chaubal and R. Pressey (1992). Chemotropic responses by pearl millet pollen tubes. Sexual Plant Reproduction **5**: 47-56.

Reiss, H. and W. Herth (1985). Nifedipine-sensitive calcium channels are involved in polar growth of lily pollen tubes. Journal of Cell Science **76**: 247-254.

Ren, H. and Y. Xiang (2007). The function of actin-binding proteins in pollen tube growth. Protoplasma **230**: 171-182.

Ressad, F., D. Didry, G.-X. Xia, Y. Hong, N.-H. Chua, D. Pantaloni and M.-F. Carlier (1998). Kinetic analysis of the interaction of actin-depolymerizing factor (ADF)/cofilin with G- and F-actins. Journal of Biological Chemistry **273**: 20894-20902.

Riquelme, M., C. G. Reynaga-Peña, G. Gierz and S. Bartnicki-García (1998). What determines growth direction in fungal hyphae? Fungal Genetics and Biology **24**: 101-109.

Robinson, K. (1985). The responses of cells to electrical fields: a review. Journal of Cell Biology **101**: 2023-2027.

Röckel, N., S. Wolf, B. Kost, T. Rausch and S. Greiner (2008). Elaborate spatial patterning of cell-wall PME and PMEI at the pollen tube tip involves PMEI endocytosis, and reflects the distribution of esterified and de-esterified pectins. The Plant Journal **53**: 133-143.

Romagnoli, S., G. Cai, C. Faleri, E. Yokota, T. Shimmen and M. Cresti (2007). Microtubule- and actin filament-dependent motors are distributed on pollen tube mitochondria and contribute differently to their movement. Plant and Cell Physiology **48**: 345-361.

Rose, A. B. (2008). Intron-mediated regulation of gene expression. In Nuclear pre-mRNA Processing in Plants, Springer Berlin Heidelberg. **326:** 277-290.

Russin, W. A. and C. L. Trivett (2001). Vacuum-microwave combination for processing plant tissues for electron microscopy. In Microwave Techniques and Protocols**:** 25-35.

Ruzicka, D. R., M. K. Kandasamy, E. C. McKinney, B. Burgos-Rivera and R. B. Meagher (2007). The ancient subclasses of *Arabidopsis ACTIN DEPOLYMERIZING FACTOR* genes exhibit novel and differential expression. The Plant Journal **52**: 460-472.

Sanchez, A. M., M. Bosch, M. Bots, J. Nieuwland, R. Feron and C. Mariani (2004). Pistil factors controlling pollination. Plant Cell **16**: S98-106.

Sanders, D., C. Brownlee and J. F. Harper (1999). Communicating with calcium. Plant Cell **11**: 691-706.

Sanger, J. W., J. M. Sanger, T. E. Kreis and B. M. Jockusch (1980). Reversible translocation of cytoplasmic actin into the nucleus caused by dimethyl sulfoxide. Proceedings of the National Academy of Sciences of the United States of America **77**: 5268-5272.

Schaefer, H., C. Heibl and S. S. Renner (2009). Gourds afloat: a dated phylogeny reveals an Asian origin of the gourd family (Cucurbitaceae) and numerous oversea dispersal events. Proceedings of the Royal Society B: Biological Sciences **276**: 843-851.

Schiøtt, M., S. M. Romanowsky, L. Bækgaard, M. K. Jakobsen, M. G. Palmgren and J. F. Harper (2004). A plant plasma membrane Ca^{2+} pump is required for normal pollen tube growth and fertilization. Proceedings of the National Academy of Sciences of the United States of America **101**: 9502-9507.

Schleiden, J. M. (1849). Principles of scientific botany. London, Longman, Brown, Green and Longmans. 616.

Schlüpmann, H., A. Bacic and S. M. Read (1994). Uridine diphosphate glucose metabolism and callose synthesis in cultured pollen tubes of *Nicotiana alata* Link et Otto. Plant Physiology **105**: 659-670.

Schnurer, J. and T. Rosswall (1982). Fluorescein diacetate hydrolysis as a measure of total microbial activity in soil and litter. Applied and Environmental Microbiology **43**: 1256-1261.

Schopfer, P. (2006). Biomechanics of plant growth. American Journal of Botany **93**: 1415-1425.

Scott, R. J. (1994). Pollen exine - the sporopollenin enigma and the physics of pattern. In Molecular and Cellular Aspects of Plant Reproduction. R. J. Scott and A. D. Stead, Cambridge University Press.

Shang, Z.-l., L.-g. Ma, H.-l. Zhang, R.-r. He, X.-c. Wang, S.-j. Cui and D.-y. Sun (2005). Ca^{2+} influx into lily pollen grains through a hyperpolarization-activated Ca^{2+}-permeable channel which can be regulated by extracellular CaM. Plant Cell Physiology **46**: 598-608.

Smertenko, A. P., C.-J. Jiang, N. J. Simmons, A. G. Weeds, D. R. Davies and P. J. Hussey (1998). Ser6 in the maize actin-depolymerizing factor, ZmADF3, is phosphorylated by a calcium-stimulated protein kinase and is essential for the control of functional activity. The Plant Journal **14**: 187-193.

Smith, L. G. and D. G. Oppenheimer (2005). Spatial control of cell expansion by the plant cytoskeleton. Annual Review of Cell and Developmental Biology **21**: 271-295.

Smyth, D. R., J. L. Bowman and E. M. Meyerowitz (1990). Early flower development in *Arabidopsis*. Plant Cell **2**: 755-767.

Snowman, B. N., A. Geitmann, S. R. Clarke, C. J. Staiger, F. C. H. Franklin, A. M. C. Emons and V. E. Franklin-Tong (2000). Signalling and the cytoskeleton of pollen tubes of *Papaver rhoeas*. Annals of Botany **85**: 49-57.

Snowman, B. N., D. R. Kovar, G. Shevchenko, V. E. Franklin-Tong and C. J. Staiger (2002). Signal-mediated depolymerization of actin in pollen during the self-incompatibility response. Plant Cell **14**: 2613-2626.

Sobol, M. and E. Kordyum (2009). Distribution of calcium ions in cells of the root distal elongation zone under clinorotation. Microgravity Science and Technology **21**: 179-185.

Sousa, E., B. Kost and R. Malho (2008). *Arabidopsis* phosphatidylinositol-4-monophosphate 5-kinase 4 regulates pollen tube growth and polarity by modulating membrane recycling. Plant Cell **20**: 3050-3064.

Staiger, C. J. (2000). Signaling to the actin cytoskeleton in plants. Annual Reviews of Plant Physiology and Plant Molecular Biology **51**: 257-288.

Staiger, C. J. and L. Blanchoin (2006). Actin dynamics: old friends with new stories. Current Opinion in Plant Biology **9**: 554-562.

Staiger, C. J., M. B. Sheahan, P. Khurana, X. Wang, D. W. McCurdy and L. Blanchoin (2009). Actin filament dynamics are dominated by rapid growth and severing activity in the *Arabidopsis* cortical array. The Journal of Cell Biology **184**: 269-280.

Stanga, J., C. Neal, L. Vaughn, K. Baldwin and G. Jia (2009). Signaling in plant gravitropism. In Signaling in Plants. S. Mancuso and F. Baluška, Springer Berlin Heidelberg**:** 209-237.

Steer, M. W. and J. M. Steer (1989). Pollen tube tip growth. The New Phytologist **111**: 323-358.

Steer, M. W. and J. M. Steer (1989). Pollen tube tip growth. New Phytologist **111**: 323-358.

Stewman, S., M. Jones-Rhoades, P. Bhimalapuram, M. Tchernookov, D. Preuss and A. Dinner (2010). Mechanistic insights from a quantitative analysis of pollen tube guidance. BMC Plant Biology **10**: 32.

Swanson, R., A. F. Edlund and D. Preuss (2004). Species specificity in pollen-pistil interactions. Annual Review of Genetics **38**: 793-818.

Szymanski, D. B., M. D. Marks and S. M. Wick (1999). Organized F-actin is essential for normal trichome morphogenesis in *Arabidopsis*. Plant Cell **11**: 2331-2348.

T'Jampens, D., K. Meerschaert, B. Constantin, J. Bailey, L. Cook, V. De Corte, H. De Mol, M. Goethals, J. Van Damme, J. Vandekerckhove and J. Gettemans (1997). Molecular cloning, over-expression, developmental regulation and immunolocalization of fragminP, a gelsolin-related actin-binding protein from *Physarum polycephalum* plasmodia. Journal of Cell Science **110**: 1215-1226.

Takayama, S., H. Shiba, M. Iwano, K. Asano, M. Hara, F.-S. Che, M. Watanabe, K. Hinata and A. Isogai (2000). Isolation and characterization of pollen coat proteins of *Brassica campestris* that interact with *S* locus-related glycoprotein 1 involved in pollen–stigma adhesion. Proceedings of the National Academy of Sciences of the United States of America **97**: 3765-3770.

Tanaka, I. and T. Wakabayashi (1992). Organization of the actin and microtubule cytoskeleton preceding pollen germination. Planta **186**: 473-482.

Taylor, L. P. and P. K. Hepler (1997). Pollen germination and tube growth. **48:** 461-491.

Tester, M. and E. MacRobbie (1990). Cytoplasmic calcium affects the gating of potassium channels in the plasma membrane of *Chara corallina*: a whole-cell study using calcium-channel effectors. Planta **180**: 569-581.

The Arabidopsis Genome Initiative (2000). Analysis of the genome sequence of the flowering plant *Arabidopsis thaliana*. Nature **408**: 796-815.

Thomas, S. G., S. Huang, S. Li, C. J. Staiger and V. E. Franklin-Tong (2006). Actin depolymerization is sufficient to induce programmed cell death in self-incompatible pollen. The Journal of Cell Biology **174**: 221-229.

Tian, G.-W., A. Mohanty, S. N. Chary, S. Li, B. Paap, G. Drakakaki, C. D. Kopec, J. Li, D. Ehrhardt, D. Jackson, S. Y. Rhee, N. V. Raikhel and V. Citovsky (2004). High-throughput fluorescent tagging of full-length *Arabidopsis* gene products *in planta*. Plant Physiology **135**: 25-38.

Tiwari, S. C. and V. S. Polito (1988). Spatial and temporal organization of actin during hydration, activation, and germination of pollen in *Pyrus communis* L.: a population study. Protoplasma **147**: 5-15.

Tollefsrud, M. M., R. O. Y. Kissling, F. Gugerli, Ø. Johnsen, T. Skrøppa , R. Cheddadi, W. O. Van Der Knaap, M. Latałowa, R. Terhürne-Berson, T. Litt, T. Geburek, C. Brochmann and C. Sperisen (2008). Genetic consequences of glacial survival and postglacial colonization in Norway spruce: combined analysis of mitochondrial DNA and fossil pollen. Molecular Ecology **17**: 4134-4150.

Tominaga, M., E. Yokota, S. Sonobe and T. Shimmen (2000). Mechanism of inhibition of cytoplasmic streaming by a myosin inhibitor, 2,3-butanedione monoxime. Protoplasma **213**: 46-54.

Tominaga, M., E. Yokota, L. Vidali, S. Sonobe, P. K. Hepler and T. Shimmen (2000). The role of plant villin in the organization of the actin cytoskeleton, cytoplasmic streaming and the architecture of the transvacuolar strand in root hair cells of *Hydrocharis*. Planta **210**: 836-843.

Toyota, M., T. Furuichi, H. Tatsumi and M. Sokabe (2008). Cytoplasmic calcium increases in response to changes in the gravity vector in hypocotyls and petioles of *Arabidopsis* seedlings. Plant Physiology **146**: 505-514.

Trewavas, A. J. and R. Malhó (1998). Ca^{2+} signalling in plant cells: the big network! Current Opinion in Plant Biology **1**: 428-433.

Trick, M. and R. B. Flavell (1989). A homozygous *S* genotype of *Brassica oleracea* expresses two *S*-like genes. Molecular and General Genetics **218**: 112-117.

Tsien, R. W., D. Lipscombe, D. V. Madison, K. R. Bley and A. P. Fox (1988). Multiple types of neuronal calcium channels and their selective modulation. Trends in Neurosciences **11**: 431-438.

Tuinstra, M. R. and J. Wedel (2000). Estimation of pollen viability in grain *Sorghum*. Crop Science **40**: 968-970.

Tung, C.-W., K. G. Dwyer, M. E. Nasrallah and J. B. Nasrallah (2005). Genome-wide identification of genes expressed in *Arabidopsis* pistils specifically along the path of pollen tube growth. Plant Physiology **138**: 977-989.

Tupý, J. and L. Říhová (1984). Changes and growth effect of pH in pollen tube culture. Journal of Plant Physiology **115**: 1-10.

Twell, D., S. K. Park and E. Lalanne (1998). Asymmetric division and cell-fate determination in developing pollen. Trends in Plant Science **3**: 305-310.

Twell, D., J. Yamaguchi and S. McCormick (1990). Pollen-specific gene expression in transgenic plants: coordinate regulation of two different tomato gene promoters during microsporogenesis. Development **109**: 705-713.

van der Woude, W. and D. Morré (1968). Endoplasmic reticulum-dictyosome-secretory vesicle associations in pollen tubes of *Lilium longiflorum* Thunb. Proceedings of the Indian Academy of Sciences **77**: 164-170.

van der Woude, W. J., D. J. Morré and C. E. Bracker (1971). Isolation and characterization of secretory vesicles in germinated pollen of *Lilium longiflorum*. Journal of Cell Science **8**: 331-351.

Vantard, M. and L. Blanchoin (2002). Actin polymerization processes in plant cells. Current Opinion in Plant Biology **5**: 502-506.

Vidali, L. and P. K. Hepler (1997). Characterization and localization of profilin in pollen grains and tubes of *Lilium longiflorum*. Cell Motility and the Cytoskeleton **36**: 323-338.

Vidali, L. and P. K. Hepler (2001). Actin and pollen tube growth. Protoplasma **215**: 64-76.

Vidali, L., S. T. McKenna and P. K. Hepler (2001). Actin polymerization is essential for pollen tube growth. **12:** 2534-2545.

Vidali, L., C. M. Rounds, P. K. Hepler and M. Bezanilla (2009). Lifeact-mEGFP reveals a dynamic apical F-actin network in tip growing plant cells. PLoS ONE **4**: e5744.

Vidali, L., E. Yokota, A. Y. Cheung, T. Shimmen and P. K. Hepler (1999). The 135 kDa actin-bundling protein from *Lilium longiflorum* pollen is the plant homologue of villin. Protoplasma **209**: 283-291.

Walker, J. W. (1971). Unique type of angiosperm pollen from the family Annonaceae. Science **172**: 565-567.

Wang, C., K. S. Rathore and K. R. Robinson (1989). The responses of pollen to applied electrical fields. Developmental Biology **136**: 405-410.

Wang, H.-J., A.-R. Wan and G.-Y. Jauh (2008). An actin-binding protein, LlLIM1, mediates calcium and hydrogen regulation of actin dynamics in pollen tubes. Plant Physiology **147**: 1619-1636.

Wang, Q. L., L. D. Lu, X. Q. Wu, Y. Q. Li and J. X. Lin (2003). Boron influences pollen germination and pollen tube growth in *Picea meyeri*. Tree Physiology **23**: 345-351.

Wang, Y.-F., L.-M. Fan, W.-Z. Zhang, W. Zhang and W.-H. Wu (2004). Ca^{2+}-permeable channels in the plasma membrane of *Arabidopsis* pollen are regulated by actin microfilaments. Plant Physiology **136**: 3892-3904.

Wasteneys, G. O. and M. E. Galway (2003). Remodeling the cytoskeleton for growth and form: An overview with some new views. Annual Reviews of Plant Biology **54**: 691-722.

Wasteneys, G. O. and Z. Yang (2004). New views on the plant cytoskeleton. Plant Physiology **136**: 3884-3891.

Webb, T. and R. A. Bryson (1972). Late- and postglacial climatic change in the northern Midwest, USA: Quantitative estimates derived from fossil pollen spectra by multivariate statistical analysis. Quaternary Research **2**: 70-115.

Weisenseel, M. H., R. Nuccitelli and L. F. Jaffe (1975). Large electrical currents traverse growing pollen tubes. The Journal of Cell Biology **66**: 556-567.

Wieland, T., H. Faulstich and L. Fiume (1978). Amatoxins, phallotoxins, phallolysin, and antamanide: The biologically active components of poisonous *Amanita* mushroom. Critical Reviews in Biochemistry and Molecular Biology **5**: 185-260.

Wilsen, K., A. Lovy-Wheeler, B. Voigt, D. Menzel, J. Kunkel and P. Hepler (2006). Imaging the actin cytoskeleton in growing pollen tubes. Sexual Plant Reproduction **19**: 51-62.

Winship, L. J., G. Obermeyer, A. Geitmann and P. K. Hepler (2010). Under pressure, cell walls set the pace. Trends in Plant Science **15**: 363-369.

Wolters-Arts, M., W. M. Lush and C. Mariani (1998). Lipids are required for directional pollen-tube growth. Nature **392**: 818-821.

Woods, C. M., M. S. Reid and B. D. Patterson (1984). Response to chilling stress in plant cells I. Changes in cyclosis and cytoplasmic structure. Protoplasma **121**: 8-16.

Wulff, H. D. (1935). Galvanotropismus bei pollenschläuchen. Planta **24**: 602-608.

Xu, J. and B. Scheres (2005). Cell polarity: ROPing the ends together. Current Opinion in Plant Biology **8**: 613-618.

Yahara, I., H. Aizawa, K. Moriyama, K. Iida, N. Yonezawa, E. Nishida, H. Hatanaka and F. Inagaki (1996). A role of cofilin/destrin in reorganization of actin cytoskeleton in response to stresses and cell stimuli. Cell Structure and Function **21**: 4.

Yalovsky, S., D. Bloch, N. Sorek and B. Kost (2008). Regulation of membrane trafficking, cytoskeleton dynamics, and cell polarity by ROP/RAC GTPases. Plant Physiology **147**: 1527-1543.

Yamamoto, Y., M. Nishimura, I. Hara-Nishimura and T. Noguchi (2003). Behavior of vacuoles during microspore and pollen development in *Arabidopsis thaliana* Plant and Cell Physiology **44**: 1192-1201.

Yang, Z. (2008). Cell polarity signaling in arabidopsis. Annual Review of Cell and Developmental Biology **24**: 551-575.

Ye, J., Y. Zheng, A. Yan, N. Chen, Z. Wang, S. Huang and Z. Yang (2009). Arabidopsis formin3 directs the formation of actin cables and polarized growth in pollen tubes. Plant Cell **21**: 3868-3884.

Yeoh, S., B. Pope, H. G. Mannherz and A. Weeds (2002). Determining the differences in actin binding by human ADF and cofilin. Journal of Molecular Biology **315**: 911-925.

Yin, H. L., P. A. Janmey and M. Schleicher (1990). Severin is a gelsolin prototype. FEBS Letters **264**: 78-80.

Yokota, E., S. Muto and T. Shimmen (2000). Calcium-calmodulin suppresses the filamentous actin-binding activity of a 135-kilodalton actin-bundling protein isolated from lily pollen tubes. Plant Physiology **123**: 645-654.

Yokota, E. and T. Shimmen (1994). Isolation and characterization of plant myosin from pollen tubes of lily. Protoplasma **177**: 153-162.

Yokota, E. and T. Shimmen (2006). The actin cytoskeleton in pollen tubes; actin and actin binding proteins. In The Pollen Tube. R. Malhó, Springer Berlin / Heidelberg. **3:** 139-155.

Yokota, E., M. Tominaga, I. Mabuchi, Y. Tsuji, C. J. Staiger, K. Oiwa and T. Shimmen (2005). Plant villin, lily P-135-ABP, possesses G-actin binding

activity and accelerates the polymerization and depolymerization of actin in a Ca^{2+}-sensitive manner. Plant and Cell Physiology **46**: 1690-1703.

Yonezawa, N., Y. Homma, I. Yahara, H. Sakai and E. Nishida (1991). A short sequence responsible for both phosphoinositide binding and actin binding activities of cofilin. Journal of Biological Chemistry **266**: 17218-17221.

Yonezawa, N., E. Nishida, K. Iida, I. Yahara and H. Sakai (1990). Inhibition of the interactions of cofilin, destrin, and deoxyribonuclease I with actin by phosphoinositides. Journal of Biological Chemistry **265**: 8382-8386.

Yoon, G. M., P. E. Dowd, S. Gilroy and A. G. McCubbin (2006). Calcium-dependent protein kinase isoforms in *Petunia* have distinct functions in pollen tube growth, including regulating polarity. Plant Cell **18**: 867-878.

Yu, Y., Y. Li, L. Li, J. Lin, C. Zheng and L. Zhang (2009). Overexpression of PwTUA1, a pollen-specific tubulin gene, increases pollen tube elongation by altering the distribution of α-tubulin and promoting vesicle transport. Journal of Experimental Botany **60**: 2737-2749.

Zerzour, R., J. Kroeger and A. Geitmann (2009). Polar growth in pollen tubes is associated with spatially confined dynamic changes in cell mechanical properties. Developmental Biology **334**: 437-446.

Zhang, C., L. Guo, X. Wang, H. Zhang, H. Shi, W. Xu and X. Li (2007). Molecular characterization of four ADF genes differentially expressed in cotton. Journal of Genetics and Genomics **34**: 347-354.

Zhao, M., J. V. Forrester and C. D. McCaig (1999). A small, physiological electric field orients cell division. Proceedings of the National Academy of Sciences of the United States of America **96**: 4942-4946.

Zhou, L., Y. Fu and Z. Yang (2009). A genome-wide functional characterization of *Arabidopsis* regulatory calcium sensors in pollen tubes. Journal of Integrative Plant Biology **51**: 751-761.

Zinkl, G. M. and D. Preuss (2000). Dissecting *Arabidopsis* pollen-stigma interactions reveals novel mechanisms that confer mating specificity. Annals of Botany **85**: 15-21.

Zonia, L., M. Müller and T. Munnik (2006). Hydrodynamics and cell volume oscillations in the pollen tube apical region are integral components of the biomechanics of *Nicotiana tabacum* pollen tube growth. Cell Biochemistry and Biophysics **46**: 209-232.

Zonia, L. and T. Munnik (2008). Vesicle trafficking dynamics and visualization of zones of exocytosis and endocytosis in tobacco pollen tubes. Journal of Experimental Botany **59**: 861-873.

Zou, J., L. Song, W. Zhang, Y. Wang, S. Ruan and W.-H. Wu (2009). Comparative proteomic analysis of *Arabidopsis* mature pollen and germinated pollen. Journal of Integrative Plant Biology **51**: 438-455.

Annex

I provided high resolution images of the well preserved actin fringe and secretory vesicles in the pollen tube of lily to Jens Kroeger, PhD student co-supervised by Dr. Geitmann, and registered at the Physics Department of McGill University. The quantitative spatial coordinates of the actin configuration and vesicle localization obtained from my images provided a crucial piece of information for his model that describes the vesicle dynamics in the apical region of the pollen tube.

The manuscript was published in 2009 in Biophysical Jounal, volume 97, pp 1822-1831.

Microfilament Orientation Constrains Vesicle Flow and Spatial Distribution in Growing Pollen Tubes

Jens H. Kroeger[†], Firas Bou Daher[‡], Martin Grant[†] and Anja Geitmann[‡]

[†]McGill University, Montréal, Québec, Canada

[‡]Institut de Recherche en Biologie Végétale, Département de Sciences Biologiques, Université de Montréal, Montréal, Québec, Canada

Received 6 January 2009;
accepted 21 July 2009.
Editor: Alexander Mogilner..
Available online 1 October 2009.

Abstract

The dynamics of cellular organelles reveals important information about their functioning. The spatio-temporal movement patterns of vesicles in growing pollen tubes are controlled by the actin cytoskeleton. Vesicle flow is crucial for morphogenesis in these cells as it ensures targeted delivery of cell wall polysaccharides. Remarkably, the target region does not contain much filamentous actin. We model the vesicular trafficking in this area using as boundary conditions the expanding cell wall and the actin array forming the apical actin fringe. The shape of the fringe was obtained by imposing a steady state and constant polymerization rate of the actin filaments. Letting vesicle flux into and out of the apical region be determined by the orientation of the actin microfilaments and by exocytosis was sufficient to generate a flux that corresponds in magnitude and orientation to that observed experimentally. This model explains how the cytoplasmic streaming pattern in the apical region of the pollen tube can be generated without the presence of actin microfilaments.

Introduction

Cells are highly compartmentalized structures and specific cellular activities are spatially confined to certain types of organelles. The dynamics of cellular organelles reveal important information about their functions and mutual interactions. One important role of organelle movement is the transport and delivery of material from the site of synthesis to the site of usance or release. This type of targeted long distance transport is often carried out by vesicles, which are small, membrane-bound

organelles. Their small size, typically between 50 and 150 nm, makes the quantification of their movements a challenge for optical microscopy, especially when they are densely packed. However, the combination of high temporal resolution confocal microscopy and spatio-temporal image correlation spectroscopy has recently demonstrated that the movement patterns of densely packed vesicles can be quantified in space and time (1).

An example for dense and extremely dynamic vesicle trafficking occurs in rapidly growing plant cells. Expansion of cellular surface in walled cells necessitates the delivery of cell wall material and membrane to the site of expansion. Much of the required material is delivered in the form of secretory vesicles whose motion requires spatial and temporal coordination to ensure targeted discharge at the location of growth ([1], [2], [3] and [4]). In general, organelle transport is mediated by the cytoskeleton, and motor proteins linking the organelles with the cytoskeletal elements provide the propelling force. In plant cells, vesicle transport is mainly actin-myosin driven.

Vesicle trafficking in growing plant cells

Among the fastest growing plant cells is the pollen tube, a cellular protuberance formed by a pollen grain upon contact with a receptive stigma. The function of the pollen is to transport the male gametes from the anther of the donor flower to the female gametes located in the ovule of the receptor flower. Similar to other cells with an invasive lifestyle such as fungal hyphae, root hairs, and neuronal growth cones ([5], [6], [7] and [8]), pollen tubes display tip growth. In this type of growth, all growth activity is confined to a very small area on the cellular surface, the apex (9). Continuous addition of cell wall material and turgor-driven expansion of the existing cell wall at the apex result in the formation of a rapidly elongating, cylindrical tube. Because of the rapid growth rate and the spatial confinement of growth activity, vesicle trafficking in these cells is extremely dense and dynamic, thus making them a very suitable system for the study of vesicle transport.

Mechanics of pollen tube growth

From a mechanical point of view, pollen tube growth is defined by two simultaneously occurring processes—the continuous addition of cell wall material, and the mechanical deformation of the existing viscoplastic cell wall, driven by the hydrostatic turgor pressure. The spatial confinement of the growth activity to the apex is reflected in a polar distribution of the cytoplasmic contents (Fig. 1). The

apical region, i.e., the growing region of the cell, beginning with the hemispherical tip of the tube and reaching to a distance of approximately one tube radius behind the tip, is almost exclusively filled with vesicles. The absence of bigger organelles gives it a clear appearance in the optical microscope (Fig. 1 *A*), as compared to the granular shank of the cell that is densely packed with various types of organelles such as mitochondria, plastids, Golgi stacks, and endoplasmic reticulum. Labeling the vesicles with the lipophilic styryl dyes FM 4-64 or FM 1-43 has revealed that in angiosperm pollen tubes, the space they occupy in the apical region has the shape of an inverted cone filling the extreme apex and pointing toward the rear of the cell (Fig. 1, *E* and *F* ([1], [10] and [11])). This cone-shaped apical region is also relatively free of prominent filamentous actin cables, whereas the cylindrical distal portion of the cell is filled by longitudinally arranged actin arrays (Fig. 1, *B* and *C* (12)).

In the transition zone between the two regions, or the subapex, these arrays become finer and form a fringelike configuration at the shoulder region of the apical dome (Fig. 1 *D*, and Figure 2 and Figure 3). This fringe is always in close proximity to the continuously advancing apex of the cell. The position of this fringe is believed to be controlled by signaling cascades involving the subapical cytoplasmic alkaline band and the cytosolic Ca^{2+} gradient present in the tube apex. Both regulate the rate of assembly of G-actin into F-actin mediated by Ca^{2+} and pH activated proteins. These ion gradients thus limit the polymerization and bundling of the actin-cytoskeleton in a space-dependent manner ([13], [14], [15], [16], [17] and [18]). Although generally the term “actin fringe” in pollen tubes denotes only the ring-shaped arrangement of actin filaments in the subapical cortex of the cell ([12] and [19]), for the purpose of our model here, we define it as the complete actin array bordering the inverted vesicle cone (marked in *gray* in Fig. 3). The role of the fringe in the control of cytoplasmic streaming, vesicle delivery, and actin polymerization is the subject of this article. It should be noted that “cytoplasmic streaming” is a term used in the biology community to designate the intracellular movements of organelles, which in the optical microscope resemble a streaming process. In reality, this process is the sum of individually controlled movements of organelles through the cytoplasmic space. Most of these movements occur along cytoskeletal arrays. The cytosol, the liquid surrounding the organelles, is not the cause for the organelle movements, but it is likely to be dragged along passively. We discuss below the role of the surrounding liquid.

In the transition zone between the two regions, or the subapex, these arrays become finer and form a fringelike configuration at the shoulder region of the apical dome

(Fig. 1 *D*, and Figure 2 and Figure 3). This fringe is always in close proximity to the continuously advancing apex of the cell. The position of this fringe is believed to be controlled by signaling cascades involving the subapical cytoplasmic alkaline band and the cytosolic Ca^{2+} gradient present in the tube apex. Both regulate the rate of assembly of G-actin into F-actin mediated by Ca^{2+} and pH activated proteins. These ion gradients thus limit the polymerization and bundling of the actin-cytoskeleton in a space-dependent manner ([13], [14], [15], [16], [17] and [18]). Although generally the term "actin fringe" in pollen tubes denotes only the ring-shaped arrangement of actin filaments in the subapical cortex of the cell ([12] and [19]), for the purpose of our model here, we define it as the complete actin array bordering the inverted vesicle cone (marked in *gray* in Fig. 3). The role of the fringe in the control of cytoplasmic streaming, vesicle delivery, and actin polymerization is the subject of this article. It should be noted that "cytoplasmic streaming" is a term used in the biology community to designate the intracellular movements of organelles, which in the optical microscope resemble a streaming process. In reality, this process is the sum of individually controlled movements of organelles through the cytoplasmic space. Most of these movements occur along cytoskeletal arrays. The cytosol, the liquid surrounding the organelles, is not the cause for the organelle movements, but it is likely to be dragged along passively. We discuss below the role of the surrounding liquid.

Theory

Profile of the actin fringe

In this section, we present a calculation of the shape of the actin fringe, based on the assumption that it maintains a steady profile while advancing in the *y* direction and that it satisfies the constraints of the tread-milling model ([31] and [32]) for microfilament polymerization. Furthermore, we assume that the fringe advances forward at a steady rate equal to the pollen tube growth rate. We begin by using a model for the actin filament aggregation ([33], [34], [35], [36], [37] and [38]) to calculate the polarity, or orientation $\Theta(x)$, of the microfilaments (MF) along the actin front, in the fringe (23). For this purpose, we fix our coordinate system such that the tube grows in the positive y-direction. As detailed in the Supporting Material, we obtain the following filament angle $\Theta(x)$ between the barbed (plus) ends of the filaments and the *x* axis

$$\Theta(x) = \frac{-\pi}{L}x - \frac{\pi}{2}. \quad (1)$$

As an initial condition for the actin filament aggregation model, we set the filaments with plus-ends pointing toward the apex at the periphery of the tube and with plus-ends pointing away from the apex in the center of the tube. These orientations are consistent with the orientations measured in the center and the periphery of angiosperm pollen tubes (23). We can now use this variable orientation of the filaments along the actin front to understand the variable protrusion rate of this front and how it forms a stable V-shape. The elongation rate, or polymerization rate, v_{MF} of a single actin microfilament, according to the treadmilling model (32), is given by

$$(2) v_{MF}=v(k_{on}G-k_{off}),$$

and depends on the local G-actin concentration G, the length per monomer v and the net rates k_{on} and k_{off} at which actin monomers polymerize at the barbed end of the actin microfilament. There are other proteins and factors such as branching, capping, and uncapping, that contribute to the polymerization of individual actin filaments and actin fronts pushing a membrane ([31] and [32]). In the absence of experimental quantification of the spatial distribution of such agents in the pollen tube, we neglect those factors and focus on the effect of the orientation change along the actin front observed in pollen tubes (23). Actin monomers are added along the orientation of the microfilament, described by the vector **n**. Consequently, the profile of the actin network will protrude at a rate

$$(3) \frac{dr}{dt} = v_{MF}(\mathbf{n}\cdot\mathbf{r})$$

in a direction along **r**, that is normal to the profile (Fig. 3). The multiplicative factor $\mathbf{n}\cdot\mathbf{r}$ ensures that the normal growth rate is maximal when the microfilaments are at a right angle to the actin profile and point out of the network. The profile stays in place when the microfilaments are parallel to the profile and retracts when the microfilaments are at a right angle to the profile but point with barbed ends into the network. Here **r** is a unit vector normal to the profile and **n** is a unit vector giving the average orientation of the actin microfilaments. The dependence of the protrusion rate of an actin front on the filament orientation has been observed in lamellipodia (39). As discussed in the Supporting Material, we assume that the microfilament orientation along the x axis in the network is given by Eq. 1.

$$\Theta(x) = \frac{-\pi}{L}x - \frac{\pi}{2}.$$

We will use this model to derive a profile $y(x)$ for the actin network advancing at a steady rate equal to the growth rate of the pollen tube. Using the relation

$\mathbf{n} = \hat{\mathbf{i}}\cos\Theta + \hat{\mathbf{j}}\sin\Theta$ for the vector describing the orientation of the microfilaments and

$$\mathbf{r} = \frac{1}{\sqrt{1 + (y')^2}}\left(-y'\hat{\mathbf{i}} + \hat{\mathbf{j}}\right), \tag{4}$$

we obtain

$$\frac{dr}{dt} = \frac{v_{MF}}{\sqrt{1 + y'^2}}\left(-y'\cos\Theta(x) + \sin\Theta(x)\right). \tag{5}$$

We will now use the assumption that the cytoskeleton profile advances at a constant rate v_p in the y direction. This constant growth or advancement rate in the y direction can be related to the protrusion rate dr/dt in the direction normal to the profile. Using the angle θ between the normal vector **r** and the y direction, one obtains

$$\frac{dr}{dt} = |\mathbf{r}|v_p\cos\theta. \tag{6}$$

This expression has been used for the calculation of the steady growth profile in the case of diffusion-limited dendritic crystal growth and fluid finger propagation ([28] and [29]). Equating the left-hand side of Eq. 6 to the right-hand side of Eq. 3 gives

$$\frac{dr}{dt} = v_{MF}|\mathbf{n}||\mathbf{r}|\cos\phi = |\mathbf{r}|v_p\cos\theta. \tag{7}$$

This relation has been obtained by expressing the right-hand side of Eq. 3 as $v_{MF}|\mathbf{n}||\mathbf{r}|$ cos Φ, where Φ is the angle between the normal vector and the actin microfilament orientation. Since both **n** and **r** have unit length, we can interpret the equation as follows: the profile of the actin fringe must be such that the angle Φ between the normal vector and the actin microfilament orientation is equal to the angle θ between the normal vector and the y axis, the direction of the overall actin cytoskeleton growth. This condition is illustrated in Fig. 3. It is important to note that for these regions of low profile curvature we neglect any surface tension between the cytoplasm and the actin network. Using $\cos\theta = r_y = (1 + y'^2)^{-1/2}$, we can express Eq. 7 in terms of y' and $\Theta(x)$:

$$\frac{v_{MF}}{\sqrt{1+(y')^2}}\left(-y'\cos\Theta(x)+\sin\Theta(x)\right)=\frac{v_p}{\sqrt{1+(y')^2}}. \quad (8)$$

We obtain an ordinary differential equation for the profile of the actin fringe

$$y'=\tan\Theta(x)-\frac{\lambda}{\cos\Theta(x)}, \quad (9)$$

which has the solution

$$y(x)=\frac{-1}{m}\ln(\cos\Theta(x))-\frac{\lambda}{m}\ln\left(\tan\left(\frac{\pi}{4}+\frac{\Theta(x)}{2}\right)\right). \quad (10)$$

Here $\lambda = v_p/v_{MF}$ and m is the slope in the expression $\Theta(x) = mx + b$. The profile velocity v_p and the maximum filament growth rate v_{MF} must be similar such that $v_p/v_{MF} \simeq 1$. The approximation of λ being constant on the fringe is based on the assumption that the concentration G of G-actin monomers, and thus v_{MF}, is a constant. The profile of the actin fringe for different values of m, b in the function $\Theta(x)$ is shown in Fig. 2 *C*. By adding the left-hand side and separating the two halves of the profile by a distance corresponding to one-fifth of the cell radius, we obtain an actin fringe that recovers the funnel shape with "shoulders" observed experimentally. Once the profile on the actin fringe is found, the vesicle flux at the fringe is obtained by evaluating Eq. 14 with Eqs. (7) and (8):

$$\mathbf{j}\cdot\mathbf{r}=v_{ve}V\left(\frac{v_p}{v_{MF}}\frac{1}{\sqrt{1+(y')^2}}-a\right). \quad (11)$$

For various values of m and b, this flux is shown in Fig. 2 *D*.

Vesicle diffusion and cytoplasmic streaming

In the pollen tube shank, the vesicles are pulled along actin filaments by motor proteins ([40] and [41]) and the cytosol is dragged along by this active movement of suspended particles. However, in the apical inverted cone, there is not much filamentous actin that could serve to guide actin-myosin driven vesicle movement. And although the vesicles clearly display Brownian dynamics in this region ([42], [43] and [44]), it is unknown whether the cytosol, the fluid surrounding the vesicles, is moving in the actin-free zone. Technical limitations have precluded quantitative measurements of individual vesicle dynamics in the densely packed apex hitherto.

Therefore, we resort to the calculation of various dimensionless numbers to determine whether bulk fluid movement or diffusion dominates the motion of vesicles in the apex. The Reynolds number is the ratio of inertial to viscous forces. For a mass density $\rho = 10^3$ kg/m^3, a tube radius $r = 6.5$ μm, a velocity $v = 0.45$ μm/s, and a dynamic viscosity $\eta = 10^{-3}$ kg/m/s (45), the Reynolds number is $Re = \rho vr/\eta = 2.9 \times 10^{-6}$. Accordingly, inertial (convective) forces are negligible ([40], [45], [46] and [47]), such that viscous (advection due to the surrounding fluid) and diffusive (vesicle collisions) forces determine the motion of vesicles. This regime is called Stokes flow, and in this regime the movement of the cytosol (i.e., the solvent) is described by the Stokes equation $\nabla p = \eta \nabla^2 v$ (46). The question remains whether the movement of the bulk fluid cytosol or the collision of vesicles dominates vesicle movement. The Peclet number $Pe = vr_v/D$, where r_v is the vesicle radius and D is the diffusion constant, gives us the ratio of the adjective (due to the surrounding fluid) to diffusive forces. The vesicle diffusion constant can be estimated from the evolution of the vesicle staining density-density correlation function (1). A broadening of the correlation function of 0.5 μm occurred in 0.1 s, which is consistent with a translational diffusion coefficient of $D_T = \langle r^2/4\Delta t \rangle = 0.625$ μm^2/s (46). For a vesicle radius $r_v = 0.075$ μm, the Peclet number is $Pe = 0.054$. Based on this number, we neglect the motion of the surrounding fluid and assume that the motion of vesicles in the apex is dominated by collision between vesicles (Brownian dynamics or diffusion). A mathematical analysis of the velocity field in the surrounding cytosol would require information on the pressure and stresses in the cytosol but also the proper treatment of the boundary conditions formed by the outer surfaces of the individual vesicles (in addition to the cell wall and the actin fringe) (46). This difficult problem has been addressed with the boundary integral approach ([48] and [49]) and the boundary element method (50), but its solution is beyond the scope of this article.

In our model, the vesicle flux is constrained by the following sources and sinks:

1. There is continuous flow of vesicles in the direction of the plus-ends of actin filaments in the polymer network modeled previously, resulting essentially in an addition of vesicles in the periphery and a removal in the center.

2. A certain number of vesicles is absorbed by the fusion process (exocytosis) at the plasma membrane located in an annular region around the very tip of the tube.

We model the vesicle flow using Fick's law $\mathbf{j} = -D\nabla V$ on the domain bounded above by the cell wall calculated in the Supporting Material and below by the fringe

calculated in the previous section. The average vesicle flow velocity **v** can be related to the flux **j** = V**v**, where V is the local vesicle density. Furthermore, the requirement of vesicle number conservation (continuity equation) leads to the diffusion equation, Eq. 12. This description is justified by the observation that organelles in pollen tubes display Brownian motion ([42], [43] and [44]). The change in vesicle density $V(x, y)$ is given by the diffusion equation

$$\frac{\partial V}{\partial t} = -\nabla \cdot \mathbf{j} = D\nabla^2 V = 0 \quad (12)$$

in the clear zone of the apex. To solve this equation, the boundary conditions must be specified on the cell wall and the fringe. The flux of vesicles normal to the cell wall $\mathbf{r}\cdot\mathbf{j} = \mathbf{r}\cdot(-D\nabla V)$ is given by the absorption of vesicle due to the fusion process

$$\mathbf{j}\cdot\mathbf{r} = -D\nabla V\cdot\mathbf{r} = \frac{R}{V_{ol}}, \quad (13)$$

where V_{ol} denotes the volume of one vesicle and the net deposition rate R is calculated in the Supporting Material (Fig. 2 *B*). We can estimate the average vesicle flux normal to the cell wall due to fusion at $\langle j_R \rangle = 0.156\ s^{-1}\ \mu m^{-2}$ from $V_{ol} = 0.0026\ \mu m^3$ and $R = 0.0244\ \mu$m/min. The net flux of vesicles normal to the actin fringe is generated by the addition of vesicles to the clear zone (inverted cone) from actin filaments with barbed ends oriented toward the tip and by vesicle recovery onto centrally located filaments that are oriented with the barbed ends pointing rearward:

$$\mathbf{j}\cdot\mathbf{r} = -D\nabla V\cdot\mathbf{r} = v_{ve}V(\mathbf{n}\cdot\mathbf{r} - a). \quad (14)$$

The quantity v_{ve} denotes the maximum rate at which vesicles are delivered into the apical cytoplasm. We can estimate the normal vesicle flux at the actin fringe (in the tube center) by $j_F \simeq v_{ve}\langle V_{3D}\rangle = 27.0\ s^{-1}\ \mu m^{-2}$. Here $\langle V_{3D}\rangle = 62.0\ \mu m^{-3}$ is the average three-dimensional vesicle density in the apical cone (1). Comparing the numbers reveals a difference of two orders of magnitude between the vesicle flux at the plasma membrane and that normal to the actin fringe. This difference explains why the vesicle flow pattern predicted by our model is largely controlled by the orientation of actin filaments. Since the orientation of the microfilaments also controls the normal protrusion rate of the actin cytoskeleton, the right-hand side of Eq. 14 is proportional to the protrusion rate of the actin cytoskeleton described by Eq. 3 (Fig. 2 *D*). The constant term a represents myosin-mediated vesicle binding onto a microfilament that is oriented parallel to the fringe profile. The constant a is

adjusted in such a way that the total number of vesicles entering the clear zone equals the total number of vesicles leaving the clear zone, i.e., the net flux is zero.

Results

A steady growth analysis (30) was used to calculate the shape of the apical cell wall during its viscoplastic expansion. The resulting cell wall shape, that minimizes the mechanical stress induced by the turgor pressure, is shown in Fig. 2 *A*. The material necessary for the steady elongation of the cell wall is supplied by vesicles. The cell wall thus constitutes a target (i.e., a sink) for these organelles (Fig. 2 *B*).

The orientation of the barbed (plus) ends of the actin microfilaments varies continuously along the radial axis to adopt the observed configuration (23), which minimizes the mechanical stress in the actin polymer network (51). Once the steady shape of the advancing actin fringe is assumed, its profile is a direct consequence of the orientation of the actin microfilaments (Fig. 2 *C*). This constraint is illustrated in Fig. 3. The orientation of the microfilaments also determines the direction in which the vesicles are delivered to or removed from the apical cone and the magnitude of their velocity (Fig. 2 *D*). Addition (positive values in Fig. 2 *D*) occurs in the periphery of the cell, removal (negative values) in the center. The fringe thus constitutes a source and sink for the vesicles. The motion of the vesicles in the apical cone is modeled with the diffusion equation together with the boundary conditions described above, which are solved with MatLab (The MathWorks, Natick, MA). After an integration time of 10 s, the vesicle density reaches a steady state shown in Fig. 4, *A* and *C*. The average density from the simulations is rescaled to 209 μm^{-2}. This average vesicle density is obtained by dividing the number of vesicles present in a typical lily pollen tube apex (average of 81,247 vesicles (1)) by the area of the clear zone (389 μm^2). In the biological sample, this average density corresponds to the density visible on a projection of a z-stack image series. Our model indicates a clear density gradient from the front of the cell to the tail of the vesicle cone. This spatial profile of vesicle density is consistent with observations in the fluorescence microscope ([1] and [11]) and the transmission electron microscope (4).

In addition to providing information on vesicle density, our model yields the relative speed and direction of vesicle motion at each coordinate in the vesicle cone. The resulting vesicle flux **j** (Fig. 4 *B*) is in excellent agreement with experimental data. Quantitative analysis of vesicle dynamics (1) revealed a vesicle flux with a direction field described by a reverse fountain pattern, qualitatively identical to the one our model produces. The microscopic observations showed very slow vesicle motion at

the immediate tip of the pollen tube whereas vesicles move rapidly in the tail region of the cone. Our model is consistent with this change in the vesicle motion.

The absence of significant vesicle motion at the very tip of the cell is due to the small value of the vesicle fusion rate at the cell wall. Since the average vesicle fusion rate is directly proportional to the pollen tube growth rate, we can model the change in the flux pattern due to an increase in pollen tube growth rate. Fig. 4 *E* shows the vesicle motion in a rapidly growing tube. The pattern was obtained by multiplying the net vesicle fusion rate by 50 (R = 1.22 μm/min when averaged over the cell wall). Although this value of R corresponds to a tube growth rate (v = 350 μm/min) that is much higher than any value observed in vitro (22), the numerical simulation displays the observed robustness of the streaming pattern to changes in the growth rate.

Our model, and especially the V-shape of the apical zone, relies on the fact that actin microfilaments are oriented with their barbed ends forward at the periphery and rearward in the center of the tube, a typical configuration in angiosperm pollen tubes (23). In gymnosperm pollen tubes, the flow direction of cytoplasmic organelles is reversed, forming a fountainlike streaming pattern (52). However, it is unknown whether this flow pattern is due to an inversion of the orientation of actin filaments (i.e., barbed ends toward the rear in the periphery and toward the front in the center), or whether a different type of myosin moves vesicles from the barbed ends of the actin filaments toward their pointed ends (53). To find out which of the two alternatives is more likely we tried to model both. First, we let vesicles move in the opposite direction to the actin polarity on actin filaments that are oriented and polymerize according to the conditions mentioned above for angiosperm pollen tubes. The vesicle flow now displays a fountain pattern (Fig. 4 *G*), but the shape of the vesicle cone remains identical to that of the angiosperm pollen tube. Importantly, a high density of vesicles is now present in the tail of the cone, whereas the density is low close to the plasma membrane (Fig. 4 *F*).

Next, we inverted the orientation of the actin filaments. Actin arrays in the periphery now point forward with their barbed ends, and the central array points rearward. We chose

$$\Theta(x) = \frac{-\pi}{L}x + \frac{\pi}{2} \quad (15)$$

for this approach. Not only do these inverse initial conditions result in a fountainlike flow pattern (Fig. 4 *H*), they also lead to a very different shape of the apical vesicle population (Fig. 4 *I*). Instead of an inverted cone, the apical vesicle population is now

crescent-shaped. Inspection of available fluorescence micrographs reveals that vesicles in gymnosperm pollen tubes indeed accumulate in such a crescent-shaped conformation ([44] and [52]), whereas the configuration shown in Fig. 4 *F* does not correspond to any phenomenon found in living pollen tubes.

Discussion

The goal of this work was to model the dynamics of vesicles in the apical region of growing pollen tubes and to relate it to the polymerization of the actin arrays bordering the apical vesicle cone. Our data show that a viscoplastic model of the cell wall and a steady-state model for the actin polymerization provide adequate inlet and outlet boundary conditions for the diffusive motion of the vesicles. When solved together, these constraints lead to a vesicle flux whose magnitude and direction are in agreement with the vesicle motion observed experimentally ([1], [11] and [54]). The continuity of the vesicle motion at the apical fringe, i.e., the conservation of the total volume of cell wall material, was used to solve the model.

The robustness of our model is demonstrated by its applicability to a system that operates quite differently, the gymnosperm pollen tube. Inversion of the actin filaments in our model produces exactly the streaming and vesicle distribution patterns that are observed experimentally ([44] and [52]). By contrast, inversion of the movement direction of the organelles, putatively mediated by a myosin motor protein operating in the opposite direction, does not produce any patterns that can be observed experimentally. This is consistent with the fact that no myosin molecules operating in unconventional direction have been identified in plants hitherto. It must be mentioned, however, that microtubules seem to be more important in gymnosperm pollen tubes, compared to their role in angiosperm counterparts (55). Drug-induced microtubule depolymerization inhibits elongation in gymnosperm pollen tubes and changes the motion patterns of organelles. However, the authors postulate that this effect is mediated by the microtubules' control of the actin array. This is corroborated by the finding that the microtubule disruption causes a reversal of organelle streaming in gymnosperm pollen tubes (52). This reversal from fountain- to inverse fountain-streaming is accompanied by a rearrangement of the actin array. Hence, these experiments are consistent with the results of our modeling. No information on the orientation of actin filaments in gymnosperm pollen tube is available, but our model predicts that actin arrays are oriented with their barbed ends toward the apex in the central cytoplasmic region, and rearward in the periphery. Vesicles are predicted to move toward the barbed ends of the arrays. Together these conditions result in the flow and distribution patterns observed experimentally.

In view of the simplistic assumptions of the model, the agreement with experimental observations is encouraging. A very important test of the vesicle diffusion picture would be the prediction of the vesicle flux after a disruption of the tubular shape of the pollen tube, e.g., through a mechanical constriction of the tube or by the application of an agent causing swelling of the apex without interfering with actin functioning. However, such tests require modeling beyond the limits of our current steady-state cell wall analysis. Refinements of the model should include a better calculation of the granular flow of the cytoplasm, a heterogeneous and polydisperse medium (i.e., containing components of different sizes). Furthermore, the spatial variation of G-actin and calcium concentrations, as well as their effects on the actin polymerization process, was not taken into account. Given the cytoplasmic calcium gradient in the clear zone of the pollen tube apex (56) and the role played by calcium during actin polymerization (57), calcium and G-actin concentrations should be considered in a future model of the polymerization process. Experimental validations of this model include a detailed determination of the polarization of the actin microfilaments in the subapical region.

Acknowledgements

We thank Prof. Luca Cortelezzi for insightful discussions.

We are thankful for the generous support of this research by the Natural Sciences and Engineering Research Council of Canada and by Le Fonds Québécois de la Recherche sur la Nature et les Technologies.

References

1 J. Bove, B. Vaillancourt, J. Kroeger, P. Hepler and P. Wiseman *et al.*, Magnitude and direction of vesicle dynamics in growing pollen tubes using spatiotemporal image correlation spectroscopy (STICS) and fluorescence recovery after photobleaching (FRAP), *Plant Physiol.* **147** (2008), pp. 1646–1658.

2 A. Geitmann and J. Dumais, Not-so-tip-growth, *Plant Signal. Behav.* **4** (2009), pp. 136–138.

3 J. Derksen, T. Rutten, I. Lichtscheidl, A. de Win and E. Pierson *et al.*, Quantitative analysis of the distribution of organelles in tobacco pollen tubes: implications for exocytosis and endocytosis, *Protoplasma* **188** (1995), pp. 267–276.

4 S. Lancelle and P. Hepler, Ultrastructure of freeze-substituted pollen tubes of *Lilium longiflorum*, *Protoplasma* **167** (1992), pp. 215–230.

5 J. Kroeger, A. Geitmann and M. Grant, Model for calcium dependent oscillatory growth in pollen tubes, *J. Theor. Biol.* **253** (2008), pp. 363–374.

6 J. Dumais, S. Long and S. Shaw, The mechanics of surface expansion anisotropy in *Medicago truncatula* root hairs, *Plant Physiol.* **136** (2004), pp. 3266–3275.

7 S. Bartnicki-Garcia, C. Bracker, G. Giertz, R. Lopez-Franco and H. Lu, Mapping the growth of fungal hyphae: orthogonal cell wall expansion during tip growth and the role of turgor, *Biophys. J.* **79** (2000), pp. 2382–2390.

8 A. Schaefer, N. Kabir and P. Forscher, Filopodia and actin arcs guide the assembly and transport of two populations of microtubules with unique dynamic parameters in neuronal growth cones, *J. Cell Biol.* **158** (2002), pp. 139–152.

9 A. Geitmann and M. Steer, The architecture and properties of the pollen tube cell wall. In: R. Malhò, Editor, *The Pollen Tube. Plant Cell Monographs 3*, Springer Verlag, Berlin (2006).

10 R. Malhó, P. Castanho-Coelho, E. Pierson and J. Derksen, Endocytosis and membrane recycling in pollen tubes. In: Šamaj, F. Baluška and D. Menzel, Editors, *Plant Endocytosis*, Springer Verlag, Berlin (2005).

11 R. Parton, S. Fischer-Parton, M. Watahiki and A. Trewavas, Dynamics of the apical vesicle accumulation and the rate of growth are related in individual pollen tubes, *J. Cell Sci.* **114** (2001), pp. 2685–2695.

12 A. Lovy-Wheeler, K. Wilsen, T. Baskin and P. Hepler, Enhanced fixation reveals the apical cortical fringe of actin filaments as a consistent feature of the pollen tube, *Planta* **221** (2005), pp. 95–104.

13 J. Feijó, The pollen tube oscillator: towards a molecular mechanism of tip growth. In: M. Cresti, G. Cai and A. Moscatelli, Editors, *Fertilization in Higher Plants*, Springer Verlag, Berlin (1999).

14 E. Yokota, M. Tominaga, I. Mabuchi, Y. Tsuji and C. Staiger *et al.*, Plant villin, lily P-135-ABP, possesses G-actin binding activity and accelerates the polymerization and depolymerization of actin in a Ca^{2+}-sensitive manner, *Plant Cell Physiol.* **46** (2005), pp. 1690–1703.

15 P. Hepler, Calcium: a central regulator of plant growth and development, *Plant Cell* **17** (2005), pp. 2142–2155.

16 J.-U. Hwang, Y. Gu, Y.-J. Lee and Z. Yang, Oscillatory ROP GTPase activation leads the oscillatory polarized growth of pollen tubes, *Mol. Biol. Cell* **16** (2005), pp. 5385–5399.

17 B. Kost, Spatial control of Rho (Rac-Rop) signaling in tip-growing plant cells, *Trends Cell Biol.* **18** (2008), pp. 119–127.

18 G. Cai and M. Cresti, Organelle motility in the pollen tube: a tale of 20 years, *J. Exp. Bot.* **60** (2009), pp. 495–508.

19 A. de Win, E. Pierson and J. Derksen, Rational analyses of organelle trajectories in tobacco pollen tubes reveal characteristics of the actomyosin cytoskeleton, *Biophys. J.* **76** (1999), pp. 1648–1658.

20 E. Yokota and T. Shimmen, Isolation and characterization of plant myosin from pollen tubes of lily, *Protoplasma* **177** (1994), pp. 153–162.

21 A. Lovy-Wheeler, L. Cardenas, J. Kunkel and P. Hepler, Differential organelle movement on the actin cytoskeleton in lily pollen tubes, *Cell Motil. Cytoskeleton* **64** (2007), pp. 1724–1769.

22 L. Vidali, S. McKenna and P. Hepler, Actin polymerization is essential for pollen tube growth, *Mol. Biol. Cell* **12** (2001), pp. 2534–2545.

23 M. Lenartowska and A. Michalska, Actin filament organization and polarity in pollen tubes revealed by myosin II subfragment 1 decoration, *Planta* **228** (2008), pp. 891–896.

24 D. Begg, R. Rodewald and L. Rebhun, The visualization of actin filament polarity in thin sections, *J. Cell Biol.* **79** (1978), pp. 846–852.

25 R. Adams and T. Pollard, Propulsion of organelles isolated from *Acanthamoeba* along actin filaments by myosin-I, *Nature* **322** (1986), pp. 752–756.

26 M. Sheetz and J. Spudich, Movement of myosin-coated fluorescent beads on actin cables in vitro, *Nature* **303** (1983), pp. 31–35.

27 S. Kuznetsov, G. Langford and D. Weiss, Actin-dependent organelle movement in squid axoplasm, *Nature* **356** (1992), pp. 722–725.

28 J. Langer, Dendrites, viscous fingers, and the theory of pattern formation, *Science* **243** (1983), pp. 1150–1156.

29 P. Pelcé, New Visions on Form and Growth, Oxford University Press, Oxford (2000).

30 J. Dumais, S. Shaw, C. Steele, S. Long and P. Ray, An anisotropic-viscoplastic model of plant cell morphogenesis by tip growth, *Int. J. Dev. Biol.* **50** (2006), pp. 209–222.

31 L. Edelstein-Keshet and G.B. Ermentrout, Models for spatial polymerization dynamics of rod-like polymers, *J. Math. Biol.* **40** (2000), pp. 64–96.

32 A. Mogilner and L. Edelstein-Keshet, Regulation of actin dynamics in rapidly moving cells: a quantitative analysis, *Biophys. J.* **83** (2002), pp. 1237–1258.

33 G. Civelekoglu and L. Edelstein-Keshet, Modeling the dynamics of F-actin in the cell, *Bull. Math. Biol.* **56** (1994), pp. 587–616.

34 W. Alt, Mathematical models in actin-myosin interactions. In: K.E. Wohlfahrt-Bottermann, Editor, *Nature and Function of Cytoskeletal Proteins in Motility and Transport*, Gustav Fischer Verlag, Stuttgart (1987).

35 A. Mogilner and E. Edelstein-Keshet, Selecting a common direction. I. how orientational order can arise from simple contact responses between interacting cells, *J. Math. Biol.* **33** (1995), pp. 619–660.

36 A.I. Mogilner and L. Edelstein-Keshet, Spatio-angular order in populations of self-aligning objects: formation of oriented patches, *Physica D* **89** (1996), pp. 346–367.

37 A. Mogilner, E. Edelstein-Keshet and G. Ermentrout, Selecting a common direction. II. peak-like solutions representing total alignment of cell clusters, *J. Math. Biol.* **34** (1996), pp. 811–842.

38 A. Spiros and L. Edelstein-Keshet, Testing a model for the dynamics of actin structures with biological parameter values, *Bull. Math. Biol.* **60** (1998), pp. 275–305.

39 S. Koestler, S. Auinger, M. Vinzenz, K. Rottner and J. Small, Differentially oriented populations of actin filaments generated in lamellipodia collaborate in pushing and pausing at the cell front, *Nat. Cell Biol.* **10** (2008), pp. 306–313.

40 M. Yoneda and R. Nagai, Structural basis of cytoplasmic streaming in characean internodal cells. A hydrodynamic analysis, *Protoplasma* **147** (1988), pp. 64–76.

41 D. Houtman, I. Pagonabarraga, C. Lowe, A. Esseling-Ozdoba and A. Emons *et al.*, Hydrodynamic flow caused by active transport along cytoskeletal elements, *Europhys. Lett.* **78** (2007), pp. 18001–18005.

42 A. de Win, B. Knuiman, E. Pierson, H. Geurts and H. Kengen *et al.*, Development and cellular organization of *Pinus sylvestris* pollen tubes, *Sex. Plant Reprod.* **9** (1996), pp. 93–101.

43 O. Terasaka and T. Niitsu, Differential roles of microtubule and actin-myosin cytoskeleton in the growth of *Pinus* pollen tubes, *Sex. Plant Reprod.* **7** (1994), pp. 264–272.

44 X. Wang, Y. Teng, Q. Wang, X. Li and X. Sheng *et al.*, Imaging of dynamic secretory vesicles in living pollen tubes of *Picea meyeri* using evanescent wave microscopy, *Plant Physiol.* **141** (2006), pp. 1591–1603.

45 M. Leonetti, Cell movement by osmotic current, *Europhys. Lett.* **32** (1995), pp. 561–565.

46 M. Ciofalo, M. Collins and T. Hennessy, Nanoscale Fluid Dynamics in Physiological Processes, WIT Press, Southampton (1999).

47 W. Pickard, The role of cytoplasmic streaming in symplastic transport, *Plant Cell Environ.* **26** (2003), pp. 1–15.

48 B. Yoon and S. Kim, A boundary collocation method for the motion of two steroids in Stokes flow: hydrodynamics and colloidal interactions, *Int. J. Multiph. Flow* **16** (1990), pp. 639–650.

49 F. Xijun and Y. Yeow, A boundary method equation method for the Stokes problem of multiparticle systems, *Phys. Fluids A* **4** (1992), pp. 1074–1076.

50 C. Pozrikidis, Boundary Integral and Singularity Methods for Linearized Viscous Flow, Cambridge University Press, Cambridge (1992).

51 S. Chandrasekhar, Liquid Crystals (2nd Ed.), Cambridge University Press, Cambridge (1992).

52 C. Justus, P. Anderhag, J. Goins and M. Lazzaro, Microtubules and microfilaments coordinate to direct a fountain streaming pattern in elongating conifer pollen tube tips, *Planta* **219** (2004), pp. 103–109.

53 A. Wells, A. Lin, L.-Q. Chen, D. Safer and S. Cain *et al.*, Myosin VI is an actin-based motor that moves backwards, *Nature* **401** (1999), pp. 505–508.

54 L. Zonia and T. Munnik, Vesicle trafficking dynamics and visualization of zones of exocytosis and endocytosis in tobacco pollen tubes, *J. Exp. Bot.* **59** (2008), pp. 861–873.

55 P. Anderhag, P. Hepler and M. Lazzaro, Microtubules and microfilaments are both responsible for pollen tube elongation in the conifer *Picea abies* (Norway spruce), *Protoplasma* **214** (2000), pp. 141–157.

56 P. Hepler, Tip growth in pollen tubes: calcium leads the way, *Trends Plant Sci.* **2** (1997), pp. 79–80.

57 M. Vantard and L. Blanchoin, Actin polymerization processes in plant cells, *Curr. Opin. Plant Biol.* **5** (2002), pp. 502–506.

58 J. Cooper, The role of actin polymerization in cell motility, *Annu. Rev. Physiol.* **53** (1991), pp. 585–605.

59 J.-B. Marchand, P. Moreau, A. Paoletti, P. Cossart and M.-F. Carlier *et al.*, Actin-based movement of *Listeria monocytogenes*: actin assembly results from the local maintenance of uncapped filament barbed ends at the bacterium surface, *J. Cell Biol.* **130** (1995), pp. 331–343.

60 K. Luby-Phelps, Cytoarchitecture and physical properties of cytoplasm: volume, viscosity, diffusion, intracellular surface area, *Int. Rev. Cytol.* **192** (2000), pp. 189–221.

61 A. Mastro and A. Keith, Diffusion in the aqueous compartment, *J. Cell Biol.* **99** (1984), pp. 180–187.

62 V. Abraham, V. Krishnamurthi, D. Taylor and F. Lanni, The actin-based nanomachine at the leading edge of migrating cells, *Biophys. J.* **77** (1999), pp. 1721–1732.

63 E. Pierson, D. Miller, D. Callaham, A. Shipley and B. Rivers *et al.*, Pollen tube growth is coupled to the extracellular calcium ion flux and the intracellular calcium gradient: effect of BAPTA-type buffers and hypertonic media, *Plant Cell* **6** (1994), pp. 1815–1828.

Table

TABLE 1 Explanation and typical value of different variables used in the model

Parameter	Symbol	Value	Source
Vesicle flux	$\mathbf{j}$		
Average vesicle density	$\langle V_{3D} \rangle$	62 μm^{-3}	*
Actin monomer concentration	G	10–50 μM	(58,59)
Diffusion constant	D	0.1–10^3 $\mu m^2/s$	(60,61)
Unit vector normal to the actin fringe	$\mathbf{r}$		
Average net vesicle deposition rate	R	0.00041 $\mu m/s$	*
Unit vector of actin microfilament polarity	$\mathbf{n}$		
Angle between the actin polarity and the x axis	$\Theta(x)$		
Angle between the $\mathbf{r}$ and the tube growth direction	θ		
Angle between $\mathbf{n}$ and $\mathbf{r}$	ϕ		
Stress in the cell wall	σ	25 MPa	(6)
Strain rate in the cell wall	$\dot{\varepsilon}$	0–0.1 min^{-1}	(6)
Maximum growth rate of a single microfilament	v_{MF}	0.25 $\mu m/s$	(62)
Vesicle delivery rate	v_{ve}	0.45 $\mu m/s$	(1)
Length of microfilament per added monomer	ν	2.2 nm	(32)
Steady growth rate, in the y direction, of the cytoskeleton	v_p	0.1–0.4 $\mu m/s$	(63)
Profile of the actin fringe	$y(x)$		

*Values calculated in this article.

Figures

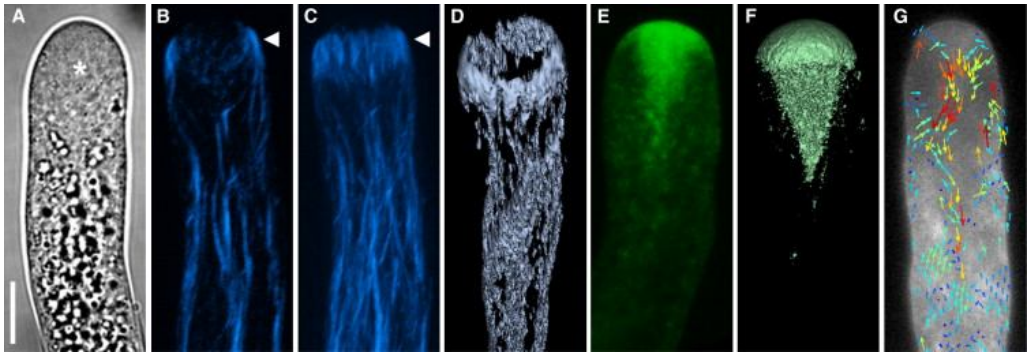

Figure 1. Cytoarchitecture of the apical region of *Lilium longiflorum* pollen tubes. (*A*) Brightfield micrograph revealing the difference between the smooth appearance of the apical cytoplasm (*asterisk*) and the granular texture of the shank. (*B–D*) Filamentous actin forming the apical fringe (*arrowhead*) revealed by label with rhodamine phalloidin. (*B*) Single optical section. (*C*) Projection of z-stack of the same tube as in panel *B*. (*D*) Surface rendering of three-dimensional z-stack reconstruction, tilted slightly to reveal spatial configuration of the apical actin fringe. (*E–G*) Vesicles visualized by label with FM1-43. (*E*) Single optical section. (*F*) Surface rendering of three-dimensional z-stack reconstruction revealing spatial configuration of the inverted vesicle cone. (*G*) Vector map of vesicle flux resulting from STICS analysis of a time series of confocal laser scanning micrographs. Panel *G*, details of the experiment and STICS analysis, were first published by Bove et al. (1) (reprinted with permission; copyright American Society of Plant Biologists). Fluorescence micrographs are false-colored. The images in this panel do not show the same tube. Bar = 10 μm. Pollen culture, fluorescent label, and image acquisition for all figures are detailed in the Supporting Material.

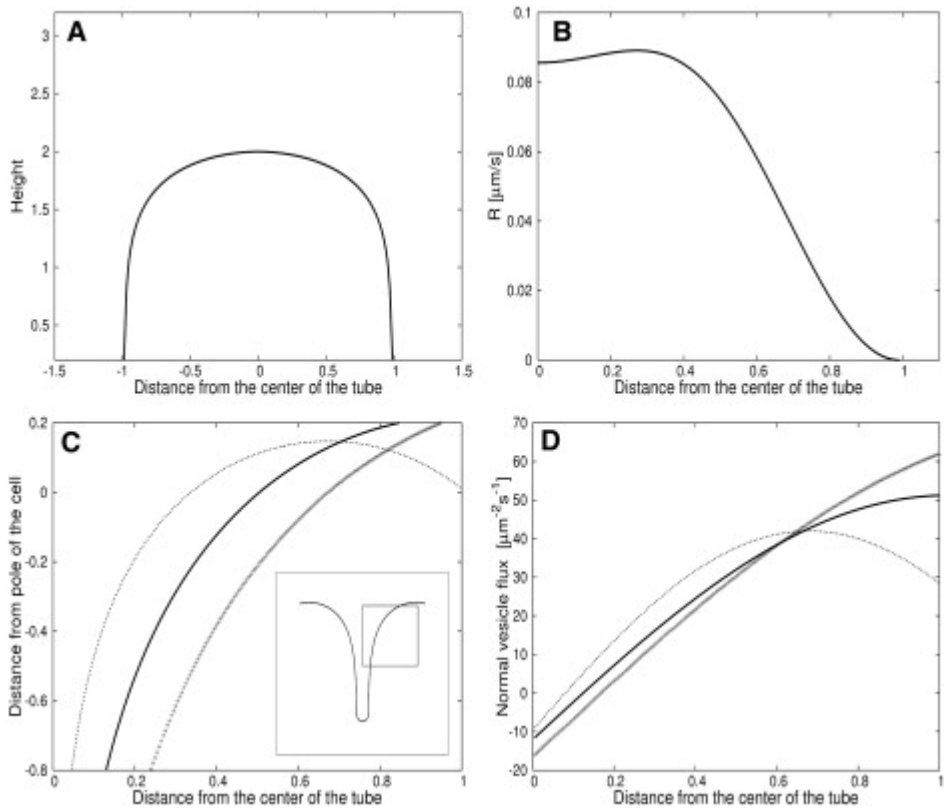

Figure 2. Geometry of the apical cone and vesicle delivery and absorption rates at its boundaries. (*A*) Shape of the apical cell wall during steady viscoplastic orthogonal growth. (*B*) Cell wall vesicle deposition rate necessary to sustain the steady viscoplastic growth. The details of their calculation are found in the Supporting Material. (*C*) Right-hand side of the actin profile given by Eq. 10. (*Solid line*) (m, b) = ($-\pi/L$, $-\pi/2$). (*Dotted line*) (m, b) = ($-3\pi/2$, $-\pi/2$). (*Crosses*) (m, $b = -5\pi/6L$, $-4\pi/6$). The inset shows two symmetric halves of the actin fringe profile. The half-circle at the tail end of the profile is due to capillary effects (Supporting Material). (*D*) Vesicle flux normal to the actin fringe given by Eq. 11. (*Solid line*) (m, b) = ($-\pi/L$, $-\pi/2$). (*Dotted line*) (m, b) = ($-3\pi/2$, $-\pi/2$). (*Crosses*) (m, $b = -5\pi/6L$, $-4\pi/6$). In all cases, $\lambda = 1$. The units of the x- and y axis are multiples of the pollen tube radius.

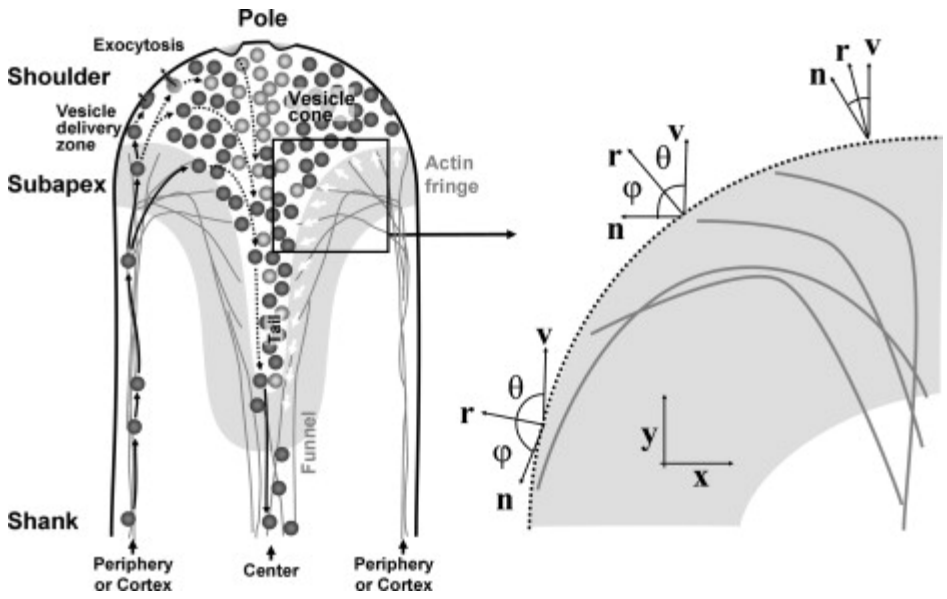

Figure 3. (*Left*) Schematic drawing illustrating the principal directions of vesicle motion (*left half* of the tube) and orientation of the actin filaments bordering the vesicle cone (*open arrows* in right half) in the apical region of a pollen tube. After delivery into the apical region on the actin filaments forming the fringe, vesicles are released into the apical cytoplasm in an annulus-shaped zone (vesicle delivery zone). Vesicles that succeed in contacting the plasma membrane undergo exocytosis. Vesicles that do not succeed in contacting the plasma membrane stream rearwards within the cone-shaped vesicle pool. Many of these vesicles are recirculated back into the forward stream immediately in the subapical region (not shown). Solid arrows indicate actin-myosin-guided vesicle movement, dashed arrows indicate movements that are presumably governed by diffusion. Objects are not drawn to scale. For clarity, except for vesicles, no other organelle or the cell wall is drawn. This figure is based on results by Bove et al. (1) and Zonia and Munnik (54). (*Right*) Orientation of the vectors along the actin fringe profile. The values **r, n**, and **v** are the vector normal to the profile, the microfilament orientation vector, and the growth vector of the cytoskeleton, respectively. The profile of the actin fringe is such that the angle ϕ between the normal vector and the actin microfilament orientation is equal to the angle θ between the normal vector and the growth direction, the y axis. Once the orientation vector **n** is fixed, the shape of the fringe profile can be determined.

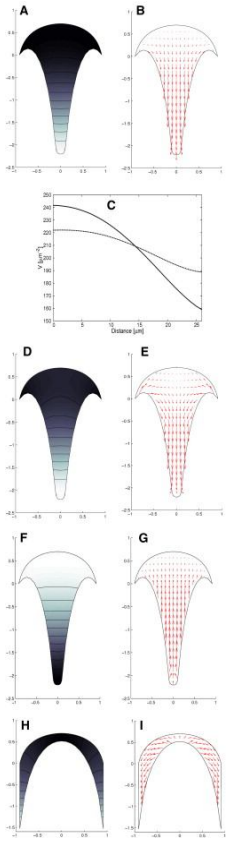

Figure 4. (*A*) Vesicle density in the clear zone of the pollen tube. Lighter shades indicate low density whereas dark shades indicate high density. The units of the *x*- and *y* axis are multiples of the cell radius. (*B*) The vesicle flux in the cell apex reveals the reverse fountain pattern. The relative magnitude of the flux velocity is given by the length of the arrows. (*C*) (*Solid line*) Vesicle density as a function of the distance from the tip, along the axis of symmetry of the tube (the *y* axis). The vesicle density from the simulation is rescaled such that its average is 209 μm^{-2} (1). (*Dashed line*) Vesicle density for a rapidly growing tube. The growth rate and the net vesicle fusion rate at the cell wall are 50 times larger. (*D*) Vesicle density in a rapidly growing pollen tube. (*E*) Vesicle flux in a rapidly growing pollen tube. (*F*) Vesicle distribution for an actin orientation identical to an angiosperm pollen tube but with inverted vesicle delivery at the fringe due to reverse myosin activity. (*G*) Vesicle flux for an actin orientation identical to an angiosperm pollen tube but with inverted vesicle delivery at the fringe due to reverse myosin activity. (*H*) Geometry of apex and density of vesicle in a gymnosperm pollen tube. This geometry is obtained by inverting the microfilament orientation at the fringe boundaries. The MF orientation profile used is $\Theta(x) = \frac{-\pi}{L}x + \frac{\pi}{2}$ (*I*) Vesicle flux in a gymnosperm pollen tube. For 5 μm, $\langle R \rangle$ = 1.22 μm/min.